

191

BOLT BERANEK AND NEWMAN INC

CONSULTING • DEVELOPMENT • APPLIED RESEARCH

N 63 82 880

**ACOUSTICAL CONSIDERATIONS IN THE PLANNING
AND OPERATION OF LAUNCHING AND STATIC
TEST FACILITIES FOR LARGE SPACE VEHICLES
PHASE I**

Report No. 884
Job Nos. 110782-9

11 December 1961

Submitted to:

George C. Marshall
Space Flight Center
Huntsville, Alabama

ILLINOIS

ACOUSTICAL CONSIDERATIONS IN THE PLANNING
AND OPERATION OF LAUNCHING AND STATIC
TEST FACILITIES FOR LARGE SPACE VEHICLES
PHASE I

FINAL REPORT
Contract NAS8-2403
BBN Job Nos. 110782-9

11 December 1961

Submitted to:
George C. Marshall
Space Flight Center
Huntsville, Alabama
Attn: Mr. O. L. Sparks, M-LOD-DL

BOLT BERANEK AND NEWMAN INC.
50 Moulton Street
Cambridge 38, Massachusetts

ACOUSTICAL CONSIDERATIONS IN THE PLANNING AND OPERATION OF LAUNCHING
AND STATIC TEST FACILITIES FOR LARGE SPACE VEHICLES PHASE ITable of ContentsPage

LIST OF FIGURES	v
1. SUMMARY	1
2. INTRODUCTION	2
3. THE ACOUSTICAL AND VIBRATION HAZARD PROBLEM	4
4. GENERAL CONCEPTS AND PROCEDURES FOR NOISE AND VIBRATION CONTROL	6
5. PLANNING IN DECIBELS AND OCTAVES	10
6. THE SOURCE	13
6.1 General	13
6.2 General Properties of the Noise Field of Rocket Engines	13
6.3 Rocket Engine Parameters and the Generation of Noise	16
6.4 Scaling Rocket Noise Data	19
6.5 Rocket Engine Parameters and the Generation of Vibrations	21
6.6 Empirical Estimates of the Near and Far Sound Fields of Large Rocket Engines	21
6.6.1 General	21
6.6.2 Near Sound Field in the Open	23
6.6.3 Far Sound Field in the Open	23

<u>Table of Contents (Continued)</u>	<u>Page</u>
6.6.4 Near Sound Field in Silo	24
6.7 Empirical Estimates of the Ground Vibration Fields of Large Rocket Engines	25
7. THE TRANSMISSION PATH	26
7.1 General	26
7.2 The Propagation of Sound through the Atmosphere . . .	27
7.2.1 The Inverse-Square Law	27
7.2.2 The Excess Attenuation	28
7.3 The Atmosphere at Representative Rocket Test and Launch Sites	34
7.3.1 Properties of the Atmosphere -- Cape Canaveral	38
7.3.2 Properties of the Atmosphere -- Site Off Cape Canaveral Shore	40
7.3.3 Properties of the Atmosphere -- Inland Site, Huntsville Area	41
7.3.4 Properties of the Atmosphere -- Point Arguello	43
7.4 Sound Attenuation by Obstacles and Barriers	45
7.5 Sound Attenuation by Structures and Enclosures . . .	46
7.6 Attenuation of Ground Vibrations	46

Table of Contents (Continued)Page

8. THE RECEIVER	48
8.1 Concept of Noise and Vibration Criteria	48
8.2 Criteria for Personnel	49
8.3 Criteria for Residential Communities	50
8.4 Criteria for Building Structures	51
8.5 Criteria for Electronic Instrumentation and other Control Equipment	53
8.6 Tentative Estimates of Noise and Vibration Criteria	54
8.6.1 Tentative Noise and Vibration Criteria for Personnel	54
8.6.2 Tentative Noise Criteria for Residential Communities	56
8.6.3 Tentative Criteria for Damage to Building Structures	56
8.6.4 Tentative Criteria for Failure of Electronic and Control Instrumentation	57
9. SUMMARY OF PROCEDURES FOR ESTIMATING SOUND PRESSURE LEVELS GENERATED BY LARGE ROCKET ENGINES, AND CORRESPONDING HAZARD RADII	58
9.1 General	58
9.2 Estimating Sound Pressure Levels Nearby	58
9.2.1 Estimating Sound Pressure Levels Along a Vehicle Launched or Statically Tested in the Open	59
9.2.2 Estimating Sound Pressure Levels Along a Vehicle Launched from a Silo	59

Table of Contents (Continued)Page

9.2.3	Estimating Sound Pressure Levels on the Ground During Static Testing or Before Lift-Off	60
9.2.4	Estimating Sound Pressure Levels on the Ground After Lift-Off	61
9.3	Estimating Sound Pressure Levels on the Ground at Remote Locations	62
9.3.1	Estimating Sound Pressure Levels During Static Testing or Before Lift-Off	62
9.3.2	Estimating Sound Pressure Levels After Lift-Off	64
9.4	Sound Pressure Levels as a Function of Time	67
9.5	Examples	67
9.6	Estimates of Acoustical Hazard Radii for Various Acoustical Criteria	72
10.	CONCLUSIONS	74
	Table of Contents for Appendix	x
	List of Figures for Appendix	xi

LIST OF FIGURES FOR TEXT

- Fig. 3-1 Typical Areas Affected by Sound and Vibrations from Launching of Large Space Vehicle.
- Fig. 3-2 Excitation and Response of Equipment Exposed to Sound and Vibrations.
- Fig. 3-3 Human Exposed to Sound and Vibrations.
-
- Fig. 6-1 Acoustic Directivity Pattern of Rocket in Flight.
- Fig. 6-2 Acoustic Directivity Pattern of Rocket with Bucket Deflector.
- Fig. 6-3 Sound Pressure Levels Near Tail Section of Space Vehicle-Static Test or Before Lift-Off.
- Fig. 6-4 Sound Pressure Levels Half-Way Along Length of Space Vehicle-Static Test or Before Lift-Off.
- Fig. 6-5 Sound Pressure Levels Near Nose of Space Vehicle-Static Test or Before Lift-Off.
- Fig. 6-6 Showing Positions for Estimating Sound Pressure Levels Near Vehicle Surface in the Open.
- Fig. 6-7 Sound Pressure Levels Before Lift-Off of Space Vehicle, 1000 Ft from Stand on the Ground (Wedge Deflector).
- Fig. 6-8 Showing Positions for Estimating Sound Pressure Levels Before Lift-Off, 1000 Ft from Stand.
- Fig. 6-9 Sound Pressure Levels During Static Testing of Space Vehicle, 1000 Ft from Stand on the Ground (Bucket Deflector).
- Fig. 6-10 Maximum Sound Pressure Levels After Lift-Off of Space Vehicle, 1000 Ft from Stand on the Ground.

LIST OF FIGURES (CONT)

- Fig. 6-11 Maximum Sound Pressure Levels During Launching from Unlined Blocked Silo. Observation Position Near Vehicle Tail.
- Fig. 6-12 Maximum Sound Pressure Levels During Launching from Unlined Blocked Silo. Observation Position Halfway Along Vehicle Length.
- Fig. 6-13 Maximum Sound Pressure Levels During Launching from Unlined Blocked Silo. Observation Position Near Vehicle Nose.
- Fig. 6-14 Maximum Sound Pressure Levels During Launching from Unlined Ducted Silo. Observation Position Near Vehicle Tail.
- Fig. 6-15 Maximum Sound Pressure Levels During Launching from Unlined Ducted Silo. Observation Position Halfway Along Vehicle Length.
- Fig. 6-16 Maximum Sound Pressure Levels During Launching from Unlined Ducted Silo. Observation Position Near Vehicle Nose.
- Fig. 7-1 Range of Values of Excess Attenuation Obtained from 20 Static Saturn Tests at MSFC in the Direction of Huntsville.
- Fig. 7-2 Estimated Dissipative Excess Attenuation in the Atmosphere.
- Fig. 7-3a Probability Distribution of Sound Velocity for Northern Sector in Winter at Cape Canaveral.
- Fig. 7-3b Probability Distribution of Sound Velocity for Northern Sector in Summer at Cape Canaveral.
- Fig. 7-4a Probability Distribution of Sound Velocity for Western Sector in Winter at Cape Canaveral.

LIST OF FIGURES (CONT)

- Fig. 7-4b Probability Distribution of Sound Velocity for Western Sector in Summer at Cape Canaveral.
- Fig. 7-5a Probability Distribution of Sound Velocity for Southern Sector in Winter at Cape Canaveral.
- Fig. 7-5b Probability Distribution of Sound Velocity for Southern Sector in Summer at Cape Canaveral.
- Fig. 7-6a Probability Distribution of Sound Velocity for Eastern Sector in Winter at Cape Canaveral.
- Fig. 7-6b Probability Distribution of Sound Velocity for Eastern Sector in Summer at Cape Canaveral.
- Fig. 7-7a Probability Distribution of Sound Velocity for Northern Sector in Winter in Huntsville Area.
- Fig. 7-7b Probability Distribution of Sound Velocity for Northern Sector in Summer in Huntsville Area.
- Fig. 7-8a Probability Distribution of Sound Velocity for Western Sector in Winter in Huntsville Area.
- Fig. 7-8b Probability Distribution of Sound Velocity for Western Sector in Summer in Huntsville Area.
- Fig. 7-9a Probability Distribution of Sound Velocity for Southern Sector in Winter in Huntsville Area.
- Fig. 7-9b Probability Distribution of Sound Velocity for Southern Sector in Summer in Huntsville Area.
- Fig. 7-10a Probability Distribution of Sound Velocity for Eastern Sector in Winter in Huntsville Area.
- Fig. 7-10b Probability Distribution of Sound Velocity for Eastern Sector in Summer in Huntsville Area.
- Fig. 7-11a Probability Distribution of Sound Velocity for Northern Sector in Winter at Point Arguello.

LIST OF FIGURES (CONT)

- Fig. 7-11b Probability Distribution of Sound Velocity for Northern Sector in Summer at Point Arguello.
- Fig. 7-12a Probability Distribution of Sound Velocity for Western Sector in Winter at Point Arguello.
- Fig. 7-12b Probability Distribution of Sound Velocity for Western Sector in Summer at Point Arguello.
- Fig. 7-13a Probability Distribution of Sound Velocity for Southern Sector in Winter at Point Arguello.
- Fig. 7-13b Probability Distribution of Sound Velocity for Southern Sector in Summer at Point Arguello.
- Fig. 7-14a Probability Distribution of Sound Velocity for Eastern Sector in Winter at Point Arguello.
- Fig. 7-14b Probability Distribution of Sound Velocity for Eastern Sector in Summer at Point Arguello.
- Fig. 7-15 Noise Reduction Afforded by Contemporary Space Capsules and Canisters.
- Fig. 7-16 Noise Reduction Afforded by Conventional Frame House Construction.
-
- Fig. 8-1 Tentative Damage Criteria Levels for Conventional Masonry Construction and for Glass.
- Fig. 8-2 Tentative Damage Criteria Levels for Conventional Wood Construction.
- Fig. 8-3 Tentative Failure Criteria Levels for Electronic and Control Instrumentation.

LIST OF FIGURES (CONT)

- Fig. 9-1 Maximum Sound Pressure Levels Halfway Along Length of Space Vehicle of 16×10^6 lbs Thrust Being Launched in the Open.
- Fig. 9-2 Maximum Sound Pressure Levels Due to Launching of Space Vehicle of 25×10^6 lbs Thrust 1000 Ft from Pad on the Ground.
- Fig. 9-3 Maximum Sound Pressure Levels at Cocoa Beach Due to Launching of Space Vehicle of 25×10^6 lbs Thrust.
- Fig. 9-4 Estimates of Maximum Sound Pressure Levels Due to Launching of Space Vehicle of about 25×10^6 lbs Thrust about 1000 Feet from Pad on the Ground.
- Fig. 9-5 Estimates of Maximum Sound Pressure Levels Due to Launching of Space Vehicle of about 25×10^6 lbs Thrust about 10 Miles from Pad on the Ground.
- Fig. 9-6 Comparison of Maximum Sound Pressure Levels Due to Launching of Space Vehicle of 25×10^6 lbs Thrust at Various Distances with Tentative Acoustical Criteria.

APPENDIX

<u>Table of Contents</u>	<u>Page</u>
LIST OF FIGURES	-xi-
A.1 Procedures Followed in Constructing Seasonal Probability Distributions of the Effective Velocity of Sound Propagation (Figures 7-3a through 7-14b in Text)	A-1
A.1.1 Cape Canaveral Area.	A-1
A.1.2 Huntsville Area.	A-4
A.1.3 Point Arguello	A-4
A.2 Selected Case Studies of the Vertical Profiles of the Effective Velocity of Sound Propagation for the Cape Canaveral Area, Huntsville Area and Point Arguello.	A-6
A.2.1 Case Studies for the Cape Canaveral Area	A-6
A.2.2 Case Studies for the Huntsville Area	A-10
A.2.3 Case Studies for Point Arguello.	A-13
A.3 Average Seasonal Profiles of Temperature and Absolute Humidity for Cape Canaveral, the Huntsville Area, and Point Arguello	A-17

LIST OF FIGURES FOR THE APPENDIX

- Fig. A-1a Individual Sound Velocity Profiles for Northern Sector in Winter at Cape Canaveral.
- Fig. A-1b Individual Sound Velocity Profiles for Northern Sector in Summer at Cape Canaveral.
- Fig. A-2a Individual Sound Velocity Profiles for Western Sector in Winter at Cape Canaveral.
- Fig. A-2b Individual Sound Velocity Profiles for Western Sector in Summer at Cape Canaveral.
- Fig. A-3a Individual Sound Velocity Profiles for Southern Sector in Winter at Cape Canaveral.
- Fig. A-3b Individual Sound Velocity Profiles for Southern Sector in Summer at Cape Canaveral.
- Fig. A-4a Individual Sound Velocity Profiles for Eastern Sector in Winter at Cape Canaveral.
- Fig. A-4b Individual Sound Velocity Profiles for Eastern Sector in Summer at Cape Canaveral.
- Fig. A-5a Individual Sound Velocity Profiles for Northern Sector in Winter in Huntsville Area.
- Fig. A-5b Individual Sound Velocity Profiles for Northern Sector in Summer in Huntsville Area.
- Fig. A-6a Individual Sound Velocity Profiles for Western Sector in Winter in Huntsville Area.
- Fig. A-6b Individual Sound Velocity Profiles for Western Sector in Summer in Huntsville Area.
- Fig. A-7a Individual Sound Velocity Profiles for Southern Sector in Winter in Huntsville Area.
- Fig. A-7b Individual Sound Velocity Profiles for Southern Sector in Summer in Huntsville Area.

LIST OF FIGURES FOR THE APPENDIX (CONT)

- Fig. A-8a Individual Sound Velocity Profiles for Eastern Sector in Winter in Huntsville Area.
- Fig. A-8b Individual Sound Velocity Profiles for Eastern Sector in Summer in Huntsville Area.
- Fig. A-9a Individual Sound Velocity Profiles for Northern Sector in Winter at Point Arguello.
- Fig. A-9b Individual Sound Velocity Profiles for Northern Sector in Summer at Point Arguello.
- Fig. A-10a Individual Sound Velocity Profiles for Western Sector in Winter at Point Arguello.
- Fig. A-10b Individual Sound Velocity Profiles for Western Sector in Summer at Point Arguello.
- Fig. A-11a Individual Sound Velocity Profiles for Southern Sector in Winter at Point Arguello.
- Fig. A-11b Individual Sound Velocity Profiles for Southern Sector in Summer at Point Arguello.
- Fig. A-12a Individual Sound Velocity Profiles for Eastern Sector in Winter at Point Arguello.
- Fig. A-12b Individual Sound Velocity Profiles for Eastern Sector in Summer at Point Arguello.
- Fig. A-13 Cape Canaveral - Avg. Seasonal Moisture Profiles.
- Fig. A-14 Cape Canaveral - Avg. Seasonal Temperature Profiles.
- Fig. A-15 Huntsville Area - Avg. Seasonal Moisture Profiles.
- Fig. A-16 Huntsville Area - Avg. Seasonal Temperature Profiles.
- Fig. A-17 Point Arguello - Avg. Seasonal Moisture Profiles.
- Fig. A-18 Point Arguello - Avg. Seasonal Temperature Profiles.

ACOUSTICAL CONSIDERATIONS IN THE PLANNING AND OPERATION OF
LAUNCHING AND STATIC TEST FACILITIES FOR LARGE SPACE VEHICLES
PHASE I

1. SUMMARY

In the planning of launching and static test facilities for space vehicles propelled by large rocket boosters consideration must be given to the many hazards involved. These hazards are important because substantial amounts of propellants, fired at substantial rates, are necessary to power the multi-stage rockets with the requisite multi-million-pound thrusts.

Hazards can be broadly classified into operational and malfunctional. The most important hazard of the first class is due to the large sound and vibration fields which occur every time a vehicle is launched or statically tested. This report analyzes this hazard and its consequences on the planning and designing of launch and static test facilities on the basis of existing knowledge. Preliminary design criteria for such facilities are formulated.

Recommendations are made for future work to close the gaps of existing knowledge in order that more definitive design criteria can be evolved.

2. INTRODUCTION

With the recent emphasis on an expanded United States space program the many hazards, operational as well as malfunctional, attendant to the launching and static testing of space vehicles propelled by large rocket engines have come in for increased attention. Among the many types of hazards, such as nuclear, toxic, blast, seismic, lightning etc., the effects of the large sound and vibration fields generated every time the engines are fired stand out as the most important operational hazard to be considered. Indeed, this study is solely concerned with the sound and vibration fields generated by the rocket engines both on the pad and in flight, and with the effects of those fields on

- a) Launching and static test site selection
- b) Planning, design and performance of launch and static test equipment
- c) Buildings and other structures on and off base
- d) Personnel on and off base

Given the importance of the acoustical hazard, it is clear that the Launching Operations Directorate (LOD) at George C. Marshall Space Flight Center has an urgent need for a comprehensive planning guide for the design of launching and static test facilities from the acoustical point of view. This guide must be detailed and specific to meet the present planning needs of LOD, yet at the same time general enough to cover future needs of NASA's expanded space operations, such as the consideration of off-shore launching sites.

A joint Air Force-NASA Hazards Board was convened in 1961. This Board has collected in a report* available data concerning the acoustical, explosion, fire and other hazards expected from the launching of very large space vehicles in the Cape Canaveral area. This report was prepared primarily to aid in a decision whether or not, from the hazards point of view, the Cape Canaveral site can be used for the launching of proposed space vehicles of thrusts one order of magnitude larger than that of Saturn. Within this narrow framework and under considerable pressure of time, the above Hazards Board Report was prepared, leaving a multitude of questions of interest to LOD unanswered. To answer these questions to the full extent of the needs of LOD and to undertake the necessary research to do so, the present study is carried out.

It was agreed in conference between representatives of LOD and Bolt Beranek and Newman Inc. (BBN) to conduct the present study and research program in two phases. The first phase consists of a general study of the problem and the formulation of as much design information as can be based on information available at present, or extrapolated therefrom. In the second phase an attempt is to be made to fill in the gaps of knowledge exposed by the first phase of the study and to prepare a more definitive planning guide for launching and static testing facilities for large space vehicles from the acoustical point of view for use by LOD.

This report constitutes the final report under Phase I of the above program.

* Joint Air Force -- NASA Hazards Analysis Board, "Safety and Design Considerations for Static Test and Launch of Large Space Vehicles," 1 June 1961 and Supplement, 29 June 1961.

3. THE ACOUSTICAL AND VIBRATION HAZARD PROBLEM

To obtain a general qualitative view of the effect of the sound and vibration fields generated by the firing of rocket-propelled space vehicles consider Fig. 3-1 showing a schematic launch facility. There are also shown schematically some typical important structures subject to excitation by the sound and vibration fields. Before lift-off, a typical building structure in the vicinity of the launch stand will be excited by the airborne sound acting on the parts of the structure above ground. A part of this energy will be transmitted into the interior via louvers or other openings in the walls, including cable ducts, pipe chases etc., and by re-radiation from the vibrating walls. Unless the structure is designed specifically to provide good acoustical isolation, a sound field of appreciable magnitude will exist in the building interior.

Ground-borne vibrations, generated by the exhaust stream of the rocket engines impinging on the deflector, are transmitted structurally from the launch stand to the parts of the building below ground, thereby exciting the rest of the building into vibrations also. Equipment and machinery located inside the structure will be affected by both types of excitation. This is schematically shown in Fig. 3-2.

The same would be true, in principle, for nearby personnel (see Fig. 3-3), although safety regulations usually prohibit the presence of personnel too close to the launch pad area. It is expected that in areas where personnel are present during launch operations, such as in the launch control center or "blockhouse," the ground-borne

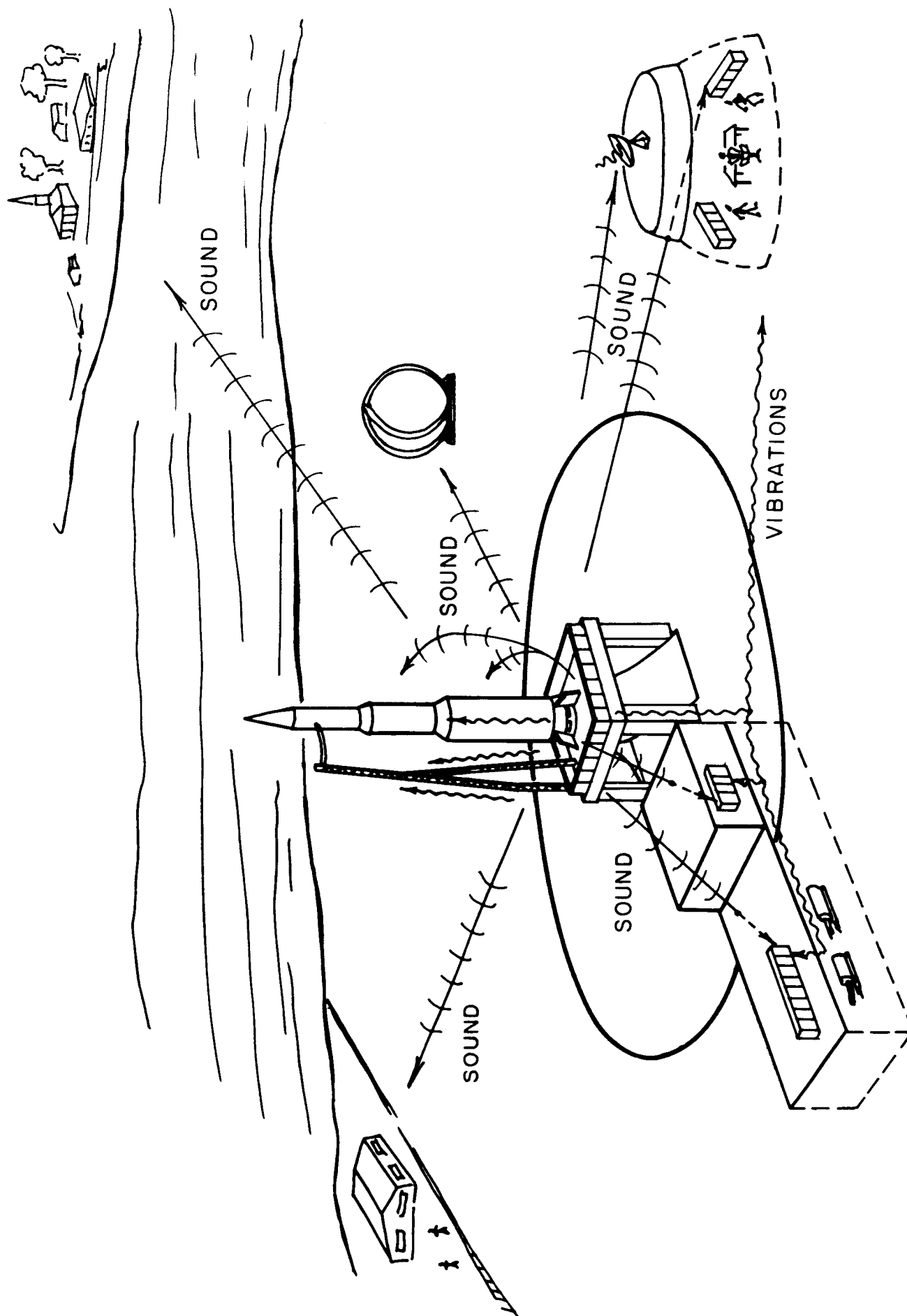


FIG.3-1 TYPICAL AREAS AFFECTED BY SOUND AND VIBRATIONS FROM LAUNCHING OF LARGE SPACE VEHICLE

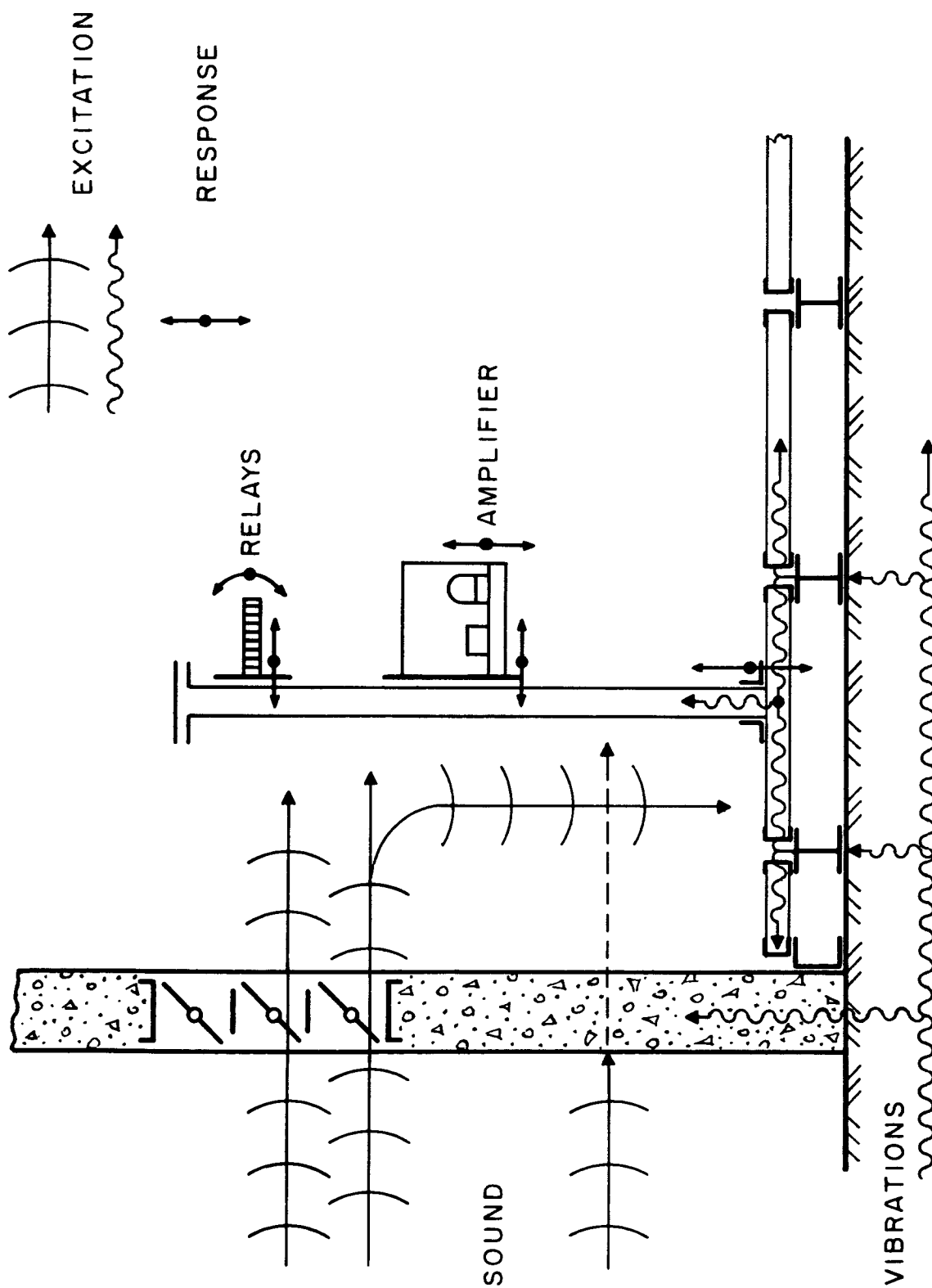


FIG. 3-2 EXCITATION AND RESPONSE OF EQUIPMENT EXPOSED TO SOUND AND VIBRATIONS

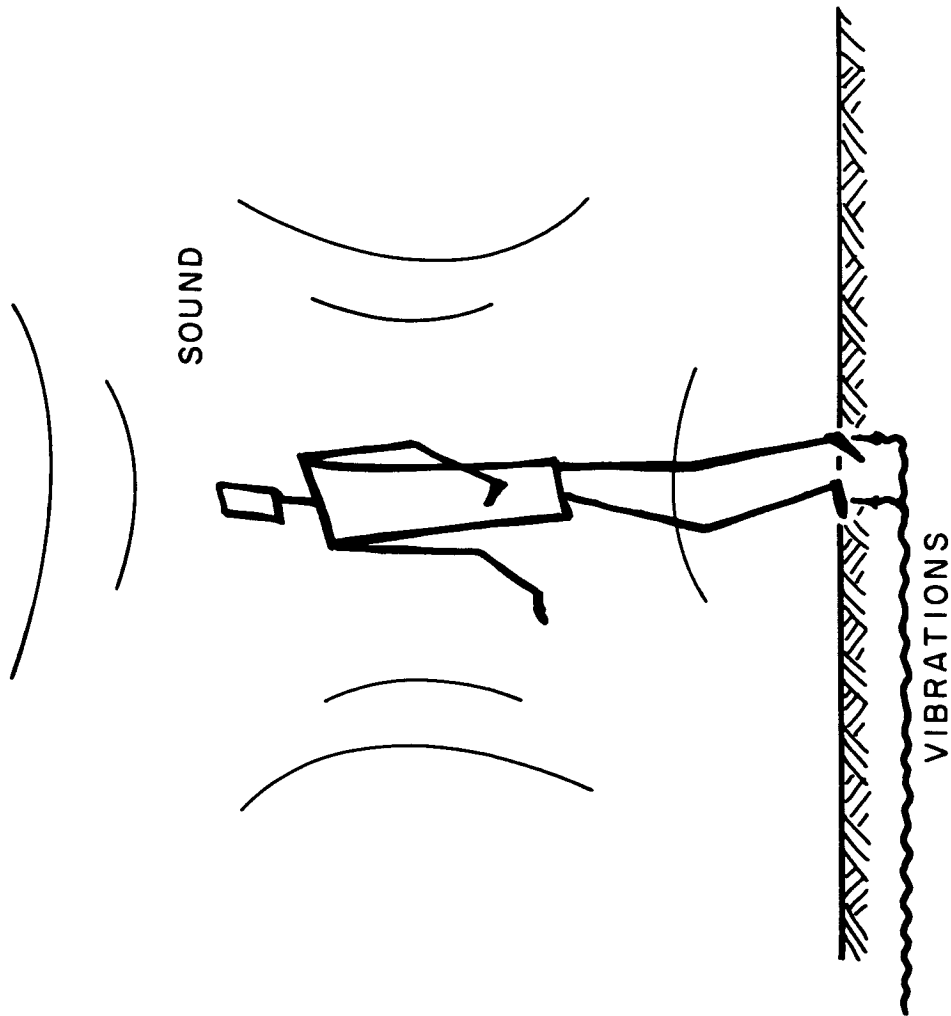


FIG. 3-3 HUMAN EXPOSED TO SOUND AND VIBRATIONS

vibrations have decayed to a level where the significant excitation takes place by airborne sound alone. This is also true for the on-base areas outside the launch complex and off-base communities within range of the rocket noise. Of course, for the vehicle itself and its payload, which may contain personnel for manned space flights, both types of excitation must be considered.

At lift-off the path of structural vibrations between the vehicle and the launch stand and other structures on the ground is broken. Vibration excitation of the vehicle and its payload continues, but in a different manner, since the tail section is now free. Likewise, acoustical excitation of the vehicle structure continues, at somewhat diminished levels, as the rocket exhaust stream begins to clear the launch deflector. Acoustical excitation continues to decrease with increasing forward speed. The acoustical excitation is nil in supersonic flight but excitation by boundary-layer noise becomes important.

Static testing conditions are akin in principle to hold-down conditions before lift-off.

4. GENERAL CONCEPTS AND PROCEDURES FOR NOISE AND VIBRATION CONTROL

It is evident from the qualitative picture given in the preceding section that the acoustic and vibration fields of space vehicles present a far from simple situation and that the design of launching and static test facilities from the acoustical and vibration point of view is an undertaking of some complexity. It shares this characteristic with most practical acoustical design problems. Nonetheless, an effective approach is possible by analyzing the problem in terms of the three basic concepts, common to any noise and vibration problem:

- a) The source of sound and vibrations, and its radiation characteristics
- b) The transmission path, and its attenuation characteristics
- c) The receiver, and its (his) response characteristics

It should be pointed out, in passing, that the words source, transmission path, receiver, etc. are used in the most general sense possible.

The general procedure for arriving at a design satisfactory from the noise control point of view is as follows:

From a knowledge of the source levels and the characteristics of the transmission path between source and receiver the excitation at the receiver is calculated, estimated, or obtained by direct measurement. This procedure is repeated for as many sources and transmission paths as are important. Then, from an analysis

of the response characteristics of the receiver, suitable criteria, i.e., levels not to be exceeded, are calculated, estimated, or obtained by direct measurement. To be more specific, the criteria levels may be in terms of vibration acceleration not to be exceeded for a critical relay exposed to the noise and vibration fields to insure reliable operation during launch. Or, the criterion may be given in terms of the sound pressure levels not to be exceeded at a person's ear to avoid permanent impairment of hearing. Or, the criterion may be given in terms of the sound pressure levels not to be exceeded in a nearby residential community, if an adverse response to the intruding noise is to be avoided. Or, the maximum sound pressure levels and ground vibration levels are specified that a given building construction can support without damage. A comparison between the criteria levels and the actual levels of excitation, in each frequency band, yields the noise or vibration reduction required. The greater this difference, the greater the severity of the problem.

It seems clear that, in the case of multiple excitation by several sources and several transmission paths, reduction of the lesser contributions is of little avail unless the level of the major excitation has been approximately reduced to that of the others. ("Balanced design for noise or vibration control"). If the criteria call for still further reduction of excitation, all sources and transmission paths must be considered.

What are some of the measures available to achieve noise and vibration reduction?

Noise reduction at the source is costly and difficult to achieve here because a muffler must not only be effective at the low frequencies but must also accommodate the high-temperature, high-velocity exhaust gases of the rocket. Moreover, effective noise reduction after lift-off is not feasible at the present state of the art.

The criteria levels at the receiver can sometimes be raised by "beefing-up" of equipment or building construction, by providing ear protection for personnel, or in certain cases, by increasing the human tolerance to annoying or frightening noise intrusion by a careful public relations effort.

But the bulk of the necessary noise and vibration reduction must come from modification of the transmission path. Noise reduction is achieved in the planning stage of a facility by interposing larger distances between source and receiver, or by buying up land in an existing situation. Barriers and heavy building construction protect critical equipment and personnel from the effects of the noise, and resilient vibration mounts effectively break the structure-borne vibration path from source to critical equipment.

These are some of the general steps available for noise and vibration reduction. A successful solution of the noise and vibration problem in any given case must be based on a detailed and thorough consideration of the physics governing the process of noise and vibration generation, transmission and reception.

Noise and vibration control measures, in order to be most effective, must be considered in the planning stage of a facility. Remedial noise control measures carried out afterwards are often far less effective and almost always more costly. And, two or more engineering solutions to a given noise or vibration control problem must often be worked out to permit critical comparison on the basis of cost, timing or other related factors.

As will be apparent from the data presented in this report, the noise reduction required is frequently greatest at the low frequencies, where it generally is most difficult to achieve. Effective noise reduction at the low audible and sub-audible frequencies is a field requiring further study in many cases. The discussion of specific noise control measures is beyond the scope of this report, but will be fully covered in Phase II of this study.

5. PLANNING IN DECIBELS AND OCTAVES

In accordance with the basic approach just outlined the main body of this report will be devoted to a detailed discussion of the characteristics of the noise and vibration generated by large rocket engines, of the transmission of this noise and vibration through the atmosphere and through the ground and other structures, and, finally, of the receiver characteristics. In each case, engineering estimates of the relevant parameters based on present knowledge will be given. Since the report is primarily intended for use in the planning of launching and static testing facilities a few general remarks concerning the required accuracy of the engineering estimates and the data supporting them are in order.

Parameters of sound and vibration fields, such as sound pressure level, acceleration level, sound power level, etc. are commonly expressed on a logarithmic (decibel) scale. There are two main reasons for this preference. First, the magnitude of the variables mentioned above (and other related ones) must frequently be considered over a range of many orders of magnitude. Second, many receiver criteria, especially those having to do with human response can best be expressed on a logarithmic rather than a linear scale. Bearing in mind that even carefully performed accoustical measurements in the field have a typical data scatter of ± 10 to 20% on a linear amplitude scale, or approximately ± 20 to 40% on a linear intensity (amplitude squared) scale, engine operating parameters, distances, receiver response criteria etc. need to be known or estimated only within the above accuracies. Furthermore, the response functions of the receivers and the resulting criteria have even greater tolerances. This simplifies the planner's task enormously. For example, in the case of estimating the noise fields of rocket

engines, it is entirely permissible, as a first approximation, to ignore the influence of a particular fuel-oxidizer combination on the specific impulse, or the influence of ambient atmospheric pressure on engine thrust, or the detailed nozzle configuration of a rocket engine of a given thrust. Likewise, the surface weight of a wall structure which determines, among other things, its sound isolation properties, need be known only approximately for preliminary estimates. Naturally, especially in critical cases, these engineering estimates should be supplemented by more accurate calculations or by measurements.

However, the importance of the frequency composition of the sound and vibrations must be stressed. Since the noise and vibrations generated by rocket engines encompass a wide frequency spectrum and since source levels, transmission path properties and receiver response vary with frequency, overall levels of sound pressure or vibration acceleration have little practical meaning.

This dependence on frequency is accounted for in practice by specifying the relevant acoustical quantities in frequency bands one octave wide over the entire frequency range of interest. Although vibration data are frequently specified in finer frequency intervals, such as bands one-third octave wide, the degree of frequency resolution provided by octave bands appears adequate at the moment for planning purposes for both acoustical and vibration data.

Finally, a few words about the decibel scale. The decibel scale is basically a logarithmic scale of dimensionless ratios, i.e., ratios of like quantities. A ratio R of quantities like power or intensity is expressed in decibels by $10 \log_{10} R$ and the decibel scale is thereby defined. Thus, for example, a value of the ratio $R = 2$ corresponds very nearly to 3 decibels ($\log_{10} 2 = 0.3010$).

The decibel definition has been extended to ratios r of quantities like sound pressure, particle velocity, acceleration, voltage or current by assuming that $R = r^2$. This assumption is equivalent to saying that sound intensity, for example, is proportional to sound pressure squared. A doubling of sound pressure corresponds therefore to a four-fold increase in sound intensity. For the quantities listed above (and other similar ones) the decibel scale is defined by $10 \log_{10} R = 10 \log_{10} r^2 = 20 \log_{10} r$. Thus, for example, a value of the ratio $r = 2$ corresponds very nearly to 6 decibels.

In acoustics, the sound pressure p is the quantity most frequently specified and always measured. The corresponding sound pressure level in decibels is defined as $20 \log_{10} p/p_0$, where p is the root-mean-square sound pressure in microbars, and p_0 is the standard reference sound pressure, equal to 0.0002 microbar. Hence, a sound pressure level of 80 decibels re 0.0002 microbar corresponds to a sound pressure of $p = 2$ microbars.

6. THE SOURCE

6.1 General

For the purpose of this study the source of sound and vibration is a vehicle propelled by a multi-stage rocket with a booster in the multi-million pound thrust class. While the booster is, of course, of primary concern here, the noise generated after booster cut-off by the upper stages can be evaluated also, if desired. Before going into the details of estimating noise levels from engine parameters, the characteristics of the noise field of rocket engines will be discussed.

6.2 General Properties of the Noise Field of Rocket Engines

Several of the general properties of rocket noise fields will now be described. Although in many cases this description is at best semi-quantitative, owing to the limited amount of data now available, the description will be adequate to lead to some important scaling relations for rocket noise fields. These scaling relations will then form the basis for the estimation procedures given later in this report.

The noise field about a sound source radiating into open space can be conveniently divided into two major regions, the near field and the far field. In the far field, in the absence of strong perturbations such as may be caused by meteorological effects (see Chapter 7), the sound pressure decreases with distance from the source in a more or less uniform and predictable manner. The near field is considerably more complicated, and empirical procedures must be utilized to obtain estimates of the sound pressure levels. For the multi-million pound thrust

boosters under consideration here, far-field conditions will generally obtain at distances from the rocket engine exceeding 500 to 1,000 ft.

Most of the noise produced by rocket engines is associated with the turbulence occurring in the exhaust stream. The principal noise sources appear to be located in the turbulent interface between the exhaust and the surrounding atmosphere, particularly in the region where the exhaust flow velocity first becomes subsonic. A wide range of turbulence eddy sizes is characteristic for these conditions and consequently the noise field will be composed of components encompassing a wide range of frequencies. Also, since the effective noise sources are intimately associated with the turbulence in the exhaust stream of a rocket engine, it may be expected that the high-frequency noise sources will tend to be located where the smaller turbulent eddies exist, i.e. further upstream, as compared to the regions further downstream where the larger eddies (and low-frequency noise sources) exist. Use of an exhaust deflector will affect the exhaust flow pattern and thus the manner in which the flow becomes subsonic and it may be expected that the rocket noise field will depend somewhat on the type and location of the exhaust deflector. Experimental evidence is in line with these general descriptions.

It should be noted that the far noise field of rocket engines exhibits a characteristic directivity of radiation. Experiments have shown that maximum radiation takes place along angles of 40-70 degrees measured from the exhaust stream. This generally holds true independent of frequency and independent of whether the exhaust stream has been deflected, as in static

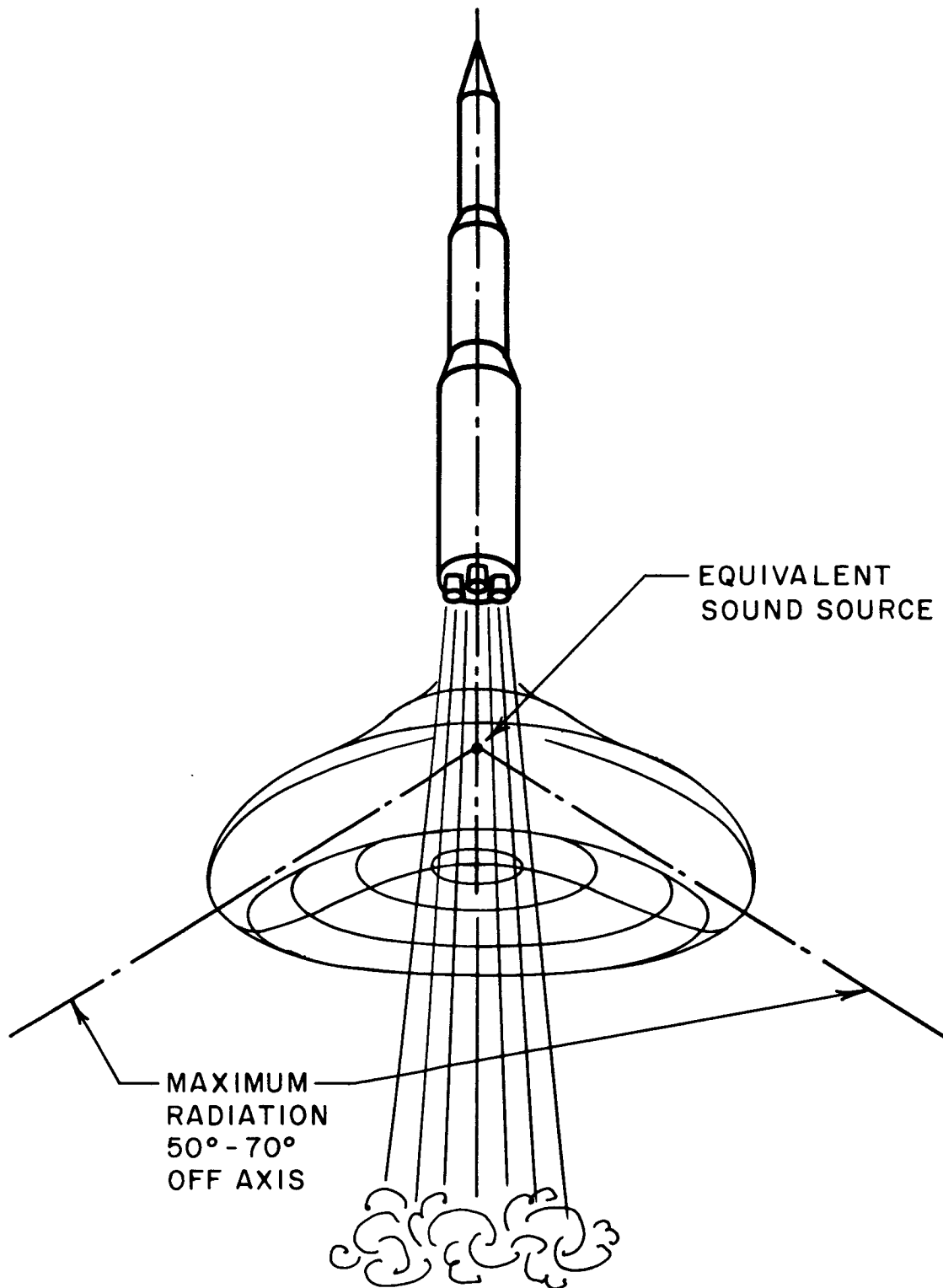


FIG. 6-1 ACOUSTIC DIRECTIVITY PATTERN
OF ROCKET IN FLIGHT

testing or on the launch pad, or whether the exhaust stream is straight as in flight. This directivity pattern is illustrated in Fig. 6-1 in polar form, where the length of the radius vector from the equivalent (point) sound source to the directivity surface gives an indication of the relative magnitude of the sound pressure level in that direction relative to the sound pressure level in some other direction. Fig. 6-2 shows the directivity pattern of a rocket engine with a bucket flame deflector. If a two-sided wedge flame deflector is used, as for launchings, the resultant directivity pattern is approximated by appropriate superposition of two patterns similar to that shown in Fig. 6-2. In this case directional radiation is less pronounced.

It should be noted that directivity patterns are meant to be used only for estimating sound pressure levels in the far field.

Although present-day liquid fuel engines vary markedly from solid fuel engines in their design and operation, both types of engines produce exhaust streams of high-velocity hot gases. Because the sound sources are primarily associated with the exhaust flow, it is expected that the noise field of the two types of engines will not be markedly different, and the limited data now available indicate that this is the case. Of course, exception must be made for non-turbulent noise sources that are particular to any engine design, such as resonant burning in a solid fuel engine or fuel line oscillations in a liquid fuel engine. In general these non-turbulent noise sources have been found to be insignificant compared with the usual turbulence noise and consequently will not be considered in the material in this report.

6.3 Rocket Engine Parameters and the Generation of Noise

In order to estimate the noise levels at particular positions on the ground or on the vehicle surface itself one must first obtain some measure of the total noise generated by the booster rocket engines. The total sound power radiated by a rocket engine has been found to range between approximately 0.1% and 1% of the mechanical power in the rocket exhaust stream. The exact value of this "conversion factor" from mechanical to acoustic power depends, among other things, on the thrust and also on details of the exhaust stream deflector. During static tests of Saturn and Jupiter rockets it was found that about 1/2% of the total stream power was converted into sound. The conversion efficiency of a large rocket engine in flight is believed to be larger (approximately 1%).

The mechanical stream power is proportional to the product of the total thrust F times the expanded exhaust velocity. This latter quantity, in turn, is proportional to I , the specific impulse. It should be noted that, for the solid and liquid fuel-oxidizer combinations currently in use, the value of the specific impulse and thus of the expanded exhaust velocity is approximately constant. A range of variation of $\pm 30\%$ corresponds to a variation in stream power of only about ± 1.5 db. Such variations are smaller than the accuracy of the acoustical data now available. For our present purpose of obtaining engineering estimates, we will therefore assume that the exhaust velocity and the conversion factor is constant for all rocket systems to be considered.*

* In this study, a conversion factor of 1/2% on the stand and of 1% in flight have been assumed as representative of large rocket boosters. Also, $I \doteq 275$ sec and hence an expanded exhaust velocity of 8500 ft/sec were assumed as representative. Corrections to the estimates for grossly different I can be made, if ever needed, by the quantity $10 \log_{10}(I/275)$.

Under this assumption the total sound power radiated is proportional to the total thrust of the rocket engine(s). However, by making use of proper scaling procedures (see section 6.4 below) it is not necessary to calculate the sound power explicitly in this study.

For those who wish to do so, the total sound power level PWL, in db re 10^{-13} Watt*, of a rocket engine of total thrust F lbs, on the stand, can be estimated as follows:

$$\text{PWL} = 10 \log_{10} F + 145, \text{ db re } 10^{-13} \text{ W} \quad (\text{Eq. 6-1})$$

It should be emphasized that this sound power level PWL does not itself represent a value of sound pressure level measured at any particular position. PWL is merely a quantity that can be conveniently obtained directly from the engine operating parameters, giving a direct measure of the total noise produced by the booster. In the succeeding sections procedures will be given for estimating the sound pressure levels at various positions on the ground or on the vehicle surface without the explicit use of PWL.

As was already noted, the jet of the rocket engine generates a sound field whose spectrum encompasses a wide range of frequencies. This is so because a large range of turbulence eddy sizes is characteristic of the turbulent mixing of the exhaust stream with the surrounding air. The maximum noise levels occur at a frequency which is related to the nozzle diameter and expanded jet velocity.

* E.g., L. L. Beranek, Acoustics, Chapter 1, McGraw-Hill Book Co., New York, N. Y., (1954).

In fact, frequency analyses of rocket noise obtained from single-nozzle engines indicate that the noise spectra, measured at similar positions, can be presented in a generalized fashion when a non-dimensional frequency parameter is utilized. This parameter is the so-called Strouhal frequency, defined by frequency times a characteristic dimension of the system (such as engine nozzle diameter) and divided by a characteristic velocity (expanded exhaust velocity). By making use again of the assumption that the characteristic velocity of all rocket systems under consideration remains approximately constant, the frequency parameter is reduced to "frequency times nozzle diameter."

Before considering the question of how to treat multiple nozzle configurations, it should be observed that the fuel-oxidizer mixtures used currently in rocket engines burning liquid or solid fuel are such that the density of the rocket exhaust gases is approximately constant. Then the total thrust of the system is proportional to the total nozzle exit area. This area can be expressed in terms of an effective nozzle diameter

$$D_{\text{eff}} = n^{1/2} D_{\text{noz}} \quad (\text{Eq. 6-2})$$

where D_{noz} is the diameter of a single nozzle in a multiple-nozzle configuration of n equal nozzles.

Thus, the generalized frequency parameter becomes "frequency times (thrust)^{1/2}" for contemporary rocket engines.* The sound pressure

* By a contemporary rocket engine is meant an engine (not necessarily in existence now) that utilizes current fuel-oxidizer mixtures and has an exhaust velocity of contemporary value (see footnote, p. 16).

level estimates presented later in this Chapter will be plotted, for convenience, in terms of both frequency parameter scales.

Summarizing, it is seen that for any liquid or solid fuel rocket engine the total noise power generated can be estimated from the total thrust. The spectral distribution of the rocket noise at various locations can be estimated from the effective nozzle diameter, or, for currently used fuel-oxidizer combinations, directly from the thrust.

6.4 Scaling Rocket Noise Data

While appropriate generalized frequency scales were developed in the preceding section for maximum utility of data presentation, it remains to consider certain geometrical relationships pertinent to similar sound fields.

It can be shown (see also Chapter 7) that in open spaces the sound pressure levels measured at a fixed distance from the stand increase 3 decibels (the sound pressure itself increases by a factor of $\sqrt{2}$) for each doubling of the thrust or total sound power generated. The sound pressure levels measured at geometrically similar distances, however, remain essentially constant. This is so because, as the thrust of a vehicle is doubled, D_{eff} increases by a factor of $\sqrt{2}$, as do approximately the total vehicle length L and booster diameter because rocket vehicles tend to be geometrically similar ($L/D_{\text{eff}} \doteq \text{const.}$). But a geometrically similar position in open space will be farther away by the same factor, namely $\sqrt{2}$, keeping the sound pressure level constant at the point of observation.

It follows from the above that the "control" area around a launch pad or test stand, i.e., the area within which the sound pressure levels exceed a given fixed criterion level, increases at least in proportion to the thrust. Since some criteria levels (e.g., building damage criteria, see Chapter 8) decrease with decreasing frequency the control area must then be increased in proportion to the square of the thrust to obtain equivalent conditions. Clearly these facts have far-reaching consequences for the facility planner.

When noise levels are measured in a launching silo, it appears that the area of the opening between the vehicle and the silo wall affects the noise levels. The sound pressure levels have been found to (de)increase by 3 db as the open annular area between vehicle and silo is (in)decreased by a factor of 2.

On the basis of these observations, it is now possible to state the following rules for scaling noise data obtained from all types of rocket engines using geometrically similar deflector configurations:

1. For rocket engine noise measured in open spaces at a fixed distance from the engines, the mean-square sound pressure* is proportional to the total thrust.
2. For rocket engine noise measured in open spaces at geometrically similar positions, the mean-square sound pressure is constant, independent of thrust.
3. For rocket engine noise measured in a silo at geometrically similar positions, the mean-square sound pressure is directly proportional to the total rocket thrust and inversely proportional to the open annular area between the vehicle and the silo.

* The sound pressure level in db re $p_0 = 0.0002$ microbar, corresponding to the mean-square sound pressure \bar{p}^2 is given by
$$SPL = 10 \log_{10} \bar{p}^2 / p_0^2.$$

4. All frequency spectra can be presented as functions of the parameter "frequency times D_{eff} ", or of the parameter "frequency times (thrust)^{1/2}" for "contemporary" engines.

6.5 Rocket Engine Parameters and the Generation of Vibrations

Unfortunately, it is not possible at the present state of the art to calculate the vibration fields of a rocket engine with anything approaching the generality of the calculations of the sound field. This is to a large extent due to the fact that the medium through which the vibrations propagate from the source is, unlike the air, a complicated structure with many resonant modes. Until it is possible to generalize, the approach to the vibration source problem must proceed along empirical lines, relying for engineering estimates on experimental results.

6.6 Empirical Estimates of the Near and Far Sound Fields of Large Rocket Engines

6.6.1 General

In this section a number of generalized plots are presented which enable the planner to estimate the sound pressure levels in the near field of large space vehicles propelled by boosters burning liquid or solid fuels for a number of typical conditions and positions.

Graphs are also presented for the estimation of the far sound field at positions on the ground. A reference distance of 1000 ft was chosen for these far-field positions, for convenience.

In the succeeding Chapter procedures will be given to enable the planner to estimate the sound pressure levels at larger distances, taking into account the properties of the atmosphere insofar as the propagation of sound through it are concerned.

The plots given in this section were prepared from data obtained during static tests of Jupiter and Saturn at MSFC, Huntsville, and from silo data obtained on Minuteman and Titan. Before using this material the reader is cautioned to bear in mind the uncertainty of the measurements on which the graphs are based. An indication of this is the "shaded band" mode of presentation. Estimating, for example, noise levels for a vehicle of the Nova class from these data entails not only extrapolation in thrust but, in addition, extrapolation to very much lower frequencies, lower even than those contained in the current measurements on Saturn. The need for additional measurements on larger engines is therefore self-evident and urgent. Special caution must be used in extrapolating from the silo data which were obtained on vehicles of thrusts one order of magnitude below Saturn.

The graphs in this section are presented in terms of the generalized frequency parameter $f \times D_{\text{eff}}$, where f is the center (geometric mean) frequency of the octave band in question, in cps, and D_{eff} is the effective nozzle diameter of the rocket engine system, in inches, as given by Eq. (6-2). For contemporary* rocket engines burning liquid or solid fuel a second scale is given, for convenience, in terms of the generalized frequency parameter $f \times F^{1/2}$, where f is the

* See footnote on p. 18.

center frequency of the octave band in question, in cps, and F is the total thrust, in lbs, of the rocket engine system.

6.6.2 Near Sound Field in the Open

Figures 6-3 through 6-5 show the octave band sound pressure levels, in db re 0.0002 microbar, to be expected in the open at three positions along a space vehicle on the test stand or prior to lift-off. These positions are near the vehicle surface and are described by a coordinate x along the vehicle axis namely,

$x/L \doteq 0$, near the nozzle plane

$x/L \doteq 1/2$, half-way up the vehicle

$x/L \doteq 1$, near the nose (payload) of the vehicle

See also Figure 6.6 for geometry.

6.6.3 Far Sound Field in the Open

In this section, data for estimating the far-field sound pressure levels at a fixed distance of 1000 ft are given. In the figures used for estimation, the ordinate is given in terms of octave band sound pressure levels in db re 0.0002 microbar, minus $10 \log_{10}[F \times 10^{-7}]$, where F is the total thrust in pounds.

Figure 6-7 is a plot which applies to full thrust conditions at launch before lift-off, assuming the use of a wedge deflector. The figure includes the expected range of azimuth dependence. The geometry relevant to Fig. 6-7 is shown in Fig. 6-8; after substituting a bucket deflector, this figure applies to static tests also.

Figure 6-9 allows the planner to estimate the sound pressure levels at 1000 ft on the ground for various azimuths during static testing when a bucket deflector is used.

Figure 6-10 allows the planner to estimate the maximum sound pressure levels on the ground after lift-off, 1000 feet away from the pad. The graph shows estimates of the maximum levels that occur in each band during launching. Because the maximum in one frequency band may not occur at the same time that the maximum occurs in another band, the graph does not necessarily give the levels at any one particular time. Note that the levels here are independent of azimuth because the rocket exhaust stream is now vertical. Doppler shift and effect of forward vehicle motion have been neglected here because these effects appear to be small. Note that the effective duration of the noise at 1000 ft is of the order of tens of seconds before tapering off.

6.6.4 Near Sound Field in Silo

For completeness several design curves are given relating to the maximum sound pressure levels along a space vehicle launched from a silo. The ordinates in all figures giving silo data are given in terms of the maximum octave band sound pressure levels in db re 0.0002

microbar minus $10 \log_{10} \left[\frac{F \times 10^{-7}}{S_a} \right]$, where F is the total thrust in

pounds and S_a is the open annular area between silo and vehicle, in square feet. The figures give estimates of the maximum levels that occur in each band during launching. Because the maximum in one frequency band may not occur at the same time that the maximum occurs in another band, the curves do not necessarily give the levels at any one particular time.

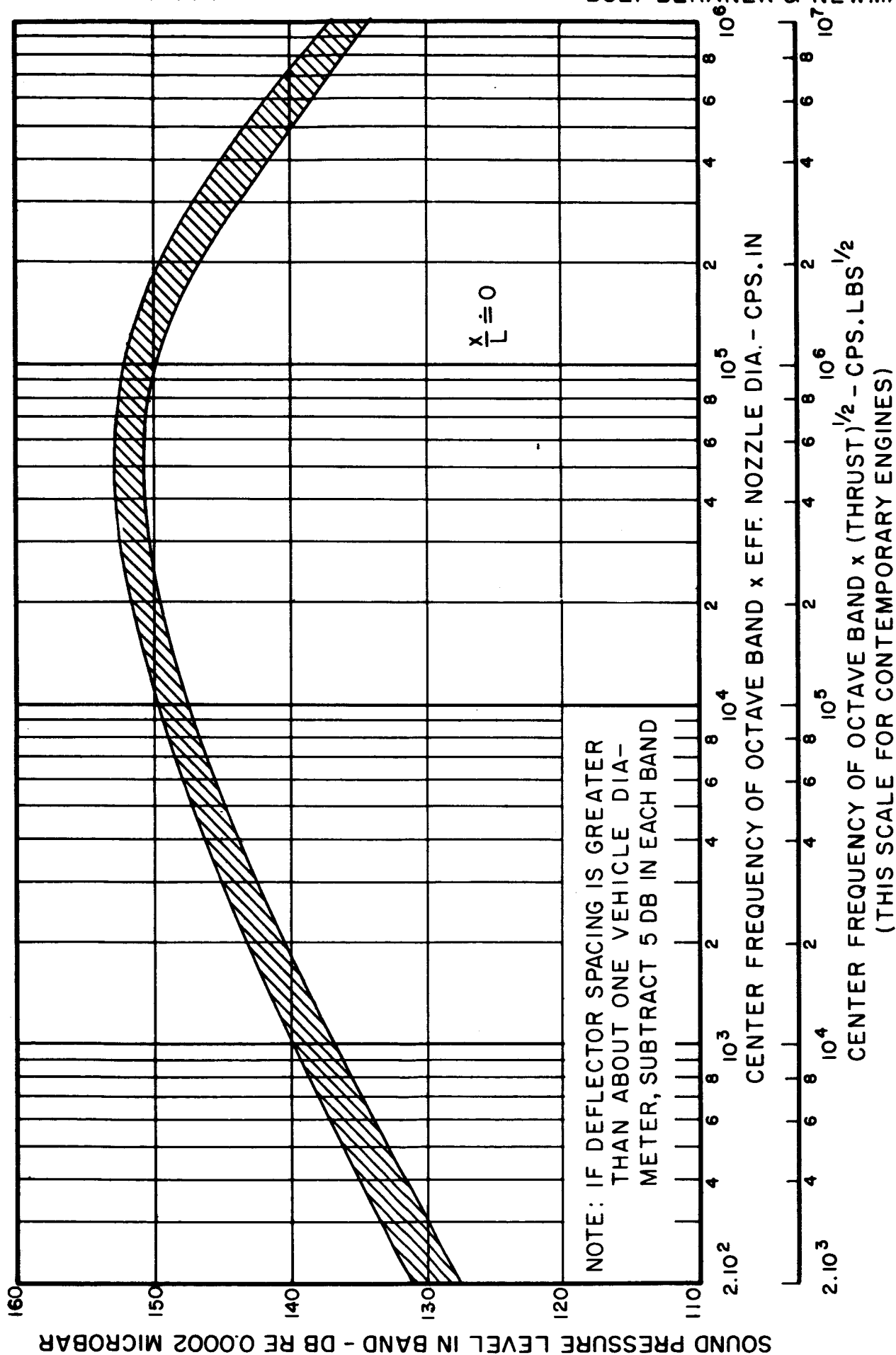


FIG. 6-3 SOUND PRESSURE LEVELS NEAR TAIL SECTION OF SPACE VEHICLE-
STATIC TEST OR BEFORE LIFT-OFF

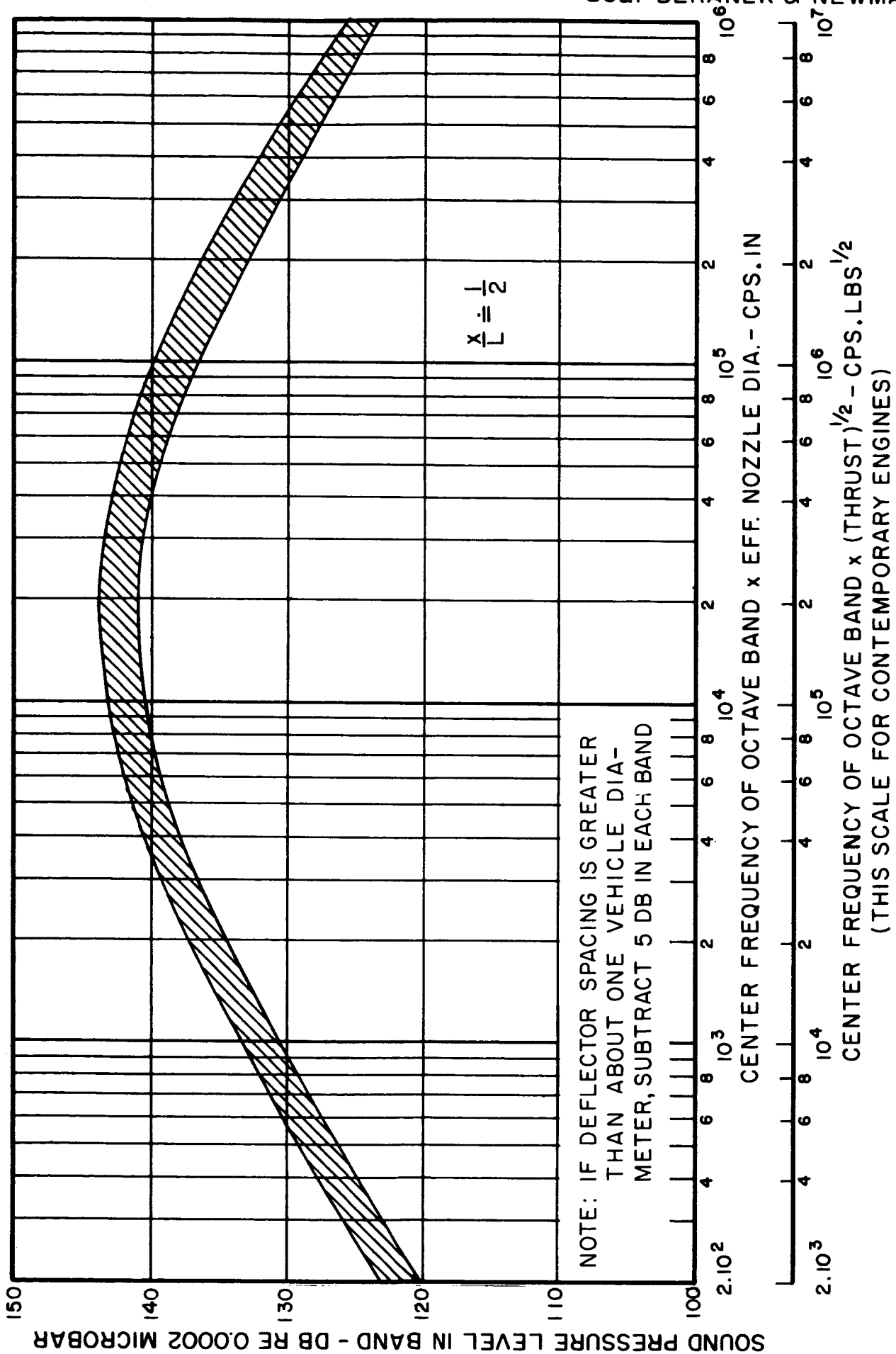


FIG. 6-4 SOUND PRESSURE LEVELS HALF-WAY ALONG LENGTH OF SPACE VEHICLE-STATIC TEST OR BEFORE LIFT-OFF

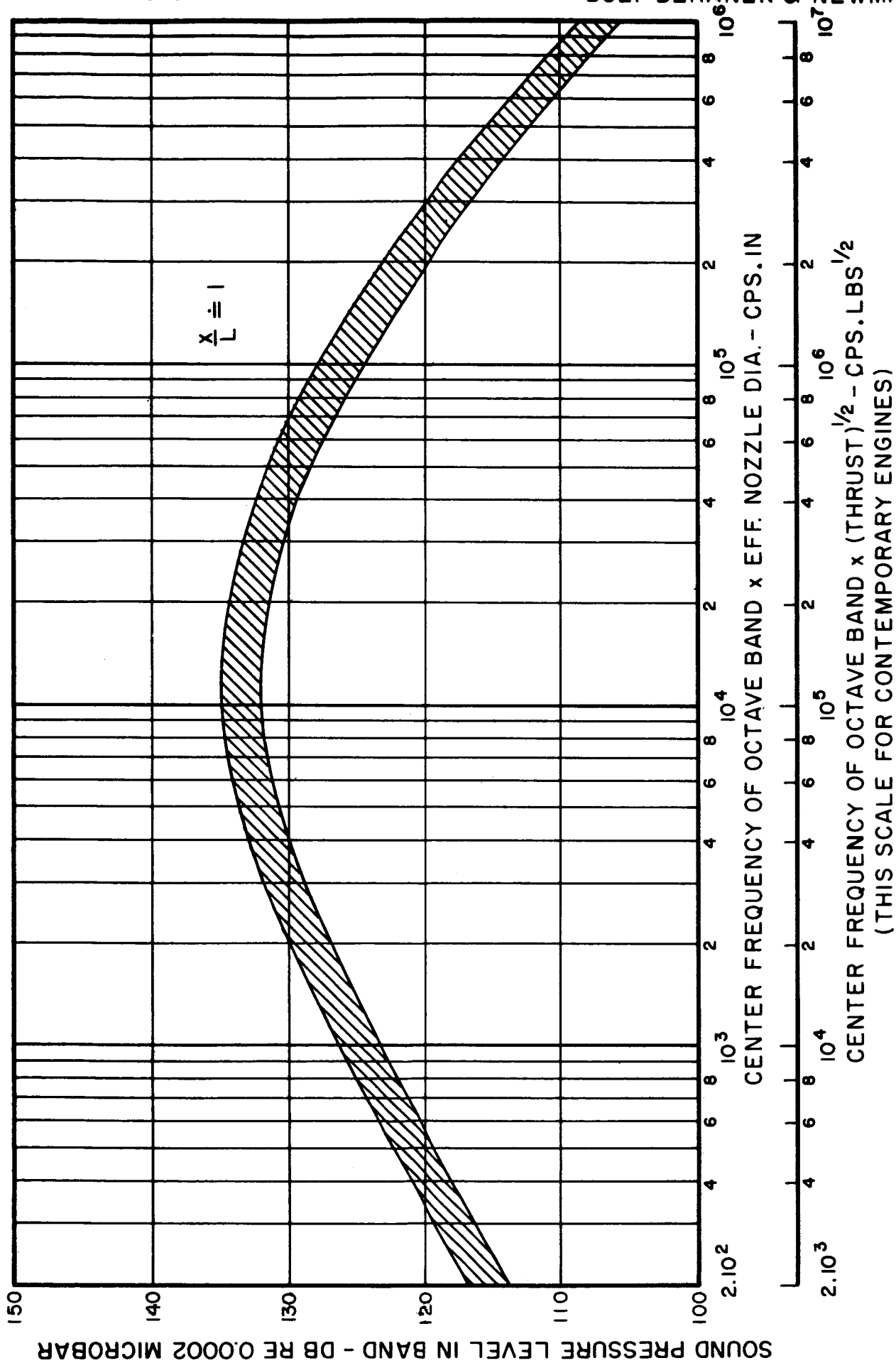


FIG. 6-5 SOUND PRESSURE LEVELS NEAR NOSE OF SPACE VEHICLE - STATIC TEST OR BEFORE LIFT-OFF

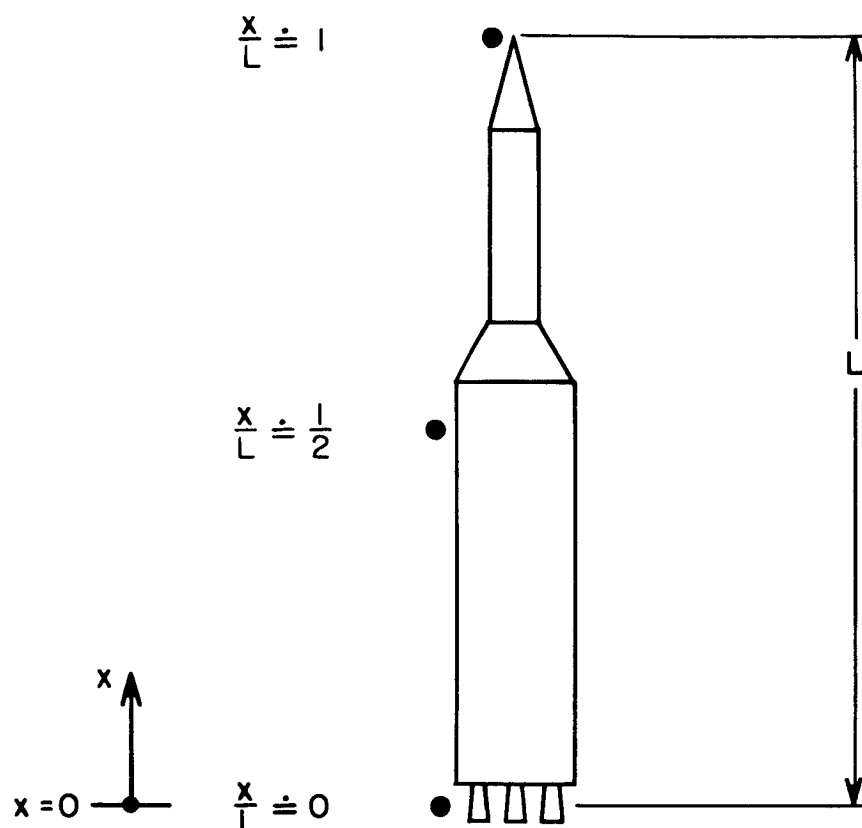


FIG. 6-6 SHOWING POSITIONS FOR ESTIMATING SOUND PRESSURE LEVELS NEAR VEHICLE SURFACE IN THE OPEN

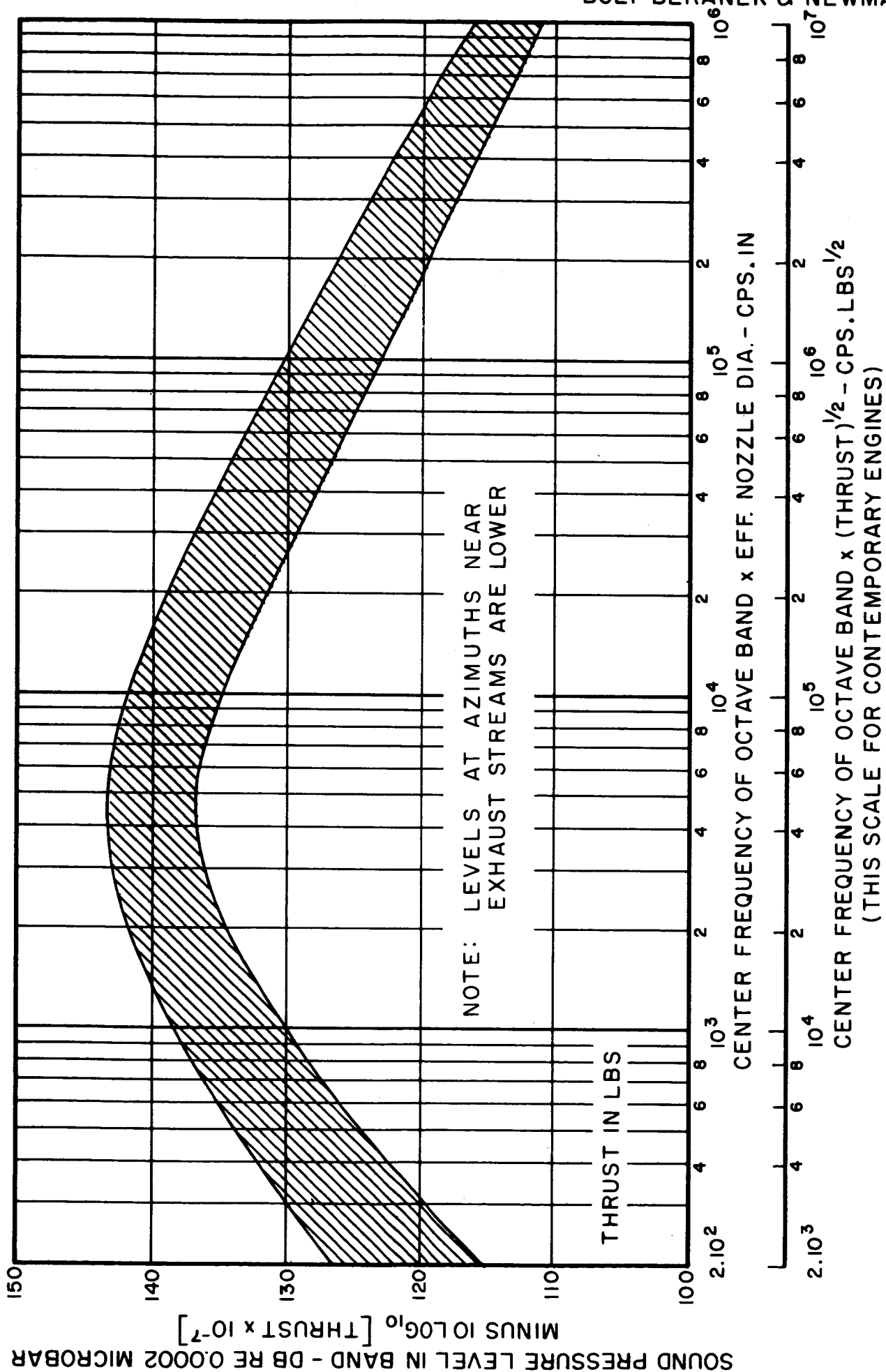


FIG. 6-7 SOUND PRESSURE LEVELS BEFORE LIFT-OFF OF SPACE VEHICLE,
1000 FT FROM STAND ON THE GROUND (WEDGE DEFLECTOR)

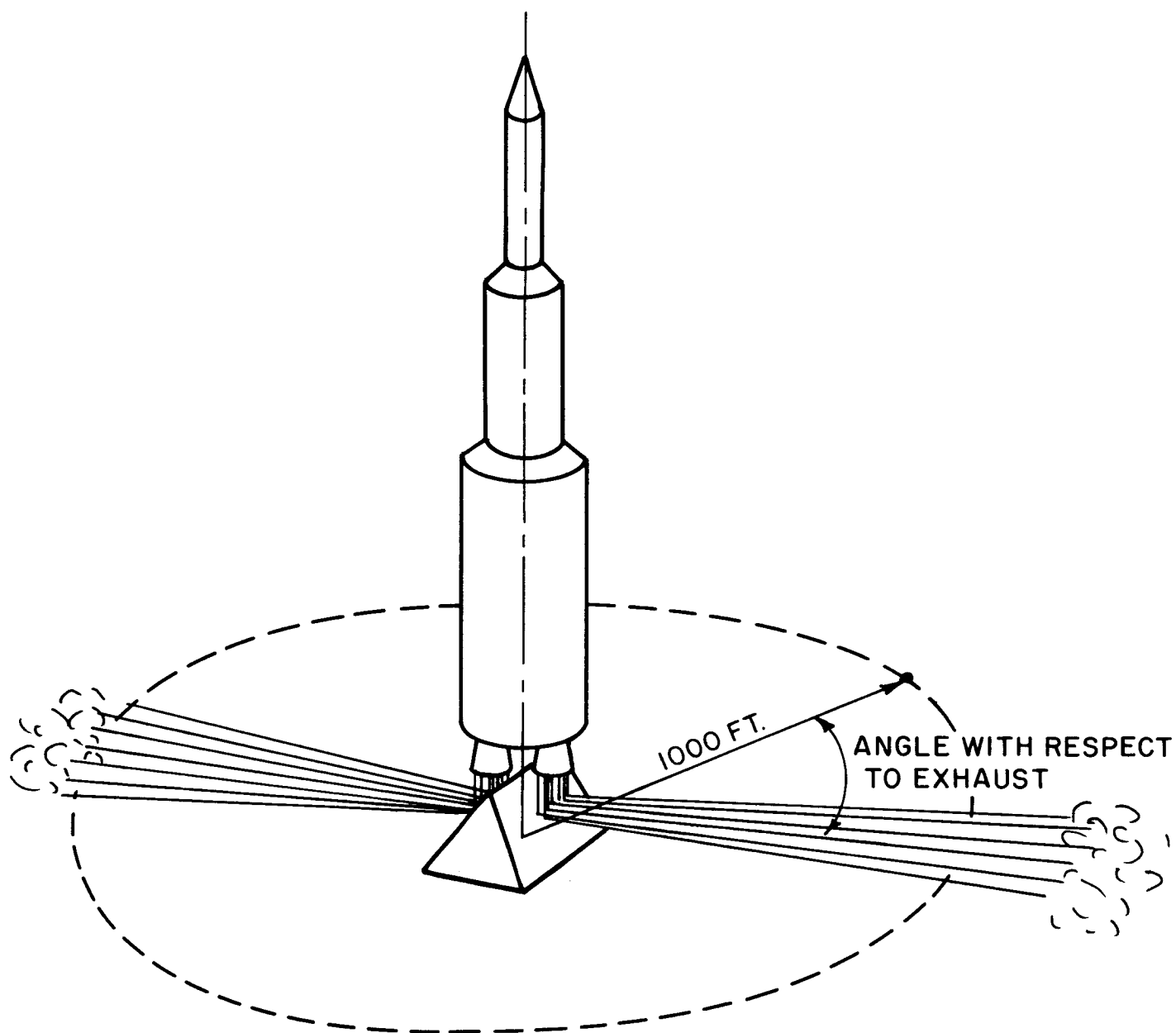


FIG. 6-8 SHOWING POSITIONS FOR ESTIMATING SOUND PRESSURE LEVELS BEFORE LIFT-OFF, 1000 FEET FROM STAND

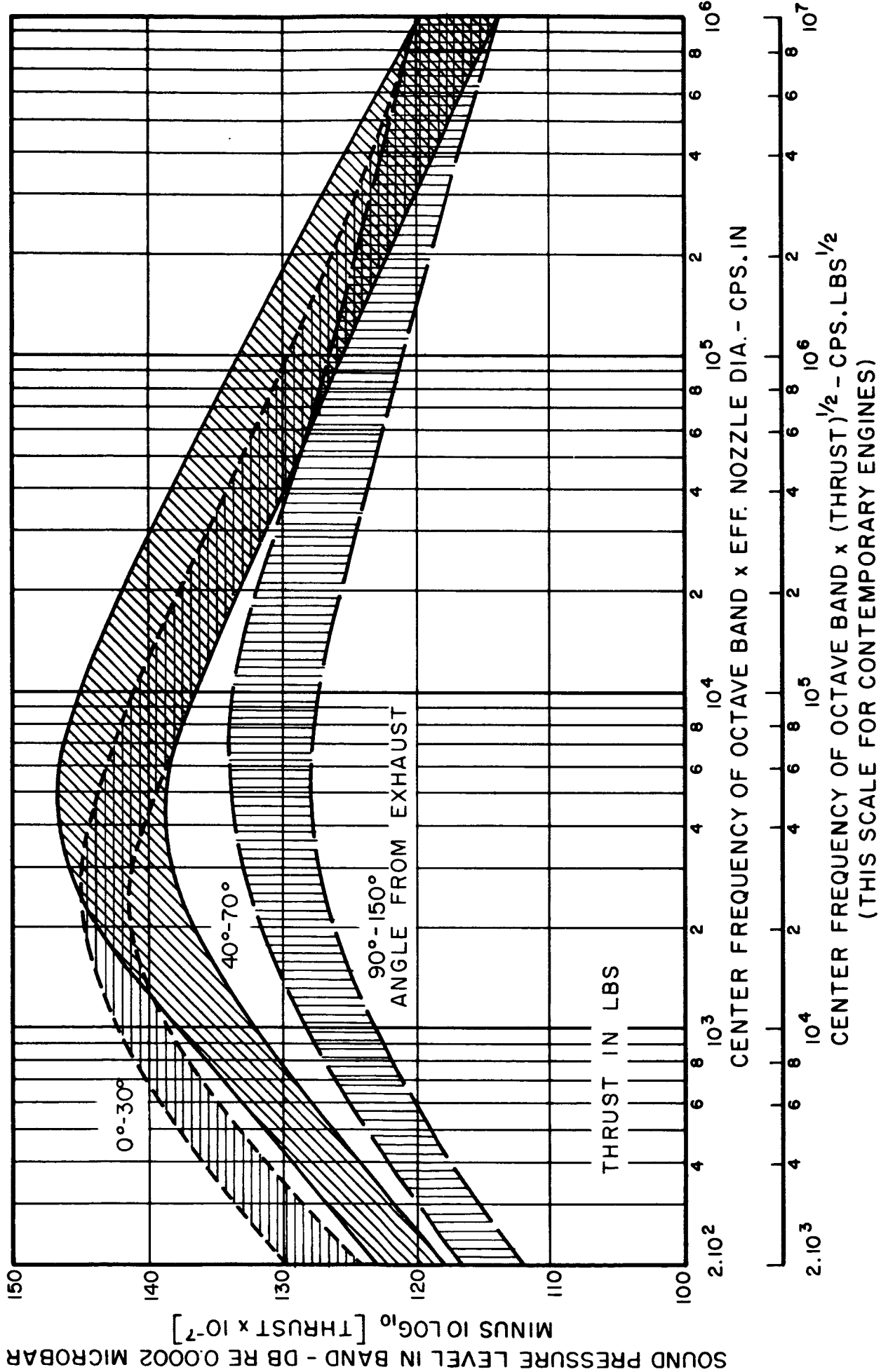


FIG. 6-9 SOUND PRESSURE LEVELS DURING STATIC TESTING OF SPACE VEHICLE, 1000 FT FROM STAND ON THE GROUND (BUCKET DEFLECTOR)

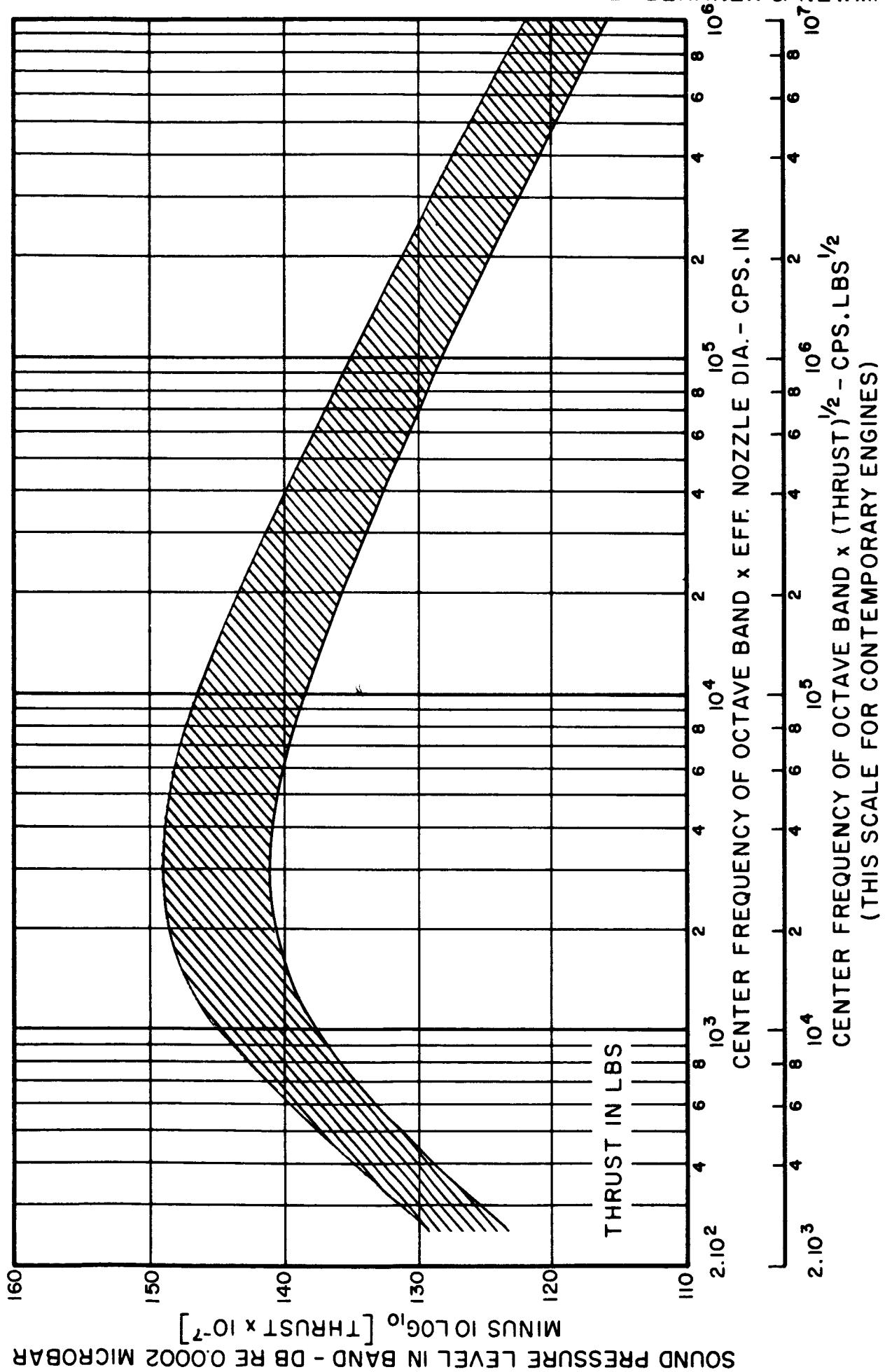


FIG. 6-10 MAXIMUM SOUND PRESSURE LEVELS AFTER LIFT-OFF OF SPACE VEHICLE, 1000 FT FROM STAND ON THE GROUND

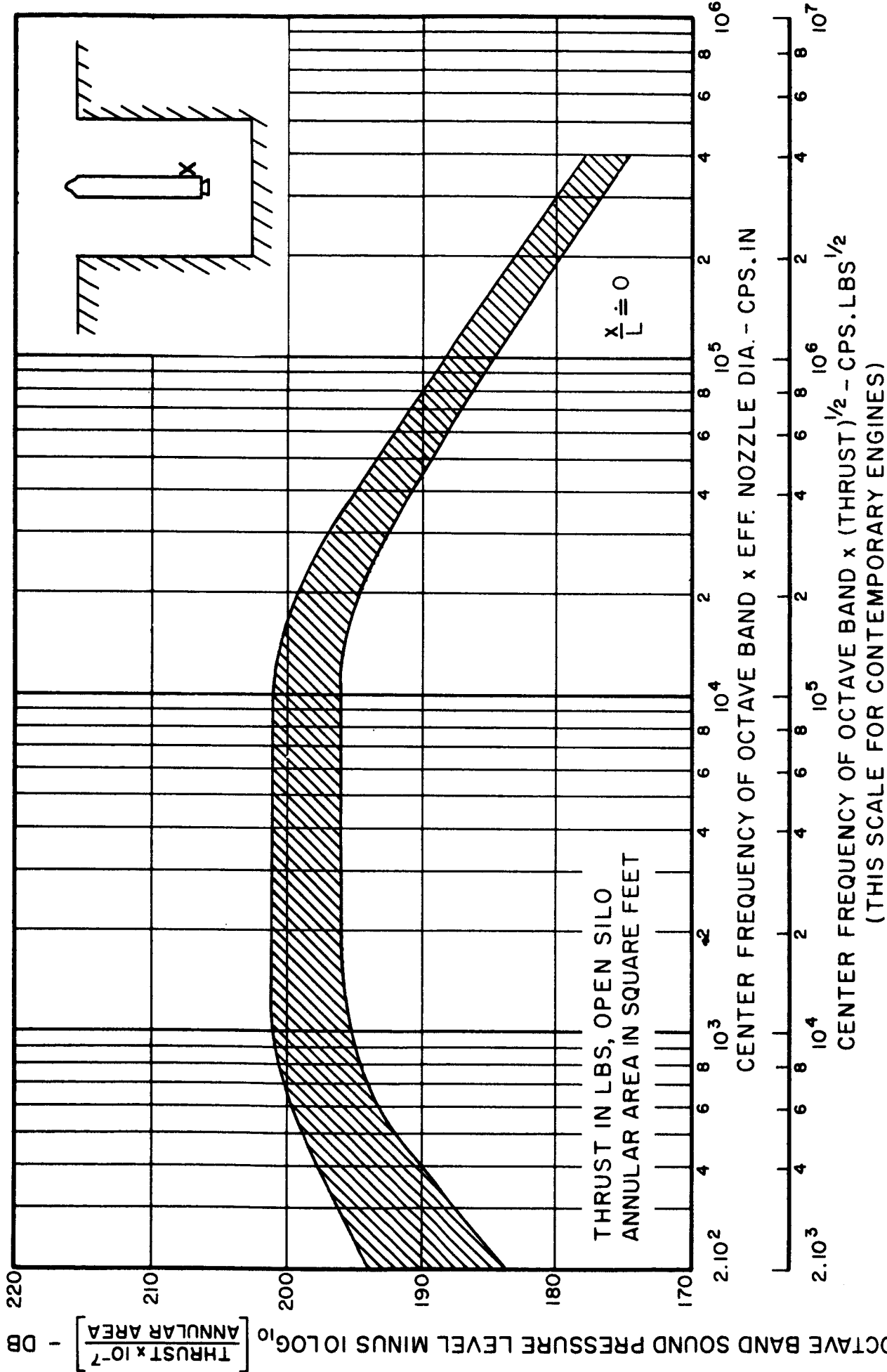


FIG. 6-11 MAXIMUM SOUND PRESSURE LEVELS DURING LAUNCHING FROM UNLINED BLOCKED SILO. OBSERVATION POSITION NEAR VEHICLE TAIL

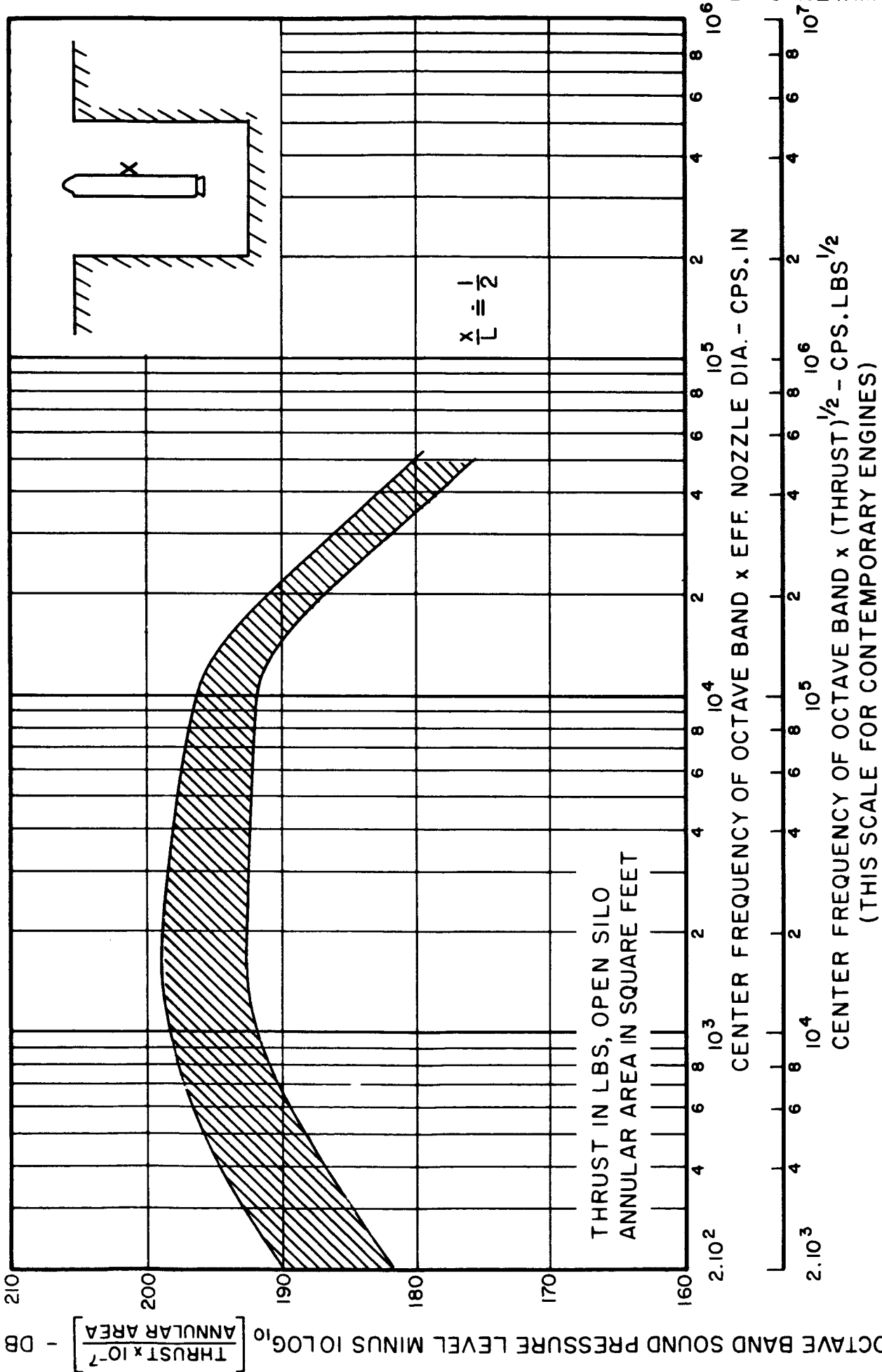


FIG. 6-12 MAXIMUM SOUND PRESSURE LEVELS DURING LAUNCHING FROM UNLINED BLOCKED SILO, OBSERVATION POSITION HALFWAY ALONG VEHICLE LENGTH

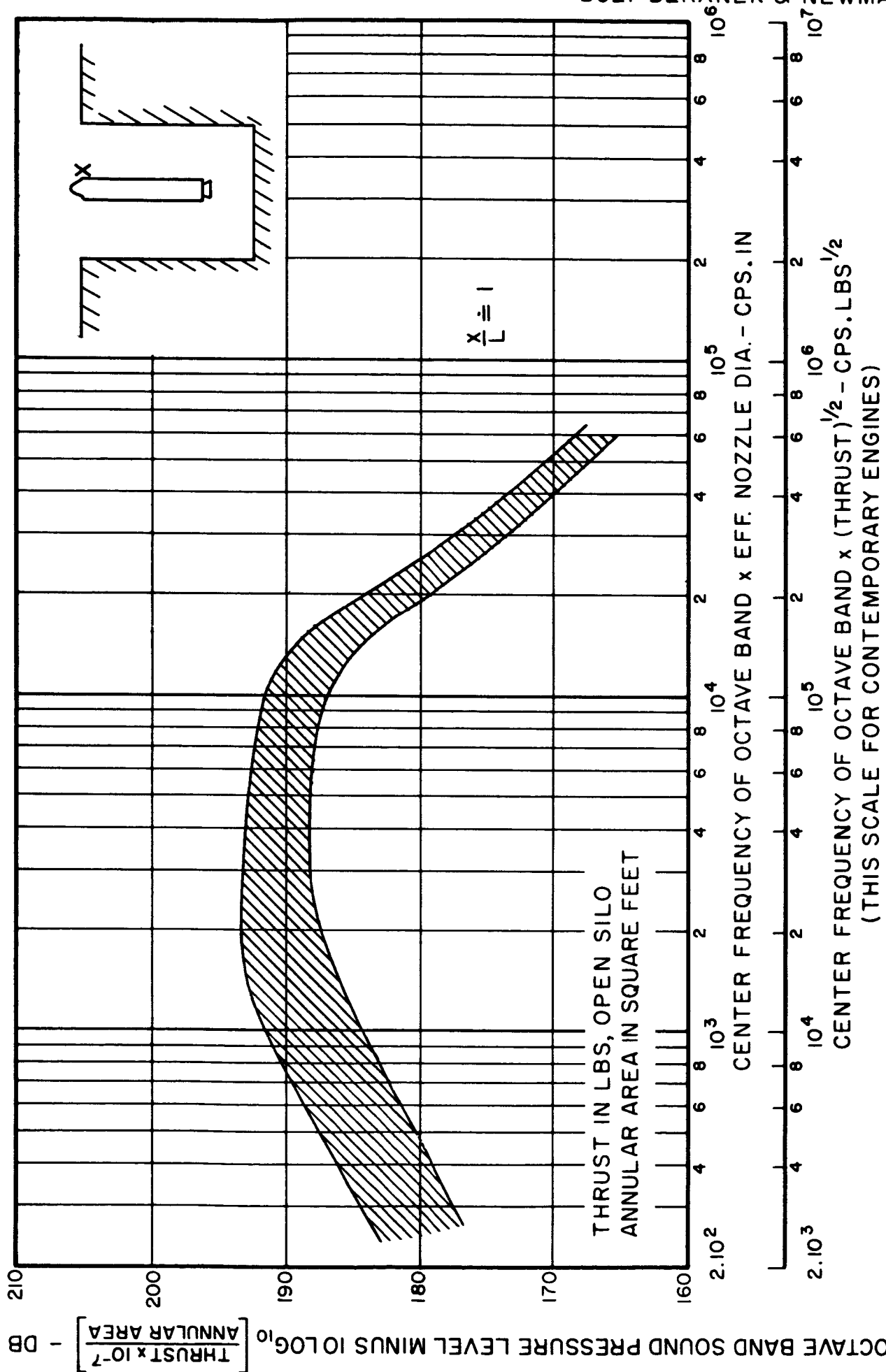


FIG. 6-13 MAXIMUM SOUND PRESSURE LEVELS DURING LAUNCHING FROM
UNLINED BLOCKED SILO, OBSERVATION POSITION NEAR VEHICLE
NOSE

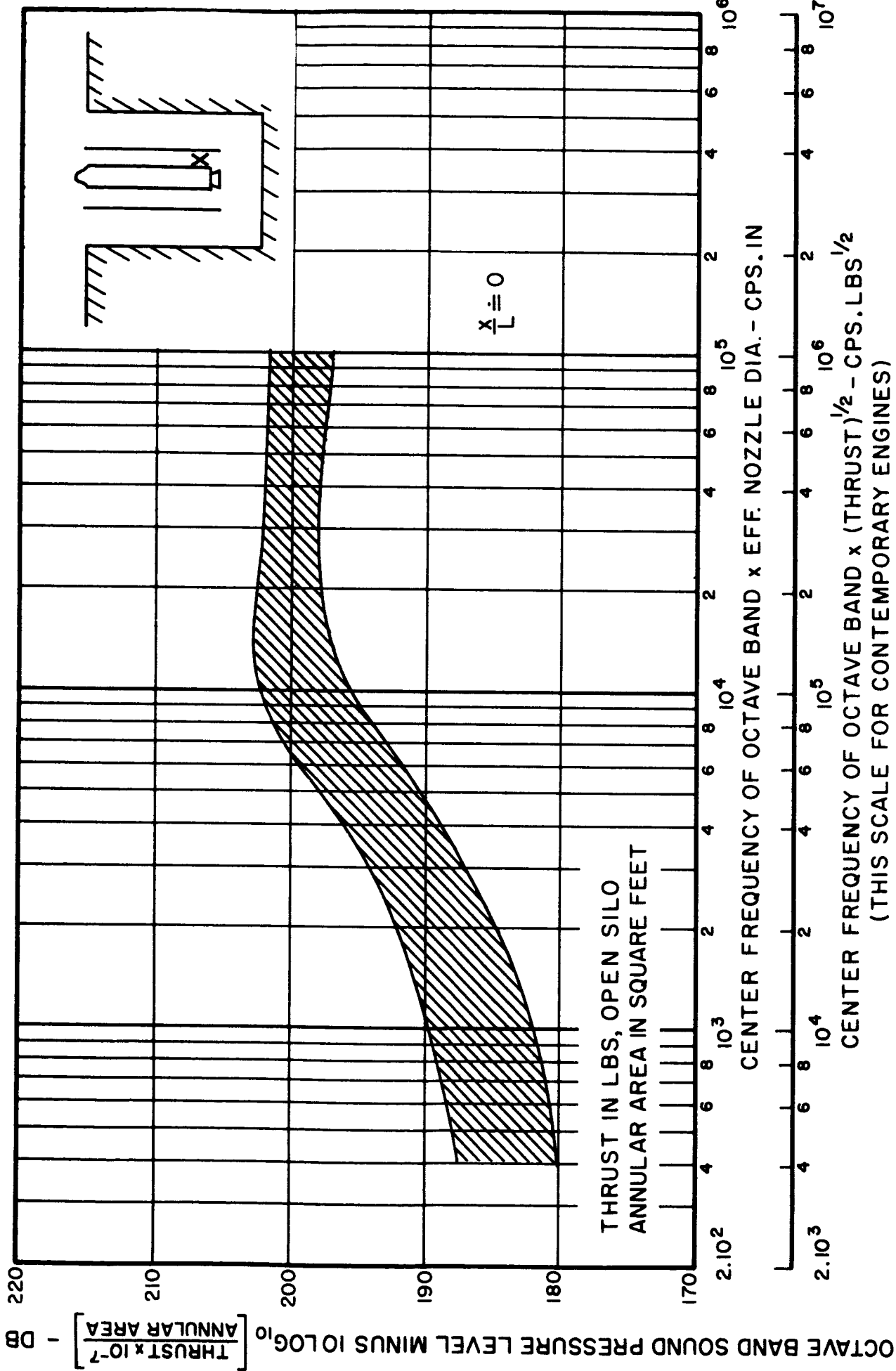


FIG. 6-14 MAXIMUM SOUND PRESSURE LEVELS DURING LAUNCHING FROM UNLINED DUCTED SILO, OBSERVATION POSITION NEAR VEHICLE TAIL

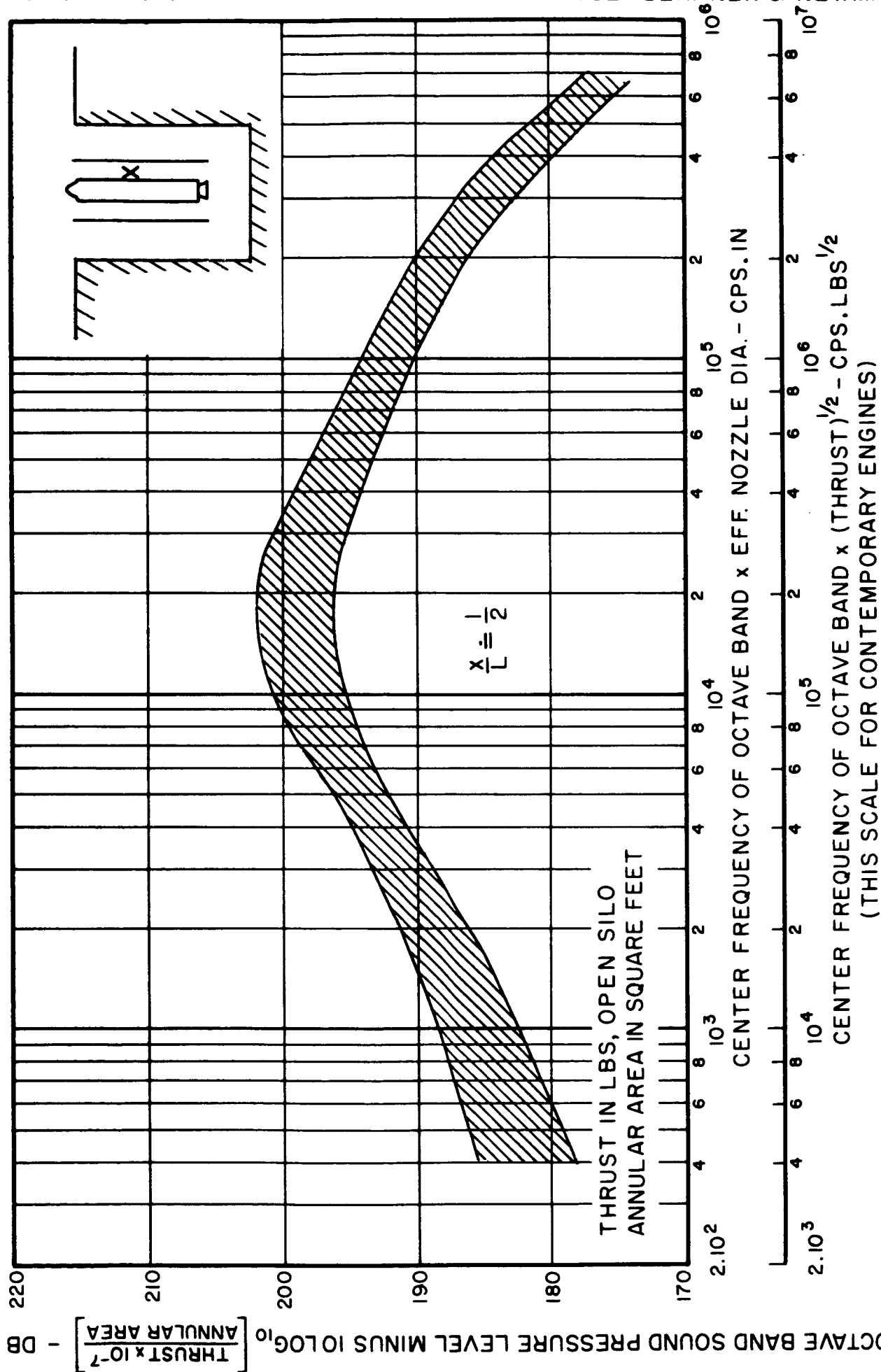


FIG. 6-15 MAXIMUM SOUND PRESSURE LEVELS DURING LAUNCHING FROM
UNLINED DUCTED SILO. OBSERVATION POSITION HALFWAY ALONG
VEHICLE LENGTH

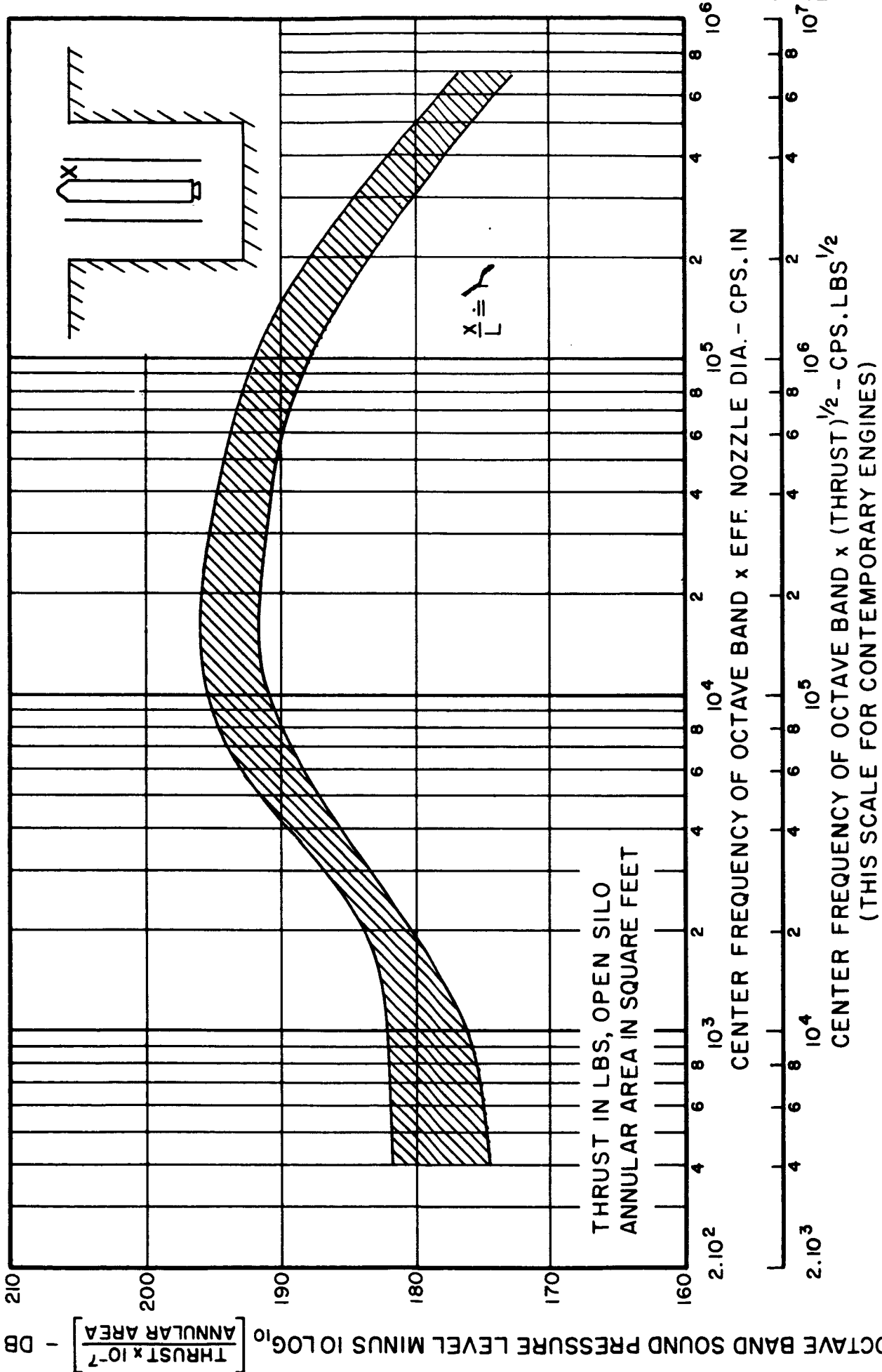


FIG. 6-16 MAXIMUM SOUND PRESSURE LEVELS DURING LAUNCHING FROM
UNLINED DUCTED SILO. OBSERVATION POSITION NEAR VEHICLE
NOSE

Additional measurements are urgently needed not only to improve our understanding of the transmission of sound through the atmosphere, but also to throw more light on the vibration transmission problem over various distances through soil of different characteristics.

7.2 The Propagation of Sound through the Atmosphere

7.2.1 The Inverse-Square Law

Let it be assumed that the noise source is surrounded by two hypothetical hemispheres of different radii r_1 and r_2 , both centered at the source. If one evaluates the acoustic power emanating from the source and carried across each hemisphere by the sound waves one arrives at a measure of how the sound pressure diminishes with distance. If the atmosphere were ideal, i.e., homogeneous, at rest, and without losses, the same acoustic power would be carried by the sound waves across each hemisphere. Since, under these conditions, the sound power per unit area of hemisphere (intensity) is known to be proportional to the sound pressure squared (with a constant factor of proportionality) one finds that the product of sound pressure p by the radius r , squared, is constant. Consequently, under these ideal conditions

$$(p_1 r_1)^2 = (p_2 r_2)^2 \quad (\text{Eq. 7-1})$$

This, in essence, is the so-called inverse-square law. Expressed in decibels, one has

$$20 \log_{10} \frac{p_2}{p_1} = 20 \log_{10} \frac{r_1}{r_2} \quad (\text{Eq. 7-2})$$

Hence, for each doubling of distance from the source, the sound pressure level decreases by 6 decibels. (See also Chapter 5)

7.2.2 The Excess Attenuation

In a real atmosphere the actual decrease in sound pressure level with distance is generally larger than the above value for ideal conditions, because there is energy being effectively abstracted from the sound waves by absorption in the air itself, by the terrain along which the sound waves may travel, and by the interaction of the sound waves with atmospheric turbulence. Moreover, there is refraction (bending) of the sound waves due to changes of the effective sound velocity with height (see below). This excess attenuation, expressed in decibels, is a measure of the additional decrease of the sound pressure level with distance beyond that given by Eq. (7-2). In some instances the excess attenuation may be negative, i.e., the attenuation actually found is less than that predicted by the inverse-square law. In such cases sound refraction is such as to neutralize or indeed overcome the dissipation attenuation. This phenomenon is illustrated in Fig. 7-1, showing the results of measurements of the overall sound pressure levels on the ground during static tests of Saturn at MSFC in the direction of Huntsville.* The results are expressed in terms of excess attenuation, i.e. departure from inverse-square law.

There are differences of opinion among workers in the field as to how best and most conveniently to separate the total excess attenuation such as shown in Fig. 7-1 into the contributions from

* These data were furnished informally by Test Division at MSFC Huntsville.

Figures 6-11 through 6-13 relate to an unlined blocked silo, whereas Figures 6-14 through 6-16 show data for an unlined ducted silo arrangement.

6.7 Empirical Estimates of the Ground Vibration Fields of Large Rocket Engines

The meager data available from static test firings of Saturn at MSFC, Huntsville, show that the accelerations measured in the ground are a very small fraction of a g^* only a few hundred feet from the stand. The attenuation of the ground vibrations with distance in the vicinity of the present test tower at MSFC, Huntsville, appears to be high.

More data are urgently needed in order to be able to estimate the magnitude of ground vibrations generated by large rocket boosters for different locations.

* g is the acceleration due to gravity.

7. THE TRANSMISSION PATH

7.1 General

In this study, two transmission media have to be considered. First, there is the atmosphere, through the lower layers of which the noise from the rocket engines is transmitted to the various points of interest on or near the ground. Second, there is the soil, through which the vibrations of the engines and their supporting structures are transmitted to nearby structures and other points of interest.

Any parameter chosen to describe the atmosphere at a point is characterized by fluctuations in its magnitude in time about a mean value. This mean value itself changes in time as well as in space. Present theoretical models are incapable of taking into account this complex behavior. However, a first approach toward exploring the effect of the inhomogenities in the atmosphere on sound propagation can be made by considering the atmosphere as consisting of a series of horizontal layers some of whose properties vary with height. In addition, the presence of some dissipative attenuation by the medium is assumed. In this Chapter the properties of the atmosphere at several typical sites are discussed, insofar as they affect the propagation of sound. In addition, a discussion of dissipative sound attenuation, or attenuation by obstacles and barriers and by enclosures is presented.

While the problem of sound propagation through the atmosphere is not yet solved to the extent desirable, the problem of propagation of vibrations through the soil is still less well understood.

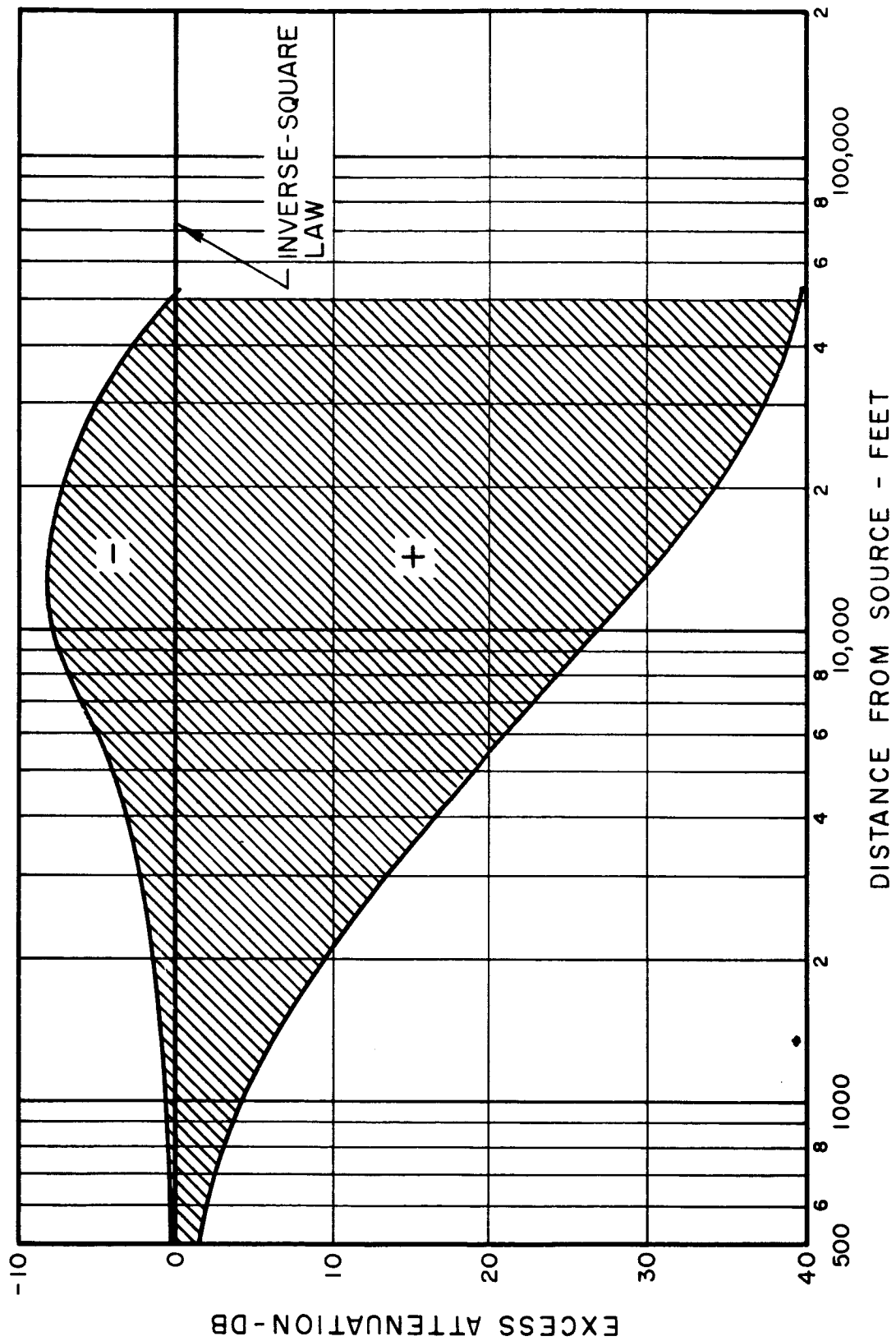


FIG. 7-1 RANGE OF VALUES OF EXCESS ATTENUATION OBTAINED FROM 20 STATIC SATURN TESTS AT MSFC IN THE DIRECTION OF HUNTSVILLE

the various mechanisms which cause the measured attenuation of sound to deviate from that calculated from the inverse-square law. The problem is also complicated by the fact that the various contributions are not independent of each other and depend on the geometry of the situation as well. These difficulties are compounded by the fact that very few data on the attenuation of rocket noise are available. Until this situation is remedied, engineering estimates must rely on the extrapolation of data obtained from airplane or similar noise over distances which rarely exceed a mile or two, to the much larger distances and much lower frequencies of interest here.

a) Excess Attenuation Caused by Energy Dissipation in the Atmosphere

Among the mechanisms which contribute to the total excess attenuation is a class that causes attenuation by energy being abstracted from the sound waves as they travel through the atmosphere. The principal contribution here is the so-called molecular absorption.* This contribution depends on humidity and temperature and increases with the frequency of the sound. It is presumed that this contribution can be expressed in terms of an attenuation coefficient in db per unit distance. If the noise is generated by a vehicle during static testing, or before and shortly after lift-off, it is reasonable to assume that energy is also abstracted from the sound waves as they travel along the ground. Little is known quantitatively about the magnitude, frequency dependence and dependence on the properties of the ground of this energy loss, as it is usually not

* E.g. see L. L. Beranek, Ed., Noise Reduction, loc. cit.

possible to isolate it from the other losses. It is usually lumped with the molecular absorption. Interaction of the sound waves with atmospheric turbulence is the cause of still another contribution to excess attenuation. This contribution is again difficult to separate from the total measured excess attenuation, but an attempt to do so has been made.* Atmospheric turbulence is also believed to contribute importantly to the fluctuations of the sound pressure level about its mean value which are almost always observed when sound is propagated through the atmosphere over appreciable distances.

Superimposed on the above-mentioned dissipative effects are the effects due to the refraction of sound by changes in the effective sound velocity with height. These changes (gradients) are caused by the gradients of temperature and wind (see below) which are generally largest near ground level. Hence their effect on sound transmission may be especially important during static testing and before and shortly after lift-off.

As the vehicle attains appreciable heights after lift-off, ground absorption becomes unimportant. But it is again difficult to isolate the remaining contributions. One reason is the fact that temperature and humidity (which determine molecular absorption) vary appreciably over the transmission path from a space vehicle high up in the atmosphere to a point on the ground. Another is that the effective sound velocity varies with height (see below).

b) The Sound Velocity Profile and its Effect on Sound Propagation

The conventional approach to a study of this aspect of the problem is that of "geometrical" or "ray acoustics." This approach considers

* H. J. Sabine, "Sound Propagation Near the Earth's Surface as Influenced by Weather Conditions," WADC Technical Report 57-353, Pt. IV, 1961.

the sound field as composed of a bundle of "rays", which, like light rays, emanate in straight lines in all directions from the source. One of the important atmospheric parameters to be considered here is the manner in which the "effective" velocity of propagation (see below) of sound varies with height. The variations of this velocity of propagation with height, as given by this velocity profile, tend to bend (refract) the sound rays. If the slope of the velocity profile of the atmosphere is positive, i.e., the effective speed of propagation of sound increases with height, the sound "rays" are bent downward. If the slope of the velocity profile is negative, the sound "rays" are bent upward away from the ground. If the source is near the ground this may result in the formation of a shadow zone into which no direct sound "rays" can penetrate. This is equivalent to stating that for receiver points well inside that shadow zone large positive values of excess attenuation will occur.

For the purposes of this study the properties of the atmosphere at a given elevation will be regarded as essentially constant along any given radius from the source. However, the inhomogeneties with height caused by variations in mean temperature, windspeed and wind direction are taken into account by this model. The important parameter to be considered is the manner in which the "effective" velocity of propagation of sound varies with height and direction. This effective velocity of propagation of sound c , at a given height, in a given direction, is equal to the speed of sound at the temperature at the point in question in quiet air, and added to it the vector component of the mean wind at that height in the direction considered. As a consequence, the effective velocity of propagation of sound c depends not only on height but also on direction, because of the influence of the wind.

While it is possible at present to estimate qualitatively the effect of a given velocity profile on excess attenuation, a thorough understanding of the problem is lacking. For example, the effect of the frequency of the signal on the excess attenuation caused by sound refraction is not well understood. The whole problem is badly in need of additional research, both theoretical and experimental, in order to be able to estimate the expected values of excess attenuation from a knowledge of the sound velocity profiles.

c) Engineering Estimates of Excess Attenuation

In the face of the present paucity of experimental sound transmission data obtained from large rocket engines in flight to points on the ground, existing data obtained from other noise sources, principally aircraft, over moderate distances must be extrapolated to larger distances and lower frequencies. The results will clearly depend on how this is done.

Dissipative Excess Attenuation

In this study it will be assumed that excess attenuation data obtained from aircraft in flight can be extrapolated to large distances by assuming that the total excess attenuation in decibels measured in a given frequency band is proportional to the distance, i.e., can be represented by an attenuation coefficient independent of distance. This includes the loss due to atmospheric turbulence. In extrapolating to the very low frequencies it is assumed that the last-mentioned type of loss is limiting. These estimates are given in Fig. 7-2 for the purpose of arriving at the engineering

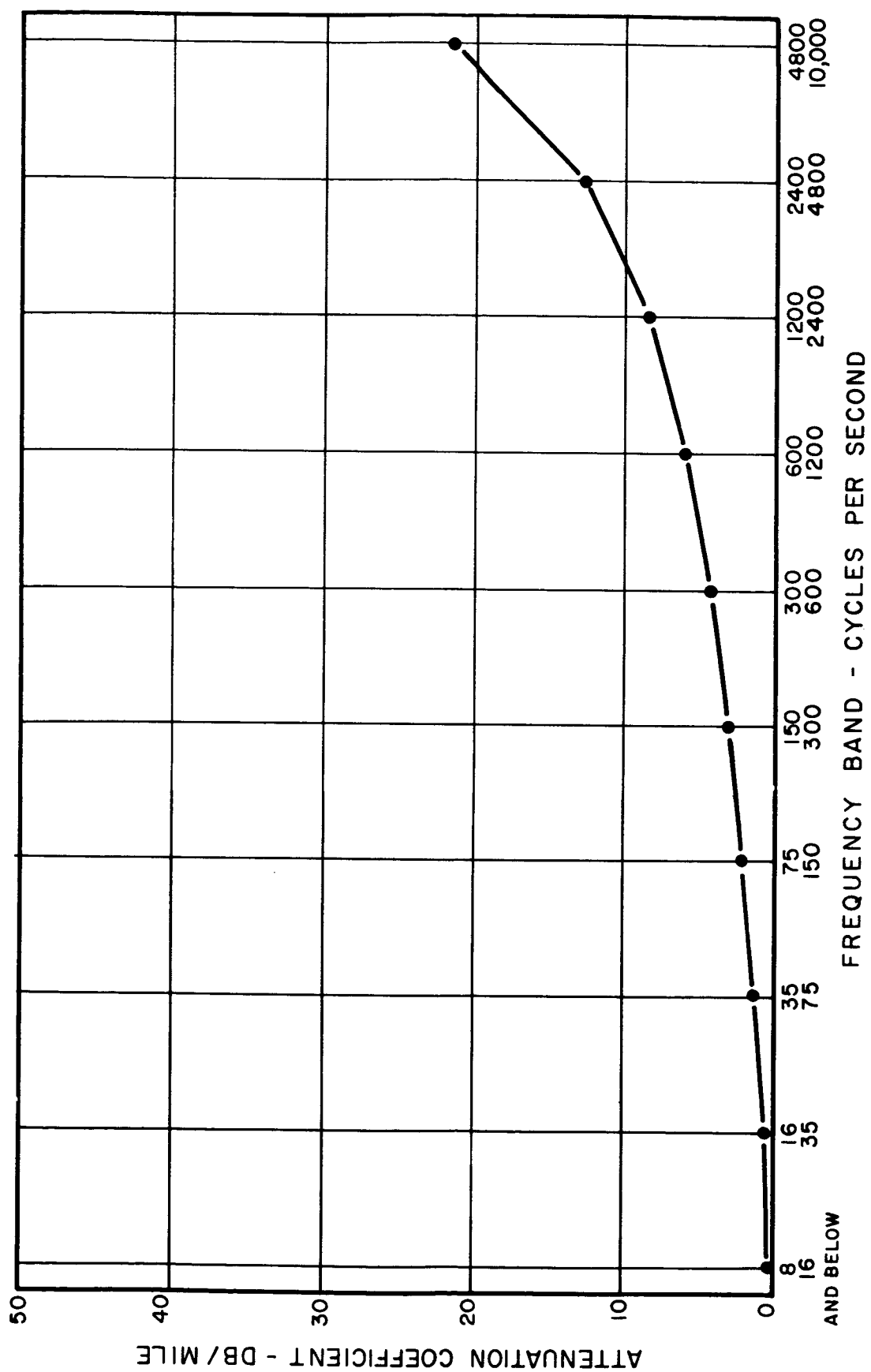


FIG. 7-2 ESTIMATED DISSIPATIVE EXCESS ATTENUATION IN THE ATMOSPHERE

estimates needed here.* Until further data are available it is also assumed that these estimates are valid for the static testing case and for the case before and after lift-off. This in effect means that ground attenuation is not specifically taken into account.

A different approach was used in the Hazards Report,** by extrapolating from the results of the WADC study.*** This resulted in appreciably higher estimates of the sound pressure levels at large distances at some frequencies.

Only by examining the results of direct measurements of the noise from large rocket engines under a variety of conditions can a decision be made as to which of the two approaches, if either, is correct.

Excess Attenuation Due to Sound Velocity Profile

From the data summarized in Fig. 7-1 and similar measurements on smaller vehicles the following general conclusions can be drawn, relevant to the effect of the sound velocity profile on the attenuation of sound propagating along the ground:

- a) When the slope of the velocity profile in the first several hundred or few thousand feet above ground is negative or slightly positive, positive excess attenuation will occur.
- b) When the slope of the velocity profile in the first several hundred or few thousand feet above ground is positive, negative excess attenuation is likely. Present indications are that an increase of 10 db or more in the level over that predicted by inverse-square law can occur in practice at the low-frequency end of the rocket noise spectrum. In order to relate

* These data are based on Fig. 9-10 in L. L. Beranek, Noise Reduction, loc. cit., appropriately modified to take into account the sloping spectrum shape of rocket noise.

** Joint Air Force--NASA Hazards Analysis Board Report, loc. cit.

***H. J. Sabine, loc. cit.

this negative excess attenuation to be expected from a certain profile shape to that shape and the magnitude of its gradients, further theoretical and experimental work needs to be accomplished.

Further theoretical and experimental work is also needed to study the effect of the wind velocity profile on the attenuation of sound propagated to a point on the ground after the vehicle has attained appreciable heights above ground level. Present preliminary indications are that negative excess attenuations of appreciable magnitude are less likely to occur than when the vehicle is close to the ground.

Fluctuations

The fluctuations of the sound pressure at a point about its mean are generally attributed to atmospheric inhomogeneities, in particular turbulence. It is known in a general way that the magnitude of the fluctuations of the sound pressure at a point near the ground tends to increase with distance from the source, with the frequency of the transmitted signal and with the level of turbulence. The fluctuations tend to decrease as the height of the source of sound above ground increases. Beyond these general observations quantitative engineering estimates of the magnitude and frequency of the fluctuations of the sound pressure level cannot be made because of our present lack of knowledge concerning this problem.

7.3 The Atmosphere at Representative Rocket Test and Launch Sites

Depending on the general meteorology of a given site, or class of sites, the vertical profile of the effective velocity of sound propagation c will be different. The form of the profile at a particular site varies with the time of day, season of the year, and the orientation of the transmission path with respect to the wind velocity vector. Hence, acoustical considerations enter into the question of

site selection, along with many other parameters. In this section of the report, the characteristic features of the sound velocity profiles in winter and summer for the Cape Canaveral area and two other important sites are discussed in detail.

Profiles of the average effective sound velocity \bar{c} and the average sound velocity $c(\bar{T})$ based on the average temperature \bar{T} alone (wind components not included) for winter and summer are presented in Figures 7-3a through 7-14b. The average effective sound velocity profiles have been calculated for the four sectors oriented North, West, South, and East from the sound source by considering the appropriate average wind components. In addition, data on the probability distribution of c are also shown.

The following procedure was used in constructing the figures: The average profiles $c(\bar{T})$ based on the average temperature \bar{T} alone were obtained directly from average seasonal temperature profiles. The effective sound velocity profiles were then derived by adding vectorially the average seasonal East-West, North-South vector wind components to the $c(\bar{T})$ profile based on temperature alone. To increase the usefulness of the data, the seasonal standard deviations of the vector wind components σ have been added to the average values of c to provide estimates of the probable range in c as a function of height. The $\pm \sigma$ and $\pm 2\sigma$ limits shown in the figures refer to this inclusion of the vector wind variabilities in the calculations of c . They roughly represent the 0.2 and 0.05 probability levels, respectively.* These data allow the planner to estimate the limits

* See Appendix for a more detailed discussion.

within which the effective velocity c will be found as a function of height, sector, and season. This means that in about 60 percent of the cases one expects to find c between the $\pm \sigma$ limits, and in about 90 percent of the cases between the $\pm 2\sigma$ limits.

The available wind data for the Cape Canaveral area are more extensive than those for other areas and the profile information contained in the Cape Canaveral figures is believed to be the most reliable of the sites evaluated. A detailed description of the data sources and procedures used in constructing the figures is provided in the Appendix.

In order to see how well individual sound velocity profiles fit the envelopes of the calculated mean profiles and to provide more detailed information on the vertical gradient of sound velocity, a number of profiles based on direct measurements are also presented in the Appendix for each site, sector, and season. In general, the data are self-consistent and the probability distribution envelopes appear to be quite satisfactory for evaluating the general trends.

Inasmuch as the detailed shape of the profile near the ground appears to be of importance in assessing the possible occurrence of negative excess sound attenuation during static testing and before lift-off, the seasonal profiles must be used with some caution. Information on the variation of sound velocity with height in any particular instance cannot be obtained from the mean profiles or their envelopes. This can easily be seen by inspection of the individual cases in the Appendix. In any practical situation, profiles obtained

by direct measurements shortly before test or lift-off should be used.

Experimental evidence shows that the wind shear in the first few thousand feet above ground level rarely exceeds $5 \times 10^{-2} \text{ sec}^{-1}$ and is generally less than $2.5 \times 10^{-2} \text{ sec}^{-1}$.* Combining these values with the mean seasonal profile by starting at the surface with zero wind component and continuing to the σ or 2σ profile, a synthetic profile can be constructed which permits (conservative) estimates of the height of the layer where positive profile slopes can be expected. When data correlating profile slope and excess attenuation become available, the expected maximum negative excess attenuation can thus be estimated. Ray acoustics indicates also that the depth of the layer in which c exceeds the value at ground level is of some importance.

After the vehicle has left the ground the shape of the profile at greater altitudes is significant. In particular, as the vehicle ascends above the point of maximum c (if any), it follows from ray acoustics, that more and more of the sound rays will be refracted away from the ground.

In anticipation of the results of the analysis of the seasonal sound velocity profiles for the various sites presented subsequently, the following general statements may be made:

- 1) Both wind and temperature must be considered in the determination of the vertical profiles of sound velocity.

* J.W. Smith and W.W. Vaughan, "Monthly and Annual Wind Distribution as a Function of Altitude for Patrick Air Force Base, Cape Canaveral, Florida," Table VIII, NASA TN D-610, July 1961.

- 2) As a result of the strong westerly winds usually present at intermediate and high levels during the winter season, positive slopes of the sound velocity profile are more likely to occur to the east of a site than in any other direction.
- 3) At any site positive slopes are also likely to be found in the lowest layers of all sectors throughout the year whenever strong wind shears occur.
- 4) Positive slopes at low levels are also produced by temperature inversions there. Such inversions are particularly common at the Point Arguello Site in summer.

7.3.1 Properties of the Atmosphere -- Cape Canaveral

The climatic regime at Cape Canaveral throughout the year is essentially oceanic in character in the lowest levels of the atmosphere. During the summer and also in the late spring and early fall, the weather is dominated by the easterly flow of tropical maritime air around the western extremity of the Bermuda anticyclone. Except for towering cumulus that develop inland and sometimes move over the Cape in the late afternoon, convective activity is capped by a weak subsidence inversion at about 8,000 ft. The easterly circulation extends to extremely high levels and is quite persistent in the lower stratosphere. During the colder parts of the year, the Cape Canaveral area experiences periodic incursions of modified polar continental air at the surface as the polar front extends its sphere of activity to low latitudes. However, the polar air masses

at Cape Canaveral are generally shallow in depth and possess a minimum of temperature contrast due to the long trajectory away from the source region. In the presence of relatively cold and dry air, small temperature inversions are formed at night in the lowest 1000 ft as the result of radiational cooling but these tend to be dissipated quickly after sunrise. Even in winter, a local sea breeze circulation characteristically develops during the solar day and dominates the temperature and wind field at low levels. During the summer, the sea breeze circulation is a daily phenomenon superimposed on the prevailing easterly flow. The most striking change produced at Cape Canaveral in winter is the presence of very strong westerly winds aloft which attain maximum values in the 30,000 to 40,000 ft layer and which persist to heights of the order of 100,000 ft. Peak values of the wind speed are of the order of 250 ft per second and the wind shear in the vicinity of the peak wind speed attains maximum values of about 50 ft per second per 1000-ft interval.* Maximum values of the gradient of c in the lowest layers appear to be of the order to 50 ft per second per 2000 ft.

These meteorological factors are reflected in the probability distributions for c shown in Figures 7-3a through 7-6b. Only one of the seasonal average profiles, that for the eastern sector** in winter (Figure 7-6a), exhibits a (small) positive slope in the troposphere. As might be expected, the probability of a positive slope for the effective sound velocity profile is a minimum for the western sector.

* J. W. Smith and W. W. Vaughan, loc. cit.

** Note that the eastern sector extends over the ocean and hence conditions there are of small engineering importance.

The winter profiles for the northern and southern sectors are quite similar in appearance. According to Figures 7-3a and 7-5a, the depth of the layer in which c is likely to exceed the value at ground level is about 10,000 ft for the 0.2 limit and about 25,000 ft for the 0.05 limit. It may be pointed out that the winter profiles for all sectors indicate a sound duct in the upper troposphere and lower stratosphere that will tend to trap sound waves generated by vehicles moving through these layers.

In summer, as shown in Figures 7-3b, 7-4b, 7-5b, and 7-6b, positive slopes of the profiles are to be expected only in the first 10,000 ft and the maximum vertical gradients of c are in general much smaller than the corresponding winter gradients. The upper-level sound duct is apparent in summer for all sectors except the eastern one where the presence of easterly high-level winds offsets the effect of the positive slope of the temperature profile.

7.3.2 Properties of the Atmosphere -- Site Off Cape Canaveral Shore

The properties of the atmosphere at a site 5-10 miles off shore will not differ appreciably from those at Cape Canaveral proper except in the very lowest layers under rather special conditions. In the presence of cold air associated with strong northwesterly flow at the surface, the over-water trajectory of 5 to 10 miles would increase the convective instability in the first 5,000 to 10,000 ft and the temperature and moisture content of the air within this layer. Also, the possibility of the formation of nocturnal radiation inversions at an off-shore site is almost negligible. The principal advantage of an off-shore site is with respect to the

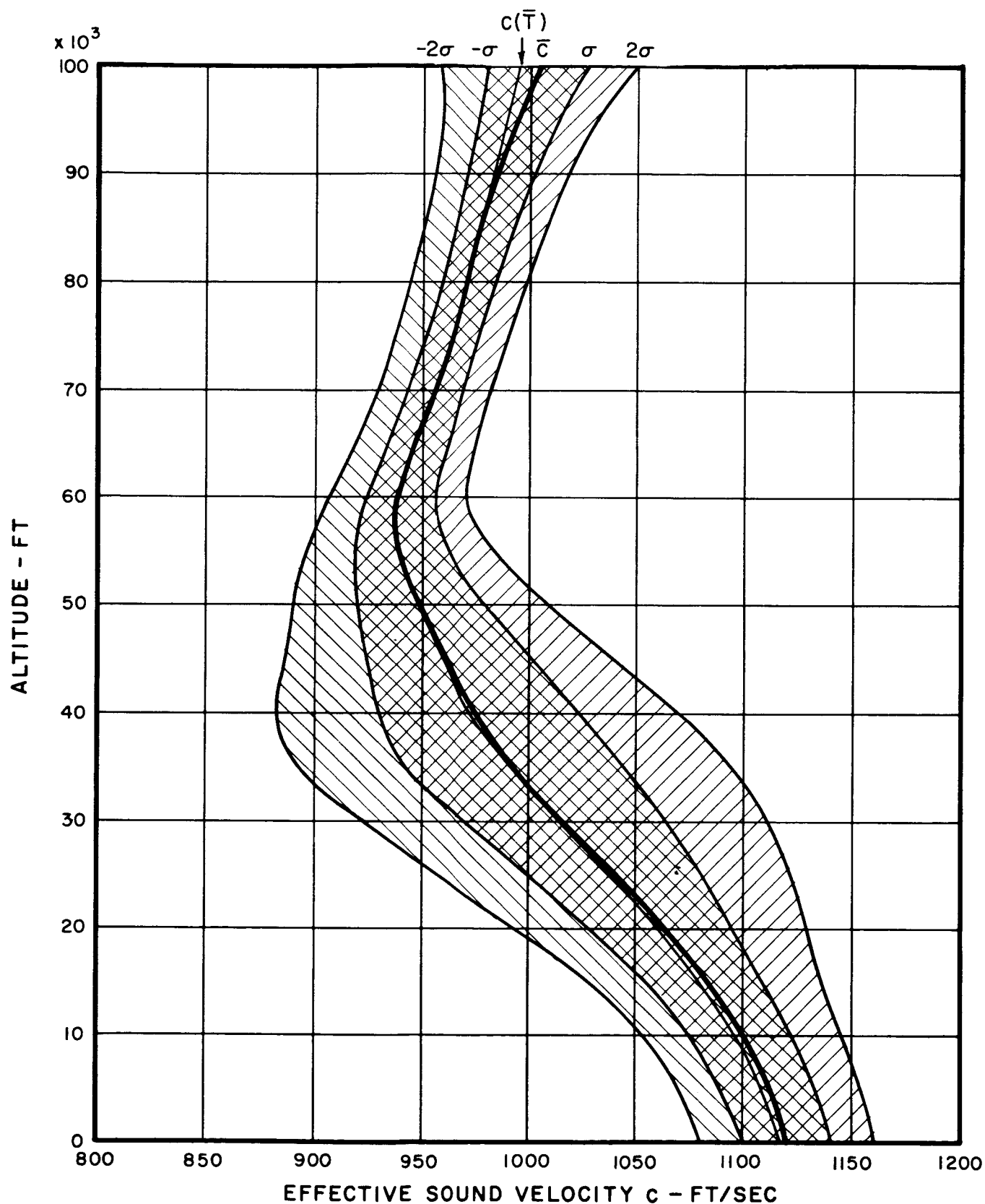


FIG. 7-3a PROBABILITY DISTRIBUTION OF SOUND VELOCITY FOR NORTHERN SECTOR IN WINTER AT CAPE CANAVERAL

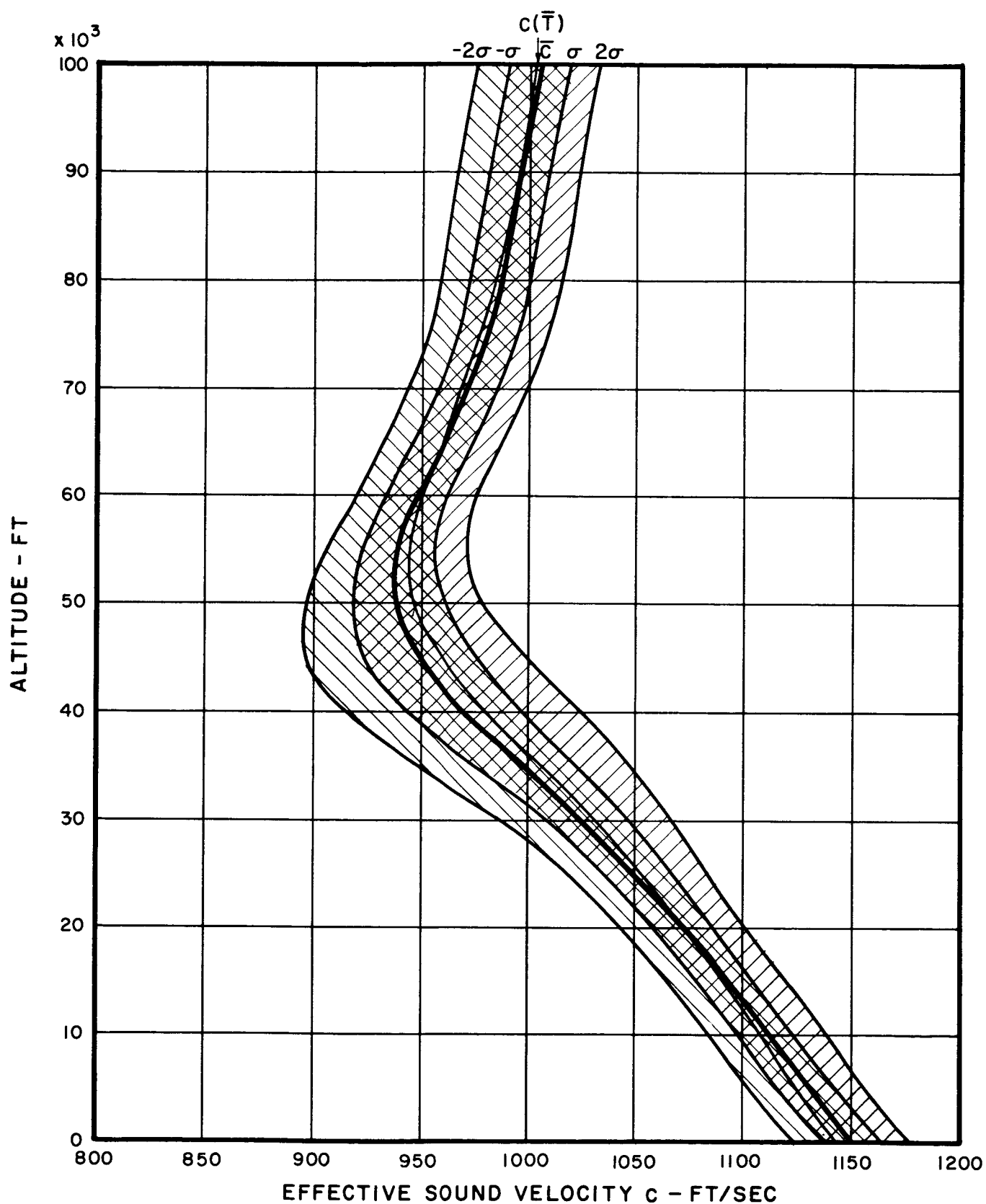


FIG.7 - 3b PROBABILITY DISTRIBUTION OF SOUND VELOCITY FOR NORTHERN SECTOR IN SUMMER AT CAPE CANAVERAL

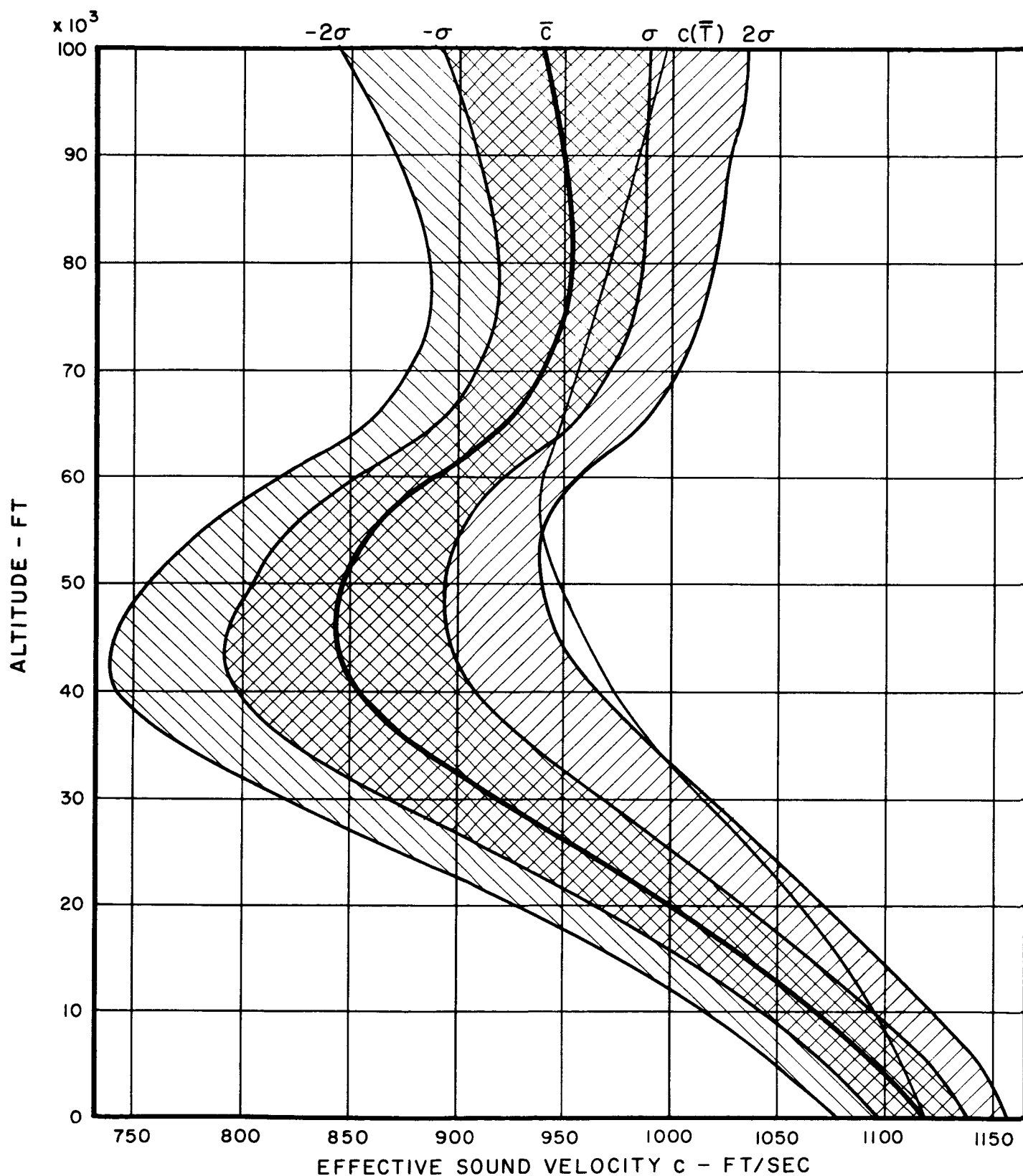


FIG. 7 - 4a PROBABILITY DISTRIBUTION OF SOUND VELOCITY
FOR WESTERN SECTOR IN WINTER AT CAPE
CANAVERAL

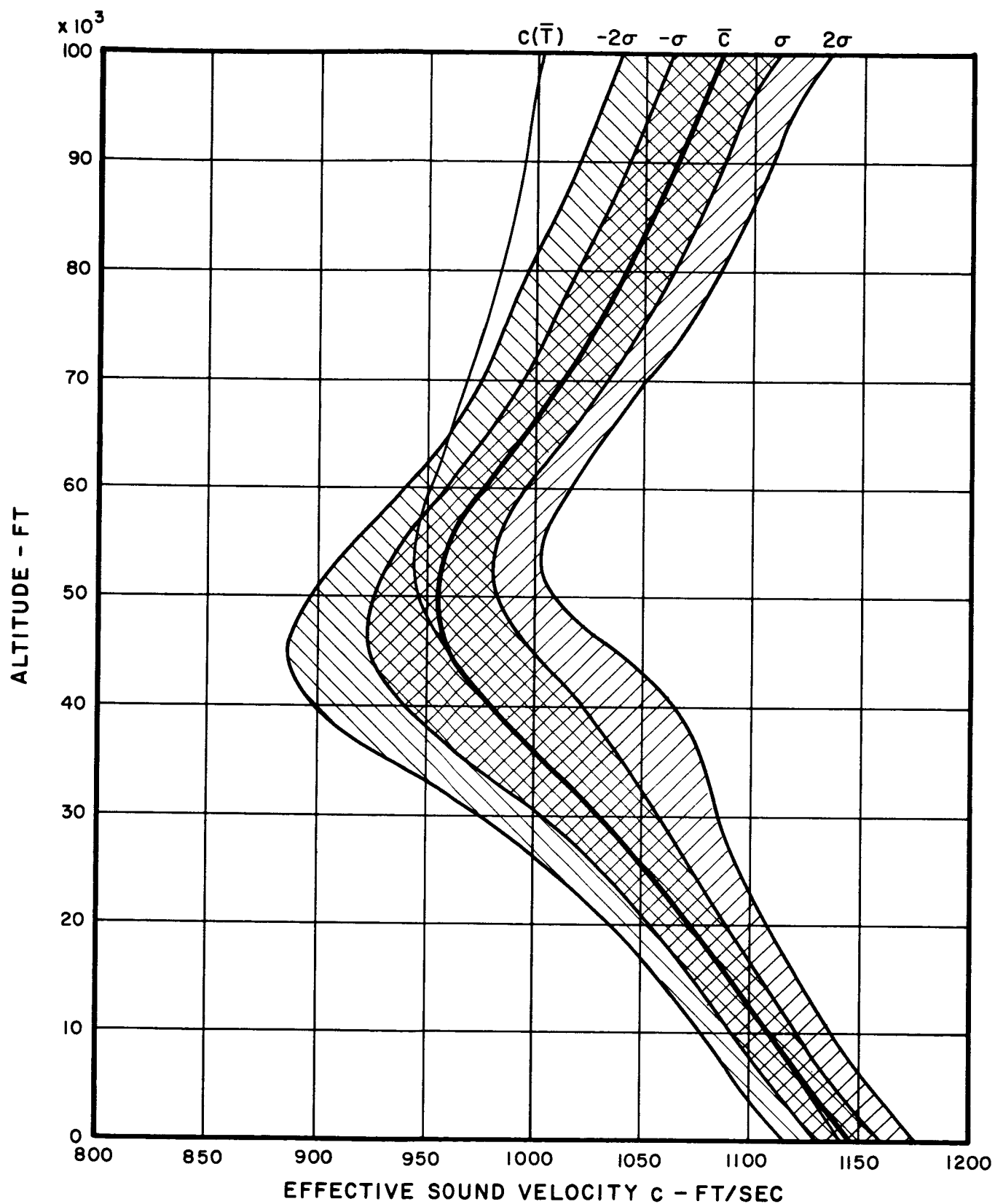


FIG. 7 - 4b PROBABILITY DISTRIBUTION OF SOUND VELOCITY FOR WESTERN SECTOR IN SUMMER AT CAPE CANAVERAL

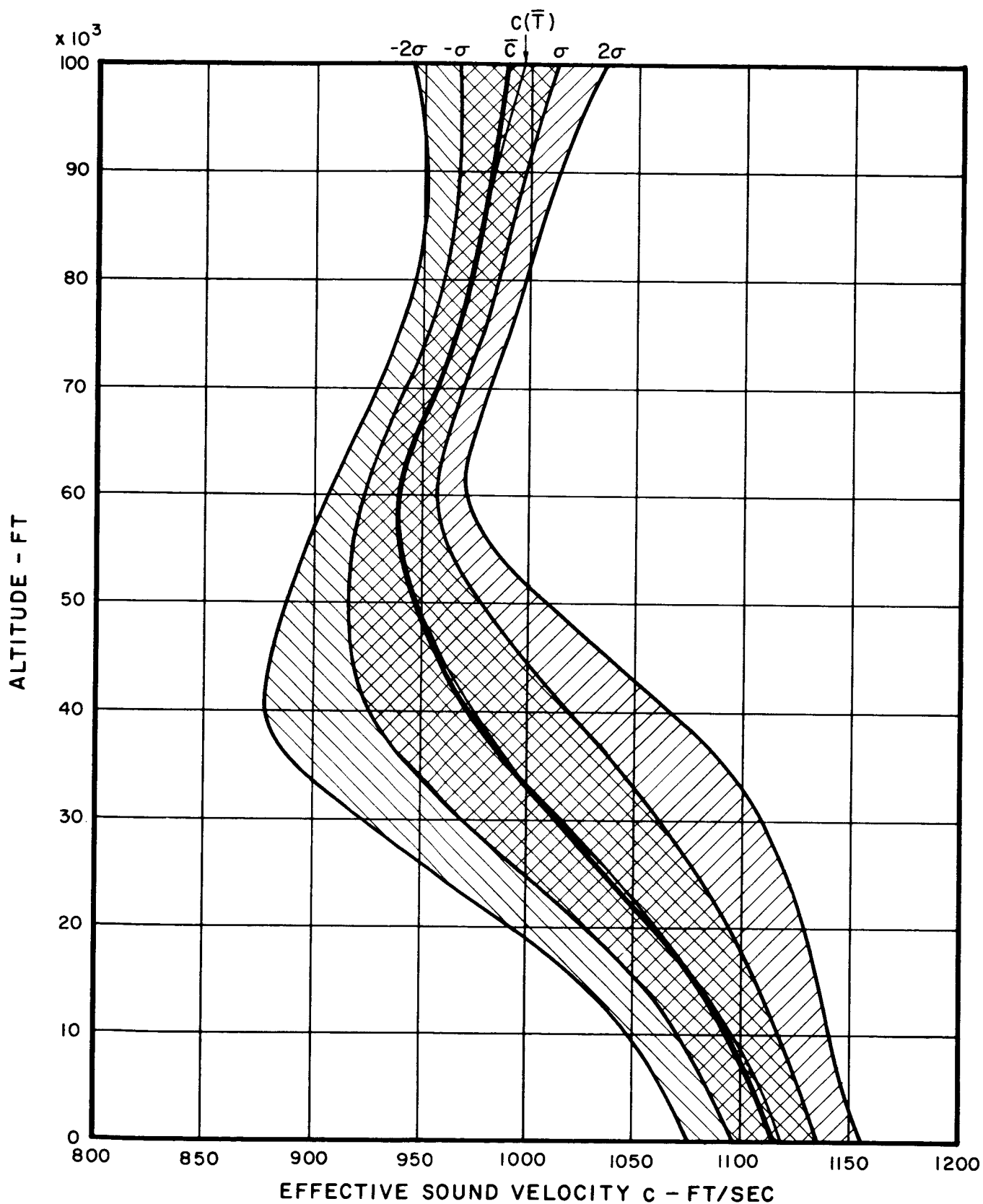


FIG. 7 - 5a PROBABILITY DISTRIBUTION OF SOUND VELOCITY FOR SOUTHERN SECTOR IN WINTER AT CAPE CANAVERAL

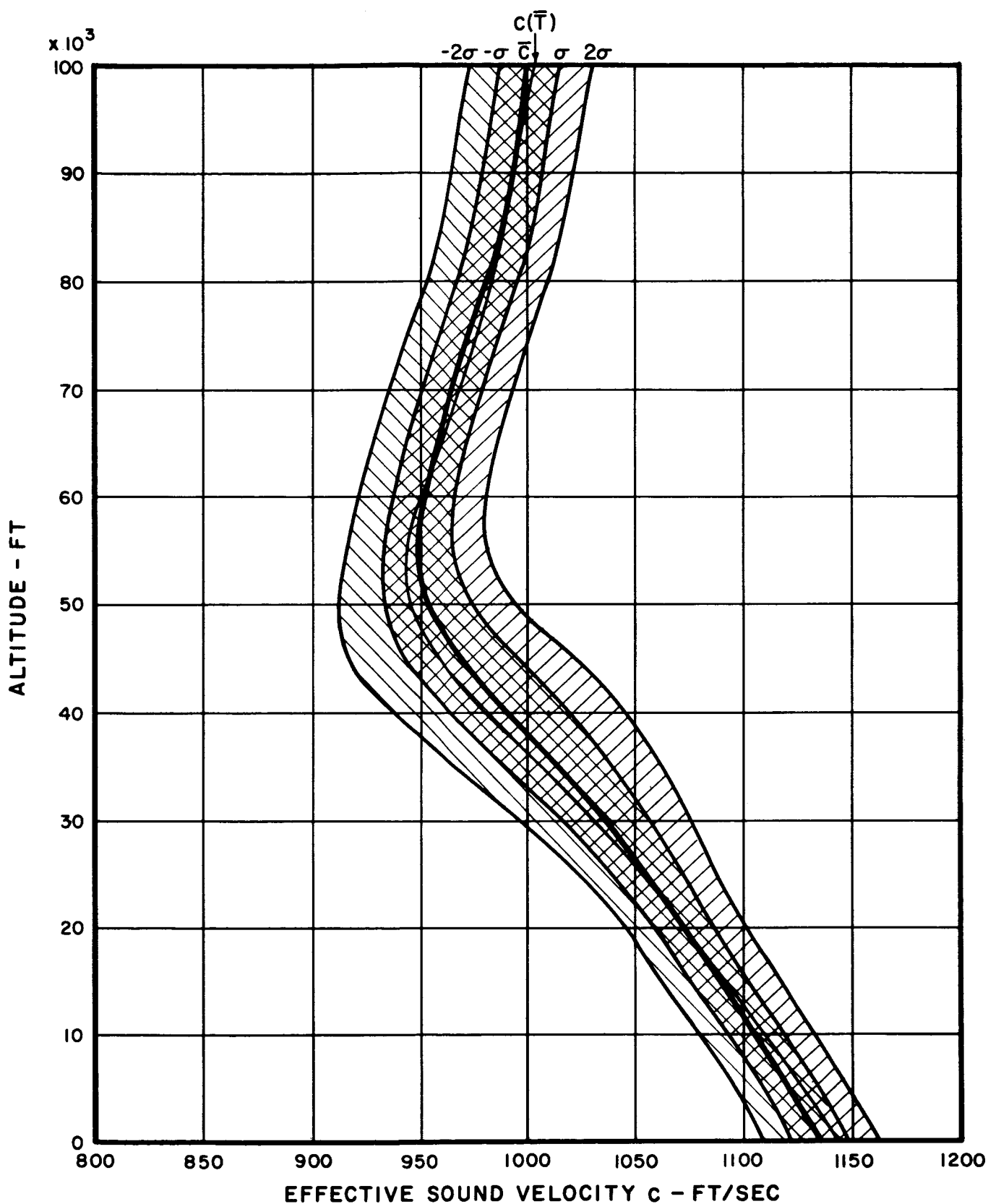


FIG. 7 - 5b PROBABILITY DISTRIBUTION OF SOUND VELOCITY FOR SOUTHERN SECTOR IN SUMMER AT CAPE CANAVERAL

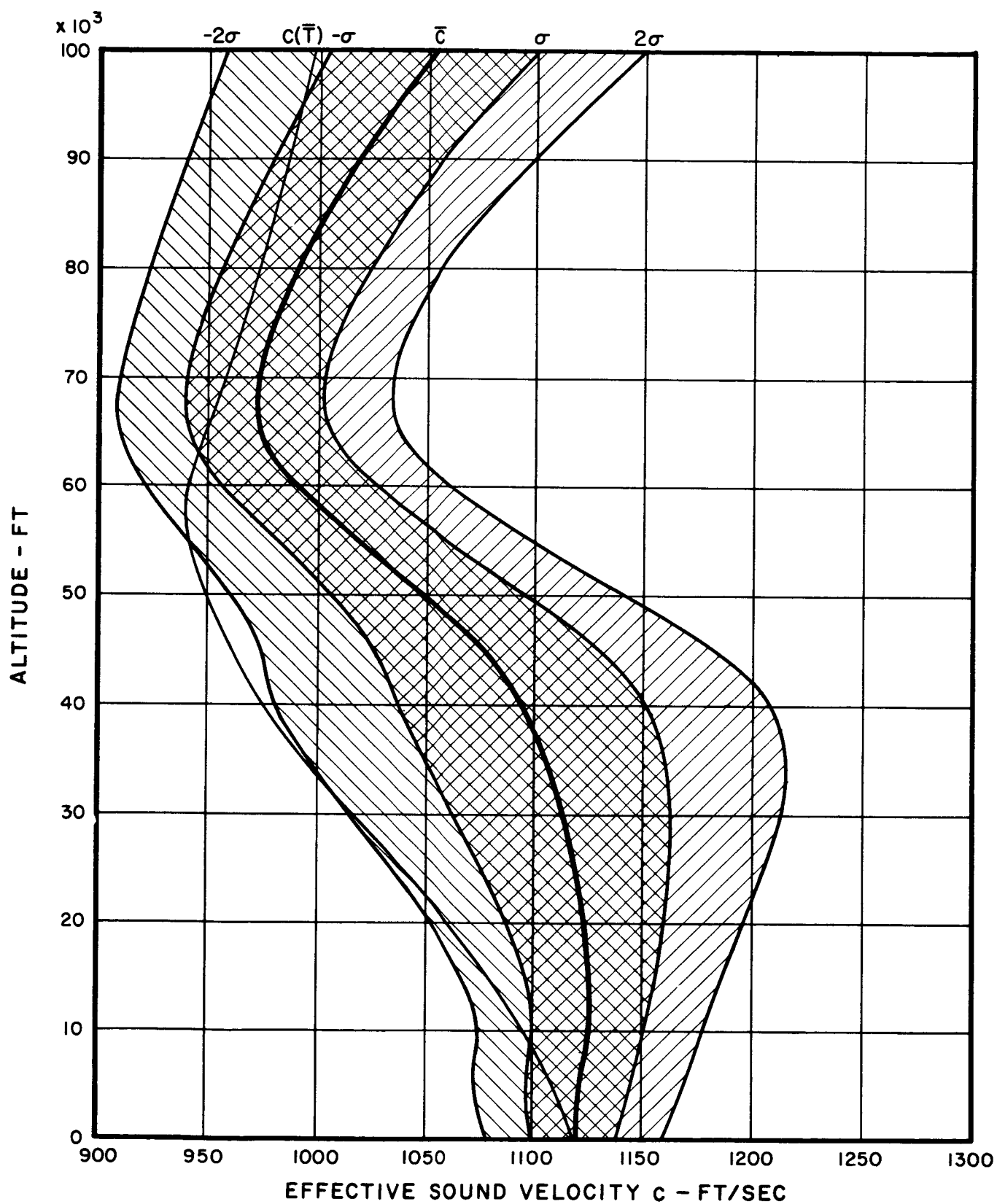


FIG. 7 - 6a PROBABILITY DISTRIBUTION OF SOUND VELOCITY FOR EASTERN SECTOR IN WINTER AT CAPE CANAVERAL

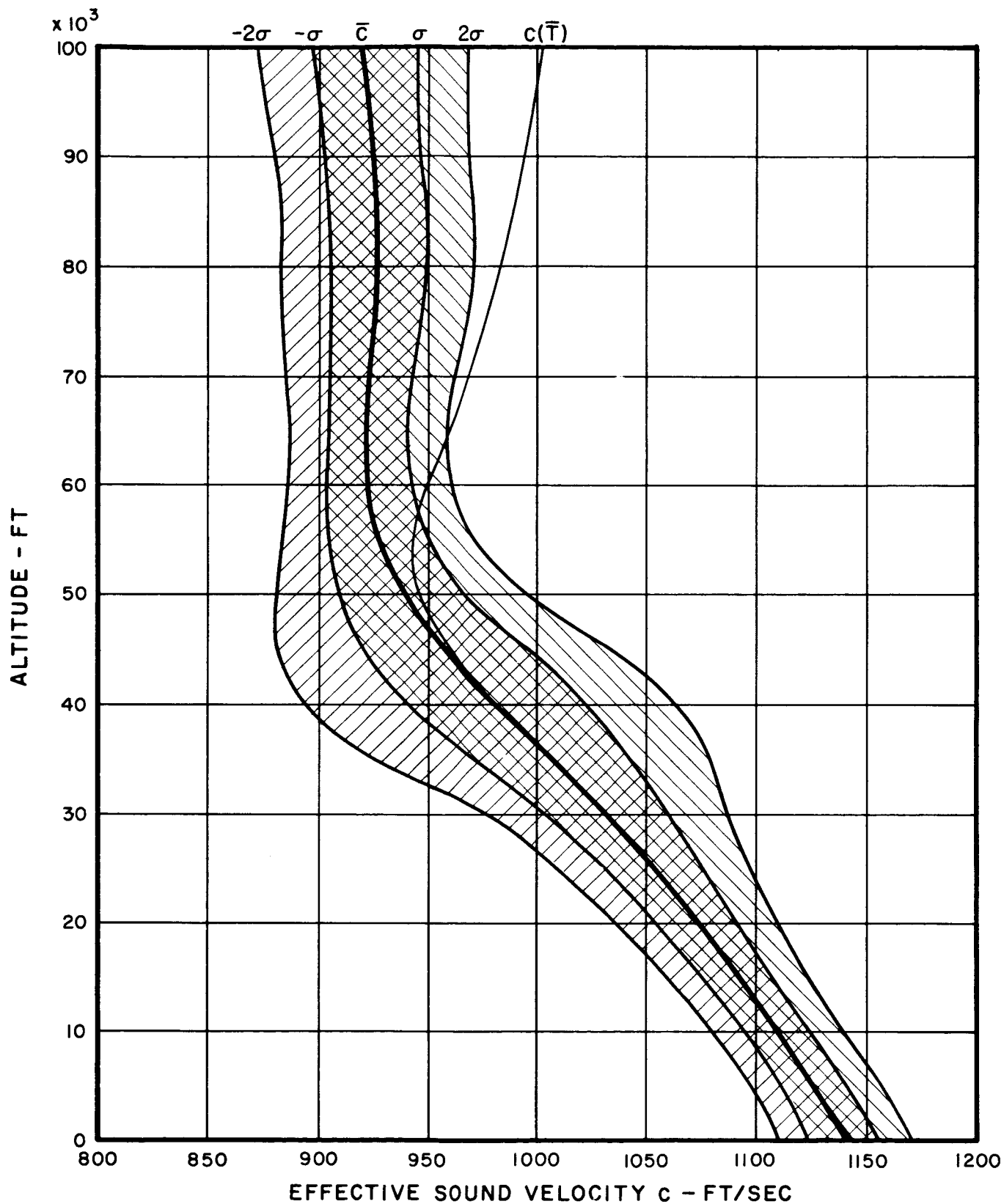


FIG. 7 - 6b PROBABILITY DISTRIBUTION OF SOUND VELOCITY FOR EASTERN SECTOR IN SUMMER AT CAPE CANAVERAL

assumption of horizontal homogeneity of atmospheric properties that is usually made in preparing estimates of acoustical hazards. This assumption is much more likely to be valid when the underlying surface is uniform than when the surface changes abruptly from water to land as it does to the west of the Cape Canaveral area. Also, water surfaces are not subject to the large diurnal variations characteristic of land surfaces and, consequently, the thermal structure of the lowest layers of the atmosphere tends to remain fairly constant. However, these considerations do not appear to be sufficient for making a strong argument in favor of an off-shore site on the basis of larger sound attenuations to be expected. Additional attenuation does accrue of course, from the increased distance of an off-shore site from existing structures and communities.

7.3.3 Properties of the Atmosphere -- Inland Site, Huntsville Area

Since the Huntsville Area is considered as a static test site, only the meteorological properties of the atmosphere in the first 30,000 ft were investigated. The continental-type climatic regime of the Huntsville area is typical of temperate-latitude sites located in moderately rough terrain. In fair weather in all seasons of the year, the thermal and wind structure of the lowest 5000 ft of the atmosphere is subject to marked diurnal variations brought about by the daytime solar insolation and nighttime radiational heat losses from the underlying surface. The sheltering effects of the topography tend to produce near-calm wind conditions at night and in the early morning at the surface with a consequent strong wind shear at the ridge lines when the prevailing flow is normal to the ridge axes. Large surface temperature inversions are characteristic

of the colder months of the year during the night and in the early morning. In winter, Huntsville is alternately exposed to invasions of tropical maritime air from the Gulf of Mexico and incursions of polar continental air from Canada. The winds aloft are generally from the west and the seasonal averages are quite similar to those observed at Cape Canaveral in winter except that the average speeds are from 10 to 20 ft per second higher. In summer, tropical maritime air brought by the southwesterly flow around the western extremity of the Bermuda anticyclone is usually present in the Huntsville area. The high moisture content and convective instability of this air mass result in considerable cumulus development culminating in frequent afternoon and evening thundershowers. Winds aloft are predominantly from the southwest.

These meteorological factors are evident in the probability distributions of the effective sound propagation velocity presented in Figures 7-7a through 7-10b. The only mean seasonal profile that shows an appreciable positive slope is that for the eastern sector in winter; in this case, the average seasonal velocity exceeds the value at the surface at all levels as shown in Figure 7-10a. The data indicate that there is at least a 50 percent probability of a positive slope (and likelihood of negative excess attenuation) in the eastern sector of the Huntsville site in winter. This is of great importance because of the proximity of important residential communities in that sector. Correspondingly, there is a very low probability of positive profile slopes in the western sector of the Huntsville site in winter as shown in Figure 7-8a. The profiles for the northern and southern sectors at Huntsville are generally similar except from 20,000 to 30,000 ft where the profiles for the northern sector (Figure 7-7a) show a smaller decrease of

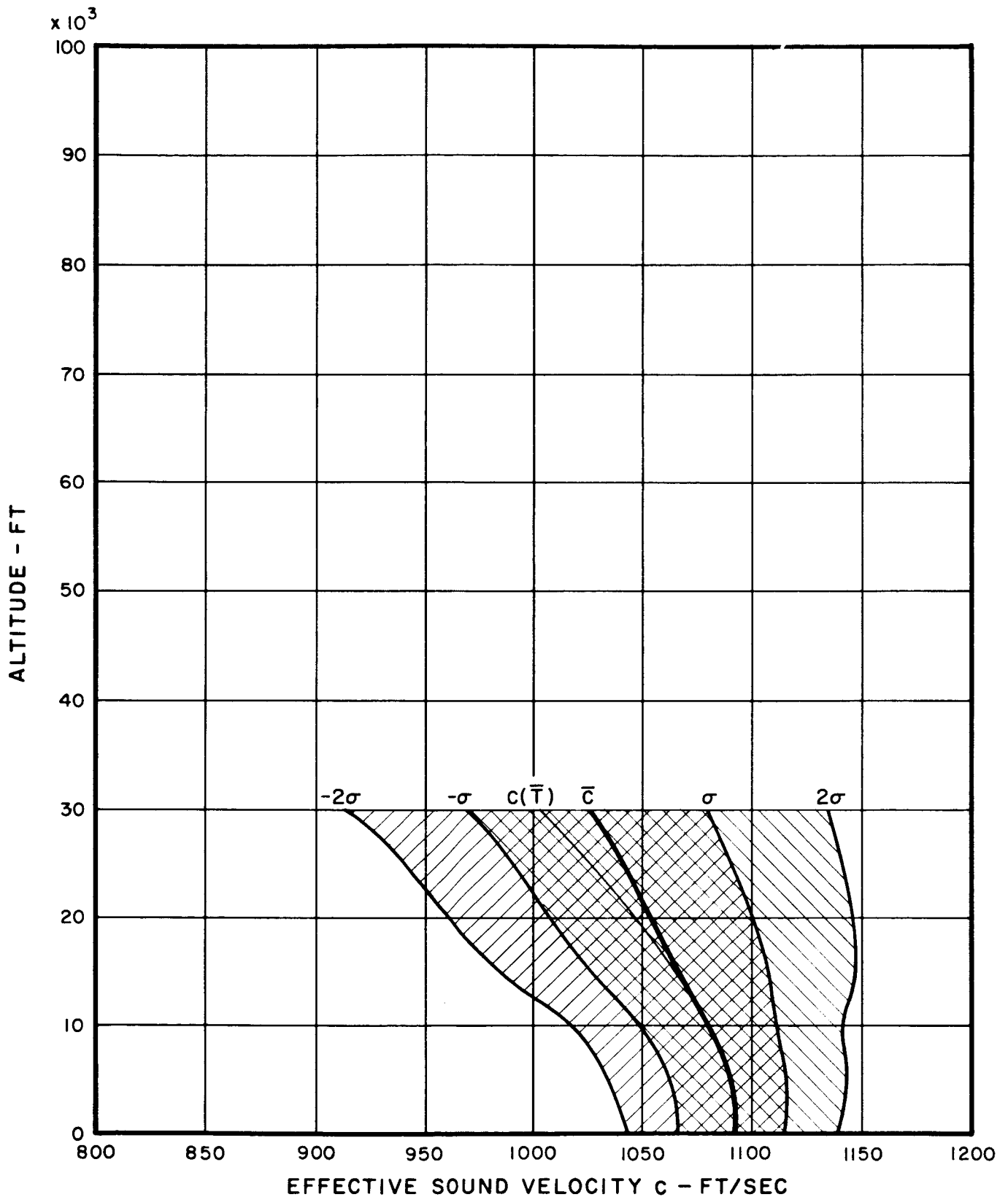


FIG. 7 - 7a PROBABILITY DISTRIBUTION OF SOUND VELOCITY FOR NORTHERN SECTOR IN WINTER IN HUNTSVILLE AREA

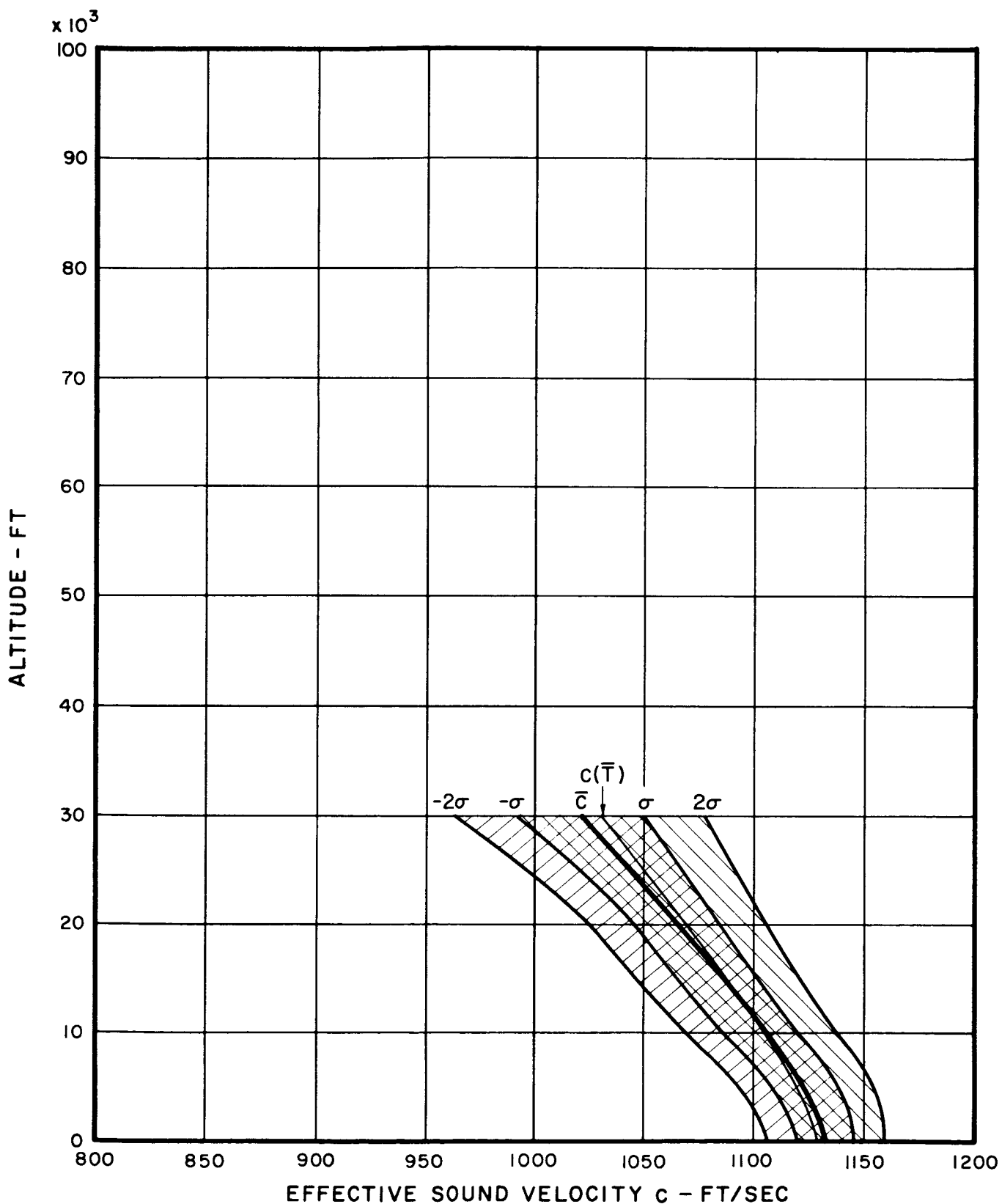


FIG. 7 - 7b PROBABILITY DISTRIBUTION OF SOUND VELOCITY FOR NORTHERN SECTOR IN SUMMER IN HUNTSVILLE AREA

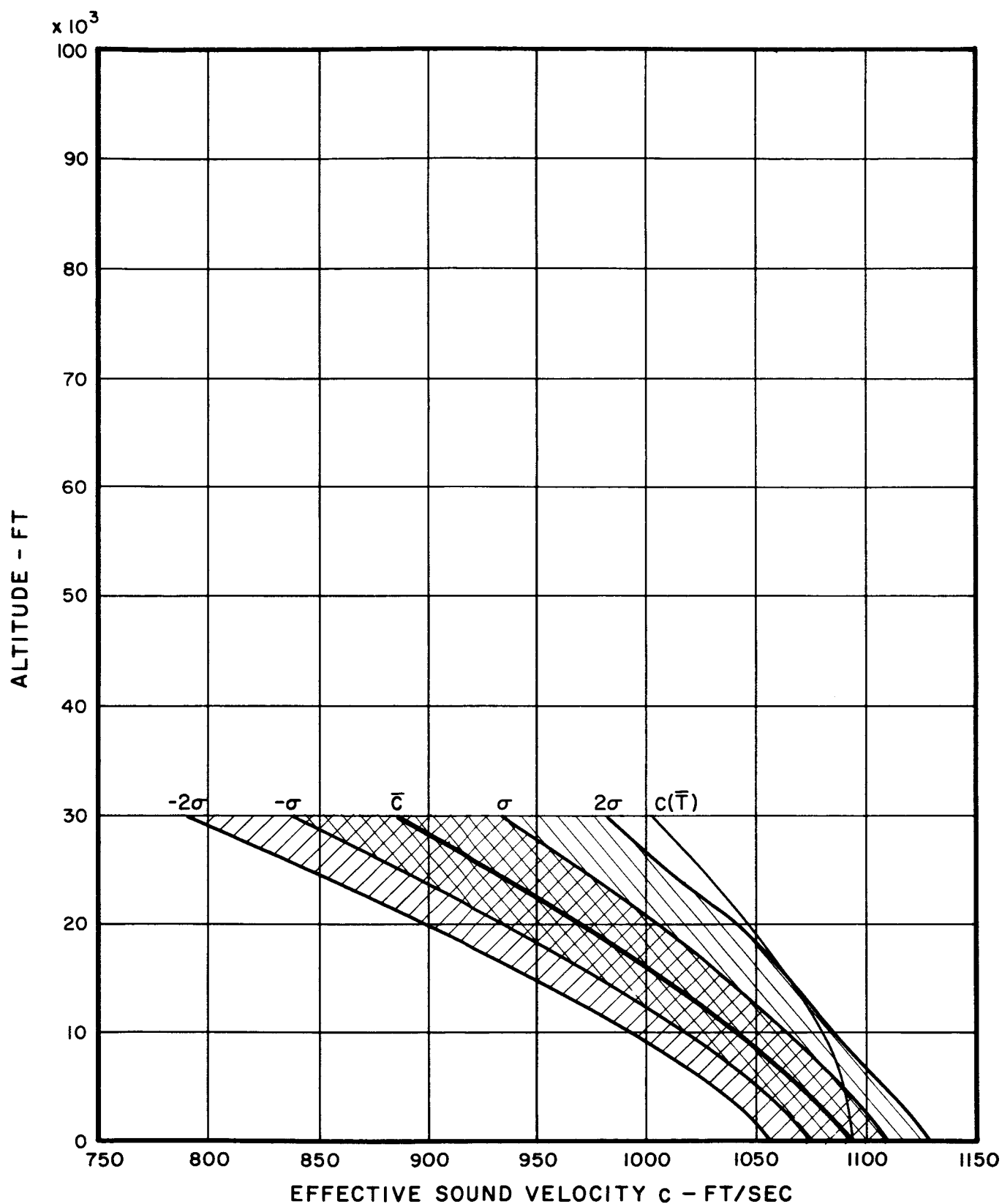


FIG. 7 - 8a PROBABILITY DISTRIBUTION OF SOUND VELOCITY FOR WESTERN SECTOR IN WINTER IN HUNTSVILLE AREA

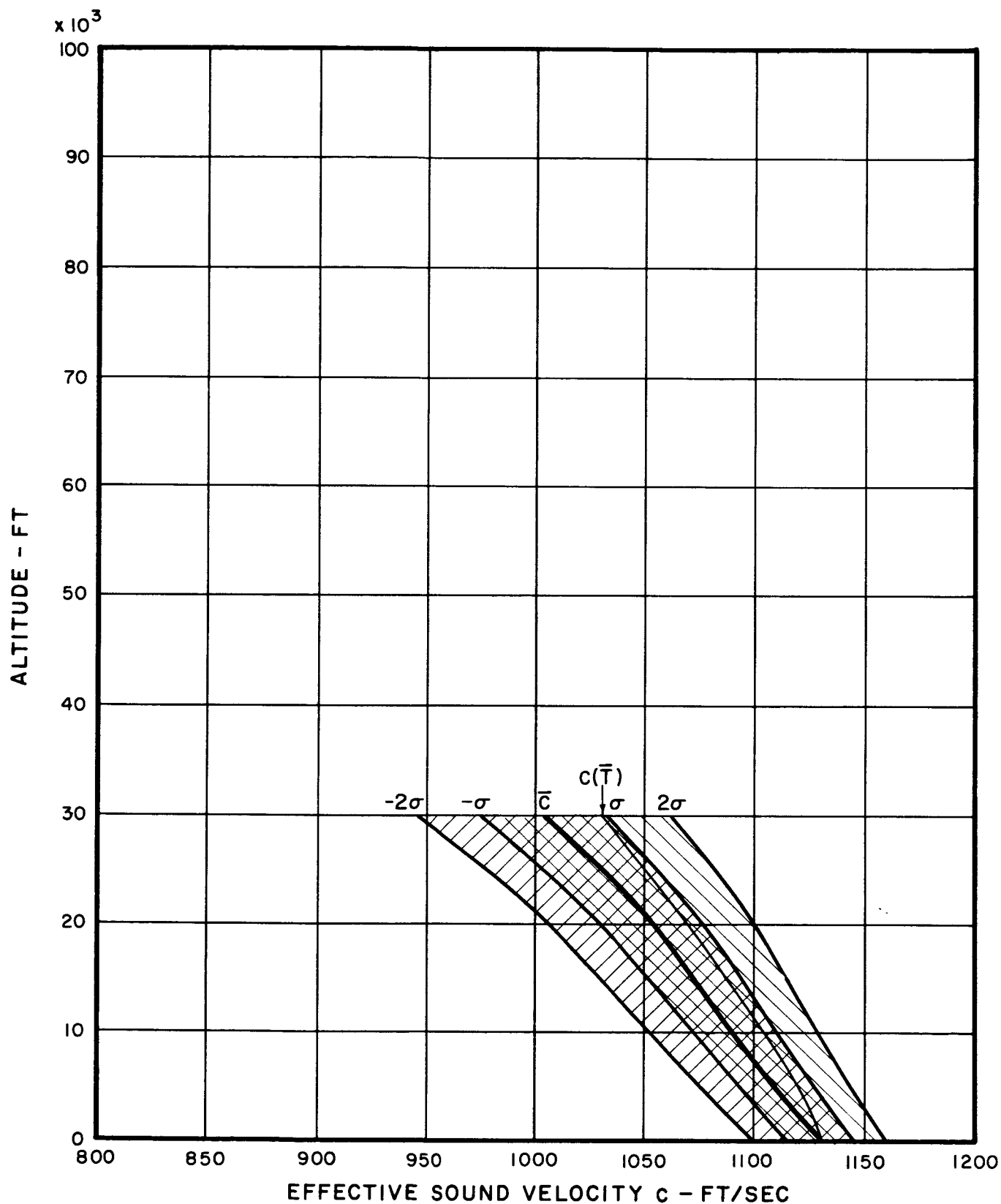


FIG.7 - 8b PROBABILITY DISTRIBUTION OF SOUND VELOCITY FOR WESTERN SECTOR IN SUMMER IN HUNTSVILLE AREA

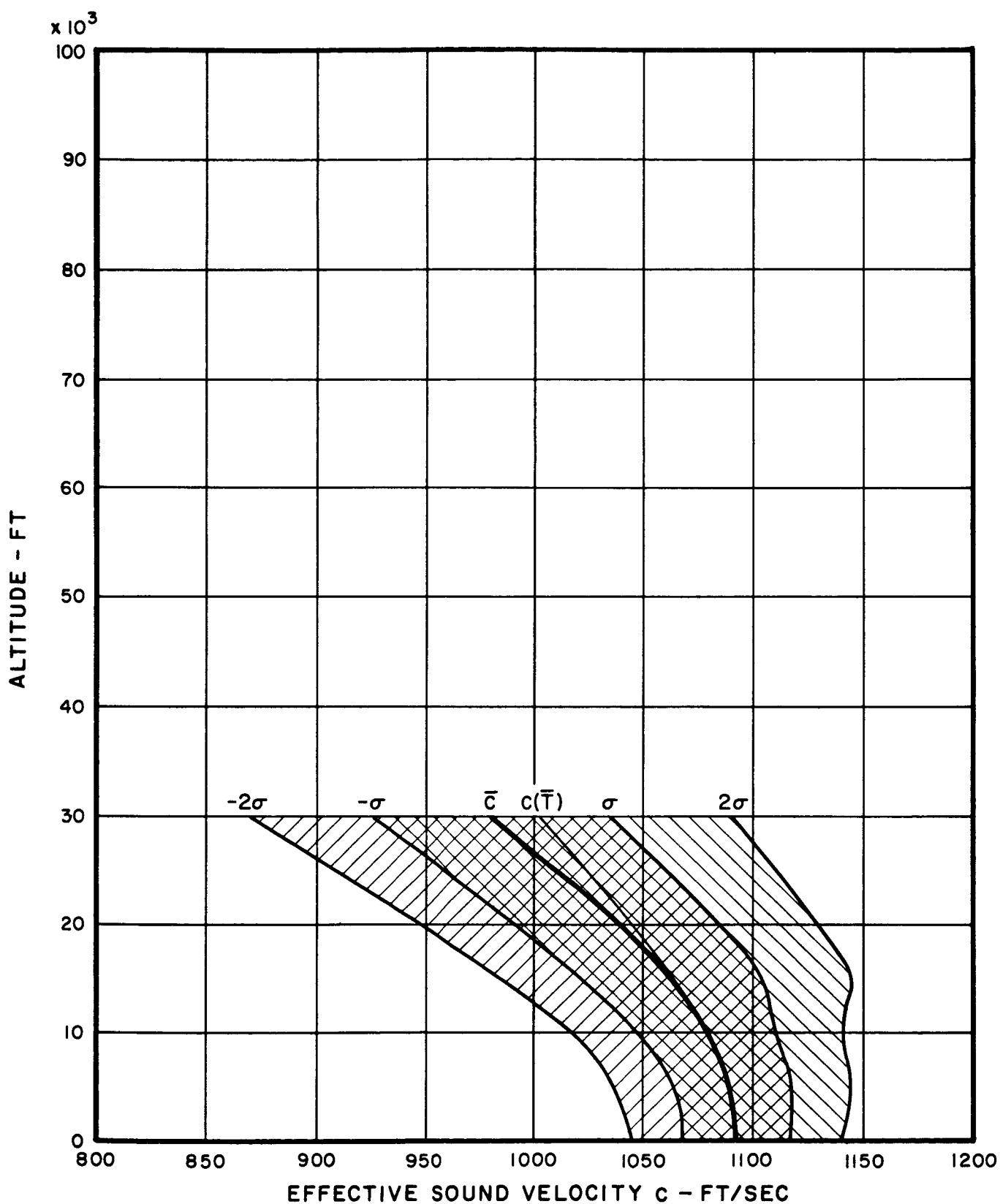


FIG. 7 - 9a PROBABILITY DISTRIBUTION OF SOUND VELOCITY FOR SOUTHERN SECTOR IN WINTER IN HUNTSVILLE AREA

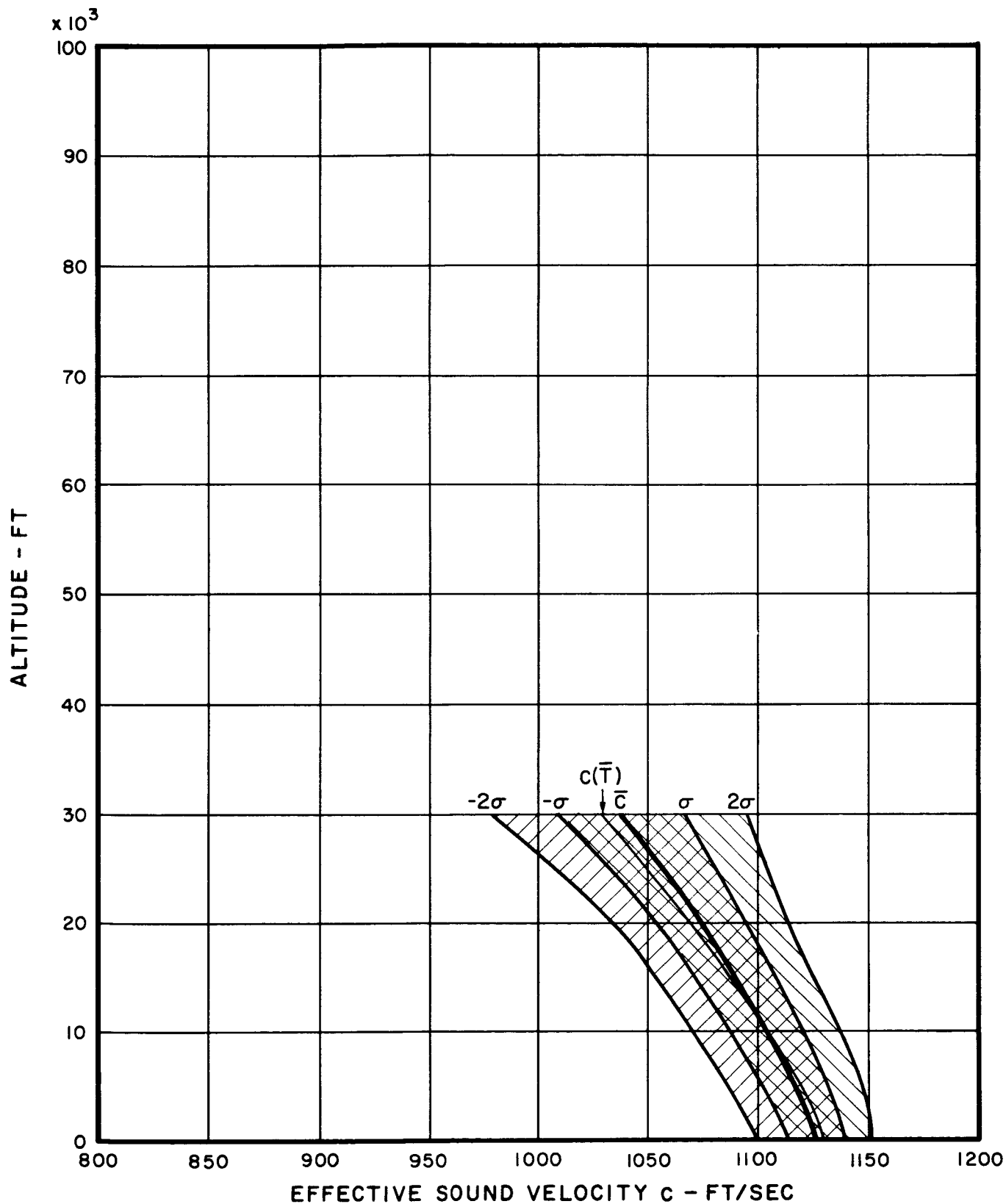


FIG.7 - 9b PROBABILITY DISTRIBUTION OF SOUND VELOCITY FOR SOUTHERN SECTOR IN SUMMER IN HUNTSVILLE AREA

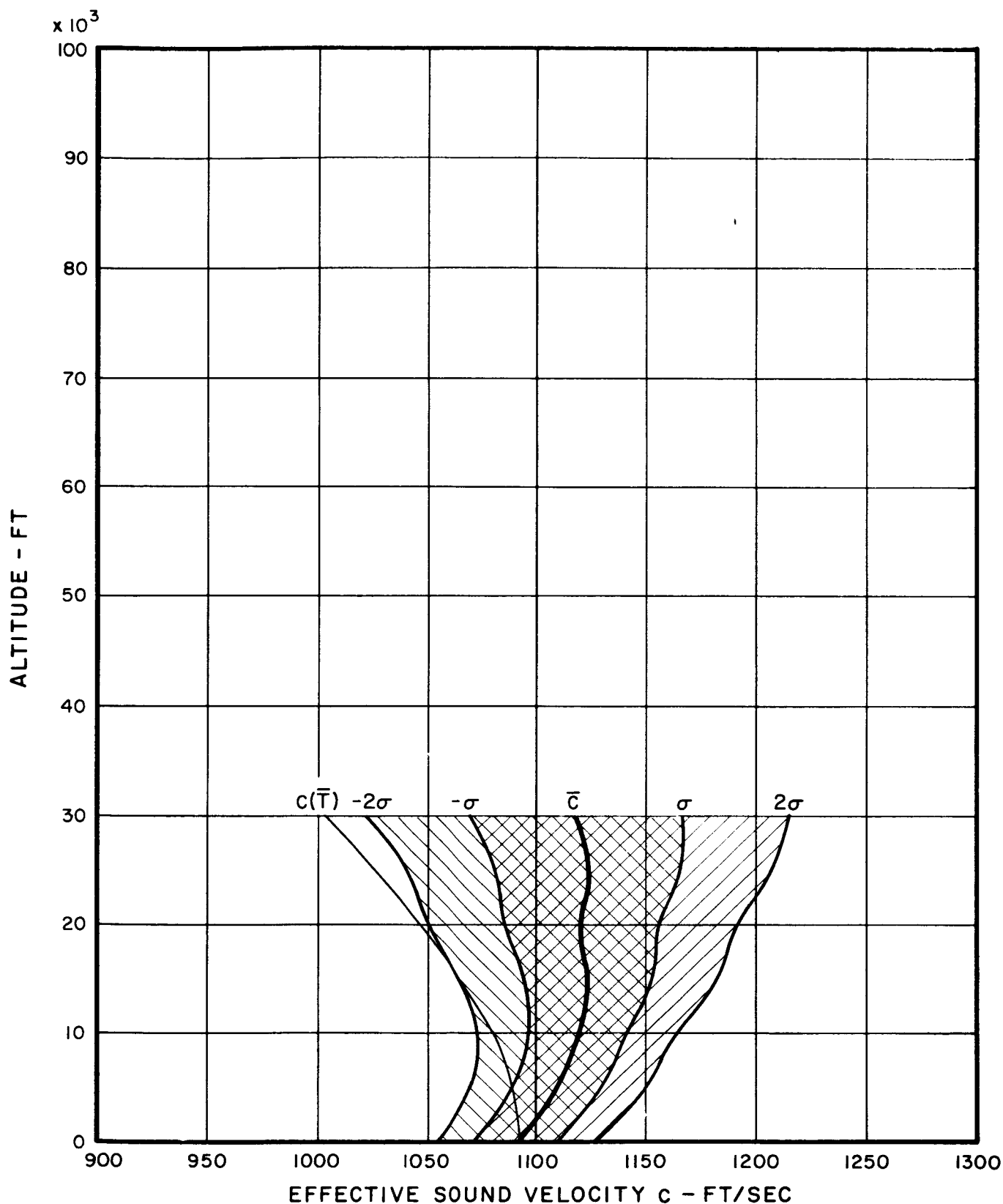


FIG. 7 - 10a PROBABILITY DISTRIBUTION OF SOUND VELOCITY FOR EASTERN SECTOR IN WINTER IN HUNTSVILLE AREA

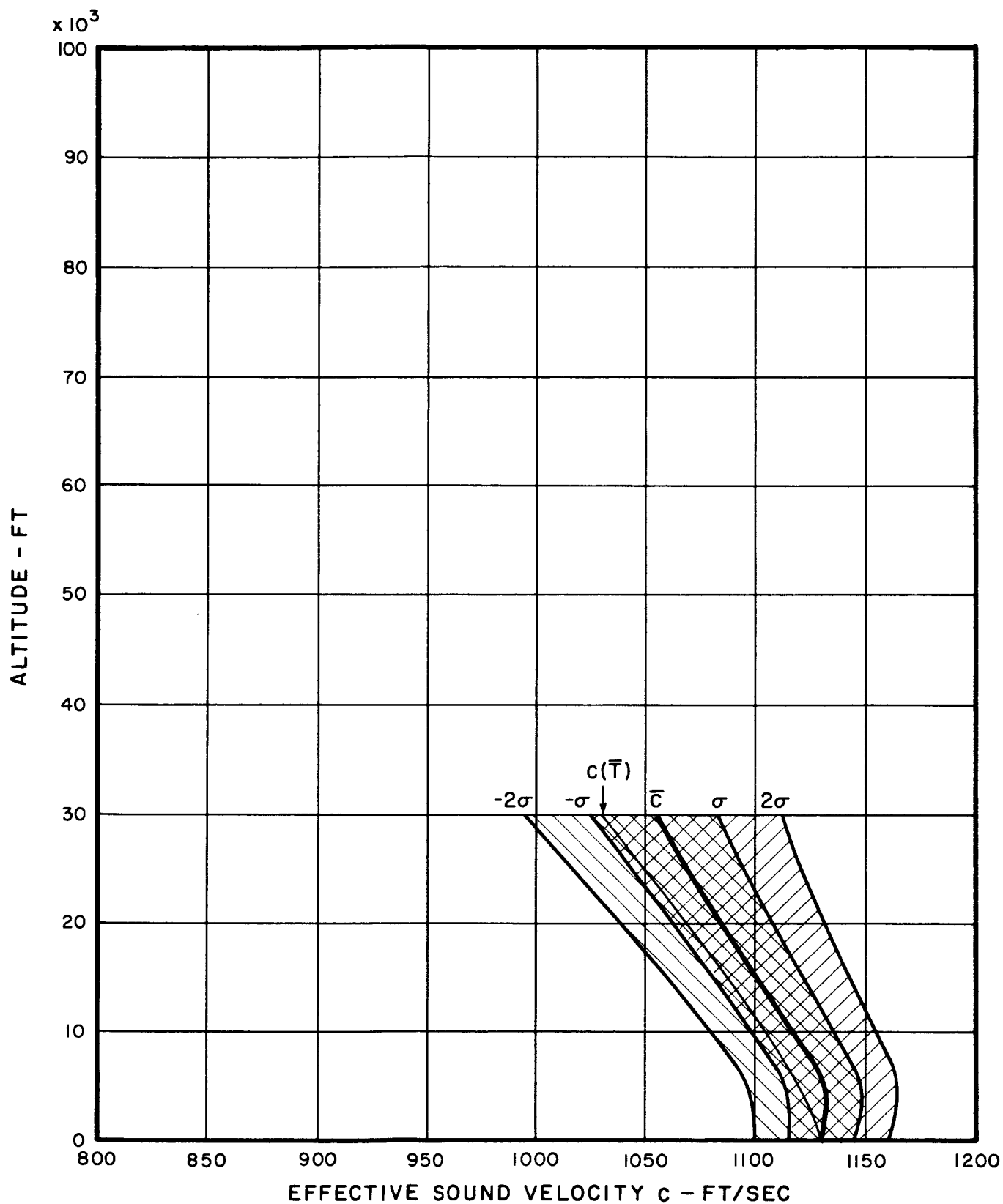


FIG.7 - 10b PROBABILITY DISTRIBUTION OF SOUND VELOCITY FOR EASTERN SECTOR IN SUMMER IN HUNTSVILLE AREA

the sound velocity with height than those for the southern sector (Figure 7-9a). It appears that there is some probability of a positive slope in the northern and southern sectors in winter in the Huntsville area within the first 5000 ft; this would be particularly valid in the late afternoon, evening, and early morning in the presence of near-neutral or stable temperature distributions along the vertical.

In summer, the eastern sector (Figure 7-10b) shows the highest probability of occurrence of a positive slope; the depth of the layer in which c might be expected to exceed the value at ground level being about 10,000 ft for the 0.2 probability level and about 25,000 ft for the 0.05 level. As shown in Figure 7-8b, the occurrence of positive profile slopes is least likely in the western slope. The probability distributions for the northern and southern sectors presented in Figures 7-7b and 7-9b, respectively, are generally similar and indicate probable occurrences of positive slopes that are approximately midway between those of the eastern and western sectors.

7.3.4 Properties of the Atmosphere - Point Arguello

The climatic regime at Point Arguello is similar in many respects to that at Cape Canaveral. During fair weather in all seasons of the year, the low-level atmospheric structure is predominantly influenced by onshore sea-breeze circulations during the solar day and by a weak land-breeze or drainage circulations at night. In winter, there are periodic incursions of polar maritime air associated with the arrival of cyclones along the Pacific branch of the polar front. The wind flow tends to be southerly in advance of

these frontal systems and then shifts sharply to the west and north after the frontal systems pass to the southeast. In summer, the thermal structure of the lowest layers at Point Arguello is dominated by the well-known West Coast temperature inversion that caps a shallow layer of marine air. This inversion is a permanent feature on the Point Arguello area during late spring, summer, and early fall; on the average, it is about 2500 ft deep. Winds aloft tend to be southwesterly below the tropopause and shift to the east in the lower stratosphere. The gradient flow at low levels in summer is from the northwest around the eastern extremity of the Pacific anticyclone.

The probability distributions of the effective sound propagation velocity for Point Arguello during the summer and winter seasons are shown in Figures 7-11a through 7-14b. The slope of the average seasonal profiles does not increase with height in the troposphere in any of the winter distributions. In the eastern sector (Fig. 7-14a) and the southern sector (Figure 7-13a) there is some probability of a positive slope. In the former case, the depth of the layer in which there is a 20 percent probability that c exceeds the ground-level value is approximately 30,000 ft while the 0.05 probability distribution indicates a depth of about 50,000 ft. In the southern sector, the corresponding layers have heights of about 15,000 ft and 35,000 ft, respectively. The western sector (Figure 7-12a), as might be expected, shows appreciable negative profile slopes. Hence, excess attenuations over the Pacific Ocean will likely be appreciable. The profiles in the northern sector (Figure 7-11a) indicate only a small probability of negative excess attenuation effects. The top of the layer in which c exceeds the value at ground level is about 20,000 ft for the 2 σ profile there. The sound duct in the upper troposphere and lower stratosphere is evident in all of the winter sectors.

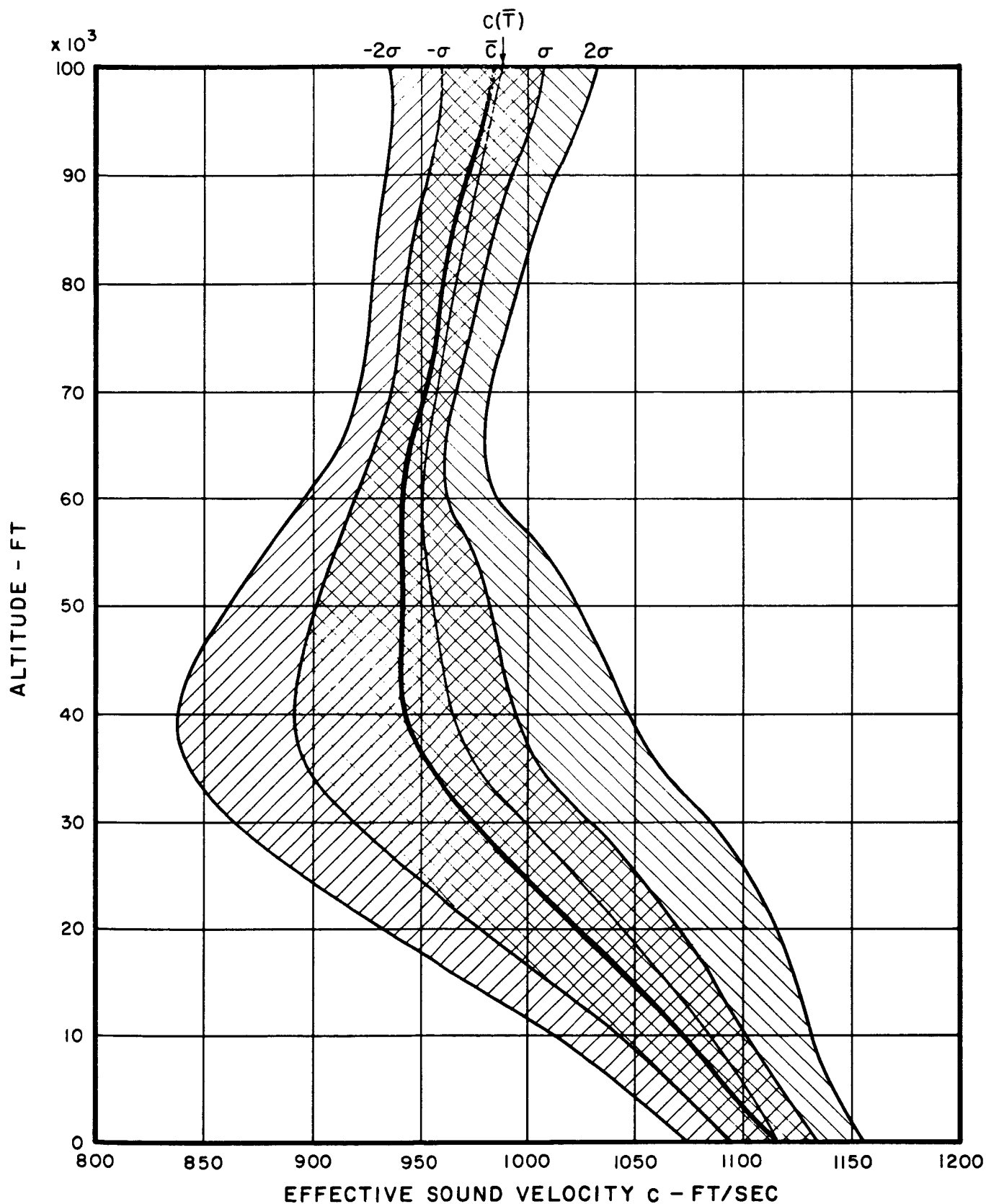


FIG. 7 - IIa PROBABILITY DISTRIBUTION OF SOUND VELOCITY FOR NORTHERN SECTOR IN WINTER AT POINT ARGUELLO

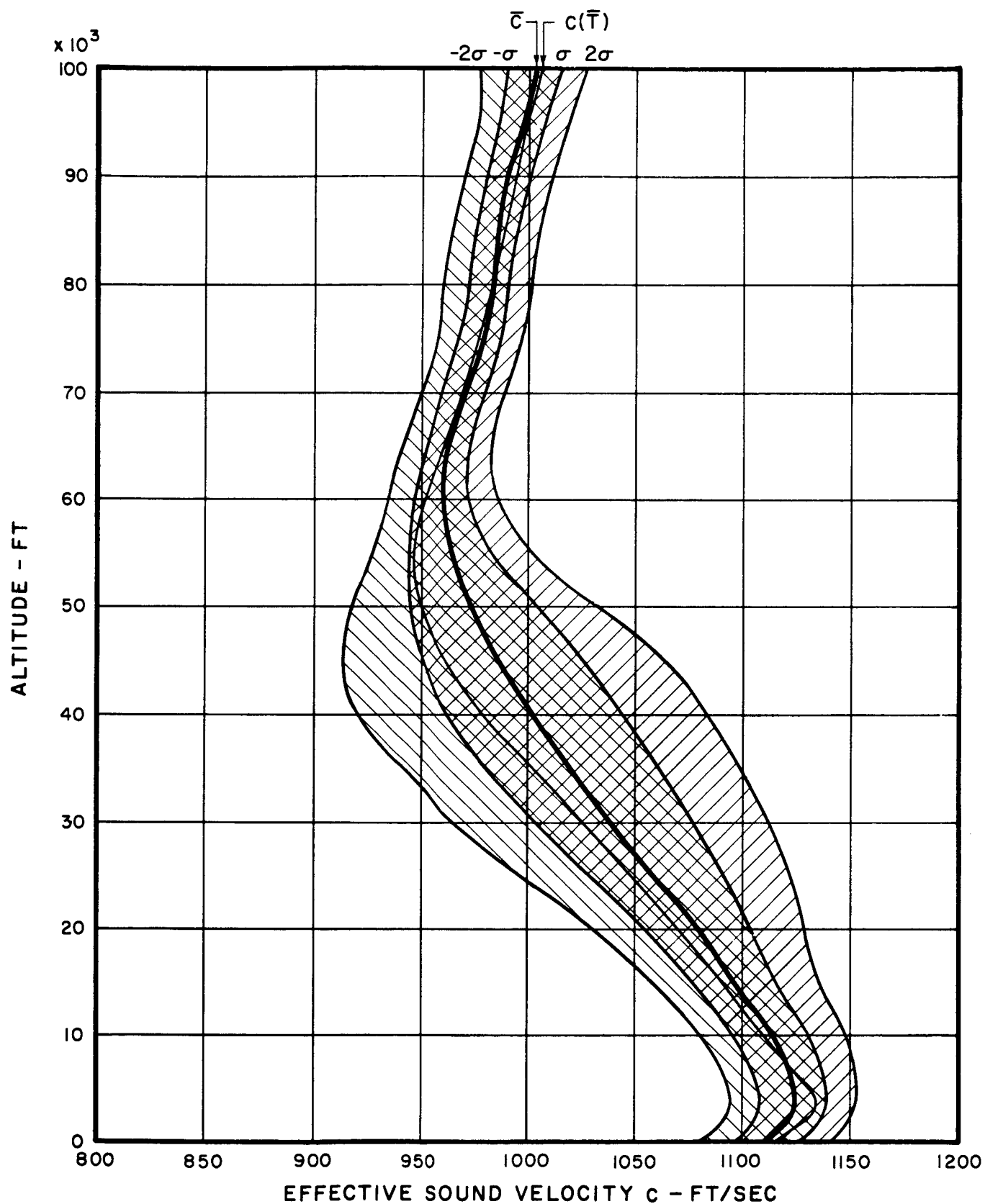


FIG.7 - IIb PROBABILITY DISTRIBUTION OF SOUND VELOCITY FOR NORTHERN SECTOR IN SUMMER AT POINT ARGUELLO

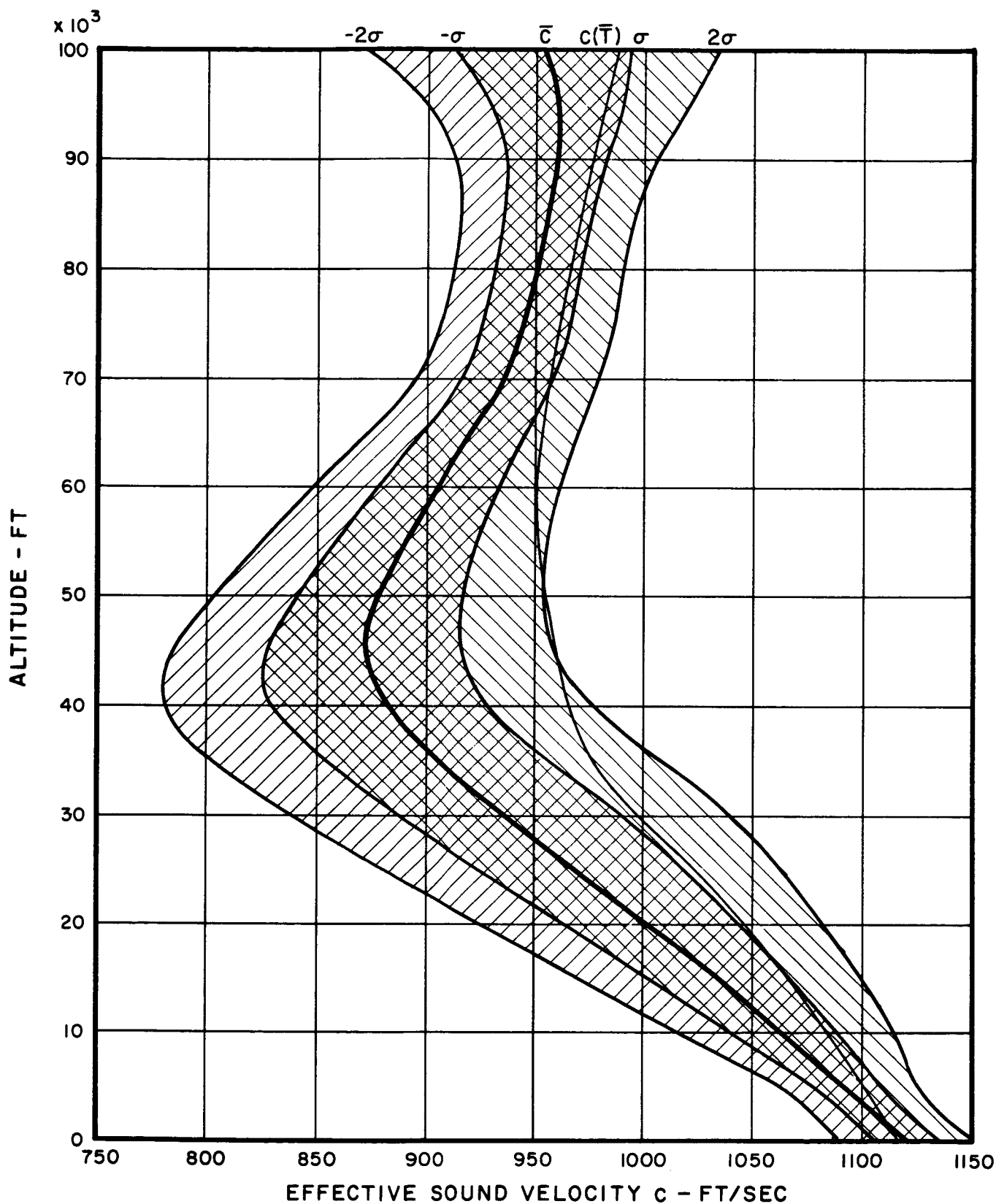


FIG. 7 - 12a PROBABILITY DISTRIBUTION OF SOUND VELOCITY FOR WESTERN SECTOR IN WINTER AT POINT ARGUELLO

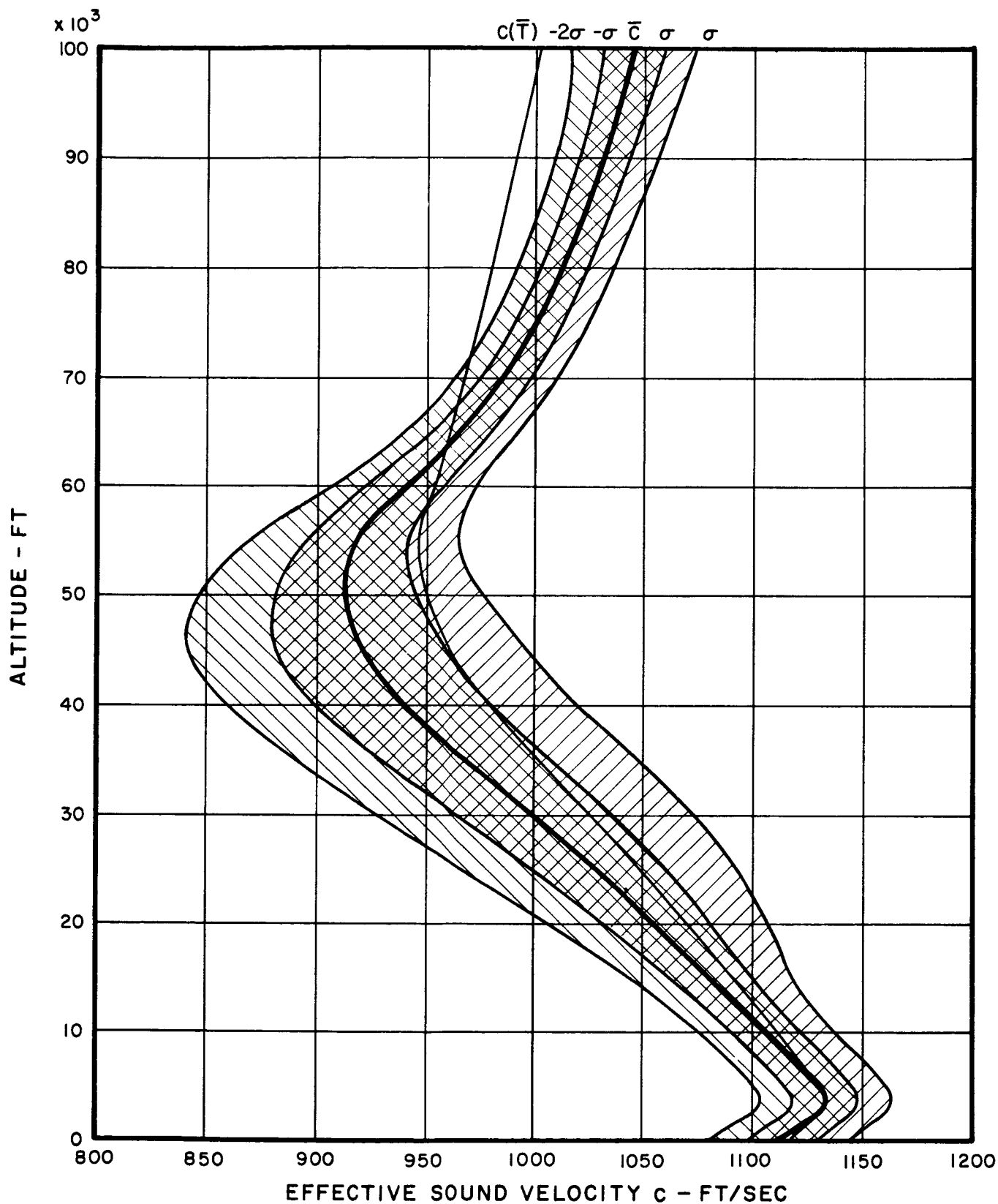


FIG. 7 - 12b PROBABILITY DISTRIBUTION OF SOUND VELOCITY FOR WESTERN SECTOR IN SUMMER AT POINT ARGUELLO

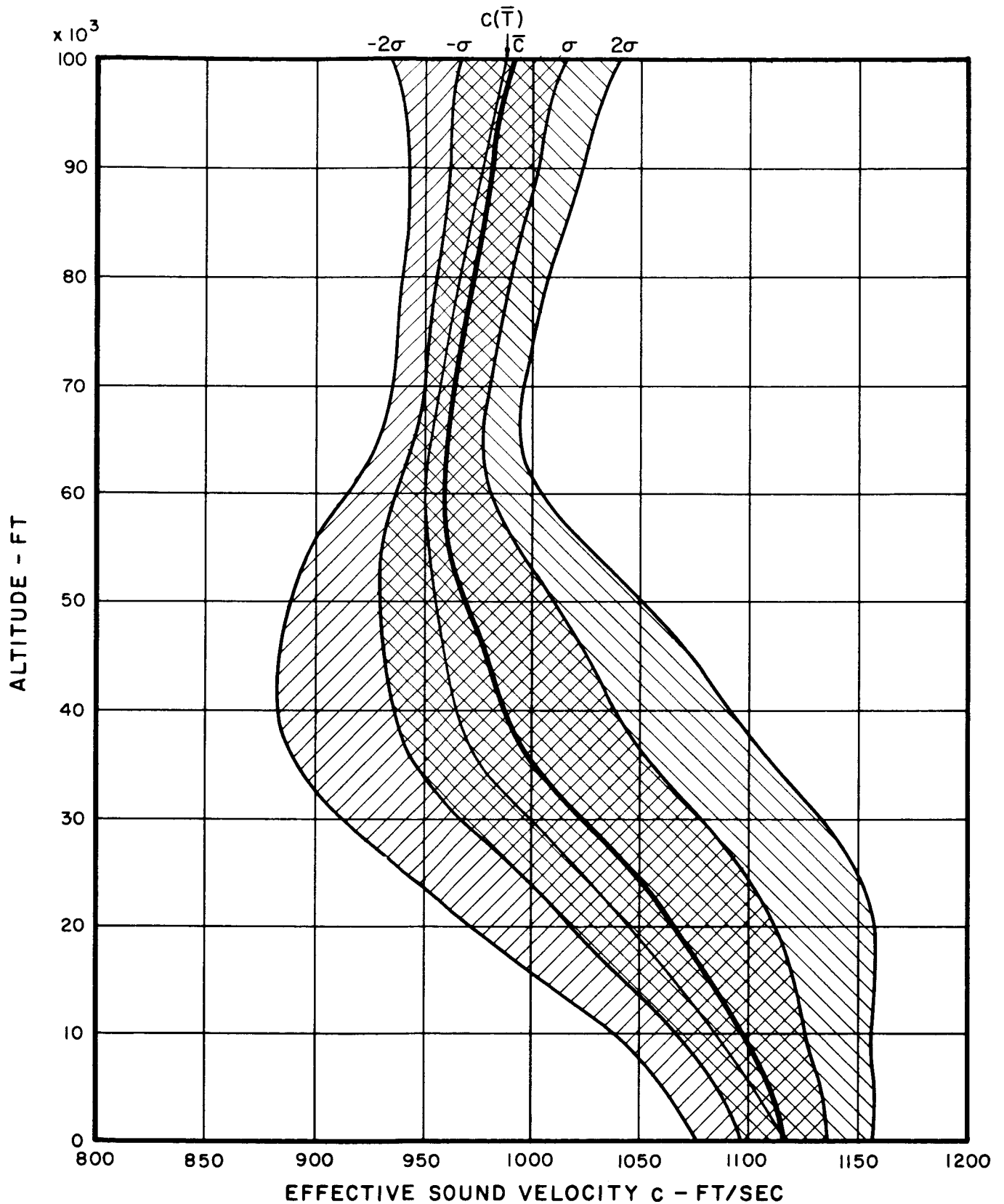


FIG. 7 - 13a PROBABILITY DISTRIBUTION OF SOUND VELOCITY FOR SOUTHERN SECTOR IN WINTER AT POINT ARGUELLO

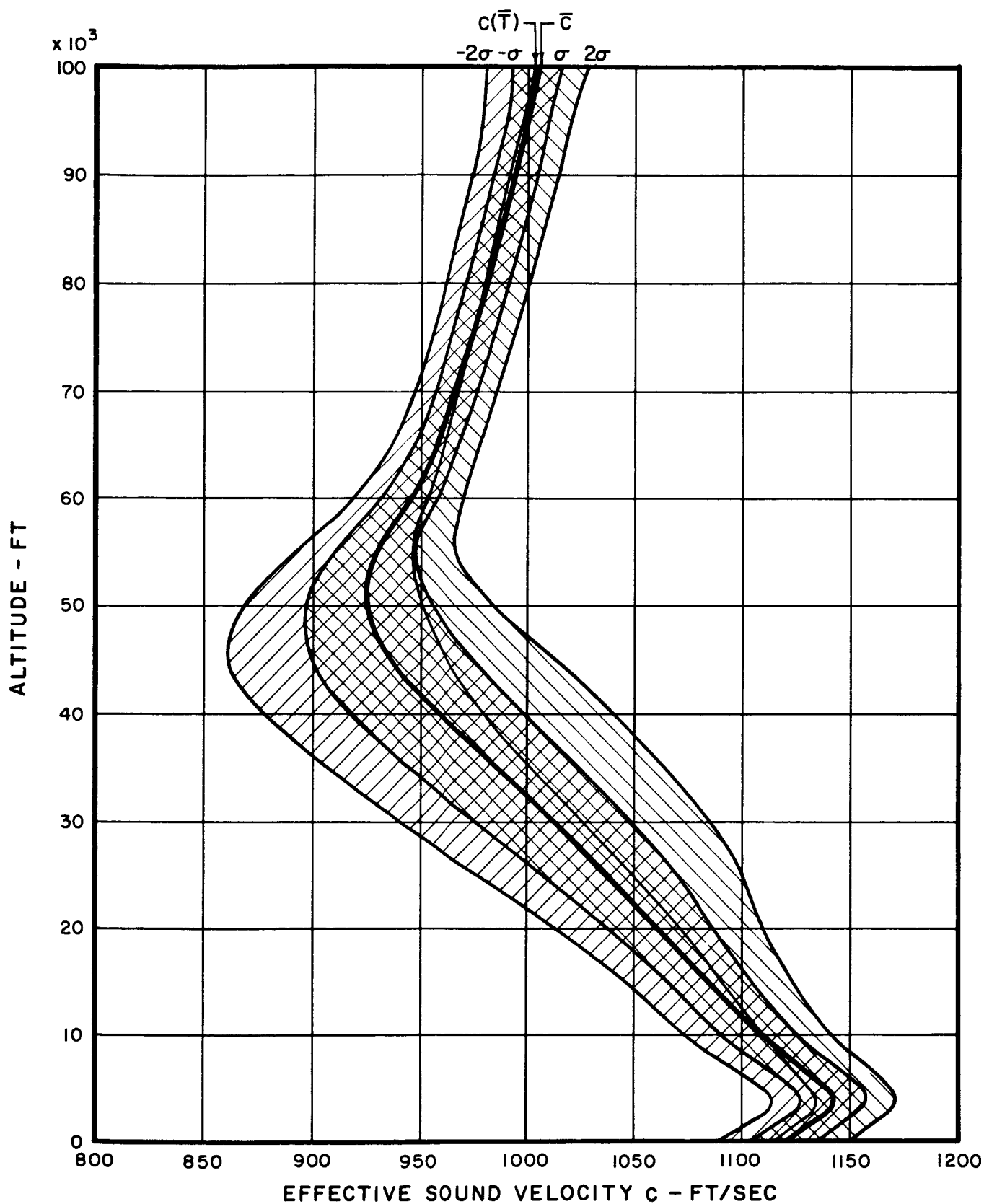


FIG. 7 - 13b PROBABILITY DISTRIBUTION OF SOUND VELOCITY FOR SOUTHERN SECTOR IN SUMMER AT POINT ARGUELLO

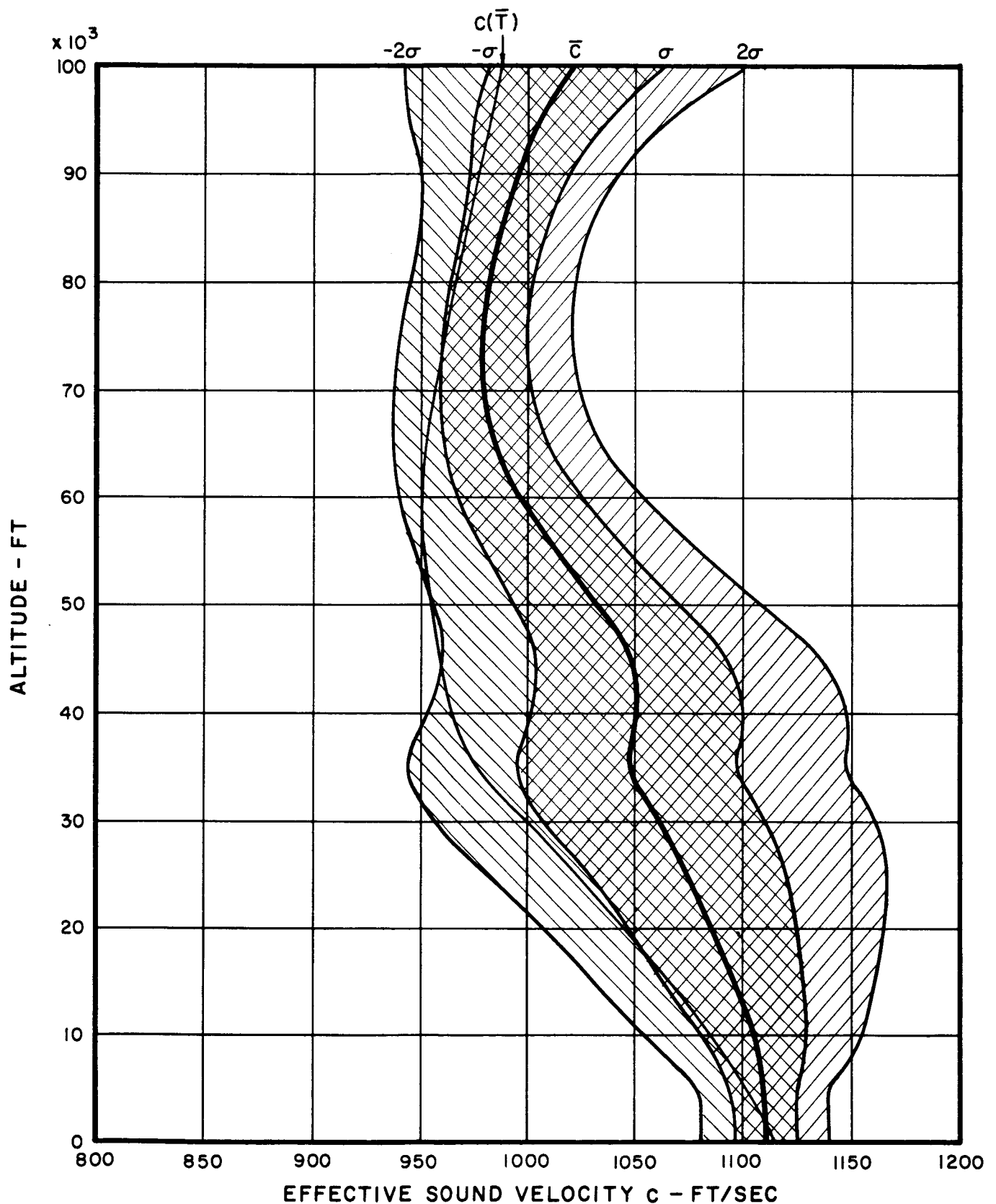


FIG. 7 - 14a PROBABILITY DISTRIBUTION OF SOUND VELOCITY FOR EASTERN SECTOR IN WINTER AT POINT ARGUELLO

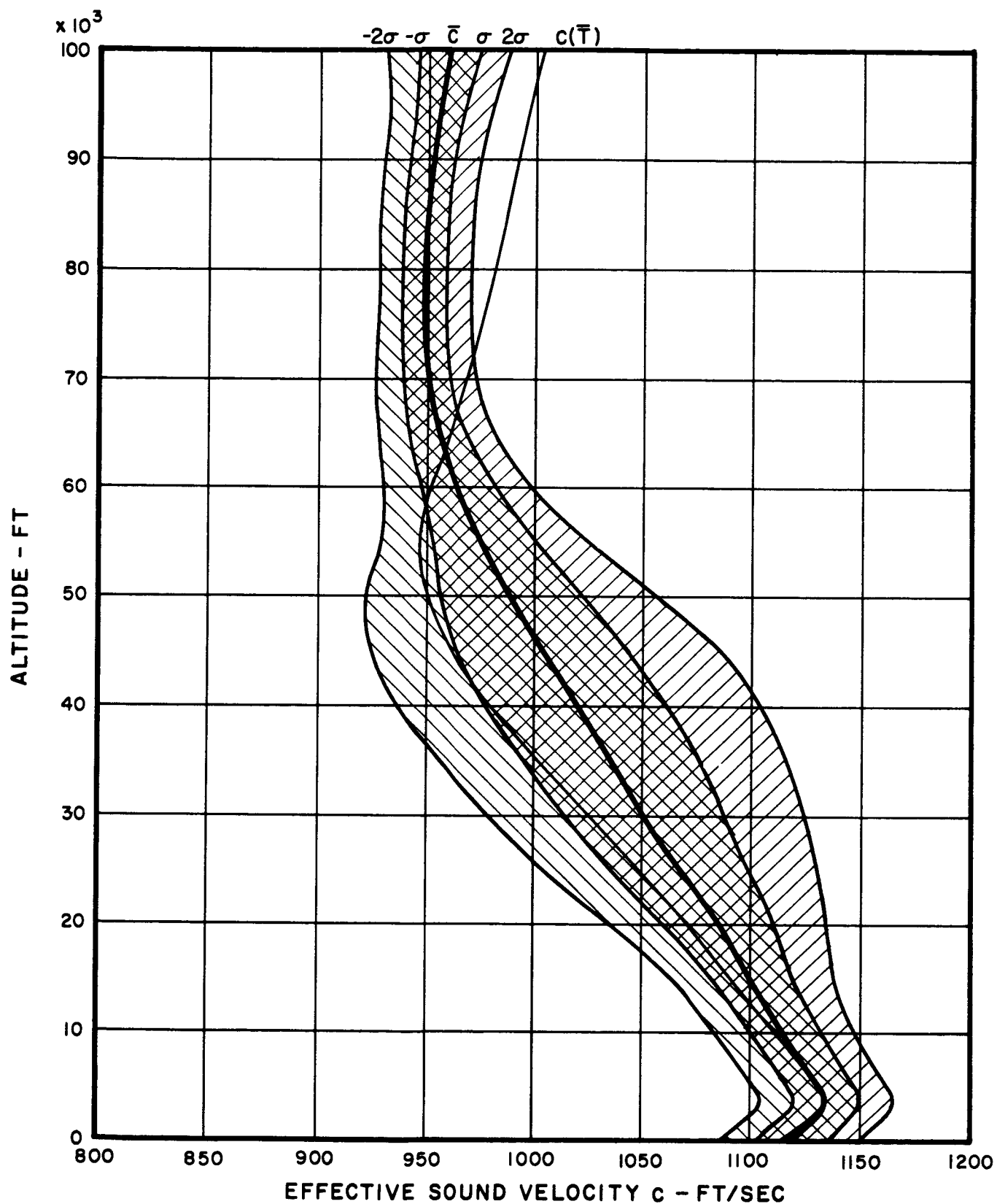


FIG. 7 - 14b PROBABILITY DISTRIBUTION OF SOUND VELOCITY FOR EASTERN SECTOR IN SUMMER AT POINT ARGUELLO

In summer, the average seasonal profiles show a positive slope for all sectors in the layer from ground level to about 3000 ft due to the low-level temperature inversion. The average value of the slope due to temperature alone is approximately 20 ft per second per 2000 ft. In summer, this inversion appears to be the principal factor in determining positive profile slopes at low levels at Point Arguello. After lift-off, the possible downward refraction of sound waves appears to be terminated when the vehicle reaches the top of the inversion.

7.4 Sound Attenuation by Obstacles and Barriers

The question is frequently asked concerning the attenuation of sound provided by natural or man-made obstacles and barriers interposed between source and receiver. These include walls, fences, woods or natural barriers provided by the terrain. Such barriers have been shown to be effective if their dimensions are large relative to the wavelength of sound and provided they are placed reasonably close to the source of sound, shielding it from the receiver. If the source can be seen directly from the receiving position effective acoustic shielding is not being provided by the barrier. Clearly, this makes barriers ineffective in any launch situation.

But even in a static testing situation where the source of sound is near the ground only very large barriers, such as natural hills or mountains can be effective, because of the predominantly low-frequency character and therefore large wave-lengths of the noise from large rocket engines. (e.g., see subsequent Fig. 9-3) Consequently, for conservative engineering estimates the effect of barriers is best neglected. Moreover, further work is needed to assess quantitatively the shielding effects of hills on low-frequency noise in the presence of wind and temperature gradients.

7.5 Sound Attenuation by Structures and Enclosures

Up to now, it was assumed that the receiver is in the open, directly exposed to the noise from the rocket engines. If this is not the case, e.g., when it is desired to estimate the sound pressure levels inside the payload capsule of a space vehicle, or inside a building on the ground, the noise reduction afforded by the enclosure must be taken into account. Again, valid data for a variety of structures at the low frequencies of greatest concern here are not available. Figure 7-15 shows the noise reduction (i.e., the difference, in decibels, of the sound pressure levels outside and inside) afforded by contemporary space capsules. The data were obtained from measurements on the guidance instrumentation canisters of the SA-1 Saturn configuration, and from measurements on a Mercury capsule for frequencies above about 50 cps. The data below 50 cps were obtained by extrapolation.

Corresponding results obtained from measurements of conventional frame houses exposed to airplane noise, and extrapolated to low frequencies are shown in Fig. 7-16.

More data obtained by direct measurements on low-frequency noise on a variety of structures of interest are needed here.

7.6 Attenuation of Ground Vibrations

The response of building structures is believed to be more critically determined by the horizontal component of the ground vibrations rather than by the vertical component. Present indications are

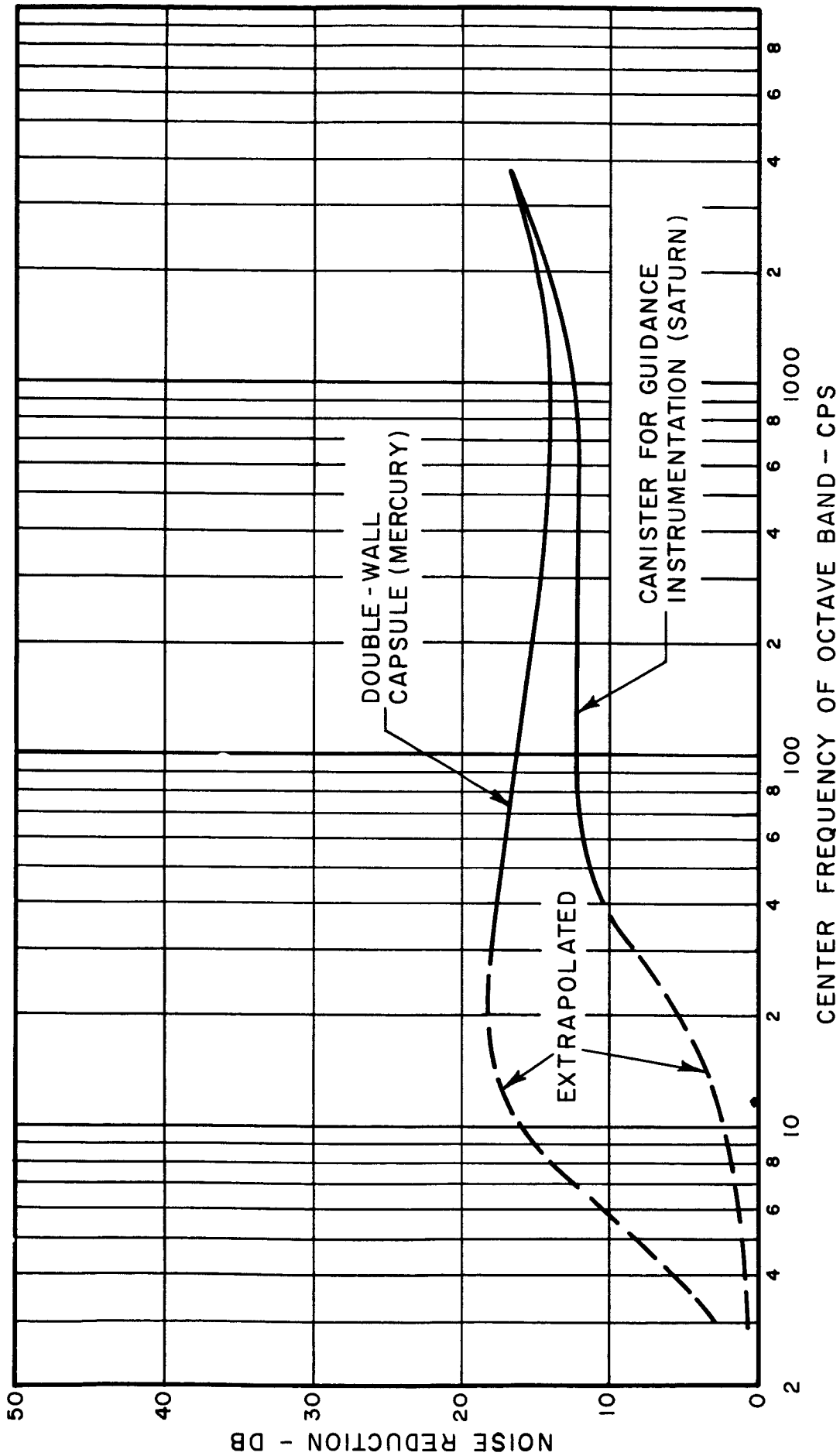


FIG. 7-15 NOISE REDUCTION AFFORDED BY CONTEMPORARY SPACE CAPSULES AND CANISTERS

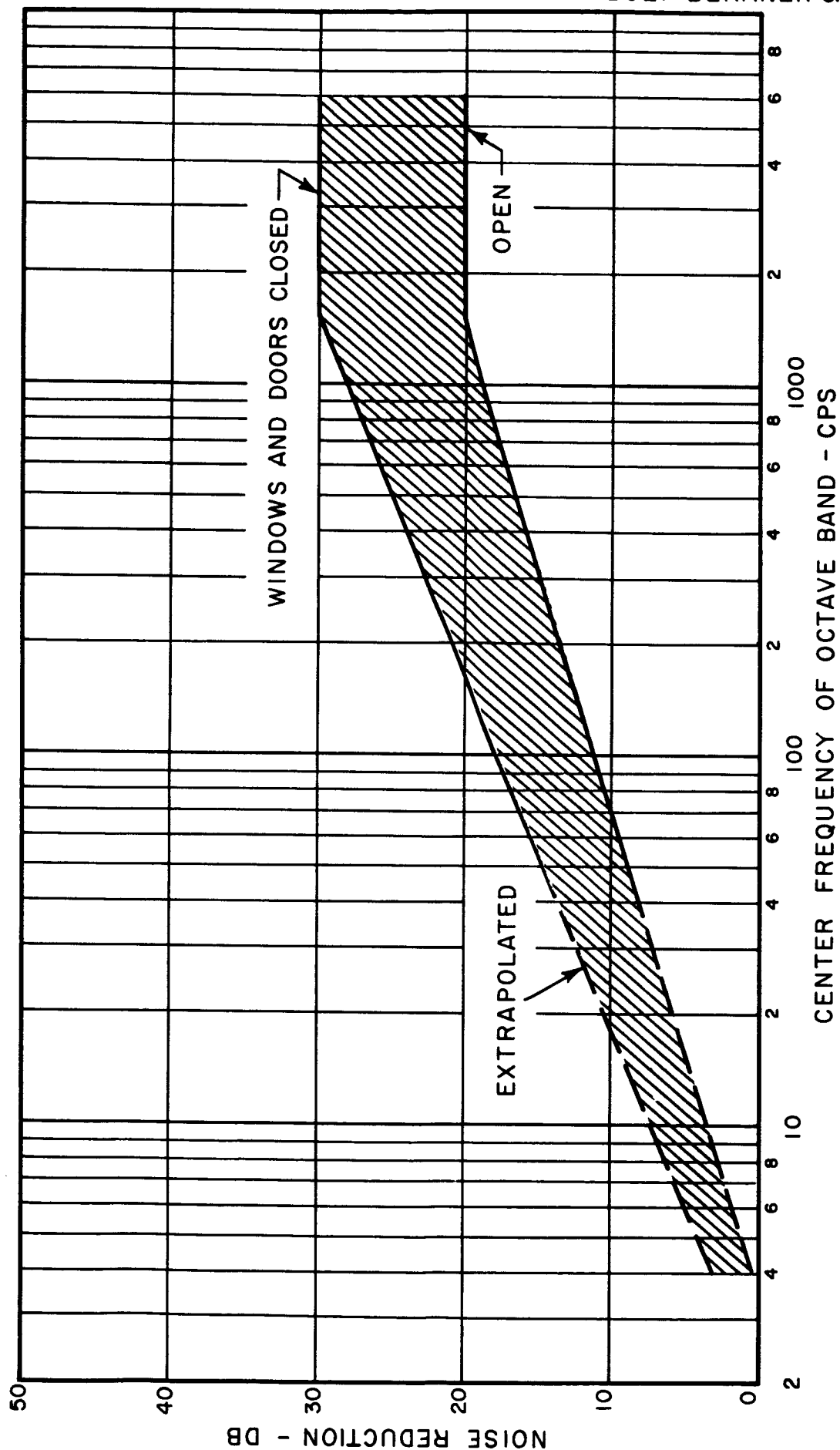


FIG. 7-16 NOISE REDUCTION AFFORDED BY CONVENTIONAL FRAME HOUSE CONSTRUCTION

that the horizontal component of ground vibrations is very rapidly attenuated in sandy or loose soil, but systematic data on the attenuation as a function of soil properties, sub-soil conditions, frequency dependence, etc., are not available.

More data are urgently needed here also.

8. THE RECEIVER

8.1 Concept of Noise and Vibration Criteria

The response of the receiver insofar as this study is concerned, is specified in terms of the noise levels not to be exceeded. The penalty for exceeding these levels, in its mildest form, may take the form of annoyance or temporary hearing loss in the case of people exposed to the noise. In case of building structures the penalty may be incurred in the form of rattling doors or windows, or cracks in masonry construction due to airborne sound or structure-borne vibrations. Excessive sound levels may lead to window breakage and other structural damage. In the case of electronic or other control equipment excessive sound pressure or structure-borne vibration levels may lead to malfunctioning and finally permanent damage of the equipment or its critical components.

Although acoustical or vibration criteria are frequently given in terms of a single number, i.e., the maximum overall sound pressure (or acceleration) level, it is absolutely essential to consider the criteria levels as a function of frequency. All receivers, be they humans, structures, amplifiers, or relays and similar equipment, respond differently at different frequencies. The acoustical properties of the transmission path change with frequency and the rocket noise levels themselves vary with frequency. Consequently, noise criteria must be given as a function of frequency. This is usually done by specifying the octave band sound pressure levels not to be exceeded. Noise criteria are at present specified in terms of octave band levels which cover the spectrum of audible frequencies only beginning at about 20 cps. However, as was seen from the preceding discussion, noise from large rocket engines

contains appreciable energy at the very low audible and sub-audible frequencies. (See also subsequent Figs. 9-2 through 9-6.) At these frequencies criteria levels are not generally available and additional work is urgently needed to fill the gap.

In the following, acoustical (noise) criteria for various classes of receivers will be discussed and estimates on the basis of existing information will be given. This will frequently have to be done, of necessity, by extrapolation in the frequency domain.

The differences, in db, between predicted noise levels and the appropriate criteria levels represent the required noise reduction in each octave band. Effective noise reduction at the very low frequencies is a field requiring further study, in many cases, and its discussion is beyond the scope of this report.

Note that the general concepts discussed above apply to structure-borne vibrations as well.

8.2 Criteria for Personnel

The effects of high-level noise on humans can be classified into various categories. Noise can affect the auditory mechanism, resulting in temporary or permanent deafness. Exposure to high-level noise may also result in other physiological changes such as respiratory and circulatory effects, dizziness and nausea and, in extreme cases, outright physiological damage. Moreover, as far as human performance is concerned the presence of high-level noise may interfere with voice communications by masking the speech sounds, it may impair visual perception by exciting the eyeballs into vibrations, it may impair psychomotor performance by directly or indirectly

stimulating receptors in skin, muscles and joints, and it may also interfere with intellectual performance.

High-level body vibrations may have effects similar to those listed above, with the exception of producing deafness. While vibration criteria have been developed for narrow-band excitation at low and medium frequencies, almost nothing is known about the effects of broad-band intense noise containing large low-frequency and sub-audible components. This is precisely the type of noise of interest here. Further work is urgently needed in this area. Moreover, data on the effectiveness of ear protection devices at the very low audible and the sub-audible frequencies are not in hand. Until such time as these data become available, criteria for personnel for low-frequency noise must be extrapolated and estimated from existing information.

8.3 Criteria for Residential Communities

While considerable information is available concerning the effects of jet aircraft noise intruding into a residential community, very little is known concerning the effects of noise from the static testing and launching of large space vehicles. If the noise levels are appreciable, reactions of annoyance, anger or fear may be elicited. These reactions might be triggered by rattling windows, doors or furnishings and perhaps by the anticipation of structural damage. Also, the noise may interfere with normal activities, such as conversation, use of the telephone, television or radio. The general attitudes of the community in question are expected to be conditioned by the economic and emotional connection of the inhabitants with the noise-producing activity.

Only very scant information on this problem is available at present and data from controlled surveys in some key communities exposed to rocket noise are needed before noise criteria can be established with any accuracy.

8.4 Criteria for Building Structures

Exposure of building structures to low-frequency, high-level sound fields may result in the generation of damaging bending stresses in the various panels and sub-elements of the structure. This is particularly true of windows and other comparatively large and thin panels.

Practical building structures are composed of many sub-elements and their response to the exciting sound field is correspondingly complicated, insomuch as many modes are being excited. However, at low frequencies it may be assumed that the damping is low enough so that the response of the structure can be analyzed on a mode-by-mode basis.

It can be shown* that, if breakage is to be avoided for repeated exposures, the critical octave band sound pressure p_{crit} is related to frequency and the material constants of the panel in question as follows:

$$p_{crit} \doteq \frac{\sigma_d}{20} \left(\frac{\omega h}{c} \right) \eta^{1/2} \quad (\text{Eq. 8-1})$$

* Ira Dyer and Francis M. Wiener "Preliminary Criteria for the Avoidance of Sound-Induced Damage to Building Structures," Paper presented at the 62nd meeting of the Acoustical Society of America 8-11 November 1961, Cincinnati, Ohio.

In this expression σ_d is the damage stress of the panel material of thickness h , c is the speed of longitudinal waves in the panel material, ω is 2π times the frequency in cps, and η is the panel loss factor. Eq. 8-1 states that for damage to occur the octave band sound pressure must equal (or exceed) the critical value p_{crit} and the octave band must contain the modal frequency of the panel. This critical pressure is proportional to frequency.

Regier* has used the design static pressure (design wind load) of a structure as a criterion for sound-induced damage. A modal analysis based on this procedure shows that for such structures the critical octave band pressure is independent of frequency. However, it seems preferable to use in this study the more general relation Eq. 8-1.

Many building structures consist of panels nailed to supports or otherwise supported by a structural framework. A vibrating panel exerts a dynamic force and possibly a moment on its supports. If this force per unit length of panel perimeter exceeds the holding strength of the nail support lines, separation will occur. It can be shown** that the critical octave band sound pressure p_{crit} is given by

$$p_{crit} = \frac{Q_d}{5h} \left(\frac{\omega h}{c} \right)^{1/2} \eta^{1/2} \quad (\text{Eq. 8-2})$$

* A.A. Regier, private communication.

** I. Dyer and F. M. Wiener, loc. cit.

where Q_d is holding strength of the support lines. Note that the frequency dependence is different here.

Although indications are that these simple theoretical approaches are not inconsistent with available case histories of noise-induced building damage, the noise criteria formulated by using these approaches are tentative at best. They must be validated by further theoretical and experimental work.

The same holds true for the investigation of the excitation by ground-borne vibrations of building structures located close to the pad.

8.5 Criteria for Electronic Instrumentation and other Control Equipment

Electronic instrumentation and other control equipment essential to the launching and operation of large space vehicles are subject to noise as well as vibration fields of appreciable magnitude. Such equipment is typically mounted on panels or chassis, which, in turn, are supported by racks, brackets and the like (see Fig. 3-2). Such structures, like the building structures discussed in the preceding section, possess many modes of vibrations and their response to both sound and vibrations is correspondingly complicated.

Laboratory tests on typical small components such as capacitors, resistors, transistors, and vacuum tubes indicate the following: direct sound damage to a component is less than the damage caused by the same sound field exciting a panel (chassis), on which the component is mounted, which, in turn, excites the component by structure-borne vibrations. In other words, the panel couples the acoustic excitation very effectively to the component via structural paths.

Using similar models as used in the preceding section on building damage, one obtains the following expression for the critical octave band sound pressure.

$$p_{crit} = \frac{1}{4} m a_d \left[1 + \left(\frac{\omega M}{2.3 m c h} \right)^2 \right]^{1/2} \eta^{1/2} \quad (\text{Eq. 8-3})$$

where M is the mass of the component in question, m is the mass per unit area of the panel on which the component is mounted and a_d is the rms damaging acceleration for the component.* This limiting acceleration a_d is usually known from pure-tone vibration tests and is usually of the order of $10g$, where g is the acceleration due to gravity. For conservative estimates, $M \doteq 0$ and p_{crit} becomes independent of frequency.

Excessive ambient noise levels must be reduced by proper enclosures or other noise control measures. Much additional work remains to be done to lead to a better understanding of the problem and to a better engineering procedure to predict the response of a given piece of equipment in situ.

8.6 Tentative Estimates of Noise and Vibration Criteria

8.6.1 Tentative Noise and Vibration Criteria for Personnel

a) Noise

Assuming that the deafness criterion controls and extrapolating to very low frequencies, the sound

* ω , c , h and η have the same meaning as in Eq. 8-1.

pressure levels should not exceed the octave band levels given in the table below if hearing damage is to be avoided. No more than one vehicle launch or static test per day, and no ear protection is assumed.

Octave Band cps	Criteria Levels in Octave Bands db re 0.0002 microbar
Below 35 cps	130
35 - 75	125
75 - 150	118
150 - 300	112
300 - 600	110
and above	

b) Vibrations

Present indications are that personnel subject to direct excitation by single-frequency vibrations in the low-frequency and sub-audible range reported unpleasant sensations when the acceleration at any frequency exceeded about $0.1g$, where g is the acceleration due to gravity.*

* C. M. Harris and C. E. Crede, Shock and Vibration Handbook, Ch. 44, McGraw-Hill Book Co., New York, 1961.

8.6.2 Tentative Noise Criteria for Residential Communities

Limited experience with the noise from static Saturn tests in the Huntsville area indicates that sound pressure levels in the low-frequency octaves of 100 to 105 db re 0.0002 microbar will elicit some complaints from residents.

8.6.3 Tentative Criteria for Damage to Building Structures

a) Noise

Figures 8-1 and 8-2 show tentative damage criteria levels for buildings of conventional masonry and wood construction. The damage criterion for glass is also indicated. These criteria levels were obtained by inserting typical values of the relevant quantities in Eqs. 8-1 and 8-2. The figures also indicate the frequency range of greatest concern, i.e. where the resonance frequencies of the structures are likely to be.

b) Vibrations

Several Government agencies on the Federal and State level have set up damage criteria for conventional building structures for excitation from earthquakes. These criteria are relevant to some extent to excitation by ground vibration from large boosters. According to one widely used criterion the maximum allowable peak displacement of the building is 30 mils for

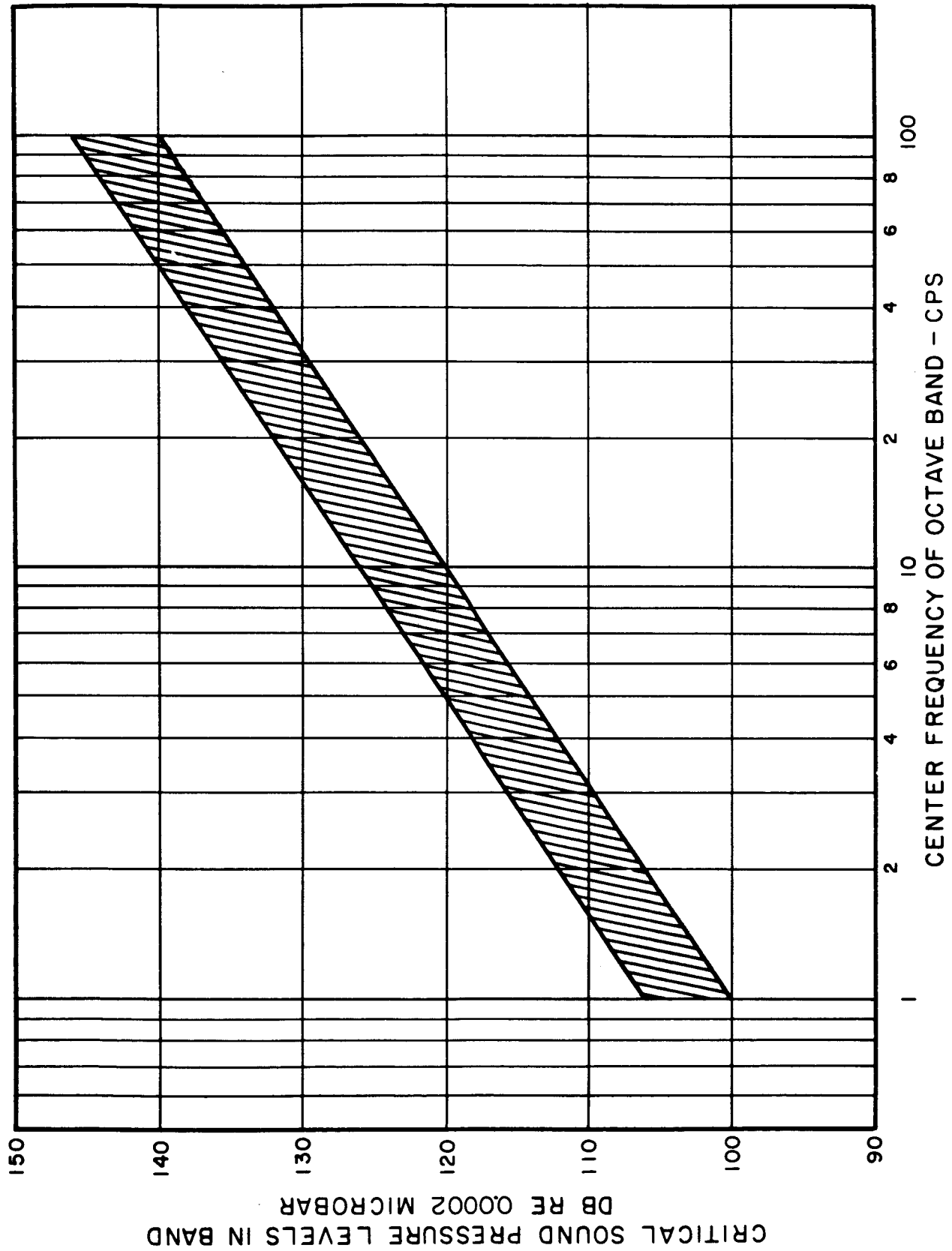


FIG.8-1 TENTATIVE DAMAGE CRITERIA LEVELS FOR CONVENTIONAL MASONRY CONSTRUCTION AND FOR GLASS

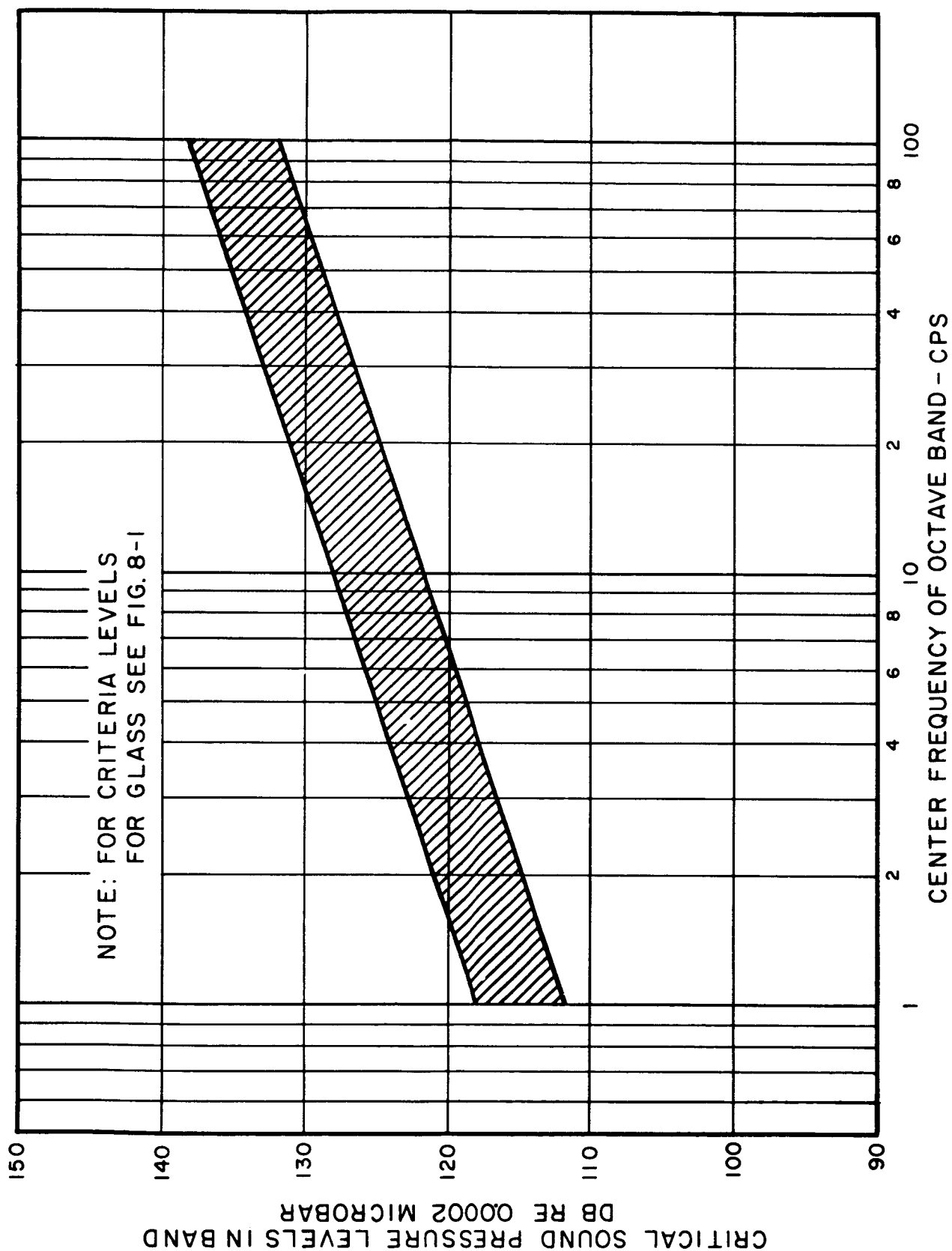


FIG. 8-2 TENTATIVE DAMAGE CRITERIA LEVELS FOR CONVENTIONAL
WOOD CONSTRUCTION

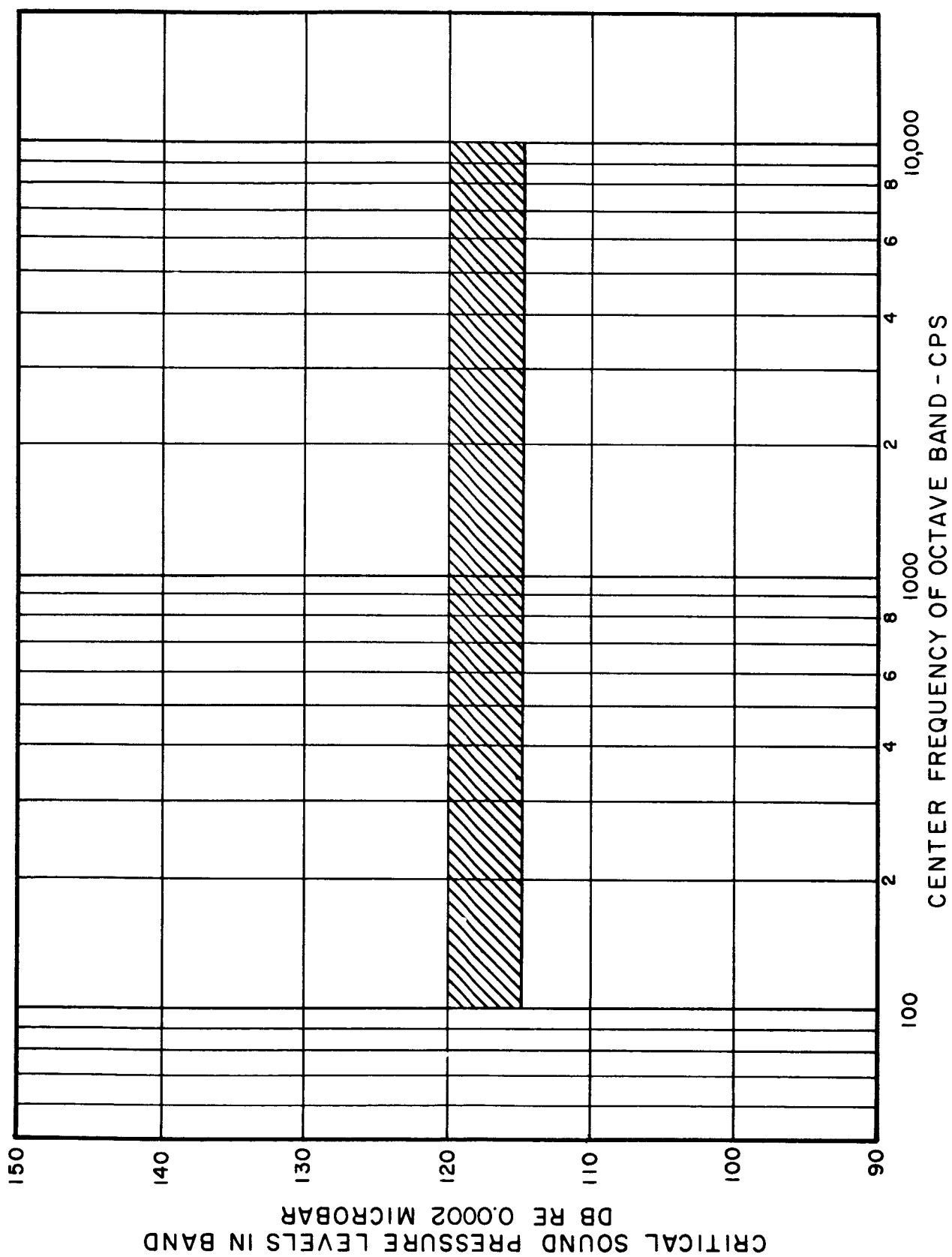


FIG. 8-3 TENTATIVE FAILURE CRITERIA LEVELS FOR ELECTRONIC AND CONTROL INSTRUMENTATION

frequencies below 10 cps. Above 10 cps a maximum allowable peak acceleration of $1/3 g$ is specified, where g is the acceleration due to gravity.*

8.6.4 Tentative Criteria for Failure of Electronic and Control Instrumentation

a) Noise

By inserting typical values of the relevant quantities in Eq. 8-3, one finds that octave sound pressure levels of 115 to 120 db re 0.0002 microbar should not be exceeded. Fig. 803 shows a plot of this criterion in the frequency range of greatest concern, i.e., where the resonance frequencies of panels and chassis are likely to be.

b) Vibrations

The acceleration of the equipment or components due to direct vibration excitation via structural paths, combined with the acceleration resulting from the acoustic excitation must be kept below the limiting value a_d . Present indications are that in most practical situations excitation of the electronic components by the sound incident on the chassis is more important than the excitation due to ground vibrations forcing the chassis rack.

*Don Leet, Harvard University, Private Communication.

9. SUMMARY OF PROCEDURES FOR ESTIMATING SOUND PRESSURE LEVELS GENERATED BY LARGE ROCKET ENGINES, AND CORRESPONDING HAZARD RADII

9.1 General

To summarize the design information presented in the preceding chapters, step-by-step procedures for estimating the sound field generated by large boosters will be given in this Chapter. Procedures will first be given for nearby locations, followed by methods applicable to remote locations. As an example of the use of these procedures, calculations of the hazard radii for the various criteria discussed in Chapter 8 are given for a particular large booster.

The source level estimates given in octave bands in Chapter 6 are furnished in terms of generalized frequency scales. In order to translate the generalized frequency scale of those graphs into actual frequencies the total thrust, in pounds, of the rocket system must be known. After calculating the quantity $(\text{thrust})^{1/2}$ the generalized frequency scale is translated into an actual frequency scale for that particular rocket engine. Alternately, if the nozzle diameters are known or if unusual fuel-oxidizer mixtures (including solid fuels) are employed, the second generalized frequency scale appearing in the figures is used.

The estimates presented here are concerned only with the mean values of the sound pressure levels, excluding fluctuations (see Chapter 7).

9.2 Estimating Sound Pressure Levels Nearby

Excess attenuation for distances less than about 1500 ft from the source can be neglected and this section is concerned with estimating the sound field within this distance limit.

9.2.1 Estimating Sound Pressure Levels Along a Vehicle Launched or Statically Tested in the Open

- 1) Figures 6-3 through 6-5 give the octave sound pressure levels expected at various locations along the vehicle positioned in the open on a launching or static firing pad.
- 2) Re-plot the abscissa in terms of frequency, using the appropriate value of the total thrust F , in pounds, of the vehicle in question.
- 3) For deflector configurations in which the spacing between the rocket exhaust nozzles and the impingement point on the deflector exceeds about one-quarter of the total vehicle length, make the appropriate level correction in each octave band as indicated on the figures. Plot the result along the ordinate axis.
- 4) The level estimates so obtained represent the maximum octave band sound pressure levels to be expected since the near sound field in the vicinity of the vehicle decreases after lift-off.

9.2.2 Estimating Sound Pressure Levels Along a Vehicle Launched from a Silo

- 1) Figures 6-11 through 6-16 show the maximum octave band sound pressure levels expected

at various locations along the vehicle during launching from various silo configurations.

- 2) Re-plot the abscissa in terms of frequency, using the appropriate value of the total thrust F , in pounds, of the vehicle in question.
- 3) Calculate the quantity $10 \log_{10} \left[\frac{F \times 10^{-7}}{S_a} \right]$ and add it to the ordinate given in the figures. F is the total thrust, in pounds, and S_a the annular area between the vehicle and the silo, in square feet. Plot the result along the ordinate axis.
- 4) The level estimates so obtained represent the maximum octave band sound pressure levels to be expected.

9.2.3 Estimating Sound Pressure Levels on the Ground During Static Testing or Before Lift-Off

- 1) Figures 6-7 or 6-9 give the octave band sound pressure levels at a distance of 1000 ft, in generalized coordinates, applicable for the case in question and the required azimuth.
- 2) Re-plot the abscissa in terms of frequency, using the appropriate value of thrust F , in pounds, of the vehicle in question.

- 3) Calculate the actual sound pressure levels by adding $10 \log_{10} [F \times 10^{-7}]$ to, and subtracting $20 \log_{10} R/1000$ from the ordinate. Plot the result along the ordinate axis.
- 4) The level estimates so obtained represent the steady-state octave band sound pressure levels to be expected.

9.2.4 Estimating Sound Pressure Levels on the Ground After Lift-Off

We restrict attention here to distances from the launch pad between 500 and 1500 ft. To estimate the sound pressure levels in octave bands at a point on the ground, R feet away from the launch pad proceed as follows. Note that $500 < R < 1500$ ft.

- 1) Figure 6-10 gives the maximum octave band sound pressure levels at a distance of 1000 ft, in generalized coordinates.
- 2) Re-plot the abscissa in terms of frequency, using the appropriate value of thrust F, in pounds, of the vehicle in question.
- 3) Calculate the actual sound pressure levels by adding $10 \log_{10} [F \times 10^{-7}]$ to, and subtracting $20 \log_{10} R/1000$ from the ordinate. Plot the results along the ordinate axis.

- 4) The level estimates so obtained represent the maximum octave band sound pressure levels to be expected.

9.3 Estimating Sound Pressure Levels on the Ground at Remote Locations

To estimate the sound pressure levels generated by a booster near the ground more than about 1500 feet from the pad, the excess sound attenuation in the atmosphere must be taken into account. At the present state of knowledge this attenuation is not accurately known and available estimates vary widely (See Chapter 7). Small errors in the sound attenuation coefficient per mile mount up to an uncertainty of very many decibels in the sound pressure level estimates. Consequently, the estimates given in this section must be used with caution. They should be verified by a well-controlled experimental measurement program as soon as possible.

9.3.1 Estimating Sound Pressure Levels During Static Testing or Before Lift-Off

To estimate the sound pressure levels in octave bands at a point near the ground, R ft away from the stand ($R > 1500$ ft) proceed as follows:

- 1) Calculate the sound pressure levels at 1000 ft according to Item 9.2.3 above.
- 2) Subtract $20 \log_{10} R/1000$ from the ordinate.

- 3) Next, consider the excess attenuation due to dissipative effects in the atmosphere. These losses are proportional to the distance between source and receiver and can be estimated, for each octave frequency band, from the attenuation coefficients given in Fig. 7-2.* Calculate the values of excess attenuation due to dissipative effects by multiplying the values from Fig. 7-2 by $R/5000$ in each band.** Subtract these values, in decibels, in each octave band from the sound pressure levels estimated in the preceding step. This result represents the sound pressure levels to be expected at a distance R from the pad from static firing or before lift-off, considering dissipative excess attenuation only.
- 4) Next, the effects of the sound velocity profile on sound propagation are to be considered. From the data presented in Chapter 7, the profile appropriate for the site, season and angular sector is examined. Since sound propagation takes place predominantly along the ground, the shape of the velocity profile between ground and heights of a few hundred or

* It is seen that the attenuation coefficient increases rapidly with frequency. Hence, the high-frequency components of the rocket noise are damped out rapidly with distance.

** 1 mile \doteq 5000 ft for the purposes of these computations.

thousand feet is important. If the slope of this part of the profile is negative, additional (positive) excess attenuation will occur. If the value of the (negative) slope of this part of the profile is small, ($< 5 \times 10^{-3} \text{ sec}^{-1}$), no further correction need be made for conservative engineering estimates. If the slope of the profile near the ground is positive, there is a likelihood that at some distances the levels estimated above may be exceeded.

These semi-quantitative conclusions were drawn from an analysis of the data contained in Fig. 7-1. More accurate estimates are not possible at this time and more data are urgently needed to obtain sound attenuation data from large rocket engines on the ground for various atmospheric conditions.

9.3.2 Estimating Sound Pressure Levels After Lift-Off

To estimate the maximum sound pressure levels in octave bands at a point near the ground, R ft away from the stand ($R > 1500 \text{ ft}$) proceed as follows:

First observe that the radiation of the source is essentially uniform in a horizontal plane* but has a maximum of radiation approximately

* For the first several miles of flight, space vehicle trajectories can be considered vertical for the purposes of this study.

60 degrees from the exhaust stream in flight (See Fig. 6-1). Ignoring the time delay due to the finite speed of propagation of sound it follows that maximum levels will occur at the point in question when the vehicle height is about $R/2$. Because the slant distance is only about 15 percent larger than R , the source distance is essentially equal to R and the following procedure is to be used:

- 1) Calculate the maximum sound pressure levels at 1000 ft according to Item 9.2.4 above.
- 2) Subtract $20 \log_{10} R/1000$ from the ordinate.
- 3) Next, consider the excess attenuation due to dissipative effects in the atmosphere. As a first approximation use the same estimates as for sound propagation along the ground (see Item 9.3.1 above). Subtract the excess attenuation values, in decibels, so obtained, in each octave band from the sound pressure levels estimated in the preceding step. This represents an estimate of the maximum sound pressure levels to be expected at a distance R from the launch pad, considering dissipative excess attenuation only.
- 4) Consider next the effect of the sound velocity profile on sound propagation. Since the source height increases in accordance with the vehicle trajectory, the profile must be considered to much larger heights than was the case before

lift-off. This, by and large, eliminates from consideration the portions of the profile possessing steep slopes. Moreover, it follows from geometric acoustics, that no sound reinforcement at ground level (appreciable negative excess attenuation) will occur unless the effective speed of sound at any point along the profile exceeds that at ground level.

At the present state of the art it is not possible to make more accurate estimates. More data are urgently needed to obtain sound attenuation data from large rocket vehicles in flight for various atmospheric conditions.

- 5) In the above it was assumed that the sound power generated by the rocket exhaust remains constant with altitude. This is a first-order approximation only, even if the propellant flow rate is constant. However, present indications are that the sound power actually decreases somewhat in flight. Hence, the above sound pressure level estimates are conservative in the engineering sense. For an observer on the ground the frequency of the noise is shifted downward due to the Doppler effect. This shift has been ignored in the present analysis.

9.4 Sound Pressure Levels as a Function of Time

While some of the procedures in the preceding sections were relevant to the calculation of the maximum levels expected at a given location on the ground, it should be realized that at appreciable distances from the launch pad levels only slightly smaller than the maximum levels will persist from a time $T + R/c_0$ to a time somewhat greater than $T + \tau + R/c_0$, where T is the time at a lift-off, τ is the time it takes the vehicle to attain a height $R/2$ and c_0 is the speed of sound at ground level. Hence, at larger distances, the duration of the noise at or near maximum levels is at least τ seconds. This consideration may be important in setting criteria levels (see Chapter 8), but our present incomplete knowledge of criteria does not enable us to take time durations into account quantitatively.

9.5 Examples

The use of the above procedures will be illustrated by two specific examples.

Example 1: Sound Pressure Levels Along a Large Space Vehicle

Let it be required to calculate the maximum sound pressure levels half-way along a large space vehicle of 16×10^6 lbs thrust burning liquid fuel, being launched in the open at Cape Canaveral.

Solution:

- 1) The maximum sound pressure levels are experienced at full thrust before lift-off.

- 2) Atmospheric conditions do not enter into the problem.
- 3) Figure 6-4 is the appropriate graph for estimating the sound pressure levels. Assuming a gas exhaust mixture similar to contemporary mixtures, the lower of the two generalized frequency scales can be used. Since $F^{1/2} = 4 \times 10^3 \text{ lbs}^{1/2}$, a frequency of 25 cps corresponds to the point marked $10^5 \text{ cps lbs}^{1/2}$ on the scale. Re-plotting the graph on this frequency scale yields Fig. 9-1. It shows the maximum sound pressure levels in octave bands as a function of frequency, assuming a closely spaced flame deflector. (The possible influence of details in deflector configuration on the sound field were ignored.)

Example 2: Sound Pressure Levels in Cocoa Beach

Let it be required to calculate the maximum sound pressure level in octave bands at Cocoa Beach due to the launching of a space vehicle powered by a rocket system of a total thrust of 25×10^6 lbs burning solid fuel. The launching is assumed to take place at Cape Canaveral in summer from a pad about 3 miles north of the present Launch Complex 34.

Solution:

- 1) Figure 6-10 is the appropriate graph for estimating the maximum sound pressure levels after

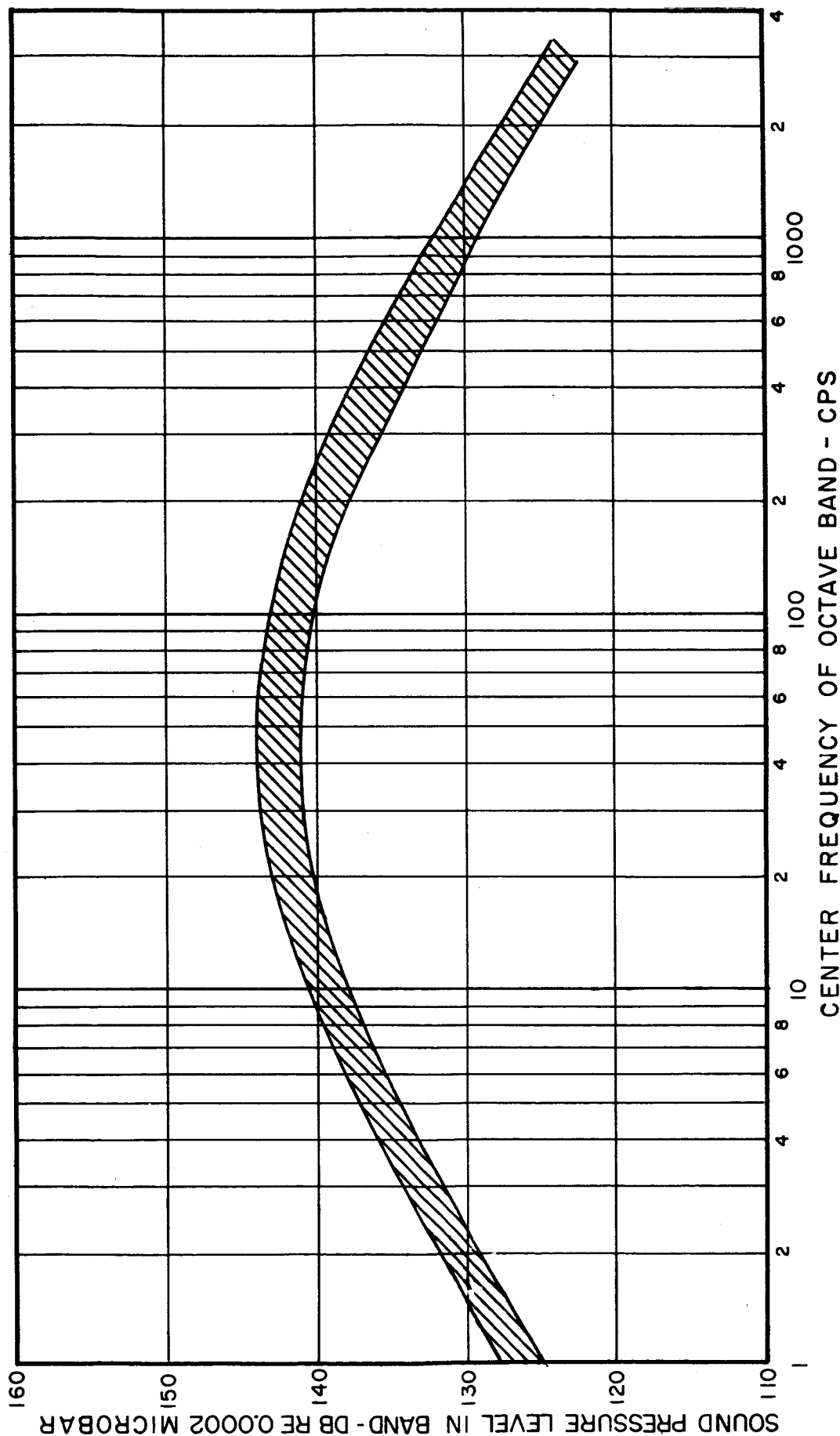


FIG. 9-1 MAXIMUM SOUND PRESSURE LEVELS HALFWAY ALONG LENGTH OF SPACE VEHICLE OF 16×10^6 LBS THRUST BEING LAUNCHED IN THE OPEN

lift-off. Assuming a gas exhaust mixture similar to contemporary mixtures, one can use the lower of the two generalized frequency scales. Since $F^{1/2} = 5 \times 10^3 \text{ lbs}^{1/2}$, a frequency of 20 cps corresponds to the point marked $10^5 \text{ cps lbs}^{1/2}$ on the scale. Re-plotting the graph on this frequency scale and adding $10 \log_{10}[F \times 10^{-7}] = 10 \log_{10} 2.5 \doteq 4 \text{ db}$ to the ordinate, Fig. 9-2 is obtained. The graph shows the maximum sound pressure levels in octave bands after lift-off as a function of frequency, at a distance of 1000 ft from the pad.

- 2) Calculate the attenuation due to inverse-square law by observing that the Cocoa Beach area is about 20 miles distance from the launching pad. This attenuation is equal to about

$$20 \log_{10} \frac{20 \times 5000}{1000} = 40 \text{ db.}$$

- 3) Next estimate the excess attenuation due to dissipative effects using Fig. 7-2. By multiplying the attenuation coefficient given in Fig. 7-2 one obtains the values shown in the Table on page 70.

Octave Band cps	Estimated Dissipative Excess Attenuation for 20 Miles, db
2-4	5 (extrapol.)
4-8	5 (extrapol.)
8-16	5
16-35	10
35-75	35
75-150	40
150-300	60
300-600	80

Figure 9-3 shows the maximum levels estimated at Cocoa Beach on that basis.

- 4) It remains to estimate the excess attenuation due to the velocity profile. Fig. 7-5b shows the seasonal sound velocity profiles for summer for the Cape Canaveral area in the southerly sector. On the average, there will be no reinforcement (negative excess attenuation). In rare cases there may be, but only while the vehicle is below an altitude of about one mile. It is concluded that sound reinforcement is not important here.
- 5) Assuming a vehicle trajectory similar to that of Saturn, it is seen that sound pressure levels at or near the maximum levels shown in Fig. 9-3 will persist in the Cocoa Beach area for well over one minute.

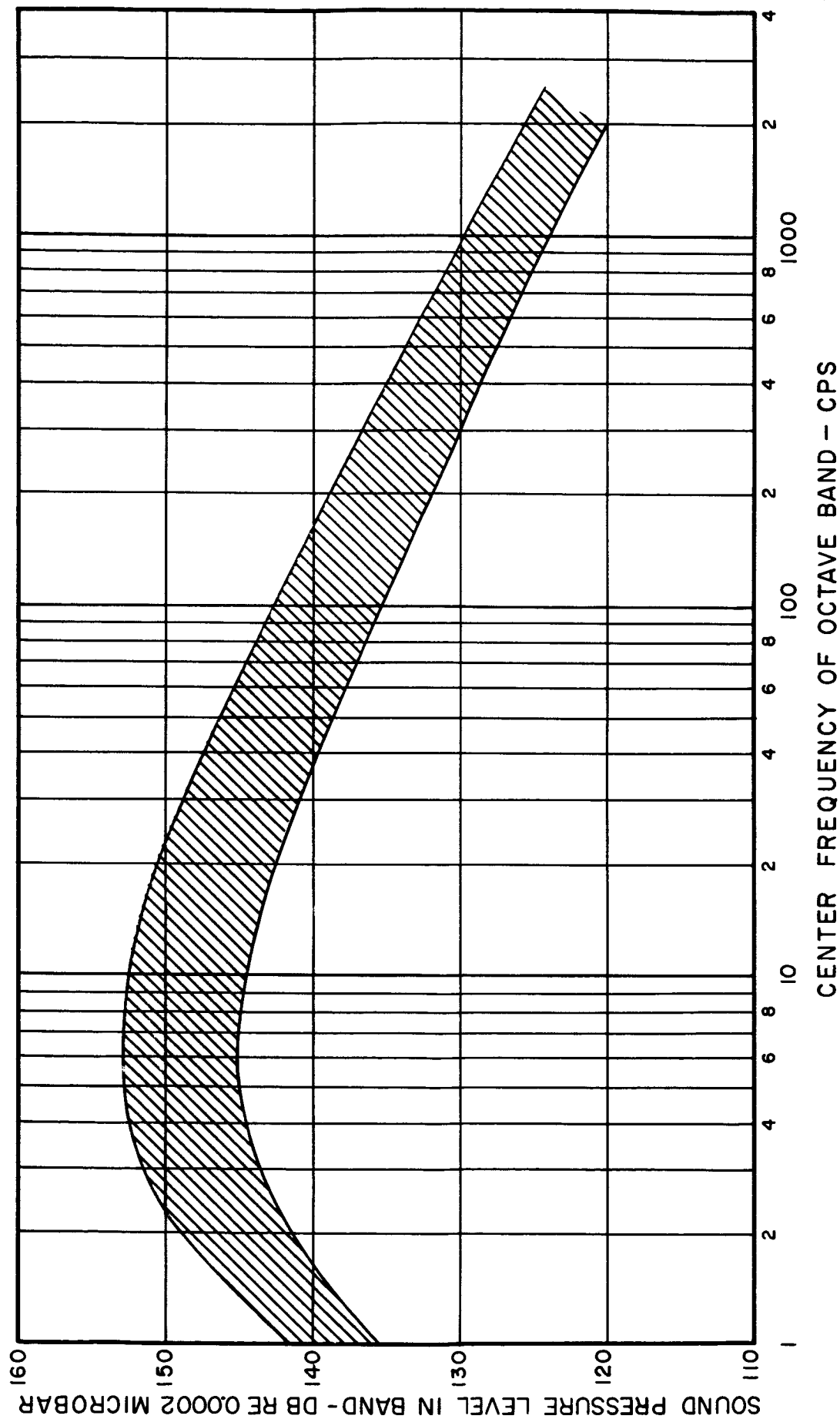


FIG.9-2 MAXIMUM SOUND PRESSURE LEVELS DUE TO LAUNCHING OF SPACE VEHICLE OF 25×10^6 LBS THRUST 1000 FT FROM PAD ON THE GROUND

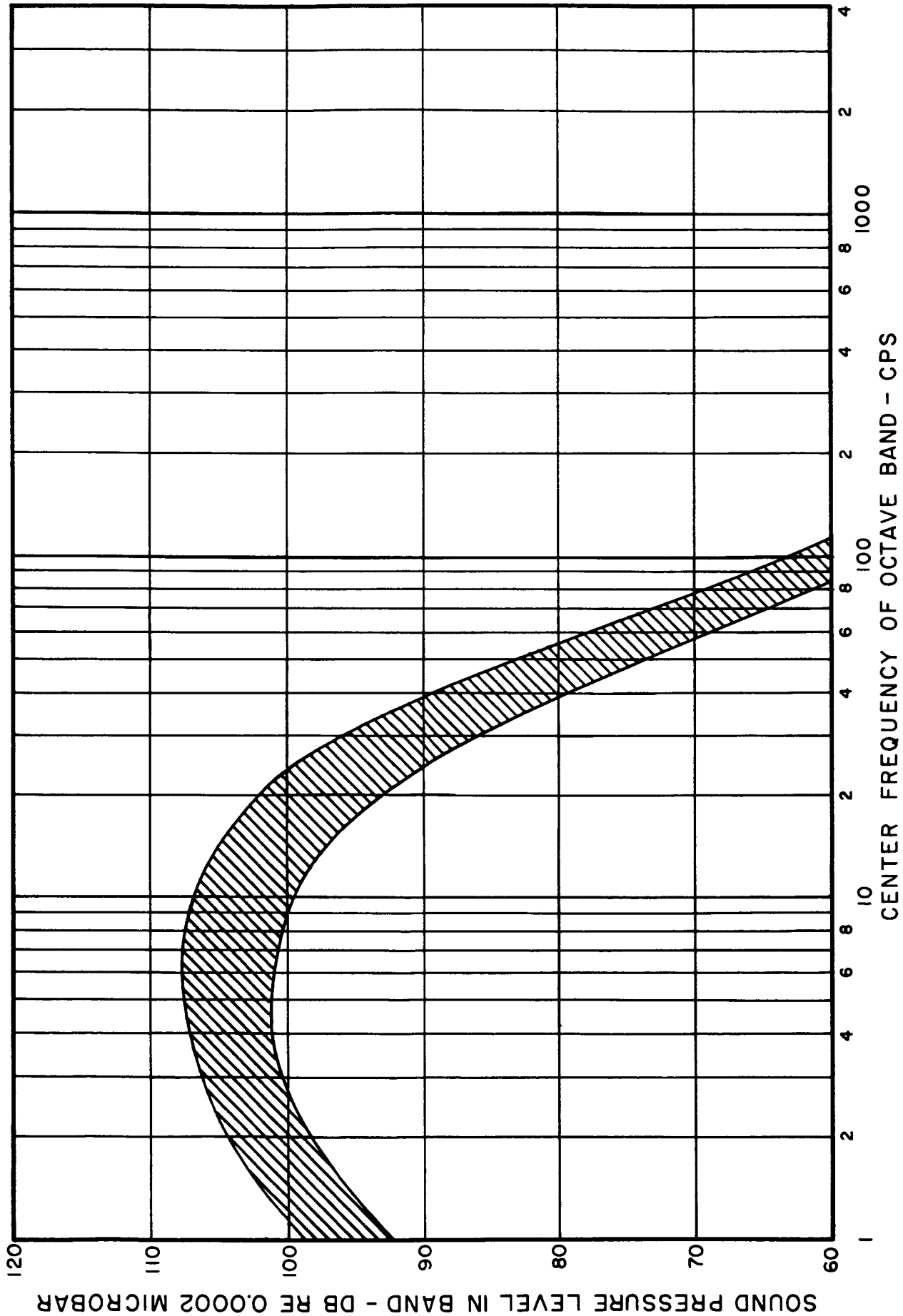


FIG. 9-3 MAXIMUM SOUND PRESSURE LEVELS AT COCOA BEACH DUE TO LAUNCHING OF SPACE VEHICLE OF 25×10^6 LBS THRUST

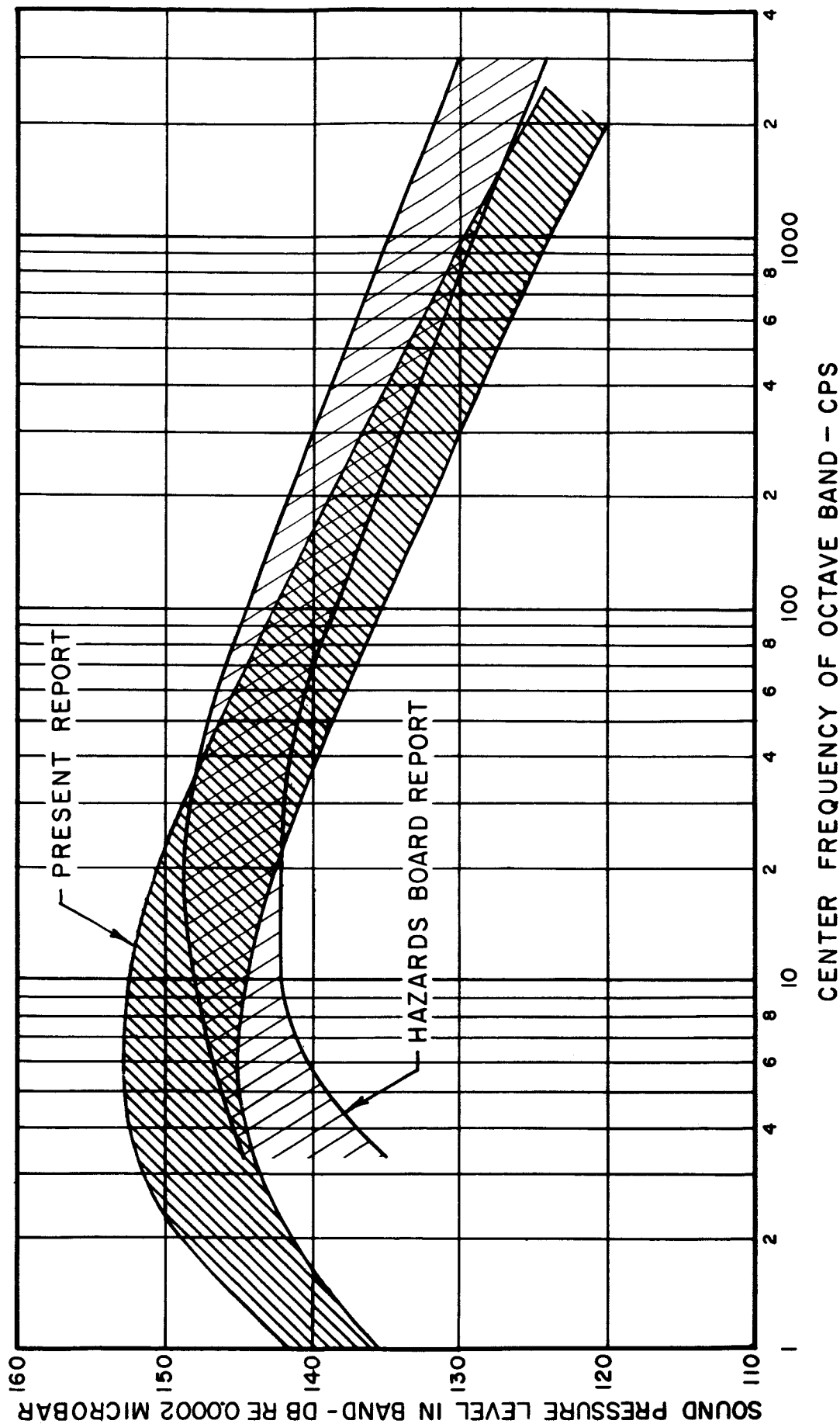


FIG. 9-4 ESTIMATES OF MAXIMUM SOUND PRESSURE LEVELS DUE TO LAUNCHING OF SPACE VEHICLE OF ABOUT 25×10^6 LBS THRUST ABOUT 1000 FEET FROM PAD ON THE GROUND

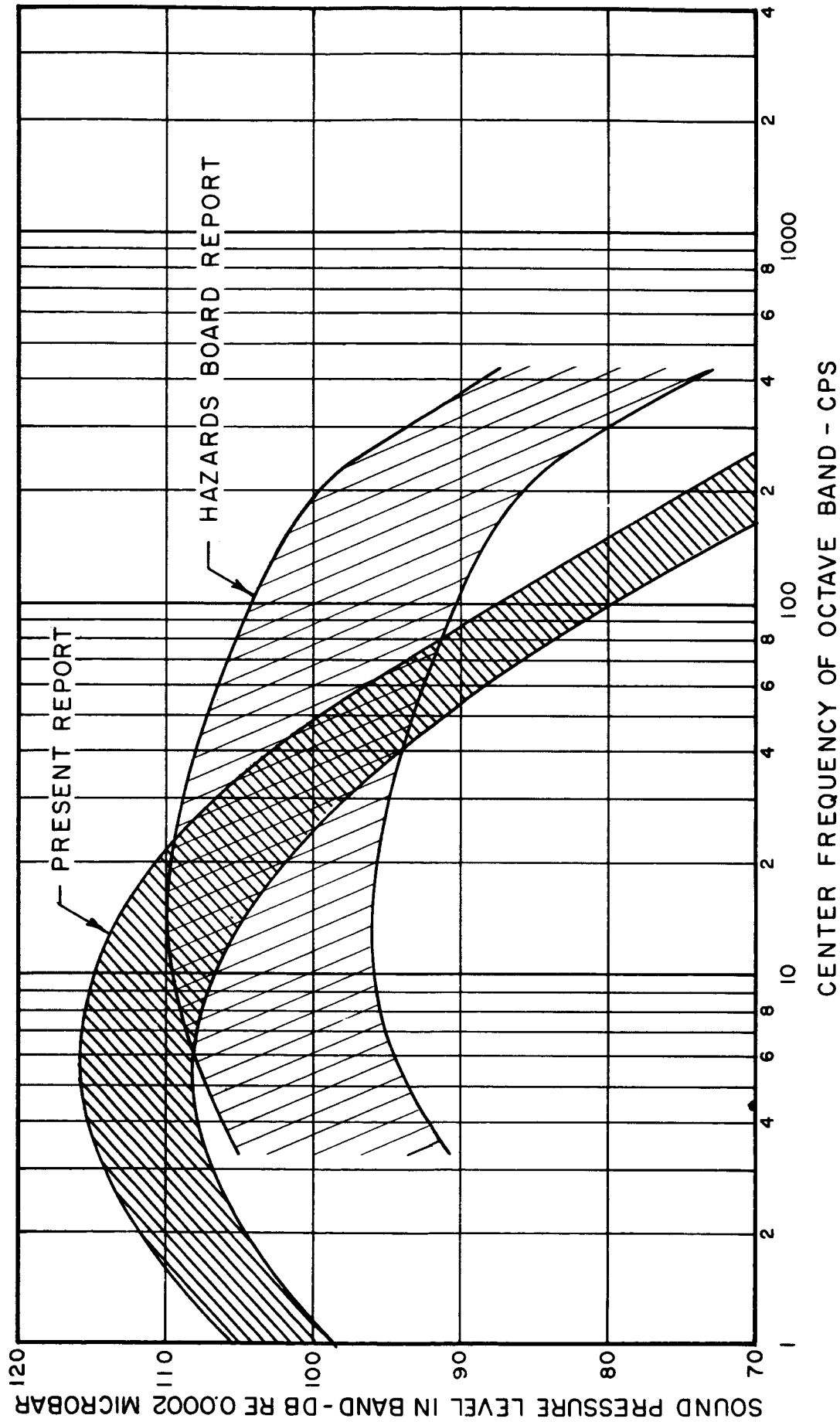


FIG. 9-5 ESTIMATES OF MAXIMUM SOUND PRESSURE LEVELS DUE TO LAUNCHING OF SPACE VEHICLE OF ABOUT 25×10^6 LBS THRUST ABOUT 10 MILES FROM PAD ON THE GROUND

Note the predominance of the very low audible and sub-audible frequencies in the estimated spectrum.

To illustrate the importance of estimating the atmospheric excess attenuation correctly the results of the above calculations will be compared with similar estimates made in the Hazards Board Report,* where somewhat different procedures were used.

Figure 9-4 compares estimates of the maximum sound pressure levels at 770 feet from the pad during launch of a vehicle of 22×10^6 lbs thrust taken from the above report (Supplement, Fig. II-B-4a) with the estimates shown in Fig. 9-2. Within the accuracy of the data available the two estimates should agree, and indeed they do reasonably well as seen from Fig. 9-4.

In Figure 9-5 the maximum sound pressure levels due to the launching of a vehicle of 25×10^6 lbs thrust were estimated for a location about 10 miles from the pad, following Example 2 above. These estimates are compared with Fig. II-B-4e of the Supplement to the Hazards Board Report giving estimates of the maximum sound pressure levels due to the launching of a vehicle of 22×10^6 lbs thrust, evaluated 50,000 ft from the pad. The wide divergence of the shape of the spectra and of the levels at the higher frequencies shows the urgent need for more theoretical and experimental work.

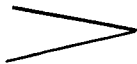
* Joint Air Force--NASA Hazards Analysis Board Report, loc cit.

9.6 Estimates of Acoustical Hazard Radii for Various Acoustical Criteria

The mean maximum octave band and pressure levels expected from the launching of a space vehicle of 25×10^6 lbs thrust have been calculated according to the procedures presented earlier in this Chapter. They are plotted in Fig. 9-6 for 1, 5, 10 and 20 miles distance from the pad. On the same graph are also plotted the various tentative acoustical criteria developed in Chapter 8.

By inspection of the figure tentative hazard radii (without regard to the effect of the sound velocity profile in the atmosphere on sound propagation) are deduced and tabulated below.

Tentative Acoustical Hazard
Radii for the Launch
of a Space Vehicle of
 25×10^6 Lbs Thrust

Criterion	Hazard Radius, Miles	
	Present Report	Hazards Board Report
Deafness	1	1
Damage to Wood Frame Construction	5	
Damage to Glass or Masonry Construction	10	
Failure of Electronic and Control Equipment	1	-
Community Reaction	20	-

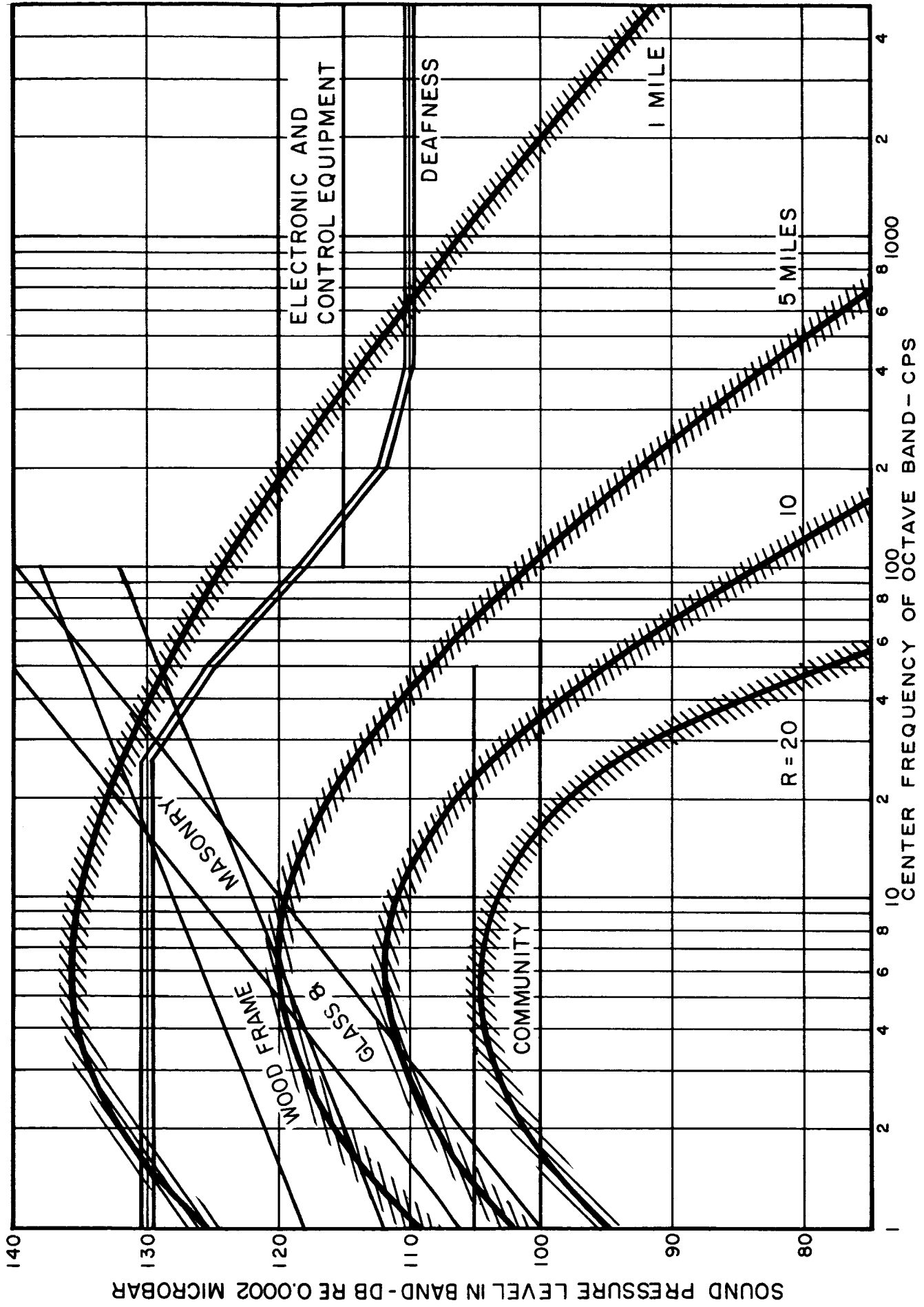


FIG. 9-6 COMPARISON OF MAXIMUM SOUND PRESSURE LEVELS DUE TO LAUNCHING OF SPACE VEHICLE OF 25 x 10⁶ LBS THRUST AT VARIOUS DISTANCES WITH TENTATIVE ACOUSTICAL CRITERIA

In the table on page 72, the estimates given in the Hazards Board Report* for certain acoustical hazard radii are also presented. Note that some of the acoustical hazard radii have not been considered in the Hazards Board Report.

It is clear that noise control measures and ear protection devices must be employed to protect personnel, equipment and buildings inside the considerable areas lying within the various hazard radii.

* Joint NASA - Air Force Hazards Board Report, loc. cit.

10. CONCLUSIONS

The following conclusions must be drawn from the material presented in this report.

1. The acoustical hazard is important. The large sound and vibration fields generated by rocket engines of large thrust must be carefully evaluated and controlled to insure successful performance and protection of personnel, equipment and structures.
2. At nearby locations most of the noise exposure has ceased a comparatively short time after lift-off.
3. At remote locations the noise is primarily due to the vehicle in flight and noise exposures are comparatively long.
4. Noise control measures at the source, (water injection, exhaust diffusion etc.) are therefore appropriate only in the static testing case.
5. Present quantitative knowledge is inadequate to deal with the problem efficiently and economically. In particular, the following areas are in need of further investigation, research, and reduction to engineering practice.
 - a. Investigation of source parameters, at frequencies as low as 1 cycle per second
 - b. Investigation of long-range sound propagation and its dependence on meteorological parameters
 - c. Equipment response and failure criteria
 - d. Building structure response and damage criteria
 - e. Human response and criteria
6. This improved information should be applied to the evaluation of launch and static test complexes, proposed and under construction, from the noise and vibration control point of view.

APPENDIX

A.1 Procedures Followed in Constructing Seasonal Probability Distributions of the Effective Velocity of Sound Propagation (Figures 7-3a through 7-14b in Text).

A.1.1 Cape Canaveral Area

The construction of probability distributions of the effective velocity of sound propagation starts with calculations of the average temperature* profile along the vertical for the summer and winter seasons at each site. The temperature profiles for the Cape Canaveral Area (see Fig. A-14) were interpolated from the 1200 Z (Greenwich Mean Time) Rawinsonde data for Miami and Jacksonville, Florida during the summer (June, July, and August) and winter (January, February, December) of 1960, the most recent year for which complete summaries are available**. The average temperatures are about 10°F warmer in summer at all levels except the surface layers, which are about 20°F warmer in summer than in winter, and near the tropopause where the seasonal variations are very small. The seasonal temperature profiles \bar{T} were converted to profiles of sound propagation velocity $c(\bar{T})$ by means of the relationship

$$c(\bar{T}) = 49 \sqrt{\bar{T}} \text{ ft sec}^{-1} \quad (\text{Eq. A-1})$$

* Strictly speaking, the absolute virtual temperature T_v should be used when the air contains appreciable amounts of water vapor. In symbols, $T_v \approx T / [1 - 0.375 e/P]$ where e and P are the vapor pressure and the barometric pressure, respectively.

** Climatological Data, National Summary, Vol. 11 Nos. 1,2,6,7,8, 12. U. S. Weather Bureau, National Weather Records Center, Asheville, North Carolina. Rawinsonde data for Cape Canaveral were not immediately available at the start of the project; a subsequent check of the interpolated values against the Cape Canaveral seasonal averages showed no significant discrepancies.

where the temperature \bar{T} is in absolute degrees Rankine. The quantity $c(\bar{T})$ is plotted in Figures 7-3a through 7-6b for the Cape Canaveral site.*

The next step in constructing the seasonal probability distributions is to add the average east-west (zonal) and north-south (meridional) vector wind components to $c(\bar{T})$ to obtain vertical profiles of the average effective velocity of sound propagation \bar{c} for each of the cardinal compass directions.** Finally, the distribution of c about the seasonal average in each of the four sectors is given by $\bar{c} \pm \sigma$ and $\bar{c} \pm 2\sigma$, where the σ 's denote the standard deviation of the meridional or zonal wind component for the winter and summer seasons. The seasonal distributions for c should properly contain some provision for variations in the temperature about the mean value. However, since the temperature and wind distributions are not independent, there is no simple method of combining the variances. At Cape Canaveral, the standard deviation of temperature is generally small compared to the standard deviations of the wind components insofar as these two parameters are related to the sound propagation velocity, and the omission of the temperature factor does not lead to significant errors in the probability distributions for c . This is also true in the majority of cases for the other sites as well. Appropriate wind data for the Cape Canaveral Area are available from a recent Air

* Similar profiles of $c(\bar{T})$ due to temperature variations alone were obtained from temperature data for the other sites considered.

** Only horizontal wind components are considered. The vertical wind components are usually small (< 3 ft/sec).

Force Study* and NASA Technical Note D-610**. If the seasonal vector wind statistics are distributed approximately according to the normal law of errors, the $\pm \sigma$ and $\pm 2\sigma$ limits of the distributions would be expected to include about 68 per cent and 95.5 per cent, respectively, of all cases. In view of the uncertainties inherent in the wind measurements and to compensate in part for the omission of temperature variations in the calculations, it is suggested that these limits be interpreted in the present study as the envelopes for about 60 per cent and 90 per cent, respectively, of the population. Alternatively, there is a probability of approximately 0.4 that c will be found outside the $\pm \sigma$ limits and a probability of about 0.1 that the $\pm 2\sigma$ limits will be exceeded. The importance of taking wind velocity as well as temperature into account in the construction of vertical profiles of sound propagation velocity is clearly seen in Figures 7-4a and 7-6a where the strong westerly winds normally present above Cape Canaveral in winter effectively preclude positive slopes of the profile in the western sector (except for a shallow layer near ground level) and significantly enhance the possibility of positive slopes throughout a deep layer in the eastern sector.

* "WBAN 120 Winds Aloft Summary, Cocoa Beach, Patrick Air Force Base Rawins, February 1950 - November 1956." Department of the Air Force, Air Weather Service, Division of Climatology, Data Control Division.

** J. W. Smith and W. W. Vaughan, "Monthly and Annual Wind Distribution as a Function of Altitude for Patrick Air Force Base, Cape Canaveral, Florida." NASA Technical Note D-610, July 1961.

A.1.2 Huntsville Area

Seasonal temperature profiles for the Huntsville Area were obtained by interpolating Rawinsonde data for Montgomery, Alabama and Nashville, Tennessee during the summer and winter months of 1960. Requisite measurements are reported on WBAN 33 forms available from the National Weather Records Center. In the vicinity of Huntsville, the average seasonal temperatures (see Fig. A-16) differ by about 35°F near the ground and by 20°F aloft. Average meridional and zonal wind components for the Huntsville Area were also interpolated from the values calculated for Montgomery and Nashville from the resultant winds available in Volume 11 of the National Summary of Climatological Data mentioned above. Standard deviations of the east-west, north-south wind components for the two seasons were obtained from an atlas of upper wind statistics for the northern hemisphere.* The average seasonal east-west, north-south wind components indicated by the atlas for the Huntsville Area were compared with the interpolated Montgomery-Nashville values based on 1960 data and no significant differences were apparent.

A.1.3 Point Arguello

Temperature profiles for Point Arguello, California are based on monthly averages for 1960 summarized on WBAN 33 forms available from the National Weather Records Center. The profiles (see Fig. A-18) are similar in most respects to the seasonal profiles for Cape Canaveral with the exception of the pronounced low-level temperature inversion present at Point Arguello in summer.

* H. L. Crutcher, "Upper Wind Statistics Charts of the Northern Hemisphere," NAVAER 50-1C-535, vols. 1, 2, August 1959 (Issued by the Office of the Chief of Naval Operations).

Average vector wind components for the east-west, north-south coordinates were obtained from the monthly resultant winds available in Volume 11 of the National Summaries of Climatological Data for 1960. The results were in general agreement with those reported in the atlas of upper wind statistics mentioned above except for a difference of about 20 ft sec^{-1} in the summer east-west component in the layer from 20,000 to 40,000 ft. These data were adjusted so that the east-west components used in constructing the probability distributions of sound velocity were about midway between the two sets of statistics. Average seasonal standard deviations of the meridional and zonal wind components were read off the charts of the NAVAER Atlas for the layer from ground level to 53,000 ft. Standard deviations above this level were estimated from the 1960 Rawinsonde data shown on the WBAN 33 records for Point Arguello.

A.2 Selected Case Studies of the Vertical Profiles of the Effective Velocity of Sound Propagation for the Cape Canaveral Area, Huntsville Area and Point Arguello.

Case studies of the vertical profiles of the effective velocity of sound propagation are essential for checking the overall adequacy of the probability distributions shown in Figures 7-3a through 7-14b, and for providing direct information on the variation of sound velocity with height. A total of ten cases, five for summer and five for winter, were chosen for each of the three sites. Selection of individual cases was limited to fair-weather situations in which no strong frontal systems or well-defined areas of precipitation were within several hundred miles of the site in question. Even though the number of examples is rather small, it is felt that the results are representative and provide an adequate check on the adequacy of the seasonal probability distributions. Data sources and brief descriptions of the weather patterns associated with individual cases are contained in the following discussion.

A.2.1 Case Studies for the Cape Canaveral Area

Sector plots of the vertical profiles of sound velocity for five summer and five winter cases at Cape Canaveral are presented in Figures A-1a through A-4b. Values for c are entered at 1000-ft intervals for the first 20,000 ft and at 5,000-ft intervals above this level. Data in the figures are based on sound velocities and wind observations tabulated in the "computer-type" records for Cape Canaveral obtained from the National Weather Records Center. With one or two exceptions, the points fall well within the envelopes of the probability distributions of Figures 7-3a through 7-6b. The general weather situations associated with the individual cases and estimates of the positive slopes of the sound-velocity profiles in the lowest layers are contained in the following summary:

Winter Cases

3 December 1960, 1126 Z

Weather: Clear skies in the presence of northeasterly flow of modified polar continental air around the southeastern side of a large anticyclone centered in the Appalachians. Winds aloft are northerly and back to the west above 40,000 ft.

Sound velocity profile: Positive slopes in the first 1000 ft of $0.9 \times 10^{-2} \text{ sec}^{-1}$ in the western sector and $0.5 \times 10^{-2} \text{ sec}^{-1}$ in the southern sector.

13 December 1960, 2335 Z

Weather: Clear skies associated with the northerly flow of modified polar continental air from an anticyclone centered in the Gulf states; northerly winds aloft become very strong westerly above 20,000 ft.

Sound velocity profile: Positive slopes in the first 1000 ft of $0.5 \times 10^{-2} \text{ sec}^{-1}$ in the western sector and $1.4 \times 10^{-2} \text{ sec}^{-1}$ in the southern sector. Also, c increases with height in the 4000-to-8000-ft layer of the southern sector and from 3000 to 30,000 ft in the eastern sector.

12 January 1961, 1127 Z

Weather: Easterly winds at low levels to the south of an extensive belt of high pressure across the Gulf states. Winds aloft are from the southwest between 5000 and 25,000 ft and from the west above 25,000 ft.

Sound velocity profile: Positive slopes of $2.1 \times 10^{-2} \text{ sec}^{-1}$ in the first 1000 ft of the western sector and $1.4 \times 10^{-2} \text{ sec}^{-1}$ in the 4000-to-5000-ft layer of the eastern sector. The slope is also positive in the northern sector from 5000 to 9000 ft.

13 February 1961, 1130 Z

Weather: Clear skies and near-calm conditions at the surface produce a 14°F radiational temperature inversion; light westerly winds aloft.

Sound velocity profile: Positive slopes of $0.6 \times 10^{-2} \text{ sec}^{-1}$ in the western sector, $2.2 \times 10^{-2} \text{ sec}^{-1}$ in the eastern sector, and $2.9 \times 10^{-2} \text{ sec}^{-1}$ in the southern sector in the first 1000 ft above the surface. The slope is positive, also, from 1000 to 4000 ft in the northern sector and from 2000 to 6000 ft in the western sector.

19 February 1961, 2330 Z

Weather: Southeasterly flow of tropical maritime air at the surface to the north of an extension of the Bermuda anticyclone. Winds aloft gradually veer through south and become westerly above 20,000 ft.

Sound velocity profile: Positive slopes of $0.5 \times 10^{-2} \text{ sec}^{-1}$ in the western sector and $2.0 \times 10^{-2} \text{ sec}^{-1}$ in the northern sector in the first 1000 ft. There is also a positive slope between 1000 and 4000 ft in the eastern sector.

Summer Cases

17 June 1960, 1135 Z

Weather: Southerly flow of tropical maritime air at the surface; winds aloft are from the south and southwest, becoming easterly above 50,000 ft.

Sound velocity profile: Positive slopes of $0.5 \times 10^{-2} \text{ sec}^{-1}$ in the eastern sector and $1.8 \times 10^{-2} \text{ sec}^{-1}$ in the northern sector in the first 1000 ft above the surface.

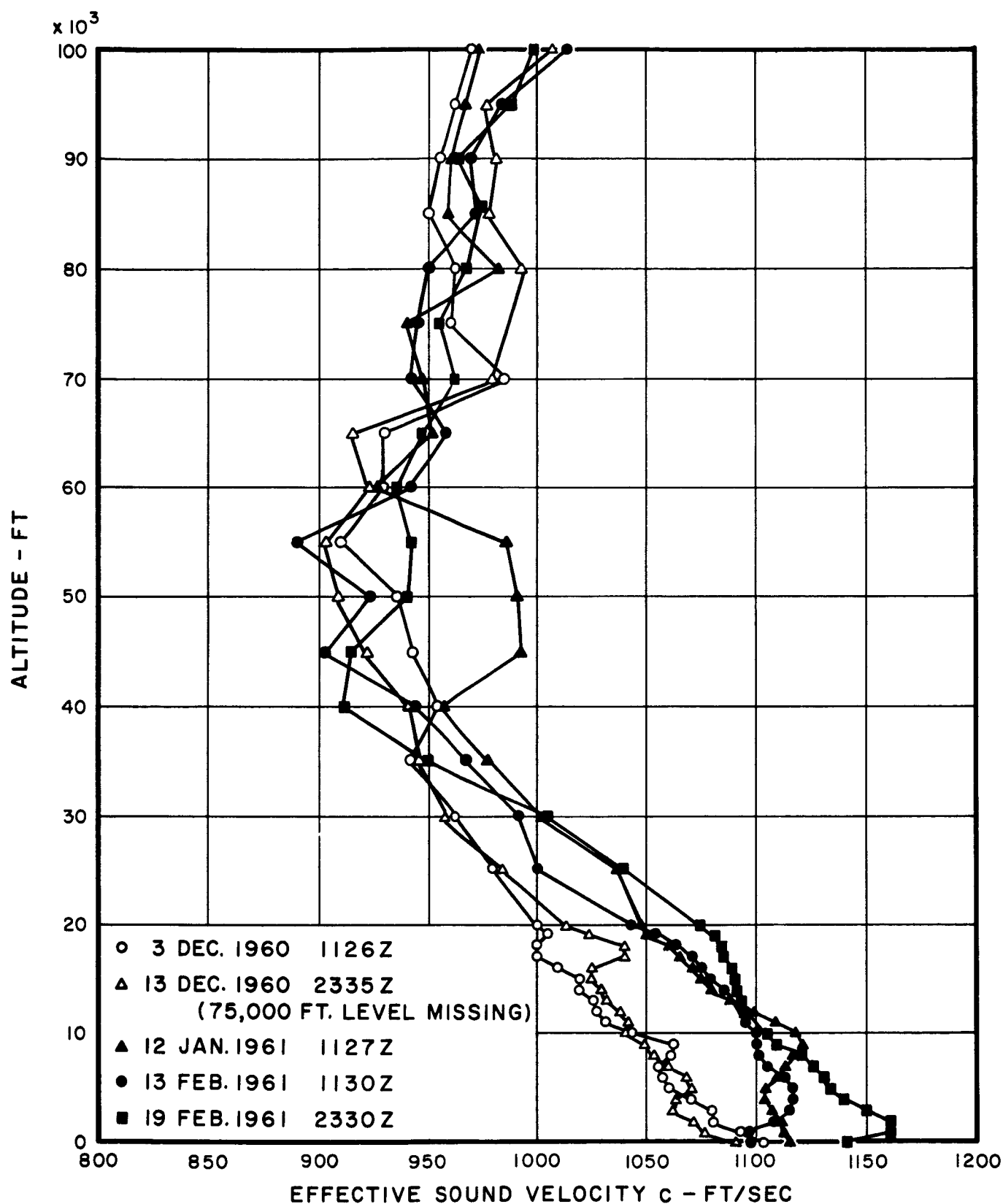


FIG. A-1a INDIVIDUAL SOUND VELOCITY PROFILES FOR
NORTHERN SECTOR IN WINTER
AT CAPE CANAVERAL

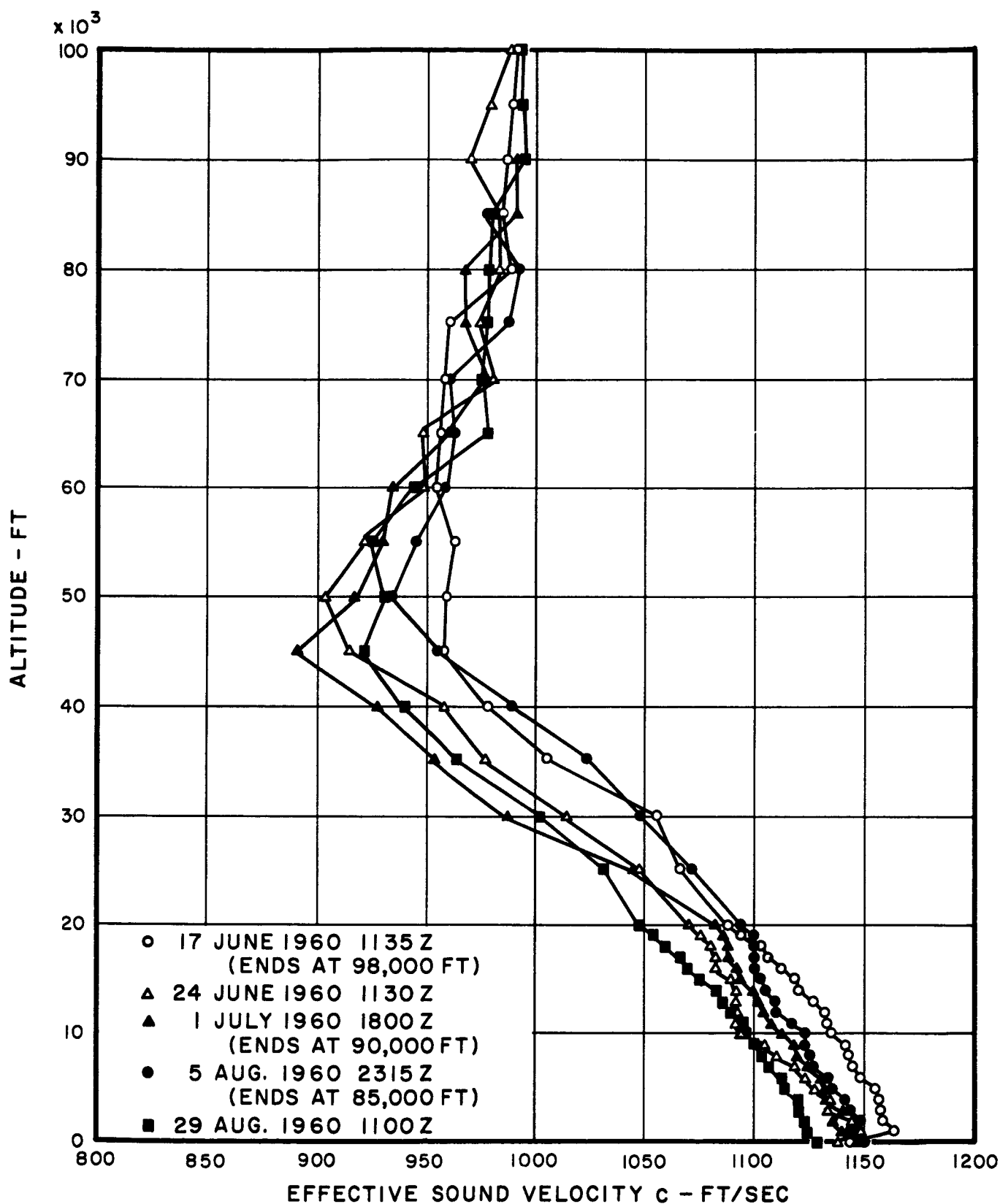


FIG. A-1b INDIVIDUAL SOUND VELOCITY PROFILES FOR
NORTHERN SECTOR IN SUMMER
AT CAPE CANAVERAL

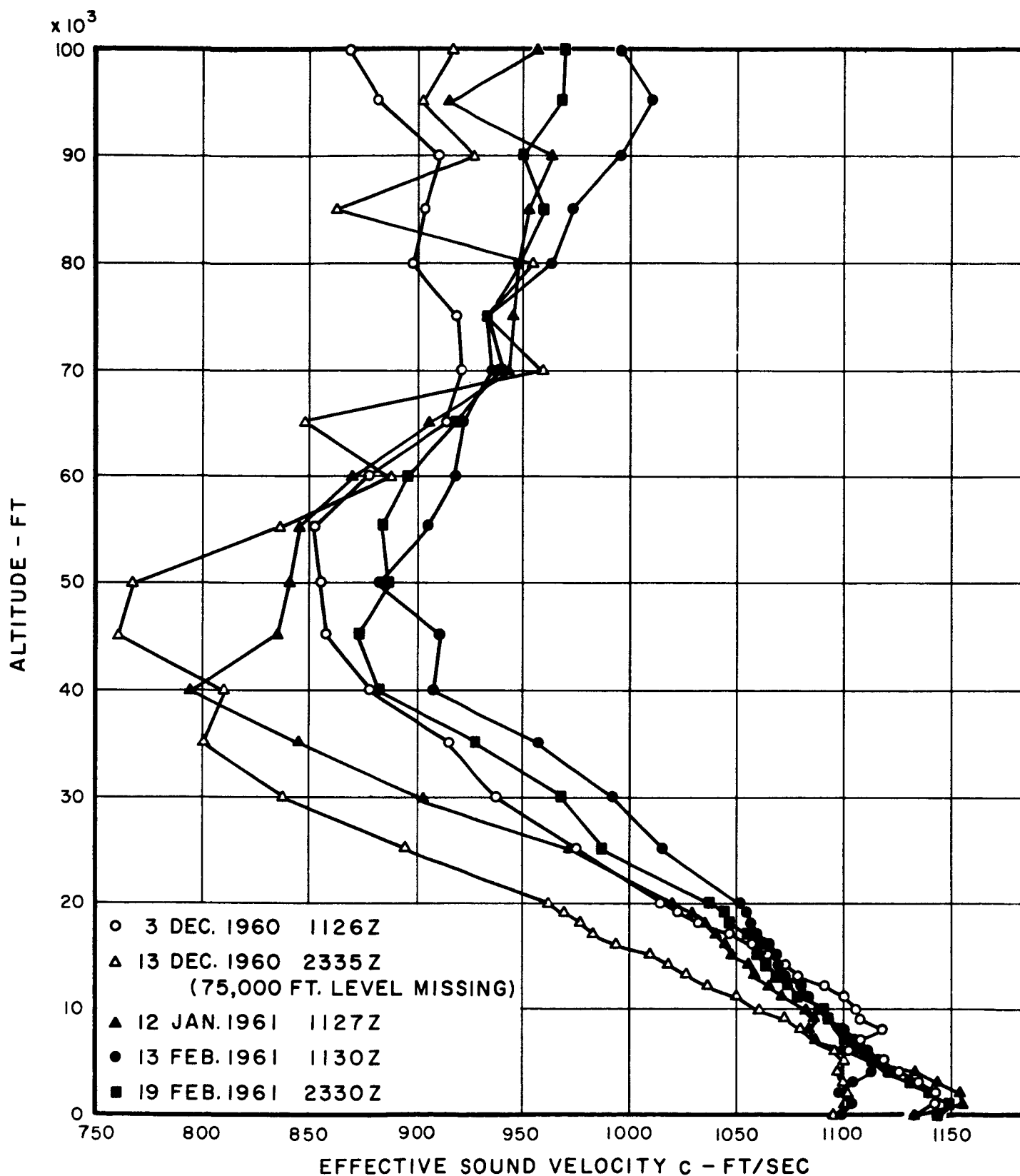


FIG. A-2a INDIVIDUAL SOUND VELOCITY PROFILES FOR
WESTERN SECTOR IN WINTER
AT CAPE CANAVERAL

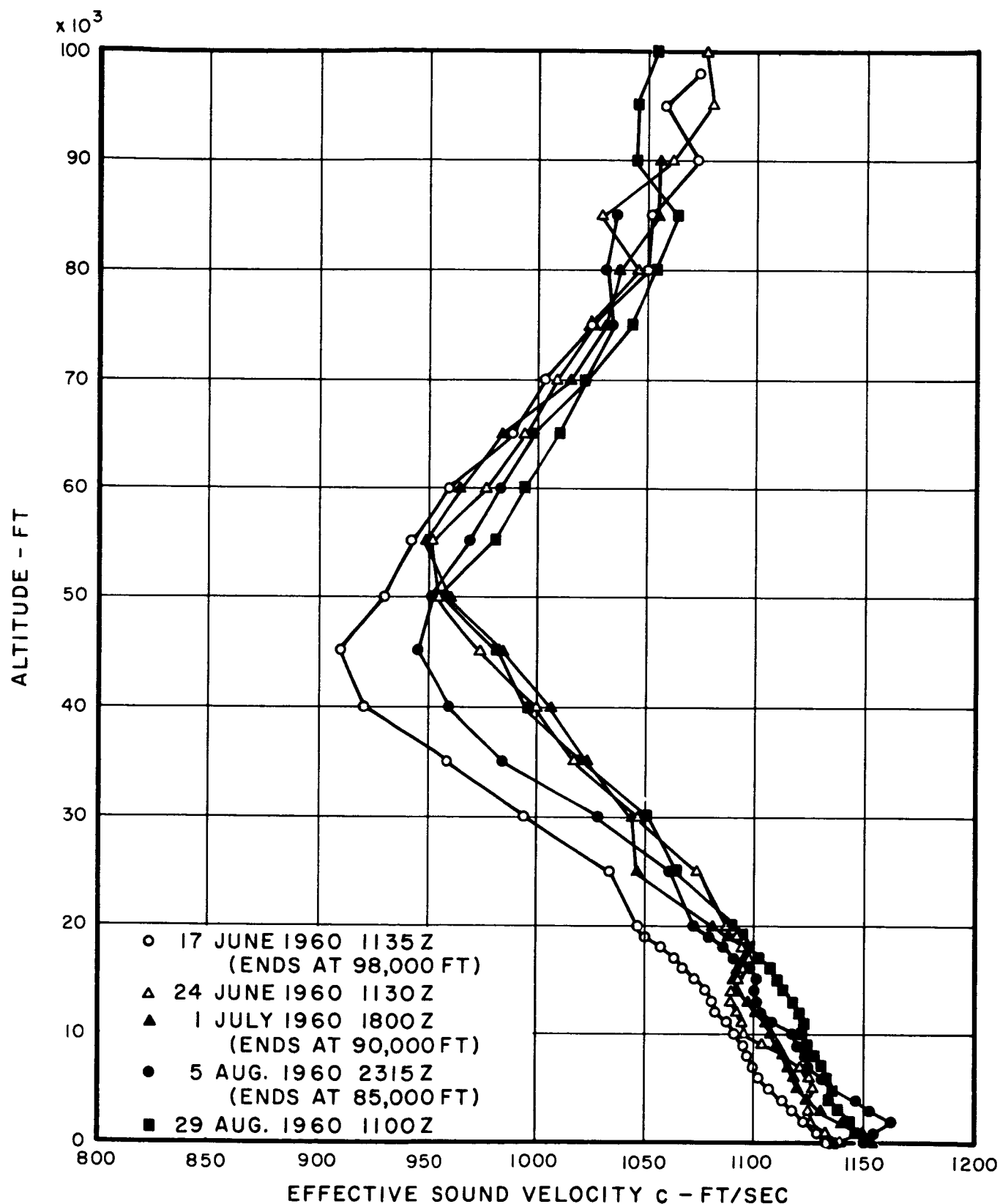


FIG.A-2b INDIVIDUAL SOUND VELOCITY PROFILES FOR
WESTERN SECTOR IN SUMMER
AT CAPE CANAVERAL

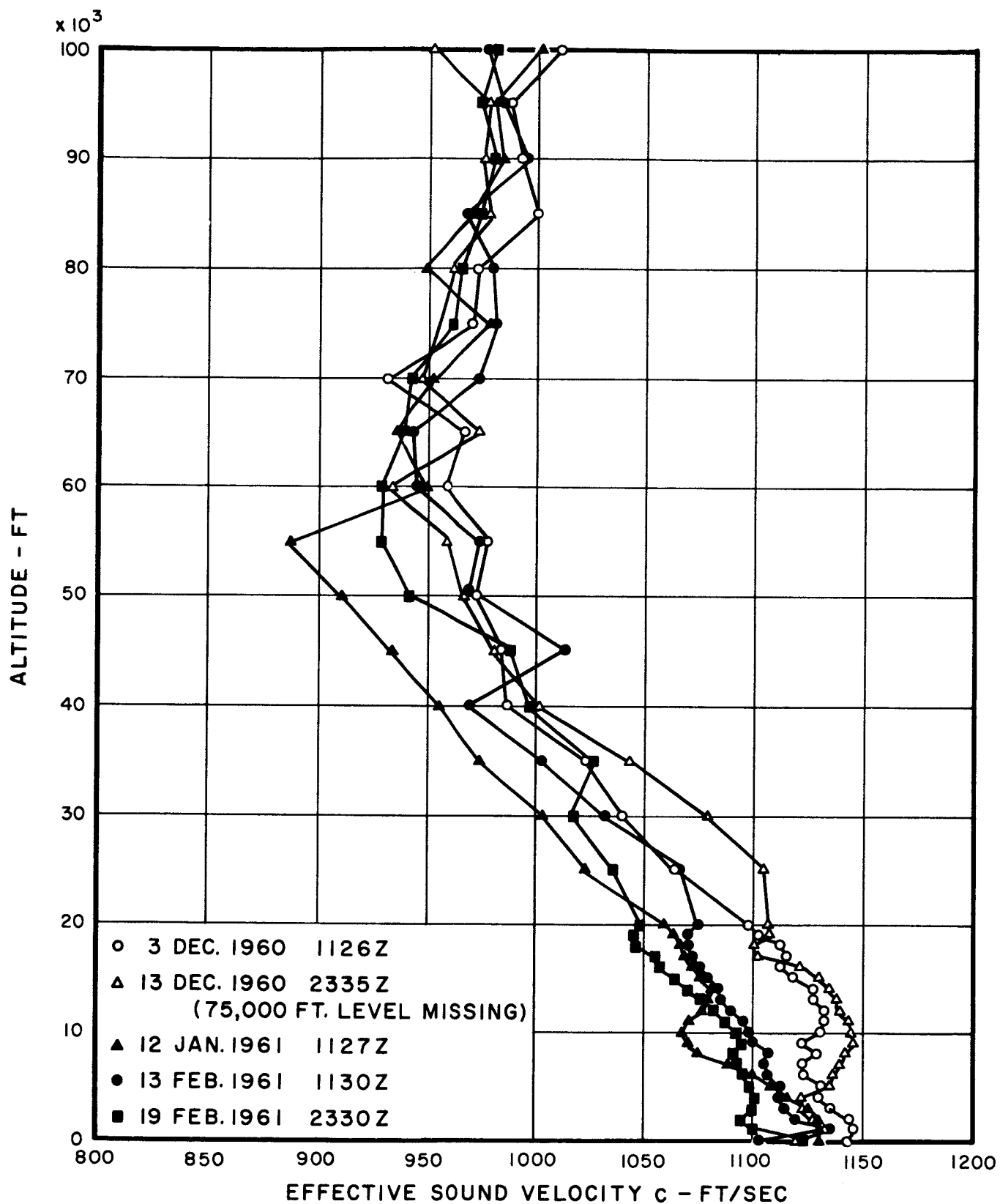


FIG. A-3a INDIVIDUAL SOUND VELOCITY PROFILES FOR SOUTHERN SECTOR IN WINTER AT CAPE CANAVERAL

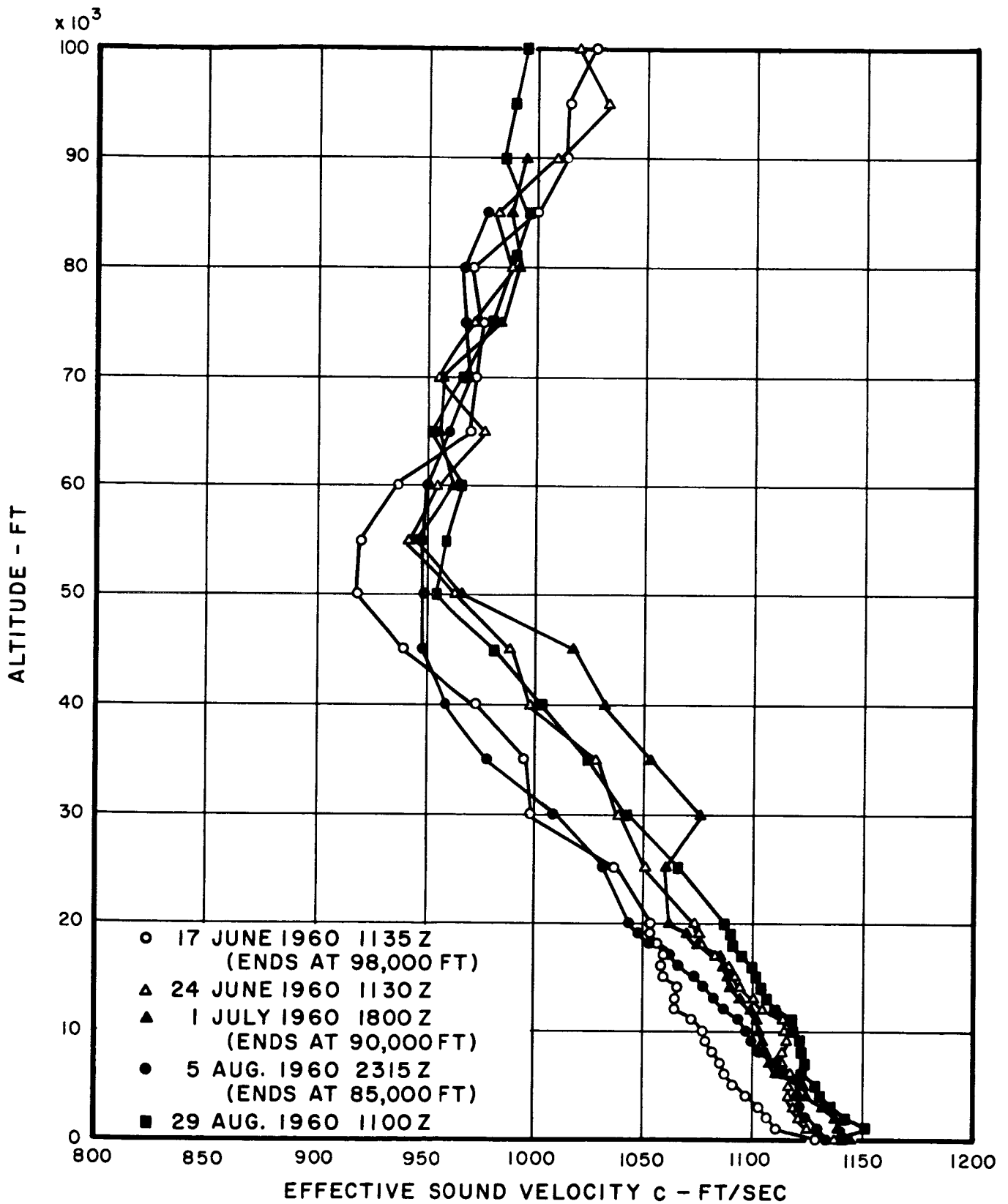


FIG.A-3b INDIVIDUAL SOUND VELOCITY PROFILES FOR
SOUTHERN SECTOR IN SUMMER
AT CAPE CANAVERAL

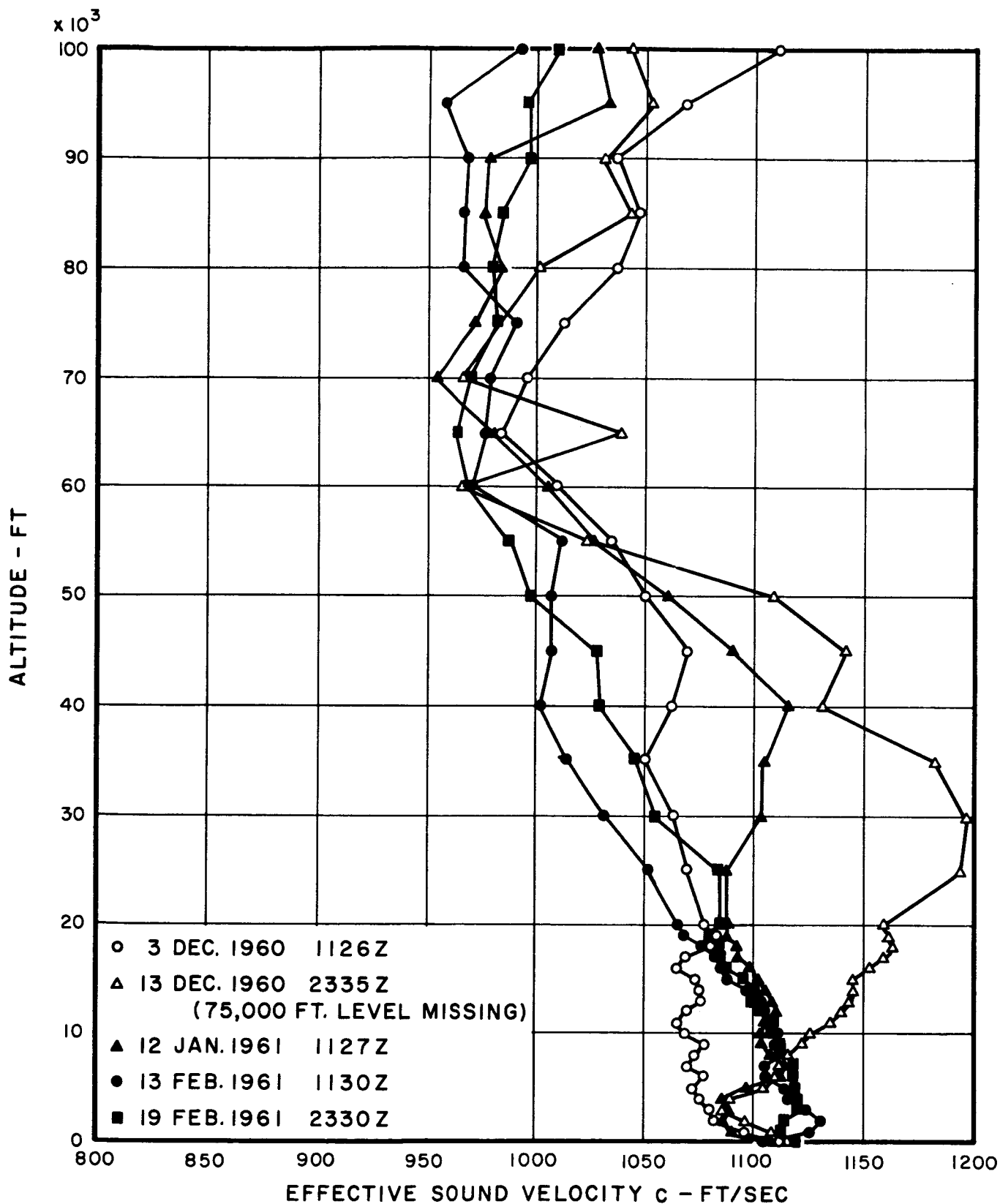


FIG. A-4a INDIVIDUAL SOUND VELOCITY PROFILES FOR
EASTERN SECTOR IN WINTER
AT CAPE CANAVERAL

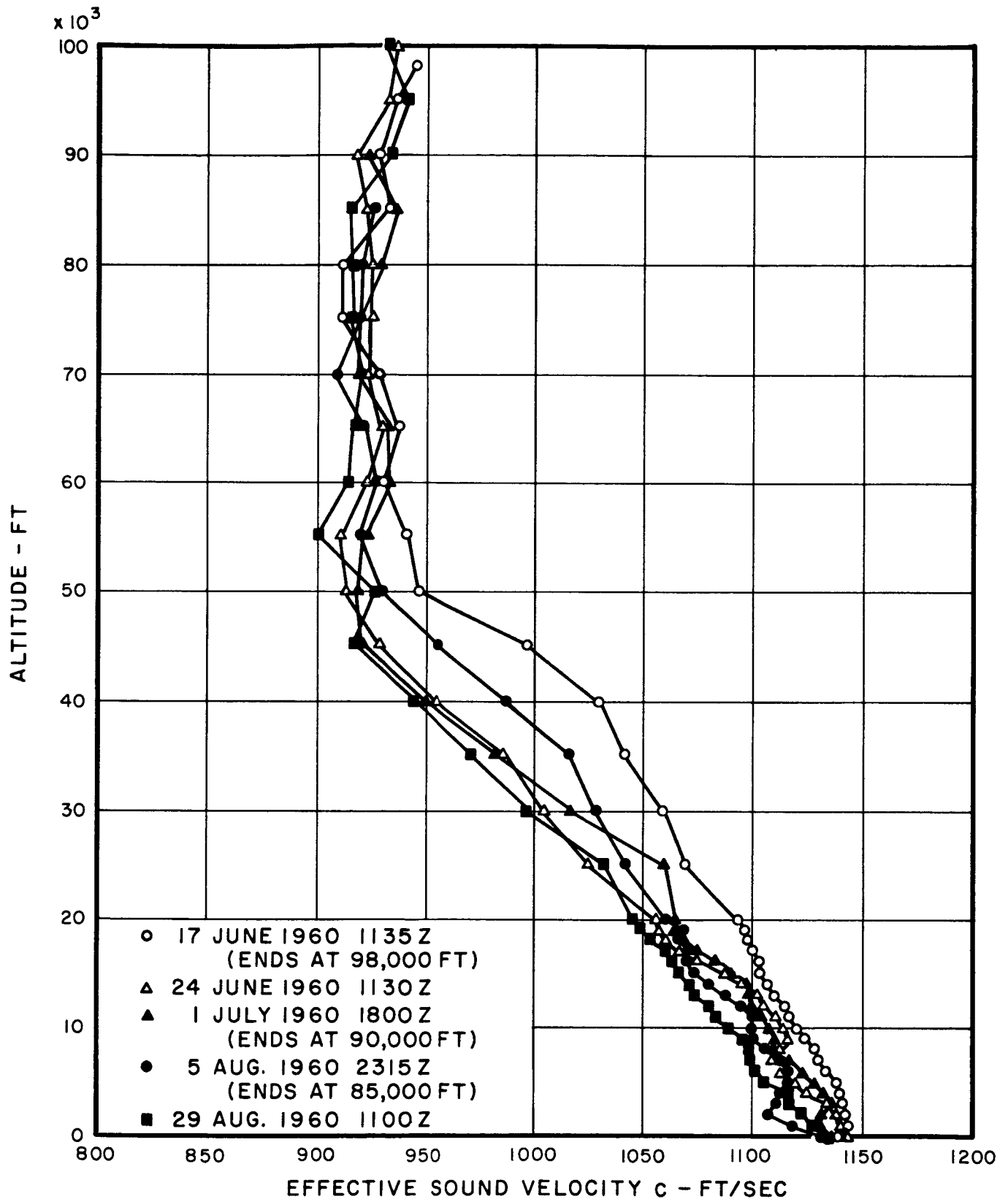


FIG. A-4b INDIVIDUAL SOUND VELOCITY PROFILES FOR
EASTERN SECTOR IN SUMMER
AT CAPE CANAVERAL

24 June 1960, 1130 Z

Weather: Near-calm conditions at the surface; light and variable wind aloft become easterly above 15,000 ft.

Sound velocity profile: Positive slopes in the first 1000 ft of $0.4 \times 10^{-2} \text{ sec}^{-1}$ in the eastern sector and $1.1 \times 10^{-2} \text{ sec}^{-1}$ in the northern sector.

1 July 1960, 1800 Z

Weather: Similar to the 24 June case above except that the surface winds are easterly in local sea-breeze circulation.

Sound velocity profile: No positive slopes of significance.

5 August 1960, 2315 Z

Weather: Southeasterly flow of maritime tropical air at low levels with easterly winds aloft except for southwesterly flow in the 35,000-to 45,000-ft layer.

Sound velocity profile: Positive slope of $0.5 \times 10^{-2} \text{ sec}^{-1}$ in the first 2000 ft of the western sector.

29 August 1960, 1100 Z

Weather: Northeasterly flow at the surface with easterly winds aloft at all levels.

Sound velocity profile: Positive slopes in the first 1000 ft of $1.0 \times 10^{-2} \text{ sec}^{-1}$ in the western sector and $1.2 \times 10^{-2} \text{ sec}^{-1}$ in the southern sector.

A.2.2 Case Studies for the Huntsville Area

Since there are no regular Rawinsonde ascents at Huntsville, the sector plots presented in Figures A-5a through A-8b are for Nashville, Tennessee, the nearest station for which appropriate data are available. Effective sound propagation velocities entered in the figures were calculated from temperature and wind data tabulated on WBAN 33 Forms (Summary of Constant Pressure Data) for the winter and summer of 1960; these forms were obtained from the National Weather Records Center. Data points are plotted at pressure intervals of 50 mb. There is good general agreement between the cases shown in the above figures and the envelopes of the probability distributions (Figures 7-7a through 7-10b). The gross weather situations associated with individual cases and the occurrence of positive profile slopes are summarized below.

Winter Cases

25 January 1960, 0000 Z

Weather: Nashville is near the center of a large polar anticyclone; light northerly winds at the surface back to westerly above 3500 ft. Sound velocity profile: Positive slope of about $1.4 \times 10^{-2} \text{ sec}^{-1}$ between 5000 and 6500 ft in the eastern sector.

9 February 1960, 1200 Z

Weather: Southerly flow of returning polar continental air at the surface; strong westerly winds above 10,000 ft. Sound velocity profile: Positive slopes in first 1000 ft of about $3.0 \times 10^{-2} \text{ sec}^{-1}$ in the eastern sector and $2.5 \times 10^{-2} \text{ sec}^{-1}$ in the northern sector. Maximum value for c at 12,000 ft in eastern sector exceeds value at ground level by 60 ft sec^{-1} .

20 February 1960, 0000 Z

Weather: Near center of very cold polar anticyclone; northerly winds at the surface and very strong westerlies above 10,000 ft. Sound velocity profile: Positive slopes in the eastern sector through deep layer between ground level and 21,000 ft where c exceeds the value at the surface by 67 ft sec^{-1} ; also, in southern sector there is a positive slope of about $1.4 \times 10^{-2} \text{ sec}^{-1}$ in the layer from 3500 to 6500 ft.

3 December 1960, 1200 Z

Weather: Near-calm conditions at the surface and clear skies near center of very cold polar anticyclone lead to 25°F temperature inversion in first 4000 ft. Winds aloft are from the southwest below the inversion and from the northwest above the inversion. Sound velocity profile: Large positive slopes in eastern and northern sectors in first 2000 ft of about $2.0 \times 10^{-2} \text{ sec}^{-1}$.

22 December 1960, 1200 Z

Weather: Near center of cold polar anticyclone. Light southerly surface winds with strong westerly winds aloft. Sound velocity profile: Positive slopes in eastern sector from surface to 30,000 ft and in southern sector from 3000 to 8000 ft.

Summer Cases

4 June 1960, 0000 Z

Weather: Weak surface pressure gradient in maritime tropical air. Winds aloft are light and variable, principally from the north. Sound velocity profile: No positive slopes.

16 July 1960, 1200 Z

Weather: Light northerly winds at the surface in a summer polar continental air mass; weak early-morning surface temperature inversion in first 1500 ft. Winds aloft are southerly from 2000 to 8000 ft and westerly above 10,000 ft.

Sound velocity profile: Positive slopes in first 1500 ft in western and northern sectors and from 2000 to 4000 ft in the eastern sector (0.7 to $1.4 \times 10^{-2} \text{ sec}^{-1}$).

3 August 1960, 0000 Z

Weather: Weak southerly flow of tropical air at the surface. Winds aloft are light and variable.

Sound velocity profile: No positive slopes of significance.

14 August 1960, 1200 Z.

Weather: Strong flow of tropical maritime air at surface with strong southwesterly winds aloft.

Sound velocity profile: Positive slope of $1.3 \times 10^{-2} \text{ sec}^{-1}$ in first 1500 ft of eastern sector and from 5000 to 7000 ft in the northern sector ($0.7 \times 10^{-2} \text{ sec}^{-1}$).

29 August 1960, 0000 Z

Weather: Southerly flow of tropical maritime air at the surface with southwesterly winds aloft.

Sound velocity profile: Positive slopes in first 1500 ft of $1.0 \times 10^{-2} \text{ sec}^{-1}$ in both northern and eastern sectors.

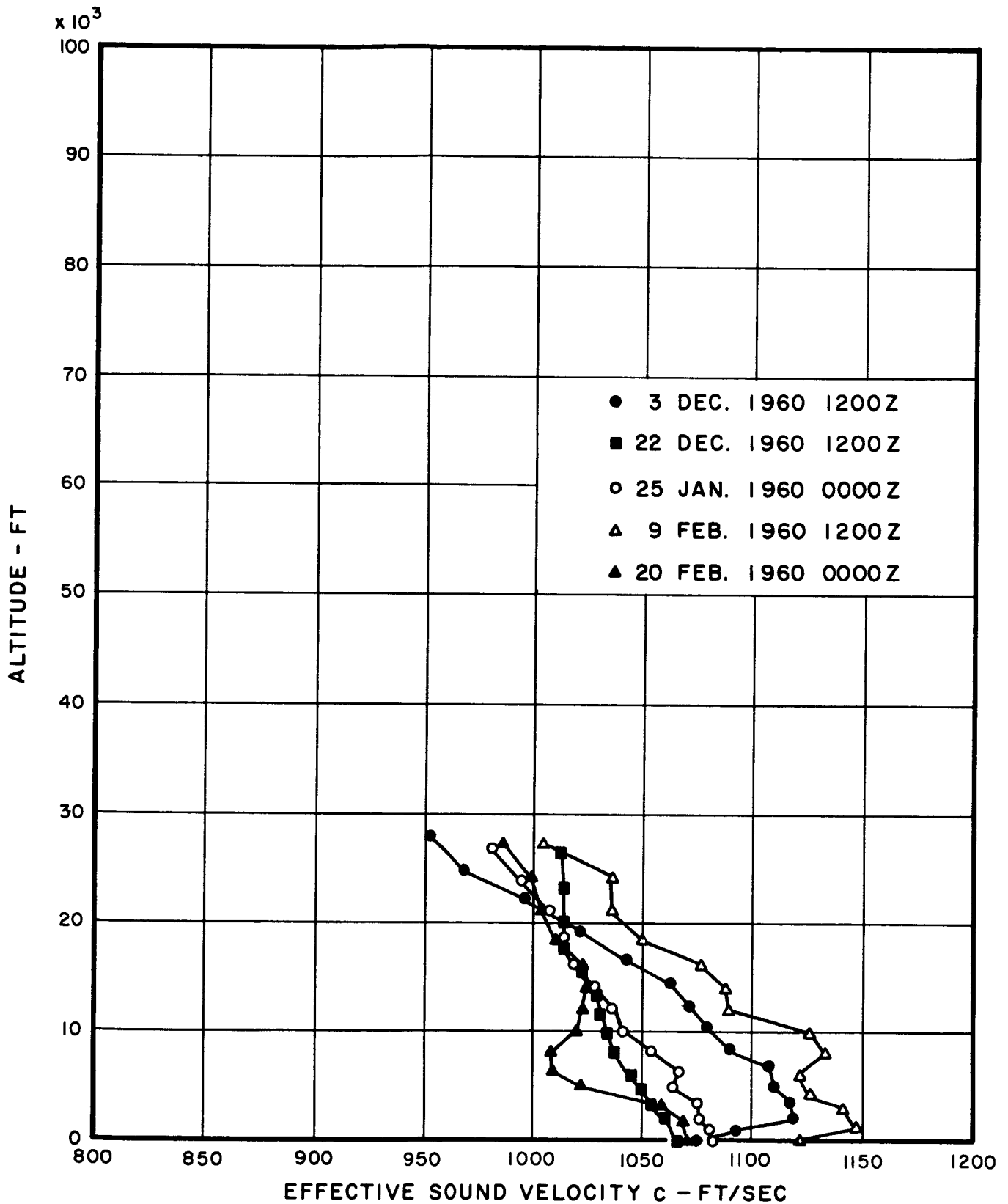


FIG. A-5a INDIVIDUAL SOUND VELOCITY PROFILES FOR
NORTHERN SECTOR IN WINTER
IN HUNTSVILLE AREA

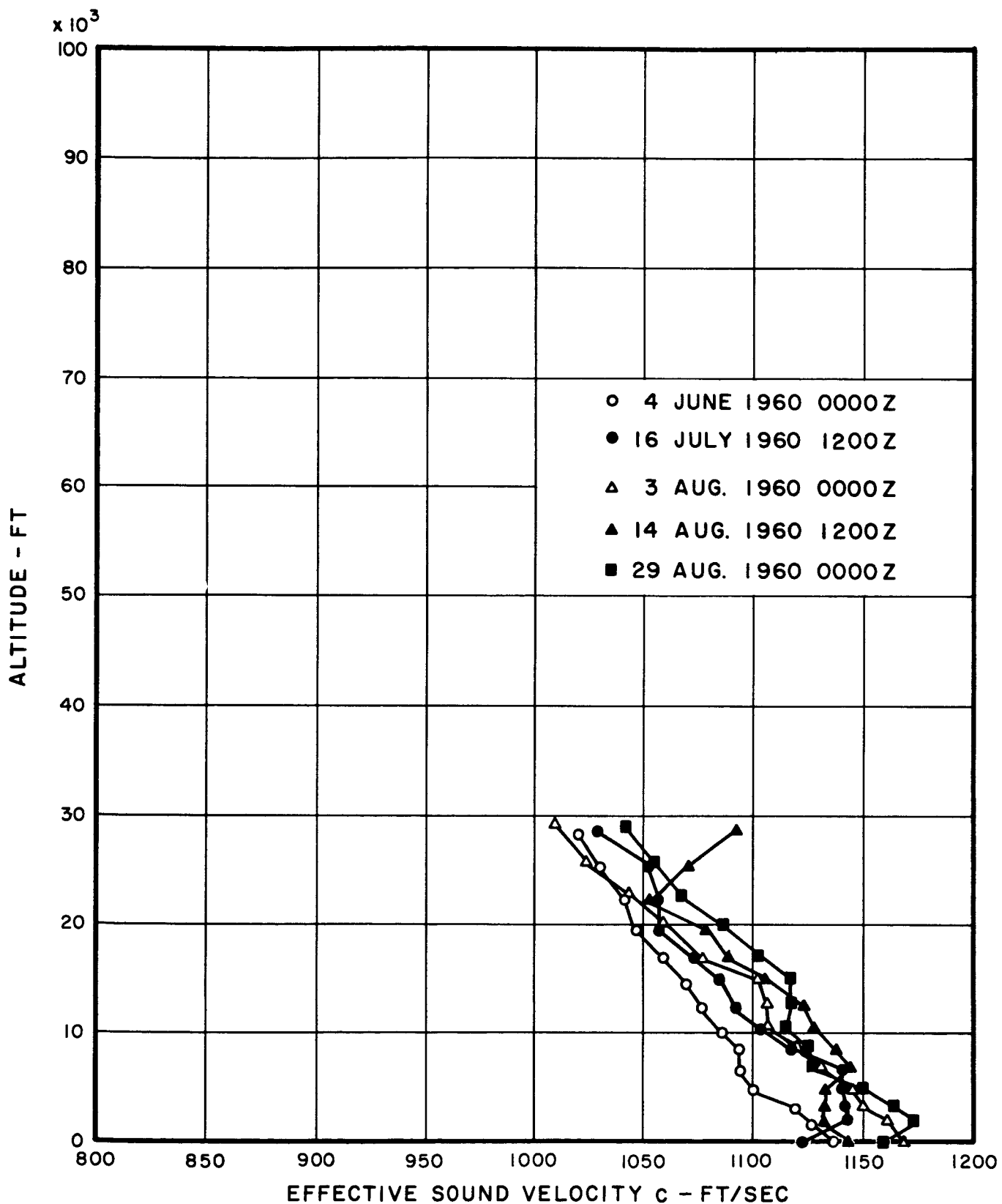


FIG. A-5b INDIVIDUAL SOUND VELOCITY PROFILES FOR
NORTHERN SECTOR IN SUMMER
IN HUNTSVILLE AREA

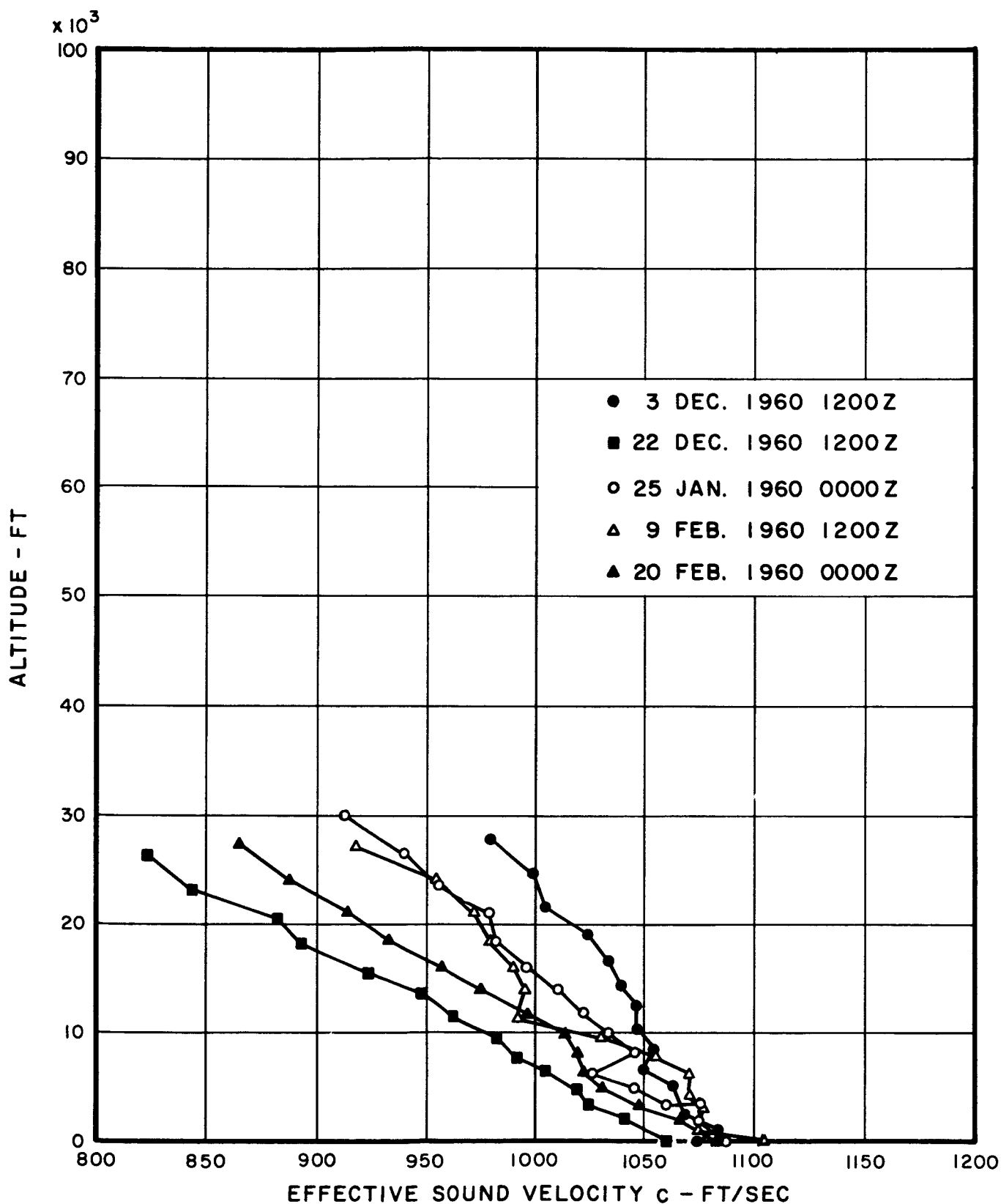


FIG. A-6a INDIVIDUAL SOUND VELOCITY PROFILES FOR
WESTERN SECTOR IN WINTER
IN HUNTSVILLE AREA

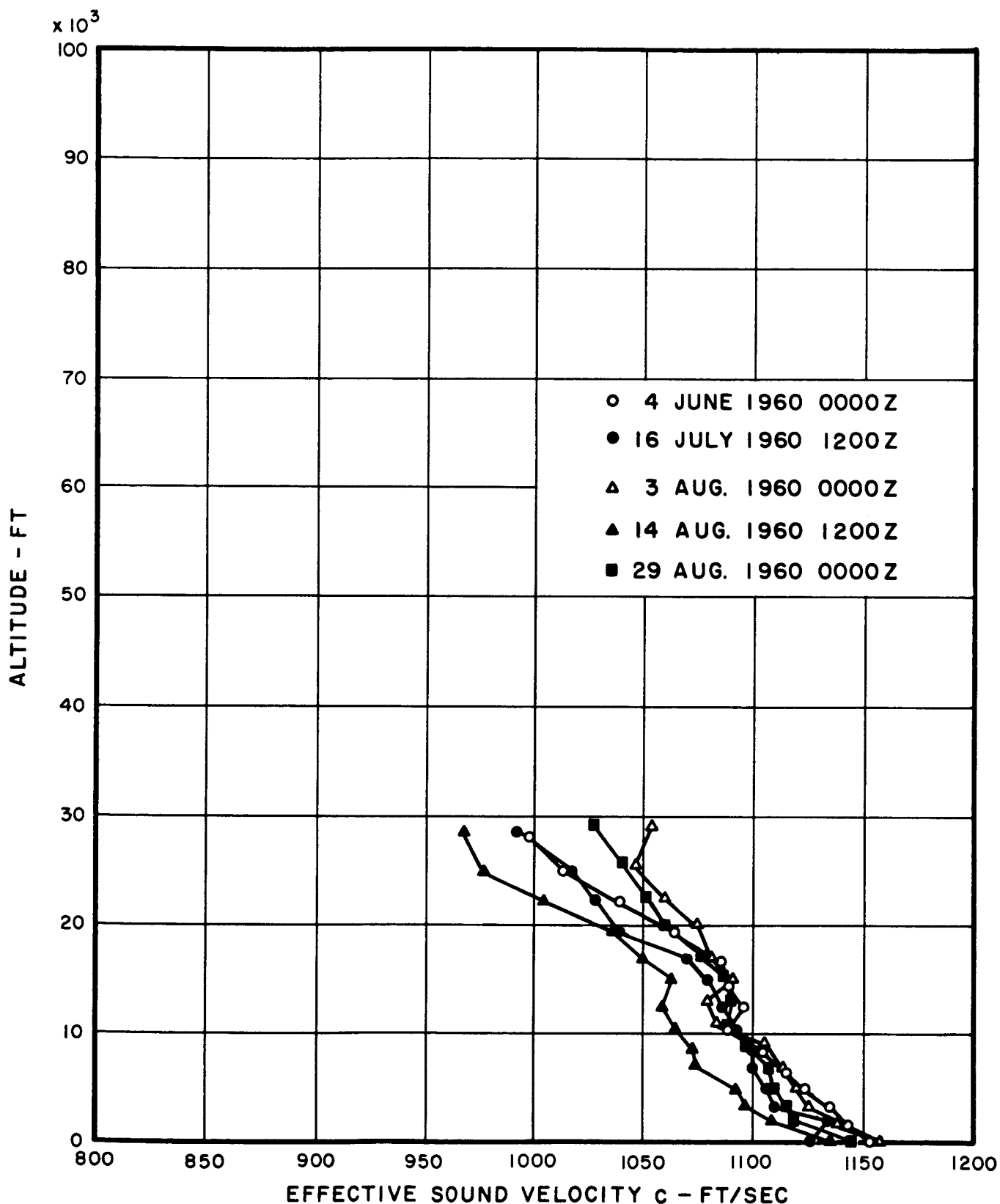


FIG. A-6b INDIVIDUAL SOUND VELOCITY PROFILES FOR
WESTERN SECTOR IN SUMMER
IN HUNTSVILLE AREA

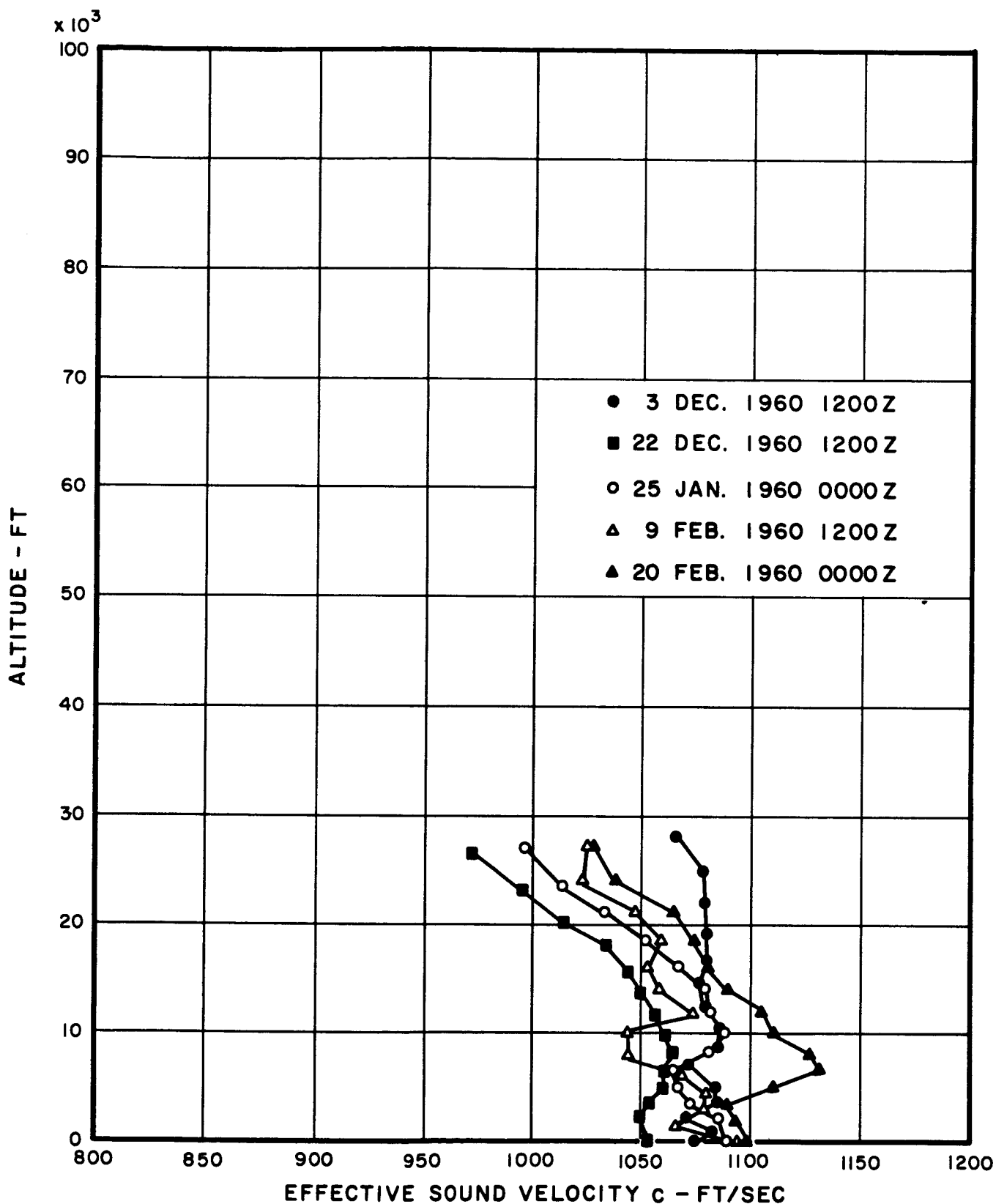


FIG. A-7a INDIVIDUAL SOUND VELOCITY PROFILES FOR
SOUTHERN SECTOR IN WINTER
IN HUNTSVILLE AREA

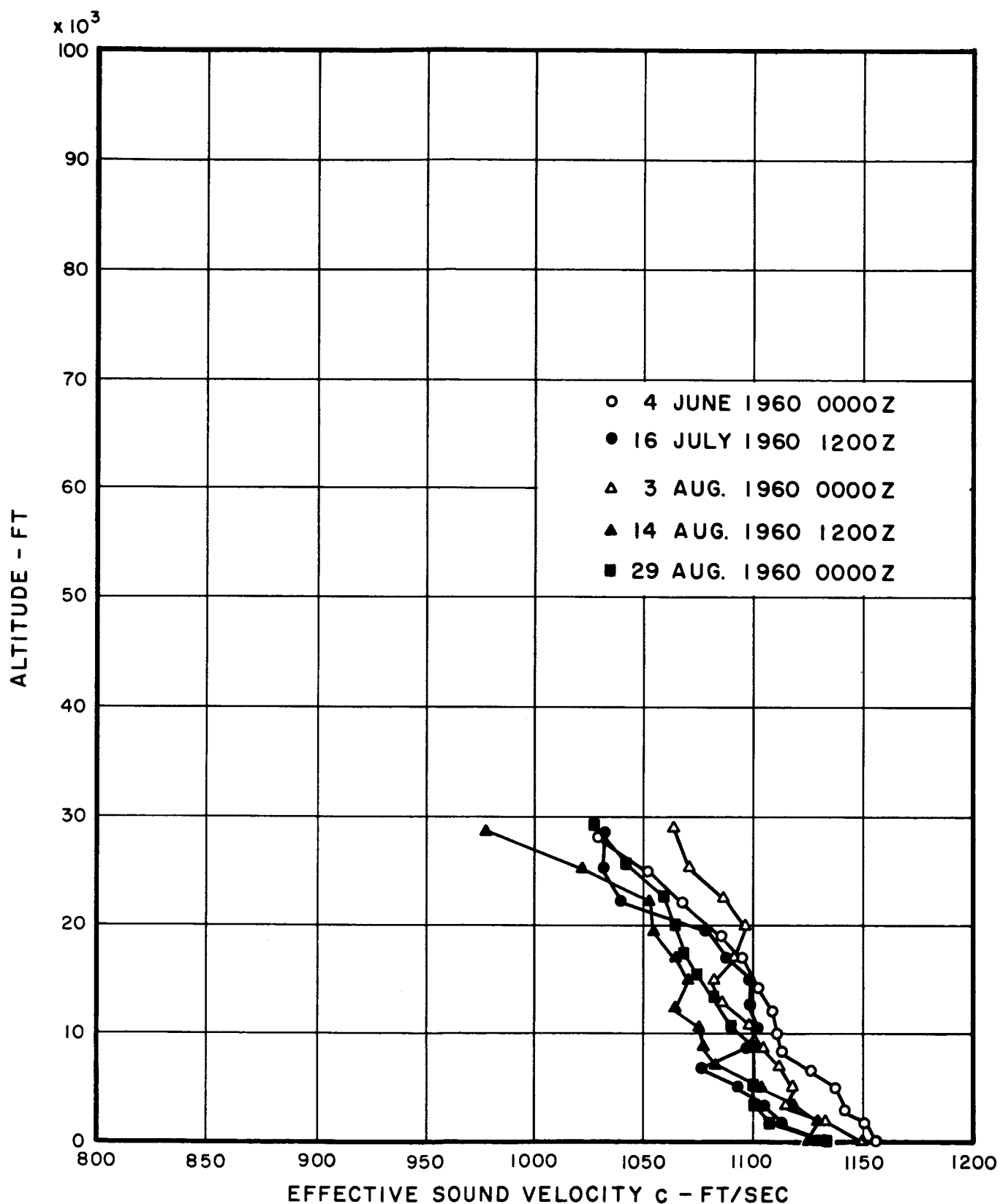


FIG. A-7b INDIVIDUAL SOUND VELOCITY PROFILES FOR
SOUTHERN SECTOR IN SUMMER
IN HUNTSVILLE AREA

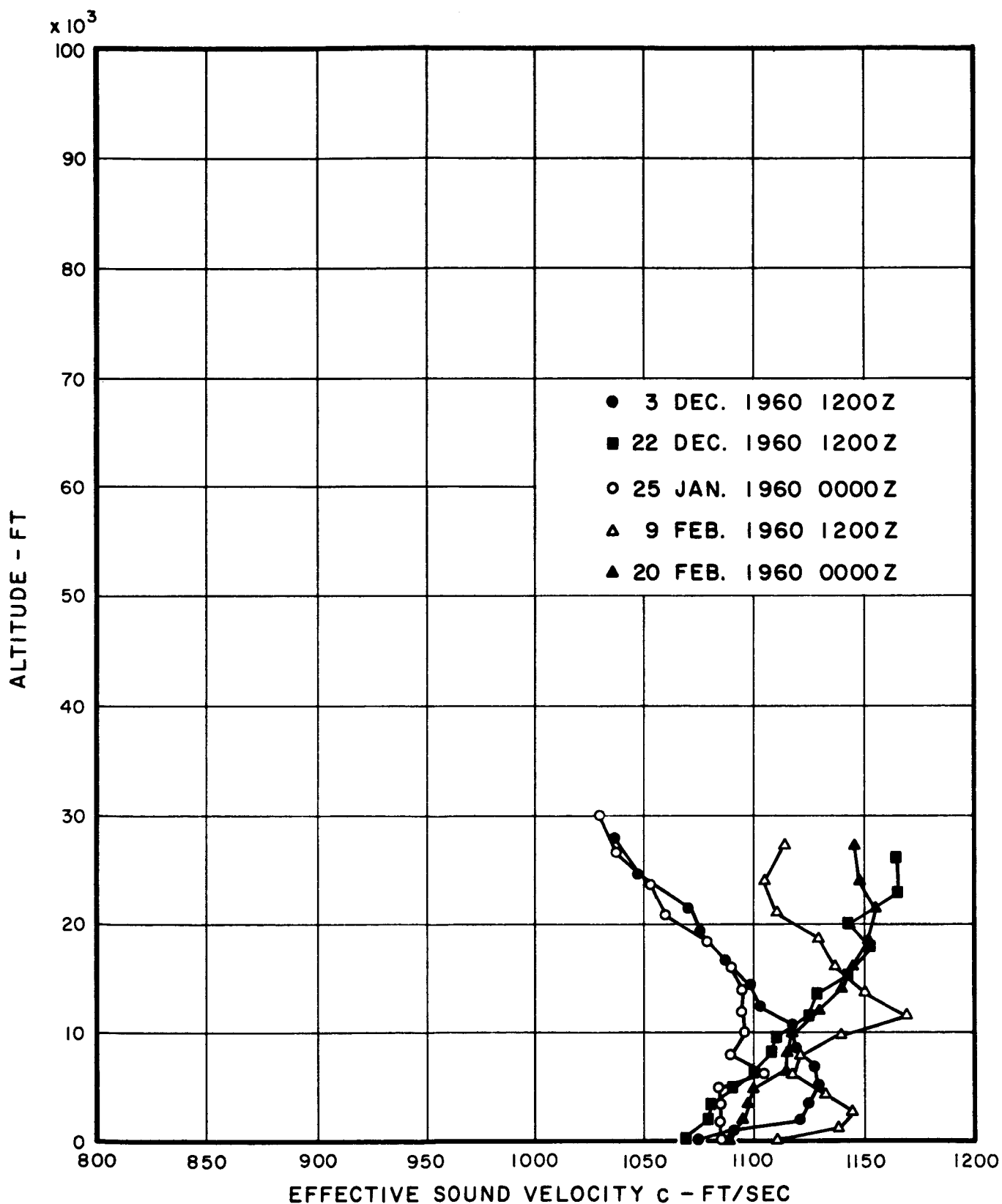


FIG. A-8a INDIVIDUAL SOUND VELOCITY PROFILES FOR
EASTERN SECTOR IN WINTER
IN HUNTSVILLE AREA

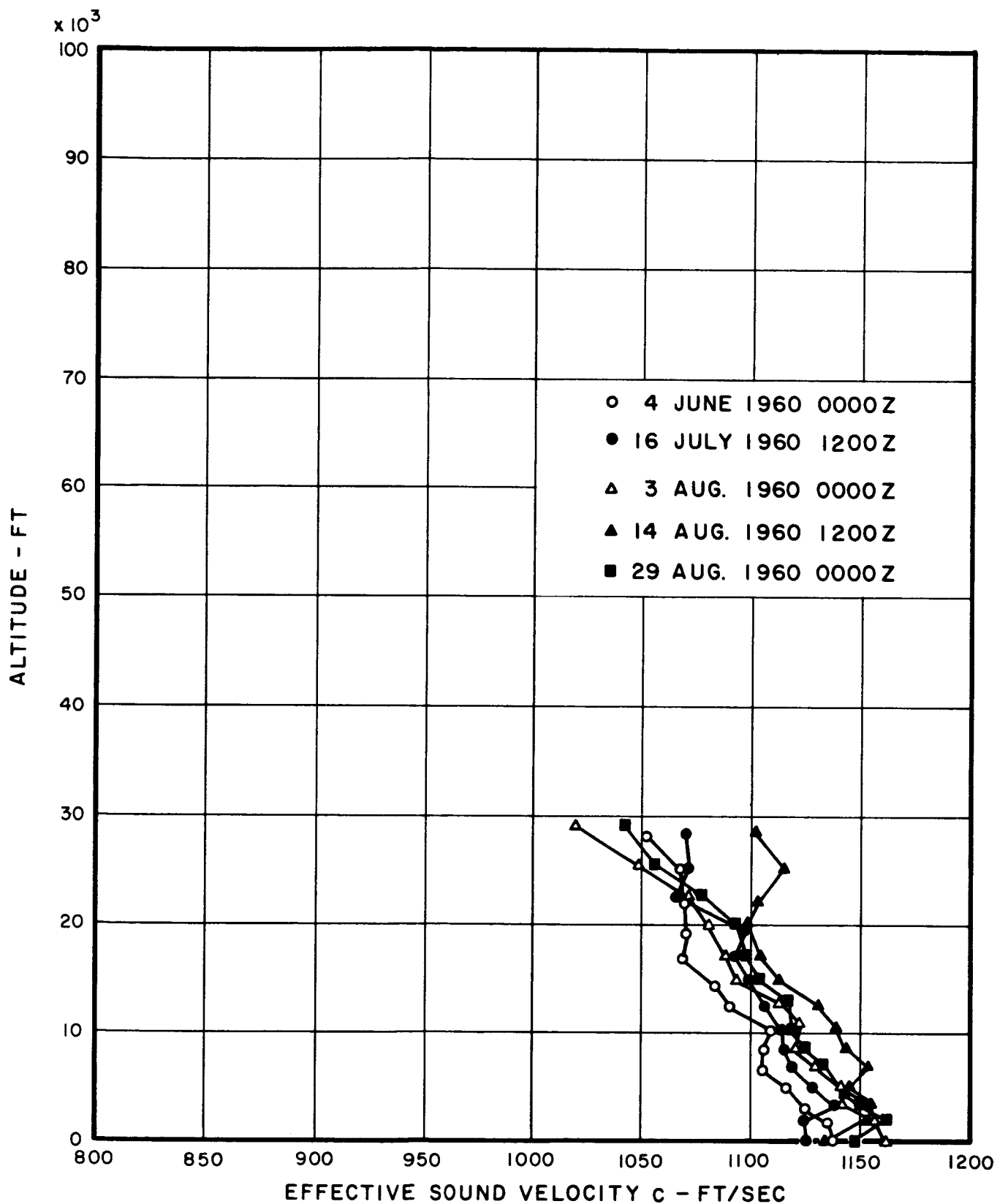


FIG. A-8b INDIVIDUAL SOUND VELOCITY PROFILES FOR
EASTERN SECTOR IN SUMMER
IN HUNTSVILLE AREA

A.2.3 Case Studies for Point Arguello

The profiles for Point Arguello presented in Figures A-9a through A-12b are based on Constant Pressure Data tabulated on WBAN 33 Forms obtained for the summer and winter months of 1960 from the National Weather Records Center. As in the previous studies of individual cases for the Cape Canaveral and Huntsville areas, the results are in good agreement with the envelopes indicated by the probability distributions (see Figures 7-11a through 7-14b). Brief descriptions of the gross weather situations identified with the individual cases and comments on the occurrence of positive slopes in the sound-velocity profiles are given below.

Winter cases

13 January 1960, 0000 Z

Weather: High pressure ridge located in northern California and Idaho; low-level flow from the northwest reinforced by sea breeze circulation. Strong northerly winds aloft between 20,000 and 35,000 ft.

Sound velocity profile: Positive slopes in all sectors except the northern one but c never exceeds the value at the surface.

28 January 1960, 0000 Z

Weather: Sea-breeze circulation at low levels with moderate northwesterly flow aloft; near center of surface anticyclone.

Sound velocity profile: Positive slope of about $0.8 \times 10^{-2} \text{ sec}^{-1}$ in western sector between 2000 and 3500 ft; positive slopes in eastern sector between 3500 and 8500 ft are less significant since c never exceeds value at ground level.

28 February 1960, 0000 Z

Weather: Light westerly winds at the surface and strong westerlies above 25,000 ft.

Sound velocity profile: Some positive slopes in the eastern sector but c never exceeds value at surface.

17 December 1960, 0000 Z

Weather: Light and variable northerly winds at low levels with moderate westerly flow aloft.

Sound velocity profile: Positive slopes of about $0.7 \times 10^{-2} \text{ sec}^{-1}$ in first 1500 ft of southern and western sectors; also, positive slopes in eastern sector from 5000 to 10,000 ft, but c does not exceed value at surface.

30 December 1960, 0000 Z

Weather: Sea-breeze circulation in surface layers superimposed on weak northerly gradient; winds aloft are from the north and northeast below 40,000 ft, westerly from 40,000 to 70,000 ft, and easterly at the highest levels. Small temperature inversion in first 2000 ft due to shift from sea-breeze circulation to northerly flow.

Sound velocity profile: Positive slopes in first 1500 ft of about $1.5 \times 10^{-2} \text{ sec}^{-1}$ in southern and western sectors; strong wind shear produces positive slopes in these sectors between 10,000 and 15,000 ft.

Summer Cases

2 June 1960, 0000 Z

Weather: Strong low-level temperature inversion (25°F difference between ground level and top of the inversion at 3500 ft); westerly winds in surface layers and northeasterly winds above the inversion. Sound velocity profile: Positive slopes in all sectors due to temperature inversion (1.0 to $2.5 \times 10^{-2} \text{ sec}^{-1}$).

21 June 1960, 0000 Z

Weather: Temperature inversion of 15°F in first 2000 ft; surface winds are from the northwest; winds above the inversion are from the northeast below 15,000 ft with a shift to westerly between 15,000 and 60,000 ft and easterly circulation at the highest levels. Sound velocity profile: Positive slopes in first 1500 ft of the southern and eastern sectors of about $2 \times 10^{-2} \text{ sec}^{-1}$ and between 2000 and 3500 ft in the western sector of about $1.3 \times 10^{-2} \text{ sec}^{-1}$.

10 July 1960, 0000 Z

Weather: Weak temperature inversion with southwesterly flow in first 5000 ft; winds are light and variable above 5000 ft. Sound velocity profile: Positive slopes of about $1.5 \times 10^{-2} \text{ sec}^{-1}$ in the first 3000 ft in the western sector and between 2000 and 3000 ft in the northern sector. Also, positive slopes of about $1 \times 10^{-2} \text{ sec}^{-1}$ between 3000 and 4500 ft in the eastern and southern sectors.

18 July 1960, 0000 Z

Weather: Strong surface temperature inversion of about 27°F in first 2000 ft; winds are from the northwest at the surface, northerly above the inversion, variable westerly between 10,000 and 50,000 ft, and easterly at the highest levels.

Sound velocity profile: Positive slopes in the first 1500 ft in the eastern sector of about $2.2 \times 10^{-2} \text{ sec}^{-1}$ and in the southern sector of about $4.0 \times 10^{-2} \text{ sec}^{-1}$; positive slope in first 3500 ft of the western sector ($1.5 \times 10^{-2} \text{ sec}^{-1}$).

15 August 1960, 0000 Z

Weather: Strong temperature inversion of about 25°F from 1500 to 3000 ft. Strong wind shear in the surface layers due to sea breeze and southwesterly flow aloft; winds are easterly above 65,000 ft.

Sound velocity profile: Positive slopes in the northern sector of about $1.1 \times 10^{-2} \text{ sec}^{-1}$ in the first 3000 ft and in the southern and northern sectors from 1500 to 3000 ft (both about $1.8 \times 10^{-2} \text{ sec}^{-1}$); positive slope of about $1.2 \times 10^{-2} \text{ sec}^{-1}$ in eastern sector between 1500 and 5000 ft.

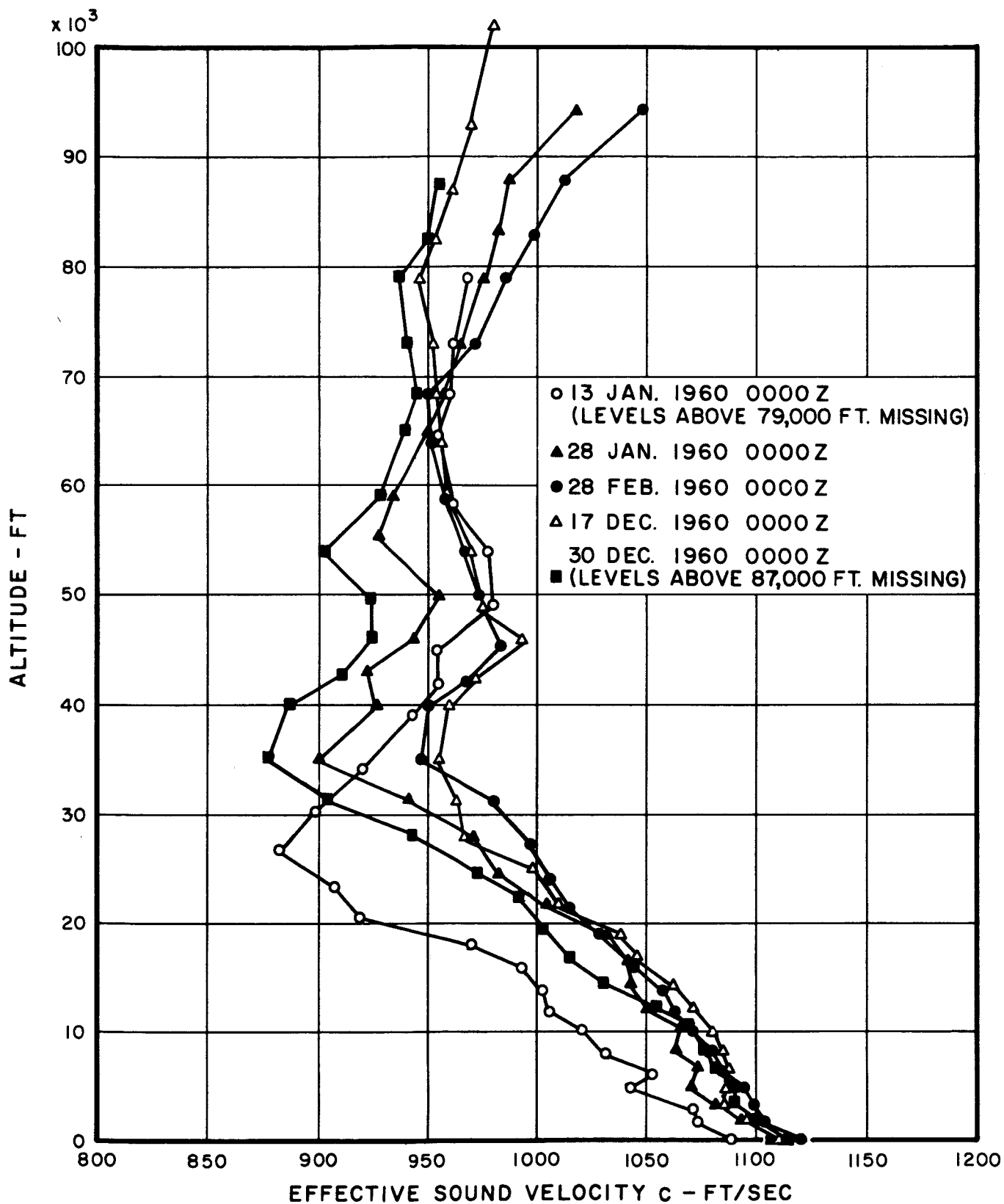


FIG. A-9a INDIVIDUAL SOUND VELOCITY PROFILES FOR
NORTHERN SECTOR IN WINTER
AT POINT ARGUELLO

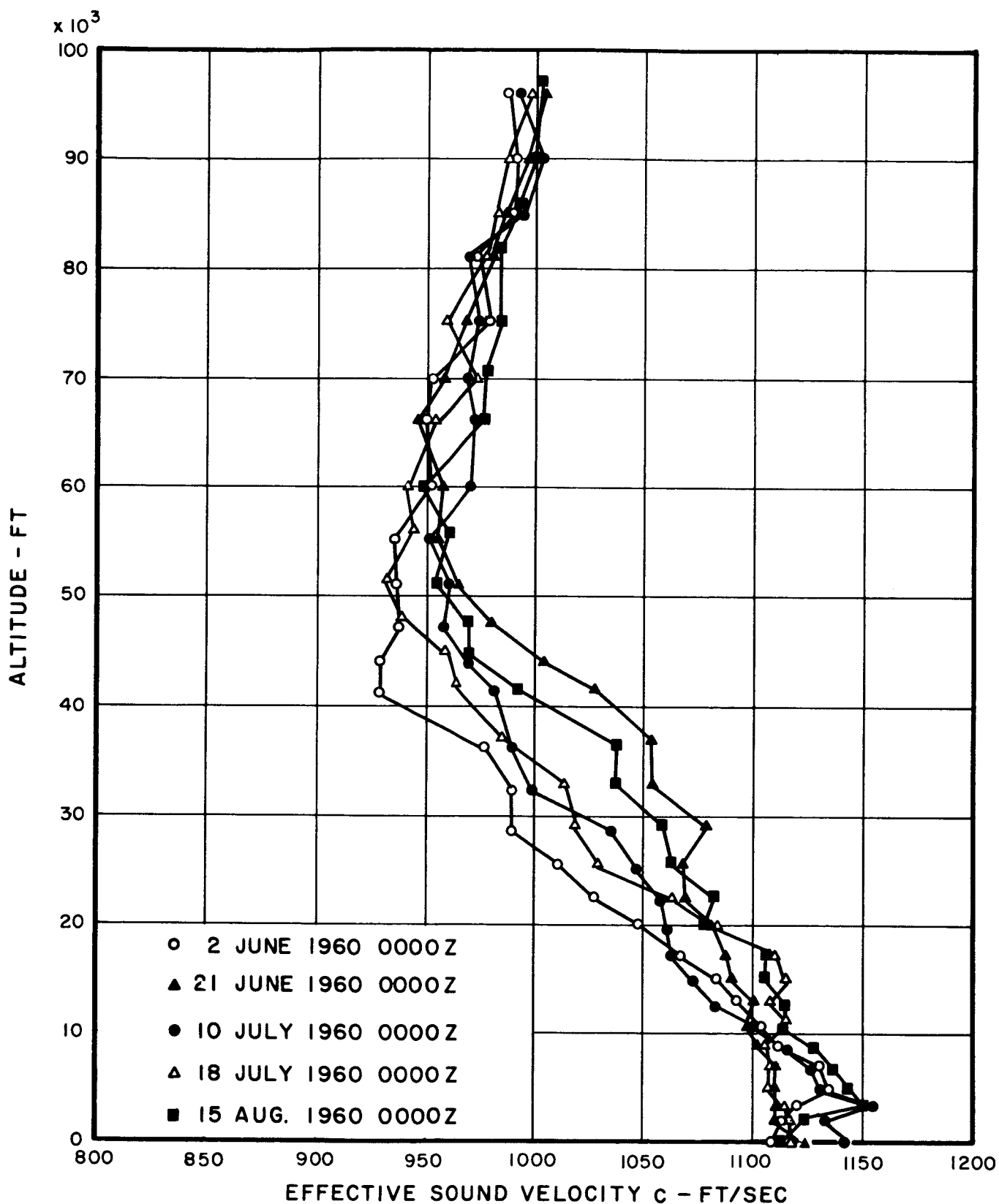


FIG. A-9b INDIVIDUAL SOUND VELOCITY PROFILES FOR
NORTHERN SECTOR IN SUMMER
AT POINT ARGUELLO

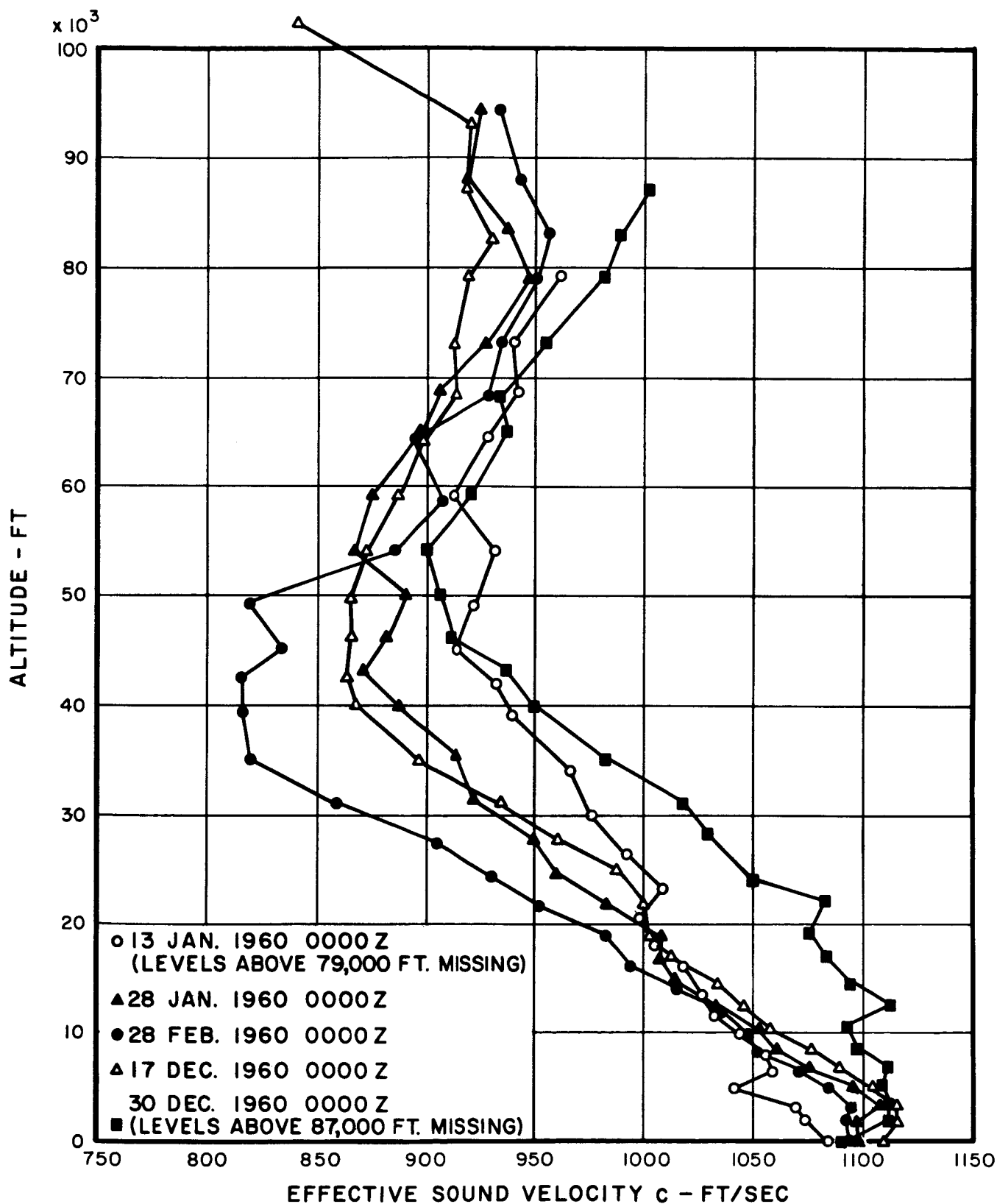


FIG. A-10a INDIVIDUAL SOUND VELOCITY PROFILES FOR
WESTERN SECTOR IN WINTER
AT POINT ARGUELLO

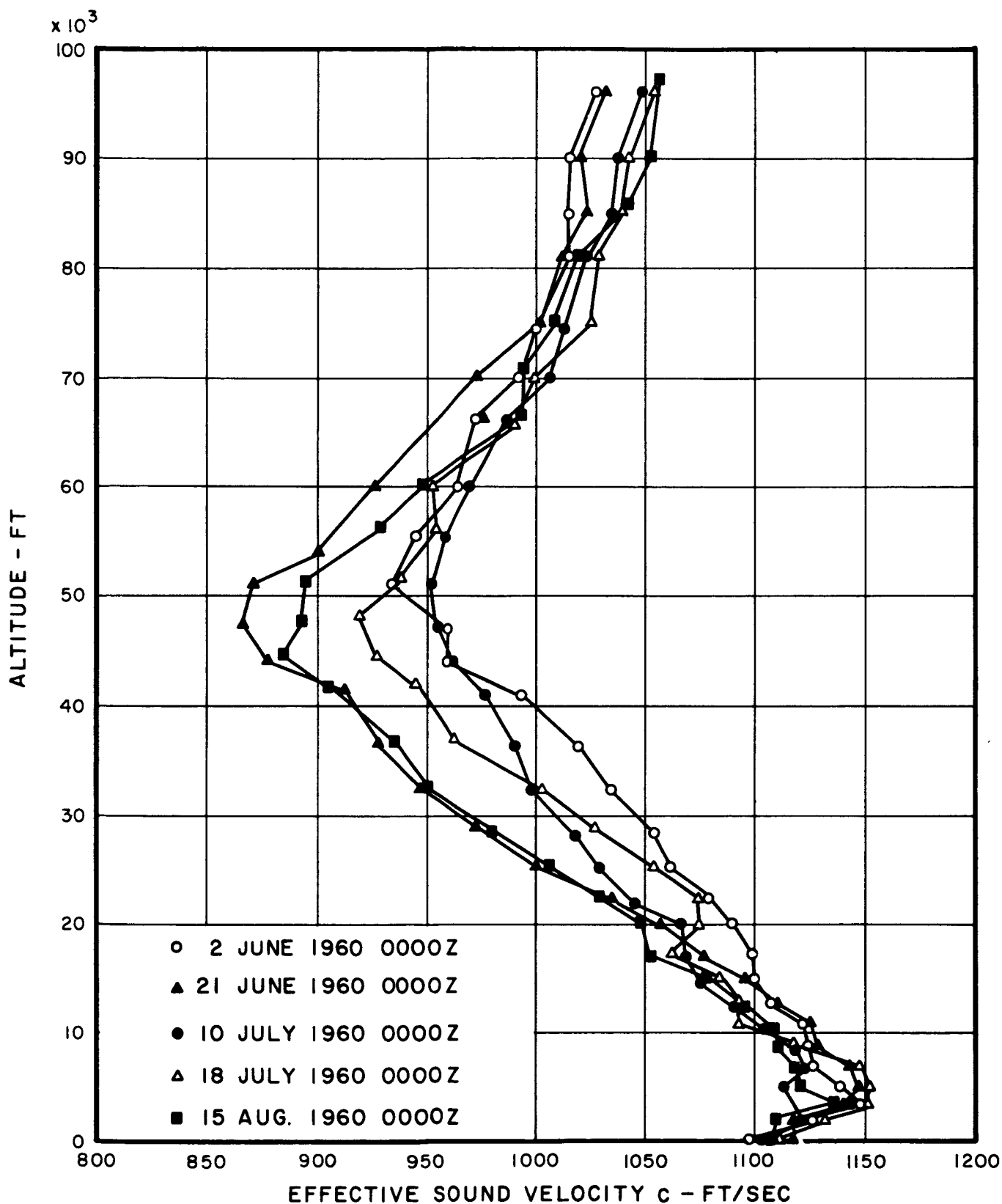


FIG. A-10b INDIVIDUAL SOUND VELOCITY PROFILES FOR
WESTERN SECTOR IN SUMMER
AT POINT ARGUELLO

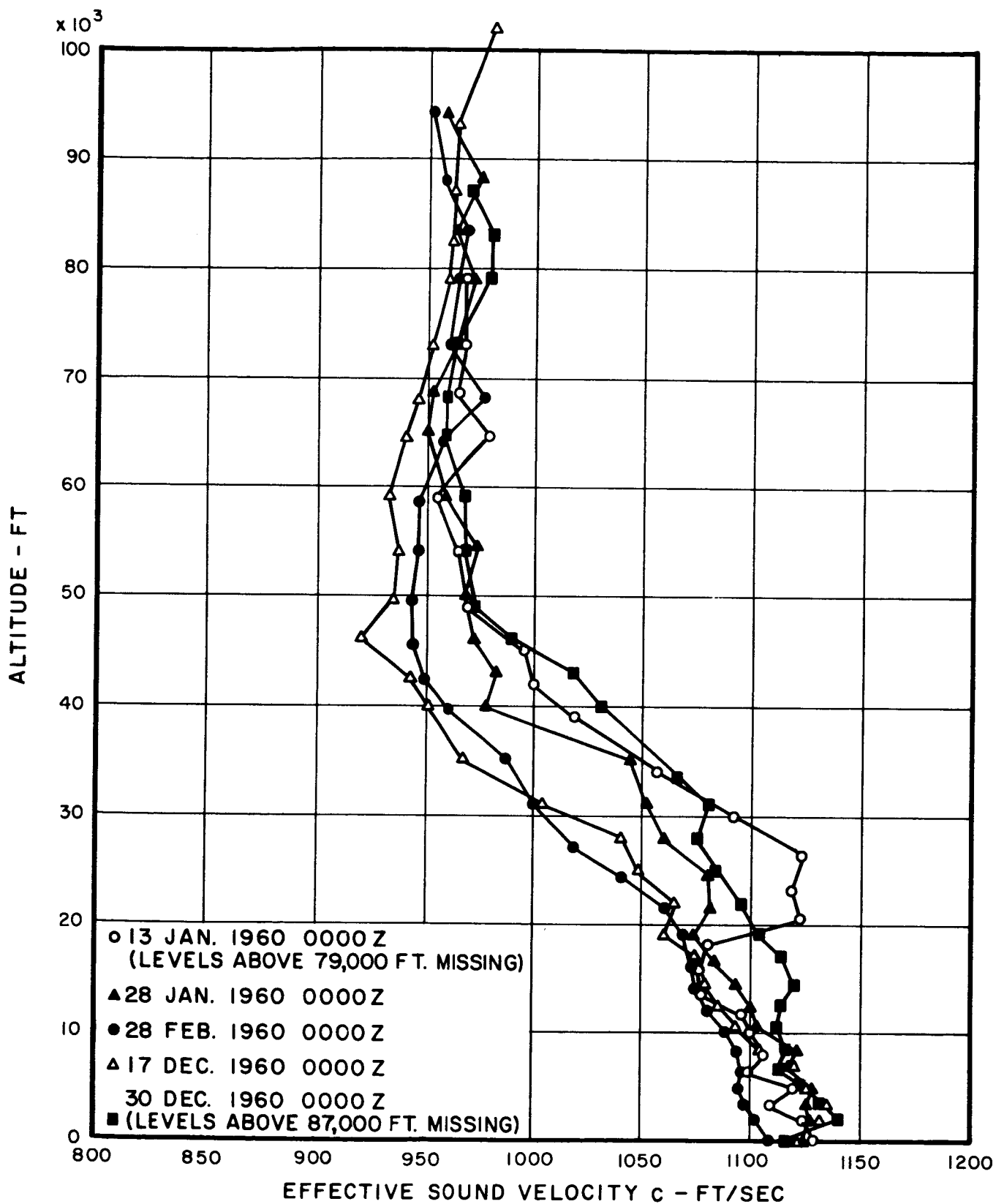


FIG. A-IIa INDIVIDUAL SOUND VELOCITY PROFILES FOR
SOUTHERN SECTOR IN WINTER
AT POINT ARGUELLO

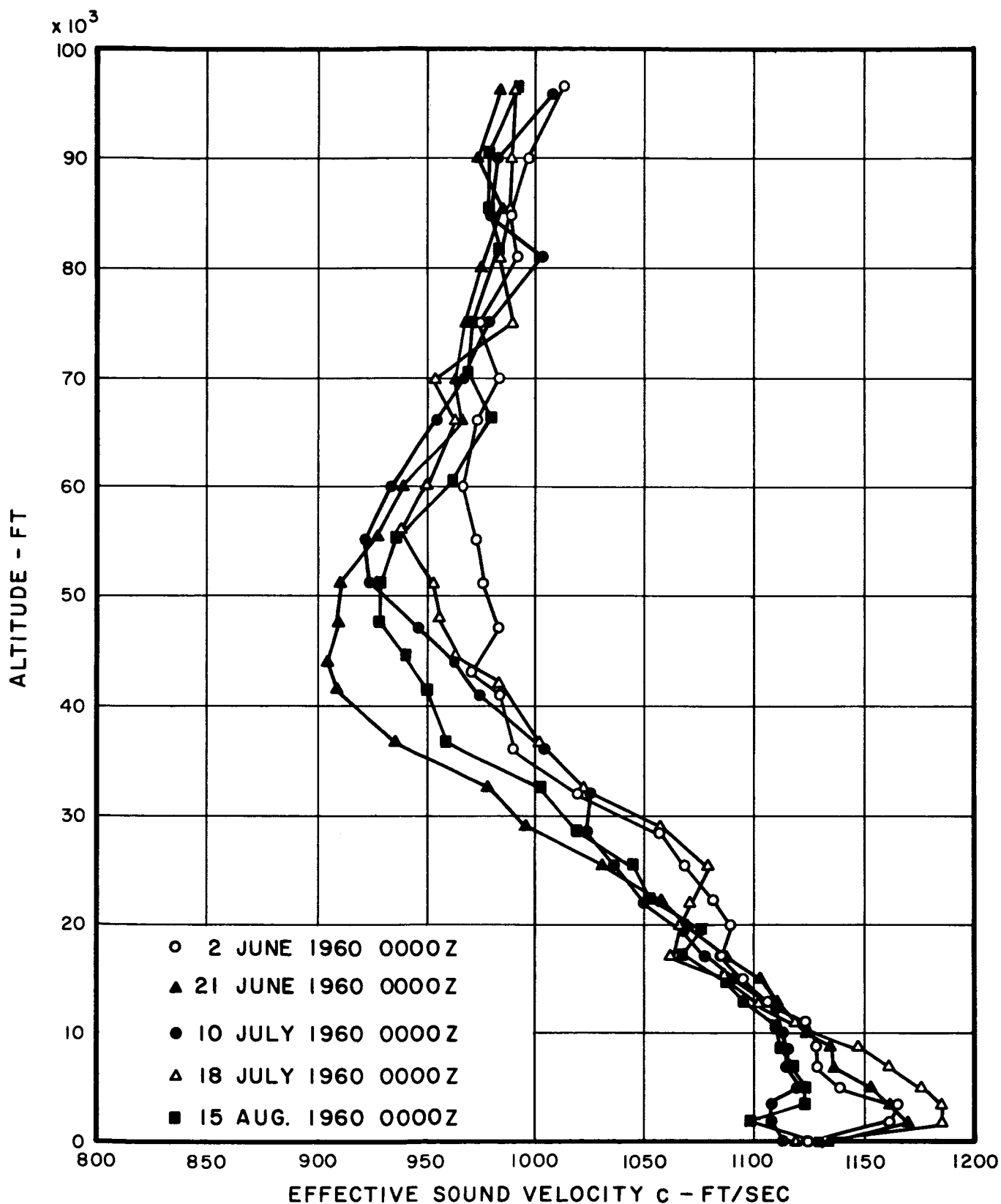


FIG. A-IIb INDIVIDUAL SOUND VELOCITY PROFILES FOR
SOUTHERN SECTOR IN SUMMER
AT POINT ARGUELLO

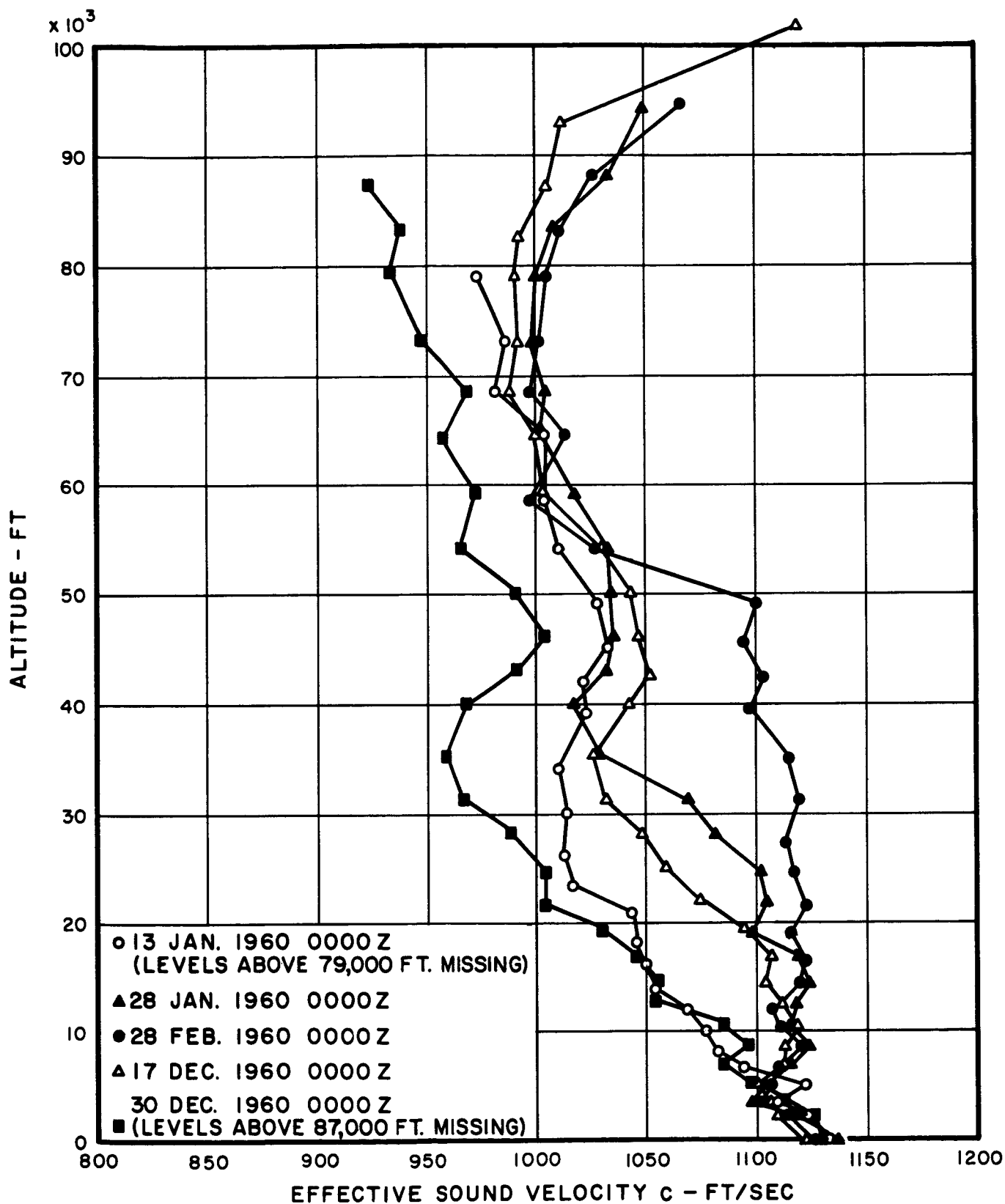


FIG.A-12a INDIVIDUAL SOUND VELOCITY PROFILES FOR
EASTERN SECTOR IN WINTER
AT POINT ARGUELLO

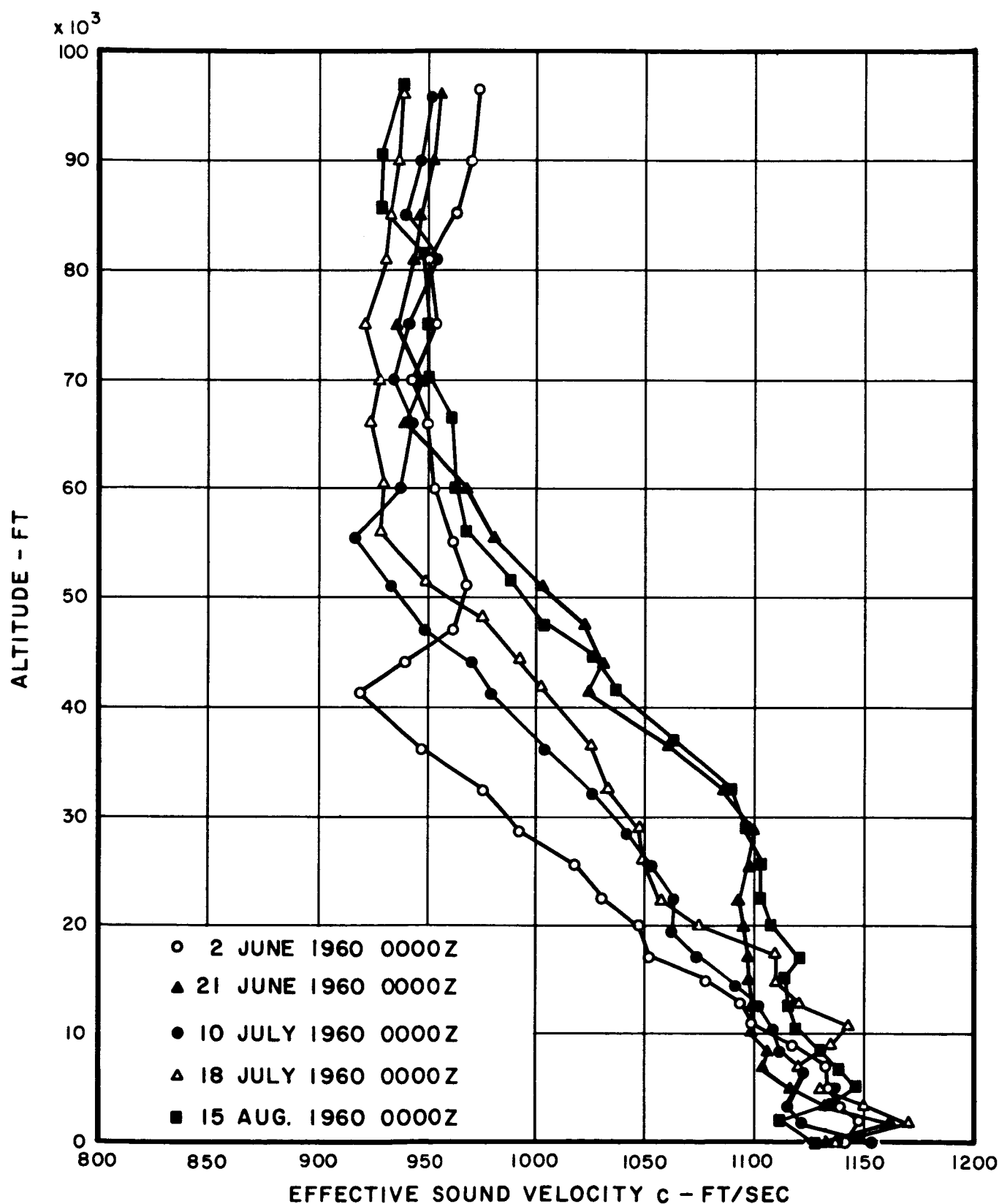


FIG.A-12b INDIVIDUAL SOUND VELOCITY PROFILES FOR
EASTERN SECTOR IN SUMMER
AT POINT ARGUELLO

A.3 Average Seasonal Profiles of Temperature and Absolute Humidity for Cape Canaveral, the Huntsville Area, and Point Arguello

Excess attenuation of sound due to molecular absorption depends, among other things, on the temperature and water content of the air. It is of interest therefore, to construct seasonal vertical profiles of absolute humidity for the various sites. These profiles are shown in Figures A-13, A-15 and A-17 together with the corresponding temperature profiles mentioned earlier (Figures A-14, A-16, and A-18).

The absolute humidity profiles are based on average seasonal relative humidities obtained from the summaries of Rawinsonde data for the summer and winter of 1960 mentioned previously, and on the values of saturation water vapor content associated with the temperatures. The measurements of relative humidity do not usually extend below 30 percent due to limitations in the Rawinsonde humidity transducers. Extrapolated estimates at low humidities have been obtained by arbitrarily assuming a constant relative humidity of 30 percent. These estimates of absolute humidity are shown as dashed lines in the figures. In general, the average seasonal absolute humidities are less than 0.1 gram per cubic meter above 30,000 ft at all sites.

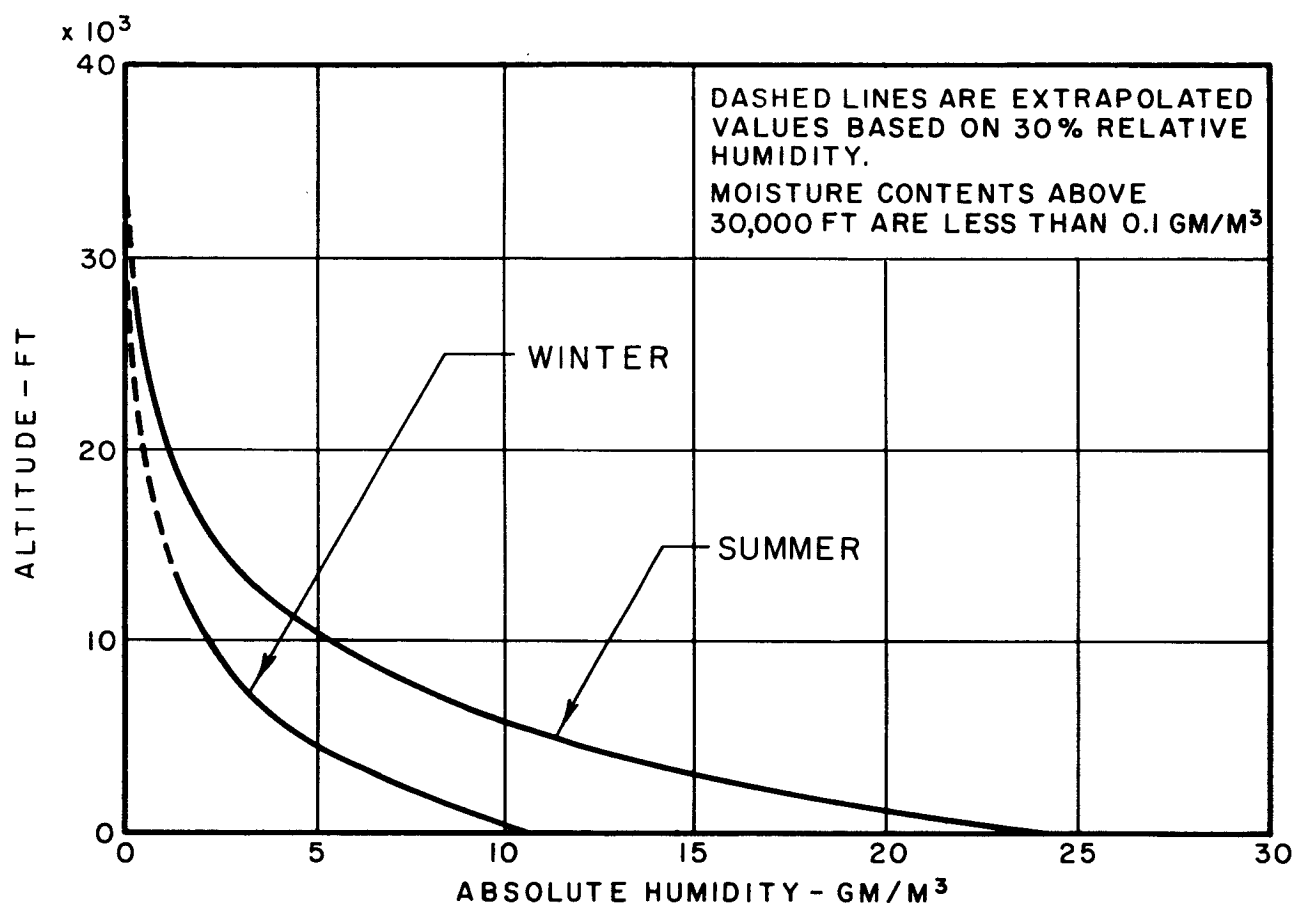


FIG. A-13 CAPE CANAVERAL - AVG. SEASONAL MOISTURE PROFILES

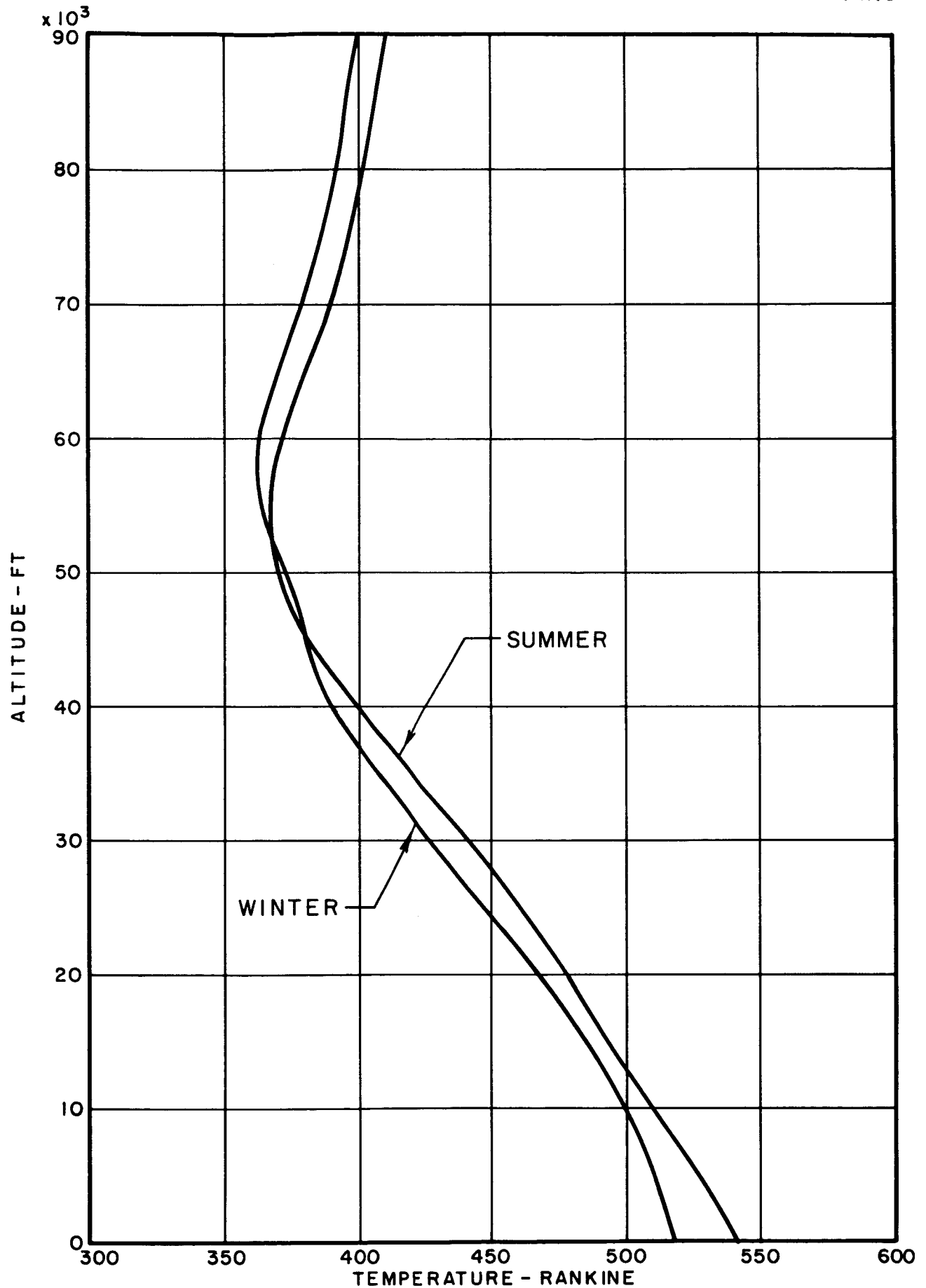


FIG.A-14 CAPE CANAVERAL - AVG. SEASONAL TEMPERATURE PROFILES

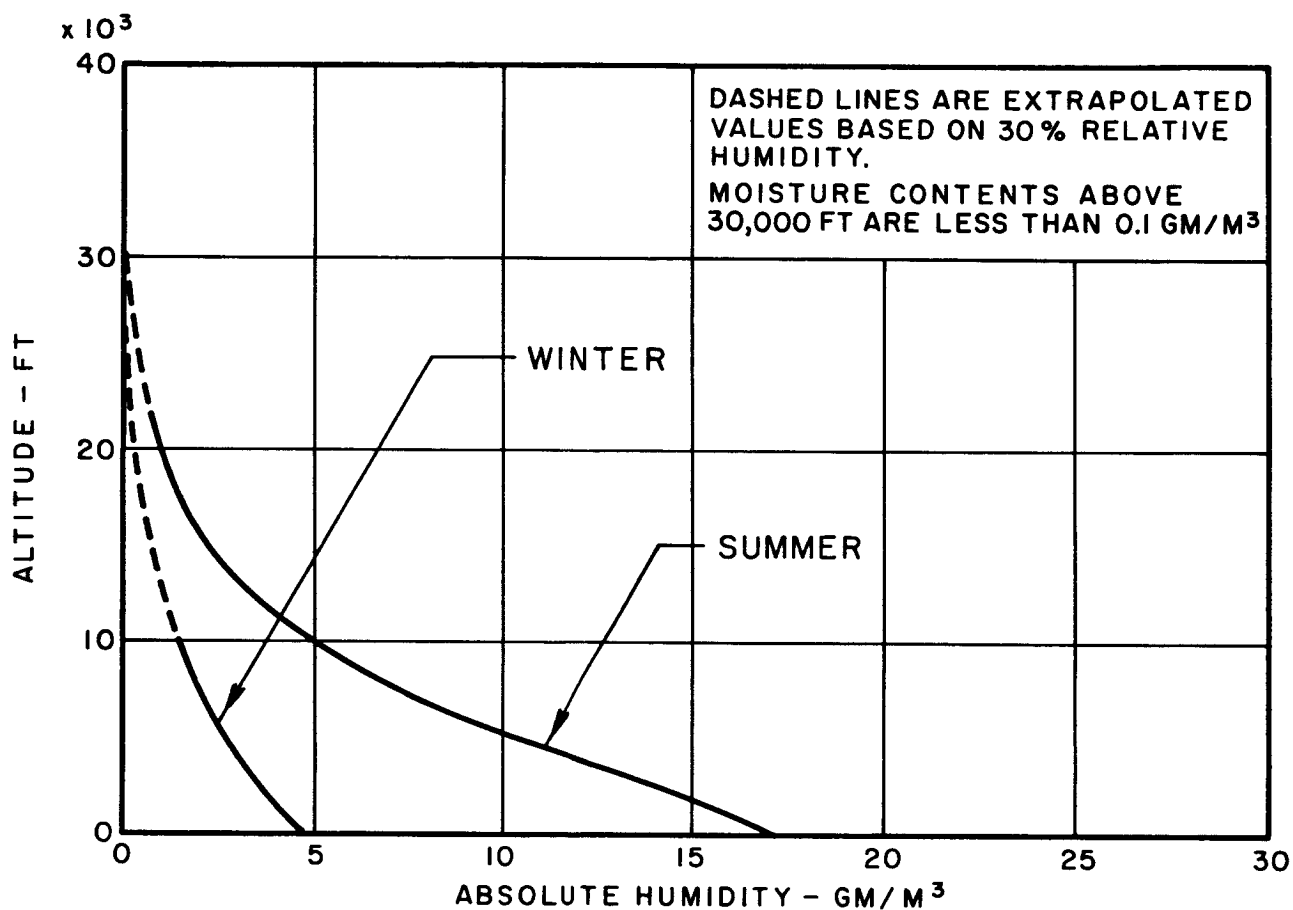


FIG. A-15 HUNTSVILLE AREA - AVG. SEASONAL MOISTURE PROFILES

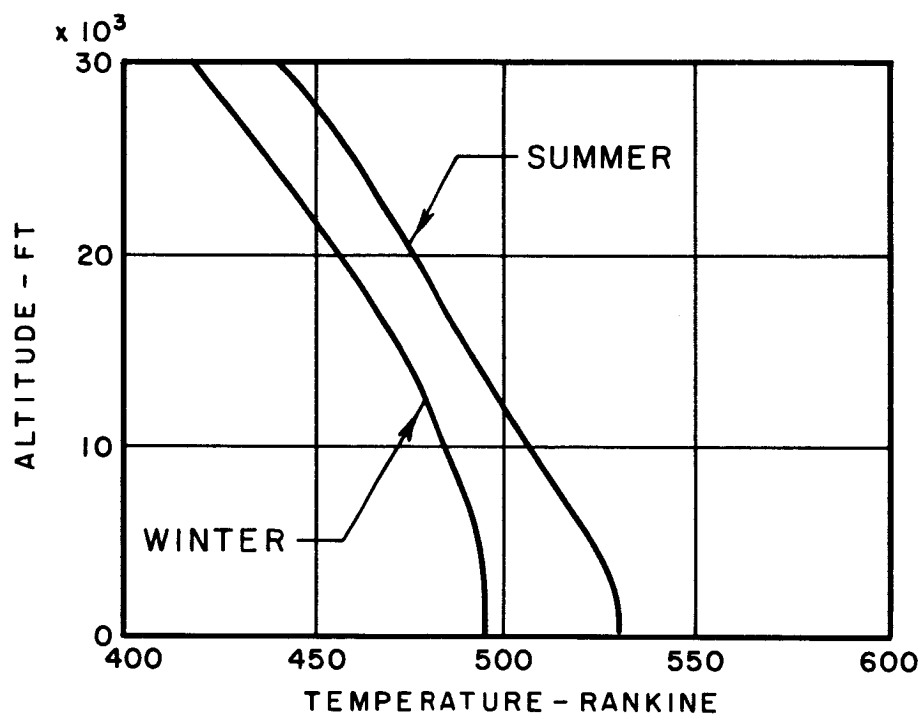


FIG.A-16 HUNTSVILLE AREA-AVG. SEASONAL TEMPERATURE PROFILES

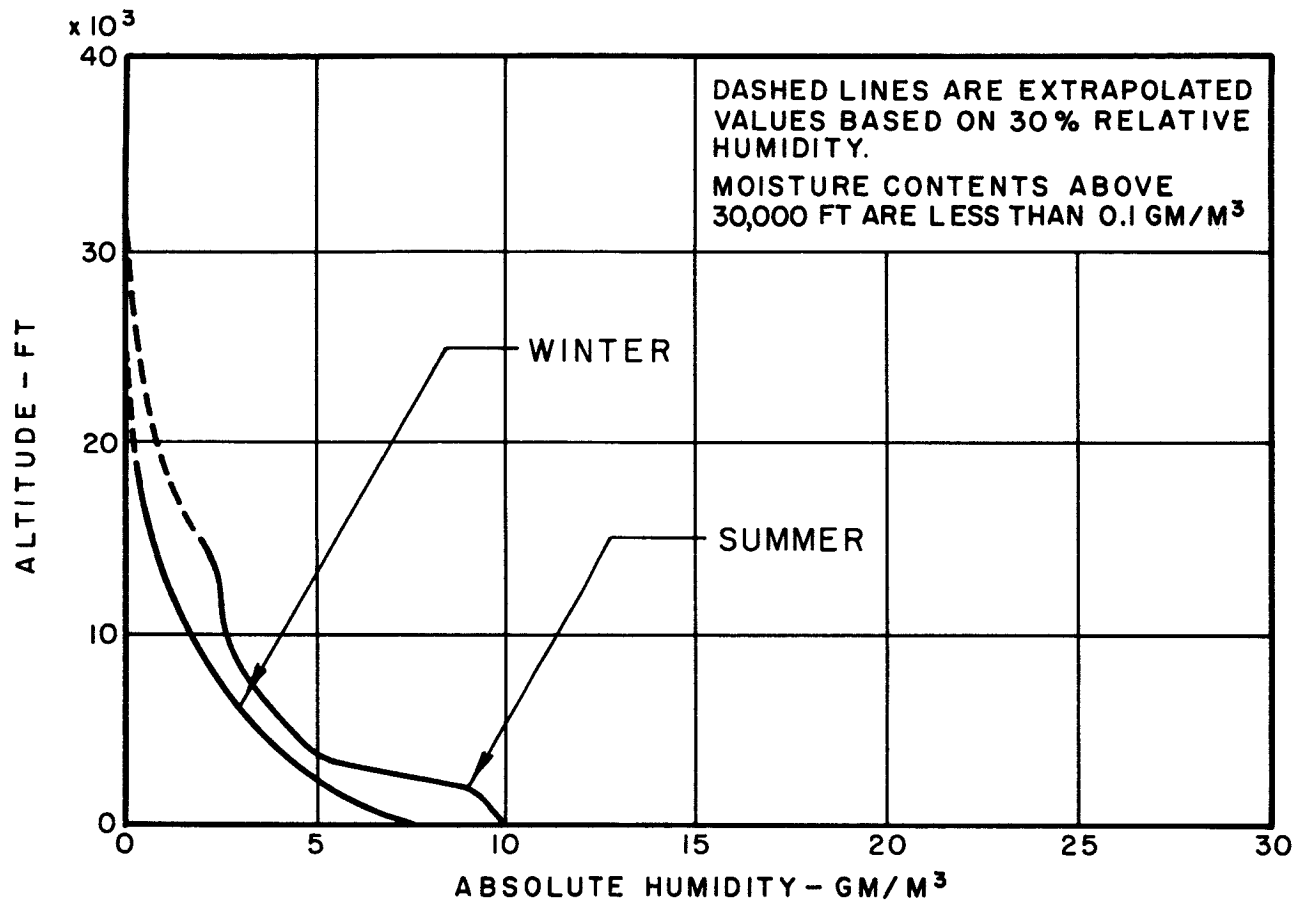


FIG. A-17 POINT ARGUELLO - AVG. SEASONAL MOISTURE PROFILES

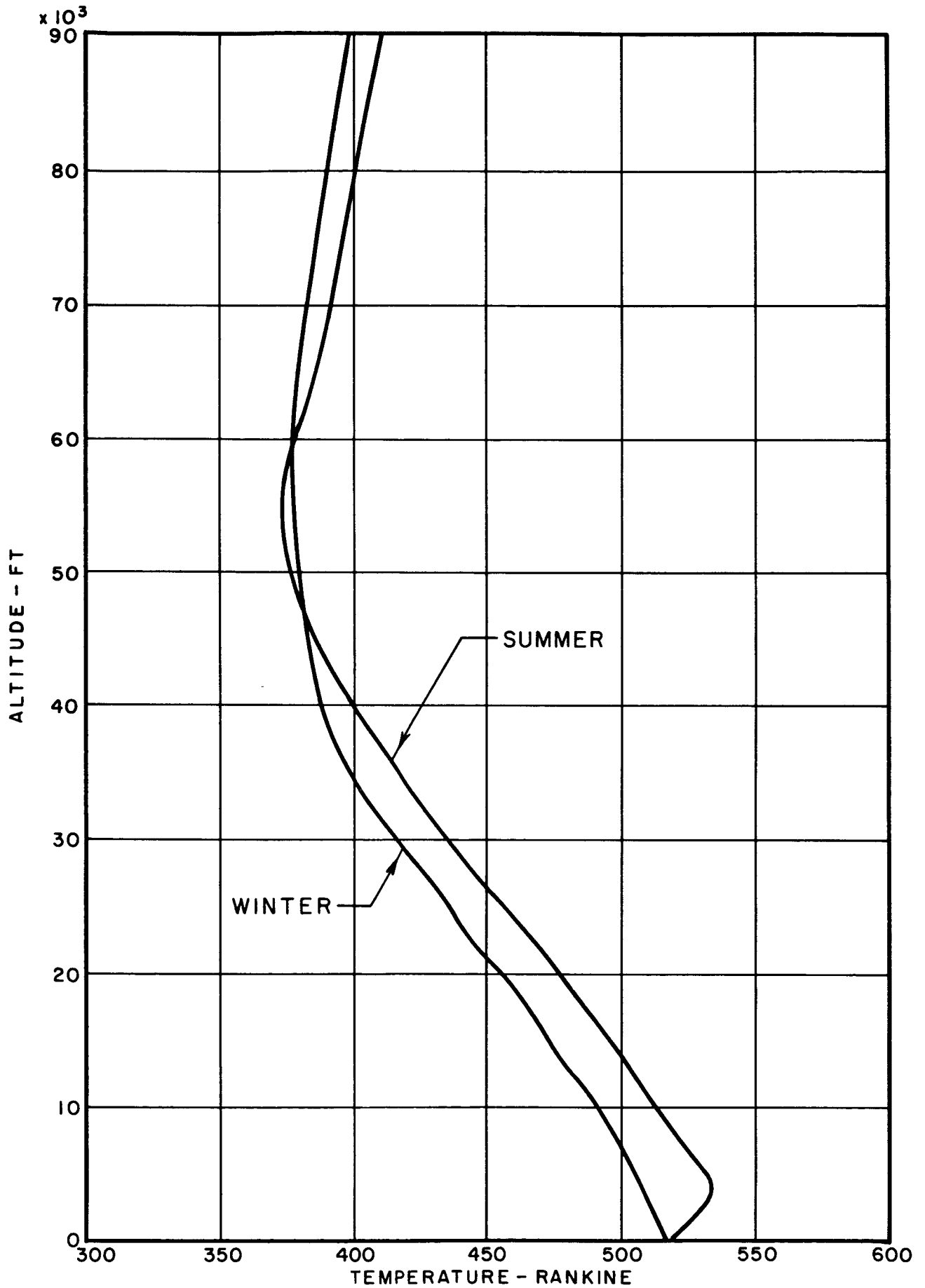


FIG. A-18 POINT ARGUELLO - AVG. SEASONAL TEMPERATURE PROFILES